Novel Cu(II)-mediated Methodologies for PET-induced Cyclizations, including Asymmetric Induction, and a Biomimetic Approach to the Basic Taxane Skeleton

DISSERTATION

submitted to the Universität Duisburg-Essen

Standort Essen

Fachbereich Chemie

in fulfilment of the Dr. rer. nat. degree

by

Yevgeny Makhynya

from

Kiev, Ukraine

Mülheim an der Ruhr

Germany

2004

Tag der mündlichen Prüfung:	21.01.2005
Prüfungsvorsitzender:	Prof. Dr. R. Boese
1. Gutachter:	Prof. Dr. M. Demuth
2. Gutachter:	Prof. Dr. R. Sustmann

This work was conducted at the *Max-Planck-Institut für Bioanorganische Chemie* (former *Max-Planck-Institut für Strahlenchemie*), *Mülheim an der Ruhr*, between August 2001 and November 2004 under the direction of Prof. M. Demuth.

My sincerest thanks goes to Prof. M. Demuth for his constant help and advises in research, for his kind help in giving the possibility to perform the practical part of my diploma thesis and for his valuable help and support at all stages of my Ph.D. studies.

I am very grateful to the State of North-Rhine Westfalia, Ministry for Education and Research, for partial support of the present Ph.D. work.

The kind support of this work at the *Max-Planck-Institut für Bioanorganische Chemie* by Prof. W. Lubitz and K. Wieghard are gratefully acknowledged.

I thank Prof. W. Gärtner for his kind help and support of this work.

I thank Prof. R. Sustmann, Department of Organic Chemistry, University of Duisburg-Essen, Campus Essen, for acting as co-referee.

I sincerely appreciated to all co-workers and friends for their assistance and friendly working atmosphere which made the work enjoyable.

Parts of this work have been published:

18. Vortragstagung der Fachgruppe Photochemie mit Sonderforum Molekulare Photomedizin, April 7-9, 2003, Muelheim an der Ruhr, Germany.
Authors: **Yevgeny Makhynya** (Talk), Mustafa E. Ozser, Andriy S. Kuklya, Martin Demuth.
Title: "Kaskadische lichtinduzierte Elektronentransfercyclisierungen von terpenoiden Polyalkenen in Gegenwart von Cu(II). Untersuchung von diastereoselektiven und enantioselektiven Photoreaktionen in Metallkomplexen",

GDCh-Jahrestagung Chemie 2003,
October 6-11, 2003, München, Germany.
Section: Radikal- und Photochemie für die Organische Synthese (gemeinsam mit der Fachgruppe Photochemie)
Authors: **Yevgeny Makhynya**, Mustafa E. Ozser, Frank Goeller, Frank Heinemann, Xuechao Xing, Martin Demuth (Talk).
Title: "Biomimetische Reaktionskaskaden mittels Photoelektronentransfer".

"Electron Transfer-Initiated Cascade Cyclizations of Terpenoid Polyalkenes in Low-polarity Solvent: One-step Synthesis of Mono- and Polycyclic Terpenoids With Various Functionalities", Mustafa E. Ozser, Huriye Icil, **Yevgeny A. Makhynya**, Martin Demuth, *Eur. J. Org. Chem.* **2004**, 3686-3692.

My Parents

My dear Viktoria

and junior

CONTENTS

1. Abstract

In this work two novel methodologies for the photo-induced electron transfer (PET) cyclizations of polyalkene terpenoids, involving Cu^{2+}-ions, are accomplished. In the first methodology the Cu^{2+}-ion acts as a co-oxidant. The presence of Cu^{2+}-ions changes the course and mechanism as compared to previously studied PET-mediated reactions. This new methodology allows to generate in a stepwise fashion two cationic intermediates from an ω-double bond of terpenoid polyalkene. The first species is a radical cation which is trapped by a nucleophile, such as water or methanol, in *anti*-Markovnikov fashion. In a further step the remaining tertiary radical is oxidized by Cu^{2+} to give a second cationic species at the tertiary centre of the former ω-polyalkene, which ultimately initiates the cascade cyclization. The mechanism of this reaction is elucidated in this thesis. The dependence on solvent, solvent proportions and temperature was also investigated.

In the previously studied PET-induced cyclization of geranyl acetate $CuCl_2$ was involved only once for mechanistic studies but no cyclic products were obtained. The possible reason could be the high nucleophilicity of the chlorine anion that leads to trapping of the formed cation. Unlike the previous reactions, the use of Cu(II)-acetate leads here to the formation of cyclic products – typical products of cationic cyclization in acceptable yields. This is because the nucleophilicity of acetate anion is much lower as the chlorine anion. Strong temperature dependence was found for this reaction. A decrease of temperature leads to a slow-down of the Cu^{2+}-mediated oxidation and an increase of product yields of the competing radical cyclization. Increasing the temperature speeds up the Cu^{2+}-mediated oxidation, but destabilizes on the other hand the cationic intermediates leading to higher yields of the double bond isomerisation products. The obtained cyclic and bicyclic products are important building blocks for the synthesis of a number of natural products.

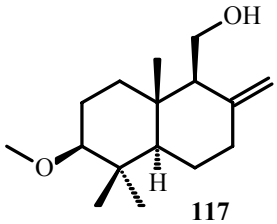

117

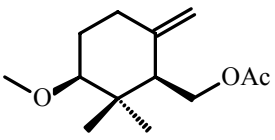

109

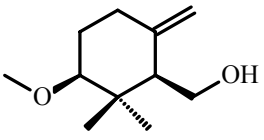

115

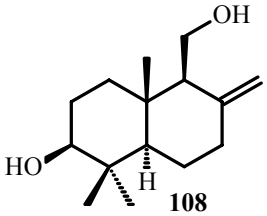

108

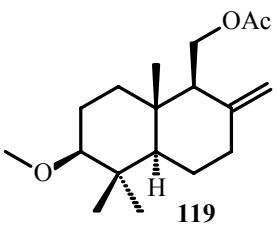

119

The second new methodology is the result of further improvement of Cu(II)-mediated PET-cyclizations where Cu(II)-acetate is employed as a co-oxidant together with another Cu^{2+}-ion involved in the complex. Different chiral and achiral Cu(II)-complexes are employed as substrates in the present phototransformations. The aim of this part of work was to develop a catalytic and enantioselective photochemical cyclization with further application in natural products synthesis. In contrast to all previously studied reactions the oxidation occurs not at the terminal double bond of the polyalkene, but from the side where the ketoester unit formes the σ,π-complex with a metal.

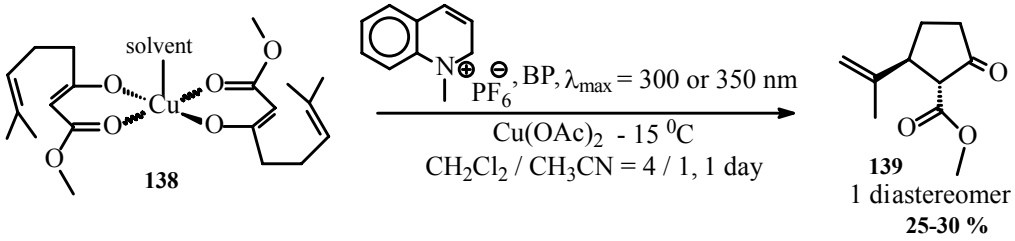

In product **139** no nucleophile is present which means that the nucleophile is not participating in the cyclization and is not necessary for this reaction. Based on the products and some mechanistic investigations we propose a reaction mechanism for this complex cyclization cascade. Further, substitution of one of the substrates in the complex with a chiral semicorrin ligand gives an enantiomeric excess which is low, but might be possible to be improved in the future.

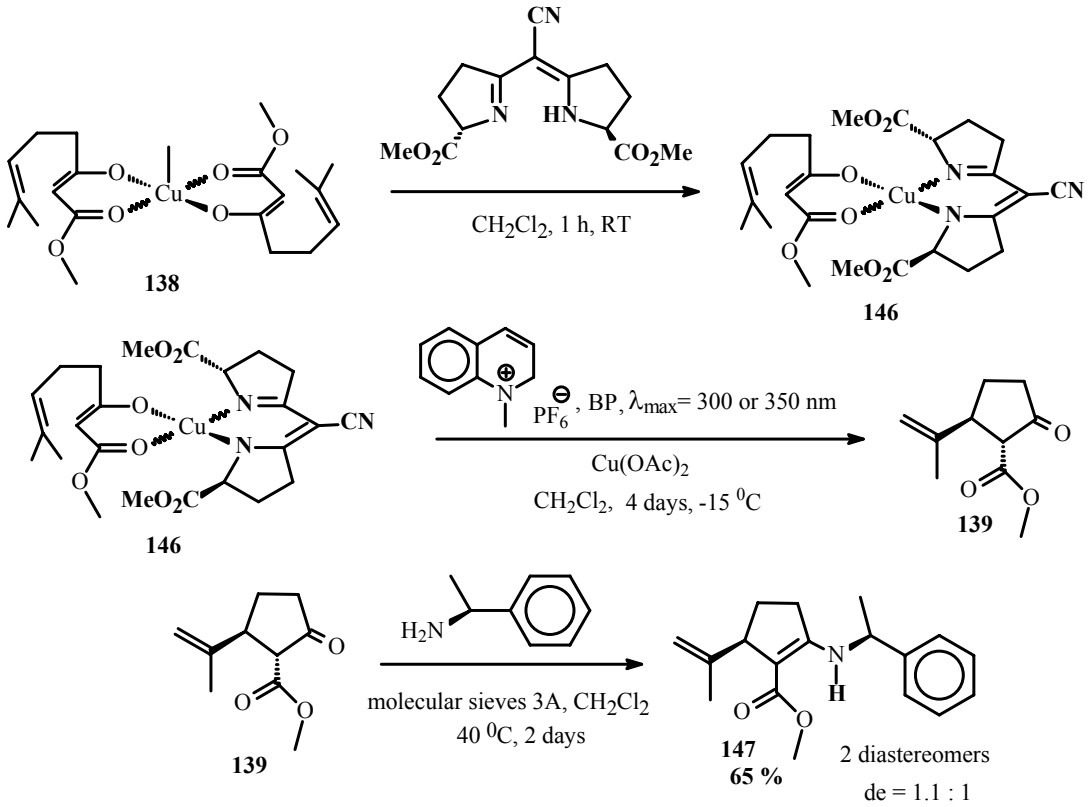

To clear the relatively low enantioselectivity of this reaction additional quantum mechanical calculations of the structures of the Cu(II)- and Zn(II)-complexes were performed to reveal the conformations shown below in (a) and (b).

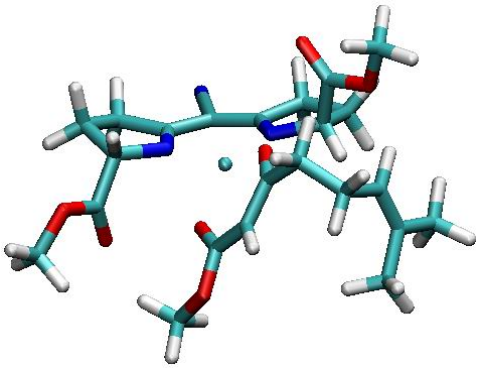

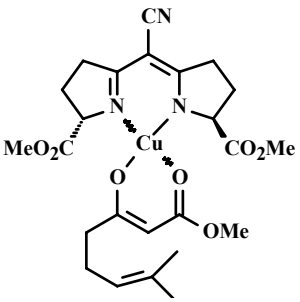

(a) Distorted square-planar Cu(II)-complex

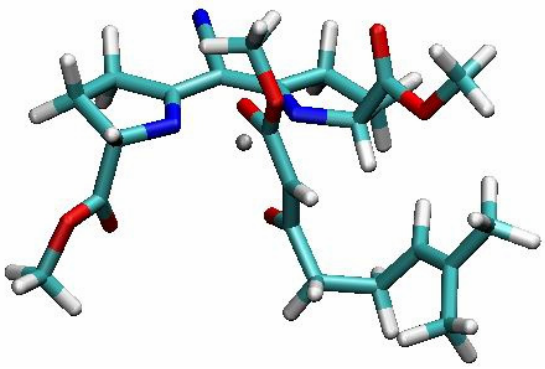

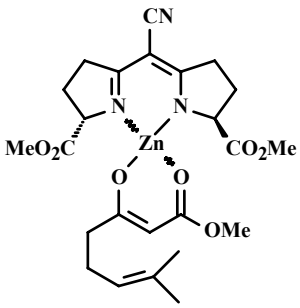

(b) Tetrahedral Zn(II)-complex

Another aim of the work was to analyze and possibly improve previously developed synthetic strategies toward the basic taxane skeleton and design the synthetic procedure to cyclize the precursor molecules to taxadiene bearing substituents or analogs thereof such as verticillene (**15**) or cembrene (**20)** (see Figure 2, page 13). Due to the long and expensive synthesis of precursors and failed cyclization attempts of these precursors in previous work (*F. Goeller*, PhD thesis), it was necessary to develop a new synthetic strategy. Possibly with a much simpler pathway to the precursors for the cyclization. We built on the positive results of previous investigations from our lab, for example fixed chiral centres and anticipating a non all-chair pre-folded conformation.

This new, efficient and cheap approach toward the basic taxane skeleton was developed as a result of this work. Additional quantum mechanical calculations were performed to elucidate preferred conformations of the potential precursors (Molecule **A**). Quantum mechanical calculations were extended to our new methodology and conformational analysis of products was performed. It was shown that the preferable non-folded conformation of precursors is highly dependent on the substituents in the star-marked key positions. The calculations with precursors bearing *tert*-butyl groups at the marked positions showed, that due

to the high bulkiness of the *tert*-butyl group (see starred positions), the energy difference between conformers becomes much higher. Hence it is possible to inhibit sterically the sterol-like pre-folding and favour conformations, such as represented by **B** and **C** (taxane-like pre-folding).

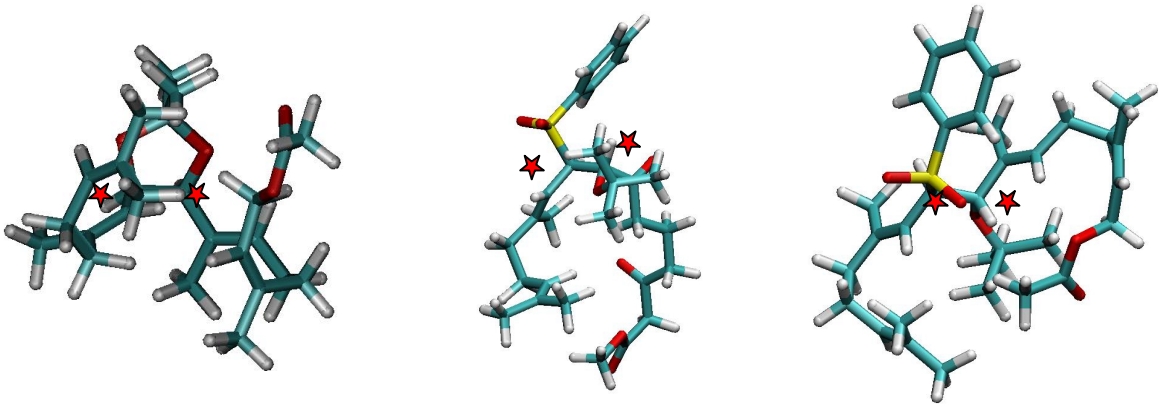

A **B** **C**

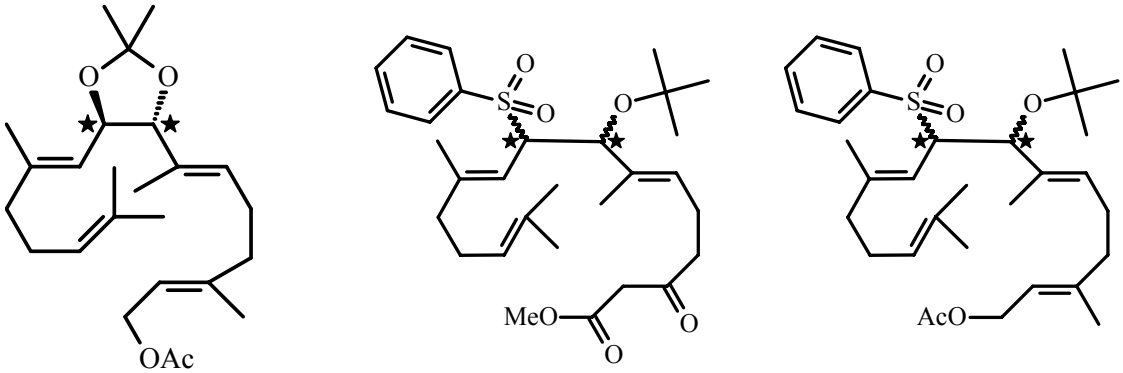

2. Introduction

2.1 Biomimetic and enzymatic cyclizations

The synthesis of natural products, mimicking the biosynthetic way, is called biomimetic synthesis. The remarkably powerful and efficient transformations catalyzed by the enzymes have provided inspiration and a big challenge for the preparative chemistry. This fact pushed the development of the biomimetic synthetic concepts in the last 50 years. *Stork* and *Eschenmoser*[1] were two of the pioneers in chemical studies on enzymatic transformations and in 1955 they formulated their postulate concerning the strategy. The biomimetic polyalkene cyclizations, done at that time, were initiated through electrophilic opening of an epoxide formed in an intermediate step at the terminal double bond of the terpenoid polyalkene. Seemingly, the conformation of the substrate rules the structure and the relative stereochemistry, *i.e.* chair-wise pre-folding was proposed[2].

2.1.1 Biotransformations of squalene: The processes catalyzed by proteins without metal cofactors

The enzymatic cyclizations of squalene (**1**) and oxidosqualene (**2**) are the most remarkable steps in the biosynthesis of steroids and triterpenoids. These polyolefins are stereoselectively cyclized and skeletally rearranged in a simple enzyme-catalyzed reaction by a wide range of microorganisms and higher eukaryotes to yield tetracyclic and pentacyclic triterpenoids including hopene (**3**), diplopterol (**4**), tetrahymanol (**5**), lanosterol (**6**), cycloartenol (**7**) and β-amyrin (**8**) (Scheme 1).

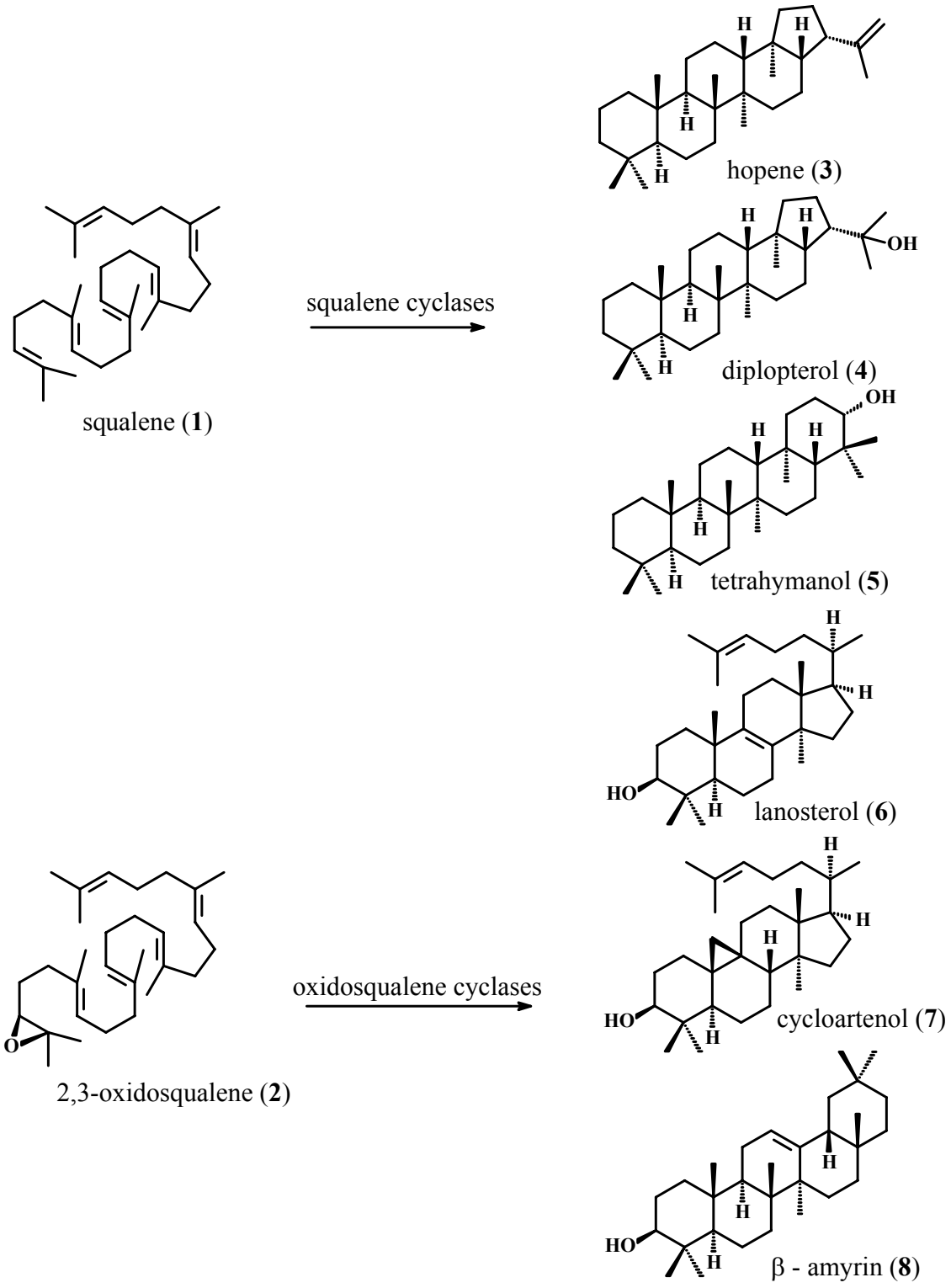

Scheme 1: Substrates and products of several polycyclic terpenes obtained through enzymatic cyclization from **1** and **2**[3].

There are two enzymatic types of transformation of squalene:

a) The oxidative cyclization, catalyzed by *squalene epoxidase* and *oxidosqualene cyclase* to lanosterol[4].

b) The non-oxidative cyclization, catalyzed by *squalene-hopene cyclase* leading to hopene and tetrahymanol (Scheme 2).

With the *oxidosqualene synthase* the substrate seems to be cyclized through the so-called "chair-boat-chair" conformation (sterol folding) and is initiated by electrophilic oxirane ring opening with participation of a neighbouring π-bond. The cyclization proceeds to give the protosteryl C-20 cation (**2**→**9**) which then undergoes a series of 1,2-methyl and hydride shifts including proton elemination to yield either the lanosterol (**6**) or cycloartenol skeleton (**7**).

In the case of the *squalene cyclase* the substrate adopts an all-chair-like conformation (non-sterol folding). Further skeletal rearrangements after cyclization were never observed. The *squalene-hopene cyclase* provides a strong catalytic acid-type activity (at least not weaker than in case of the *oxidosqualene cyclase*) to initiate the cyclization and after trapping of the intermediate cation results **3** and tetrahymanol (**4**). Notably, both reactions are catalyzed by proteins containing no metal. It is anticipated that both cyclases have the same phylogenic origin. It is assumed that the more complex *oxidosqualene cyclase* is the product of the evolutionary development of *squalene-hopene cyclase*.

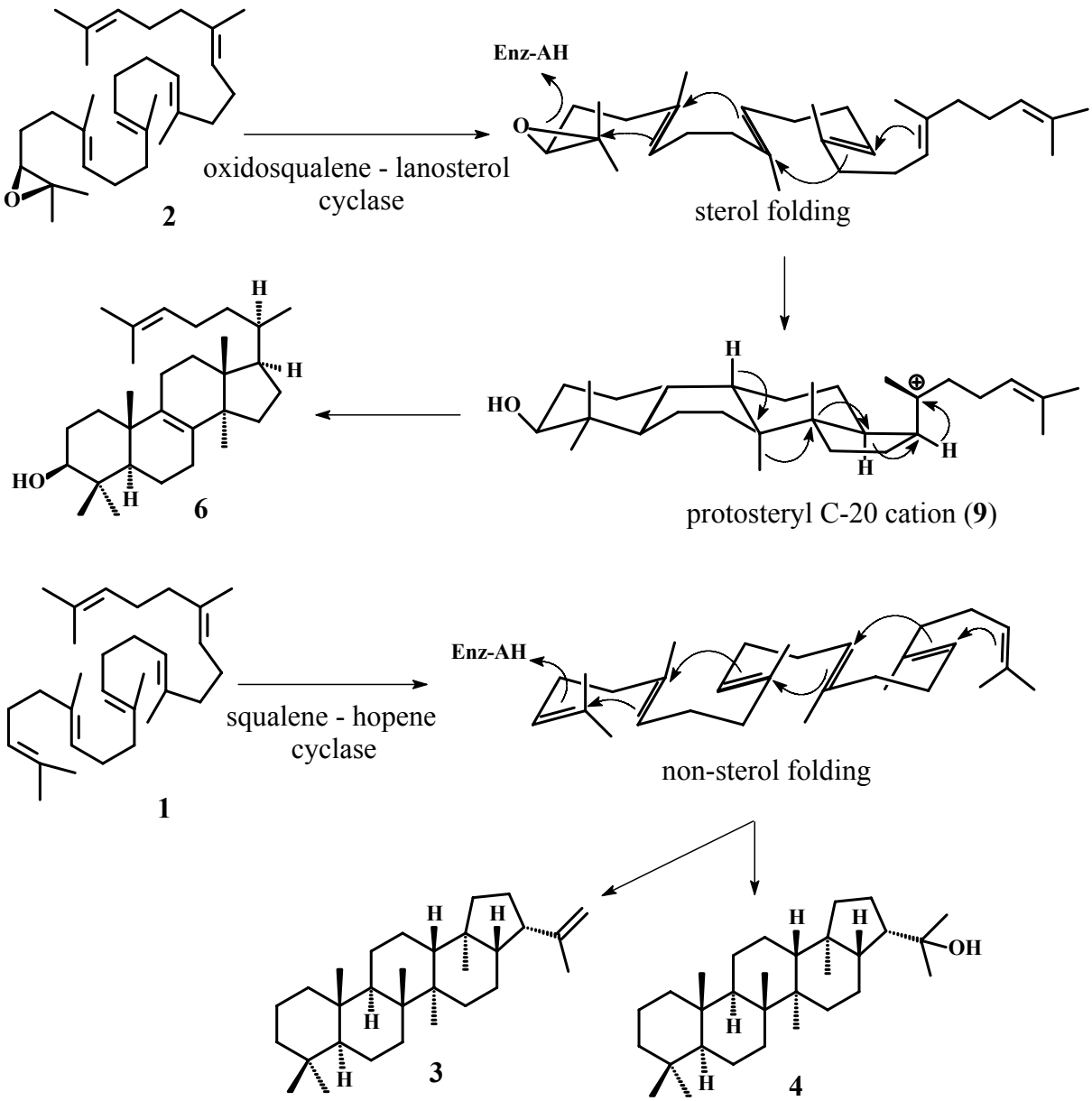

Scheme 2: Putative substrate conformation and overall mechanism of the reactions catalyzed by *oxidosqualene-lanosterol cyclase* (**2** → **6**) and by *squalene-hopene cyclase* (**1** → **3** + **4**)[3, 5].

2.1.2 Biosynthesis of taxadiene. A process catalyzed by the *taxadiene cyclase*, being a protein with a metal cofactor

The biosynthesis of taxol, which is an important anticancer agent, proceeds in a key step from geranylgeranyldiphosphate (GG-OPP, **10**) to taxa-4(5),11(12)-diene (**18**) (Scheme 3) catalyzed by the *taxadiene cyclase*, a metalloprotein with at least one Mg^{2+} ion. The exact number of metal ions is unknown up to now. The crystal structure of the protein is still unsolved. Nevertheless, the numerous terpene cyclases are the product of evolution. One example of direct interest to us concerns the solved structure of *bornyl diphosphate synthase* which produces (+)-bornyl diphosphate from geranyl diphosphate[6] and could serve as a convenient structural model for the yet unknown terpene synthase (Figure 1).

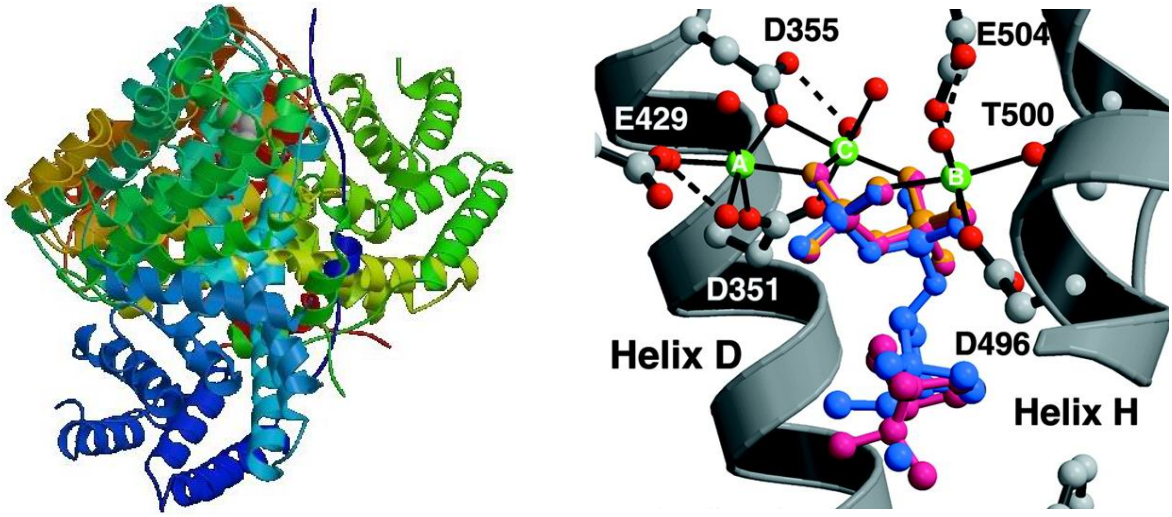

Figure 1: Crystal structure (left) and active site (right) of bornyl diphosphate synthase (PDB entry 1N1Z)[6].

As a result of the crystal structure a cluster of three Mg^{2+} ions is present in the protein. According to evolutionary similarity one could assume the presence of such a cluster also in *taxadiene cyclase*. This assumption also implies a similar cyclization mechanism in case of geranylgeranyl diphosphate (GG-OPP, **10**), which in fact was investigated[7] and is described below (Scheme 3).

The cyclization starts with ionisation of the geranylgeranyl diphosphate ester **10**, followed by migration of the OPP group to position 3 allowing rotation around the C2-C3 bond. Finally, compound **12** is again ionised and it promotes the C-C bond formation between

C-1 and C-14. The product of *anti*-Markovnikov addition (**13**) closes then the ring A *via re*-face attack at C-10. Deprotonation of the resulting 11α-verticillyl cation (**14**) by removal of the 11α-hydrogen finally affords 1S-verticillene (**15**). This intermediate, bound to the enzyme, is rapidly reprotonated at C-7 (**16**) *via* the same enzyme being responsible for the previous deprotonation step, to initiate transannular cyclization generating the taxenyl cation (**17**). Upon final deprotonation at C-5, **17** yields the endocyclic double bond of the taxadiene product **18**.

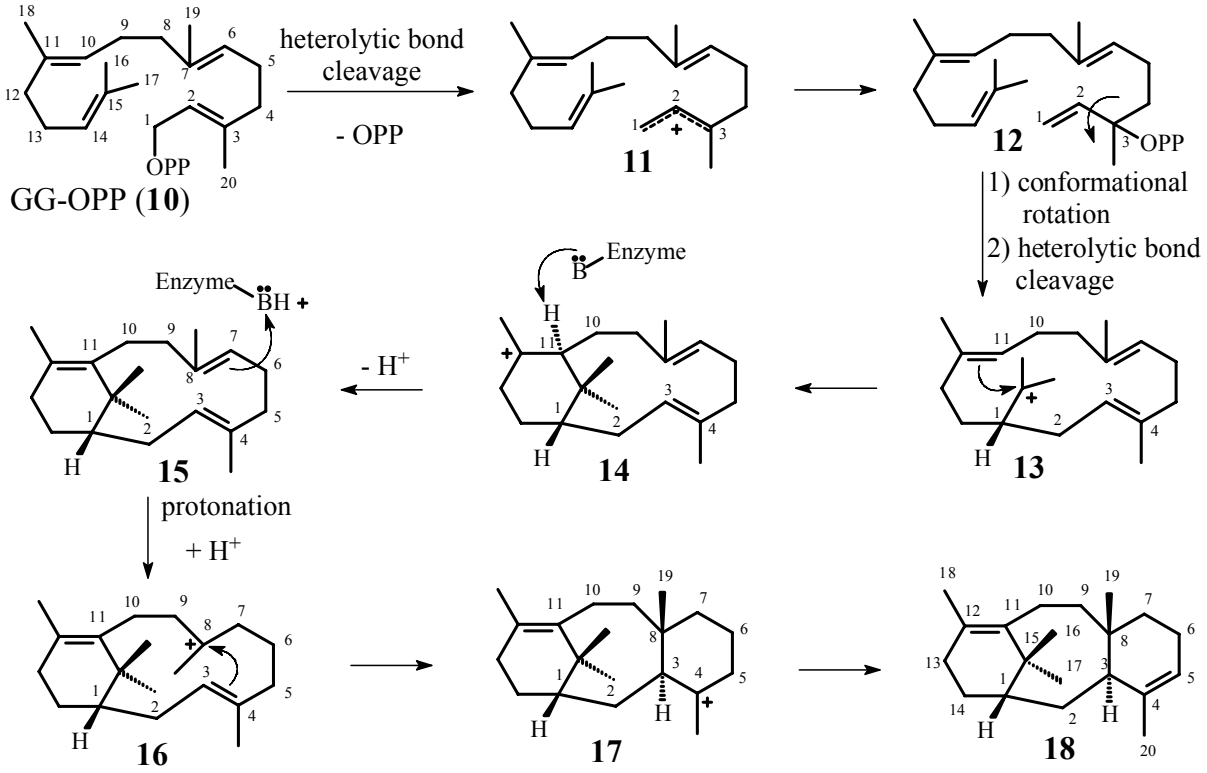

Scheme 3: Proposed mechanism for the cyclization of geranylgeranyl diphosphate to taxa-4(5),11(12)-diene involving *1S*-verticillene (**15**) as an intermediate[7].

Upon investigations of the reaction mechanism it was shown that compounds like casbene (**19**) or cembrene-type olefins (**20**) are not involved as intermediates (Figure 2). Also, in the final step **17** → **18** no taxa-4(20),11(12)-diene is formed and **18** is the sole product. Another proposal was that the OPP group plays a role of "molecular key" for the substrate recognition by the enzyme. It is also possible that the cleavage of the diphosphate group could be the energy source for reaction. The conformational changes are highly defined by the cavity size at the binding site. Remarkably, in case of many other terpene cyclases the first step is the macrocyclizaton *via anti*-Markovnikov addition.

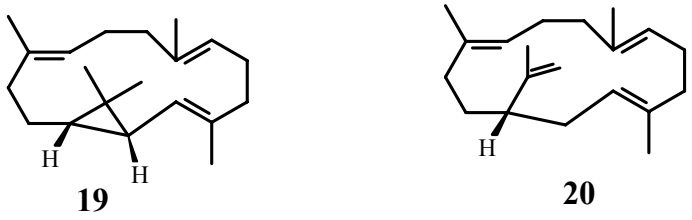

Figure 2: Structures of proposed intermediates in the taxadiene biosynthesis[7].

The importance of conformation and type of protein (metalloprotein *vs.* non-metalloprotein) in biochemically performed cyclization of geranylgeranyl diphosphate is illustrated by the recent work of *Eguchi* and *Kakinuma*[8]. They have analyzed the isoprenoid biosynthesis and reaction mechanism of the transformation of geranylgeranyl diphosphate into terpentetriene **25**, catalyzed by *streptomyces diterpene cyclase*. It seems that this enzyme is a non-metalloprotein, or even if it is one, the metal ion is not participating in coordination to the OPP-group. This enzyme acts similarly to *squalene-hopene cyclase* and arranges the substrate in the partial chair conformation. The proposed mechanism is depicted below in Scheme 4.

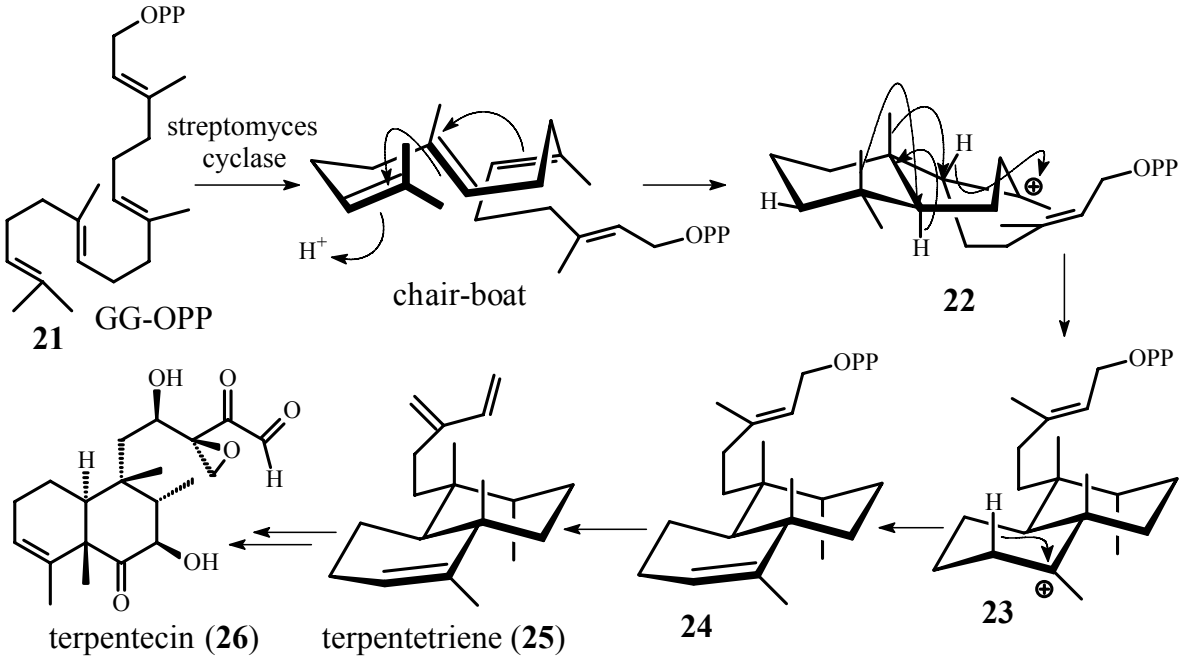

Scheme 4: Reaction mechanism of the cyclization of **21** catalyzed by *streptomyces cyclase*[8].

2.1.3 Biomimetic transformations

Based on the *Stork-Eschenmoser's* proposal a large number of biomimetic synthetic concepts were developed. Most of them were the attempts to reproduce the oxidative biosynthetic way *via* cationic cyclization. One of the pioneering works was the acid- or lewis acid-catalyzed cyclization of polyene epoxides performed by *van Tamelen*[9]. Further work was initiated by *Johnson*[10] (Scheme 5) and *Nishizawa*[11]. They gave rise to the synthesis of a number of natural products. However most of them in racemic form.

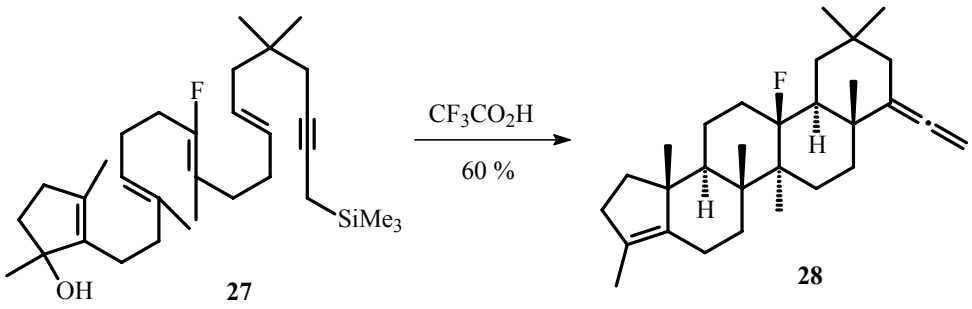

27 **28**

Scheme 5: Biomimetic cationic cyclization of **27** by *Johnson*[10].

A real highlight was the development by *Yamamoto* and co-workers[12], so called "Artificial cyclase", where the enantioselective cyclization of polyalkene terpenoids, using the combined system of a Lewis acid and a chiral Brønsted acid (LBA), was achieved. Cyclization of (E,E)-homofarnesol **29** using tintetrachloride ($SnCl_4$) and (R)-2-hydroxy-2'-methoxy-1,1'-binaphtyl ((R)-BINOL-Me) results in a synthesis of (-)-Ambrox (**30**) in 54 % yield and 42 % ee (enantiomeric excess).

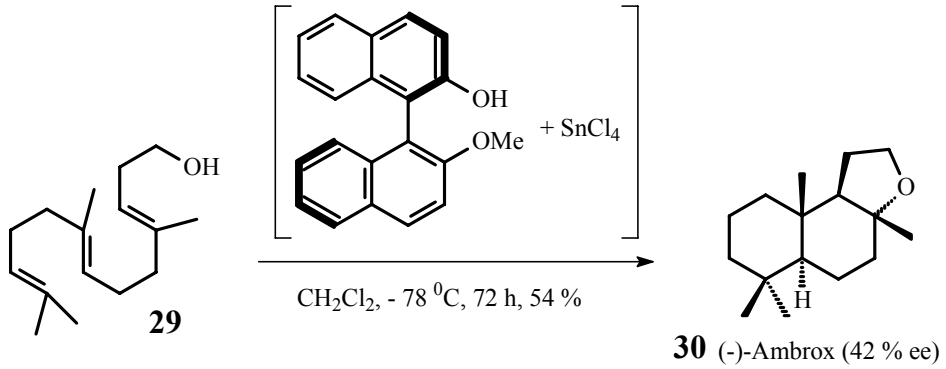

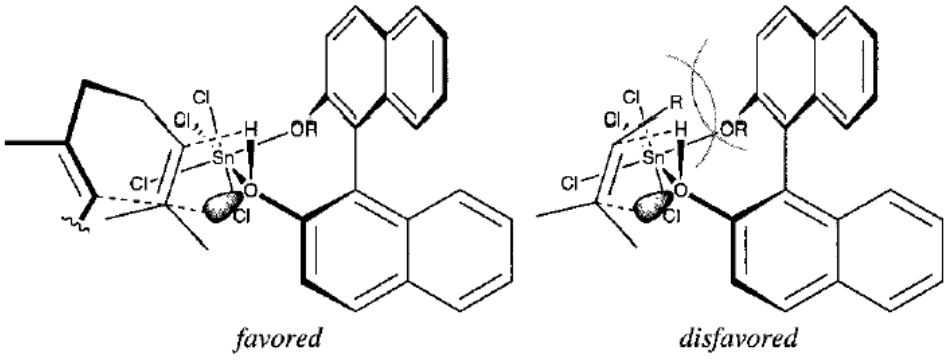

Scheme 6: Biomimetic cyclization of **29** which includes the proposed transition-state assemblies[12].

Biomimetic concepts were also investigated using radical cyclizations, where the first attempts to cyclize some di- and polyalkene terpenoids, such as geranyl and farnesyl acetate, were achieved by *Breslow*[13] (Scheme 7).

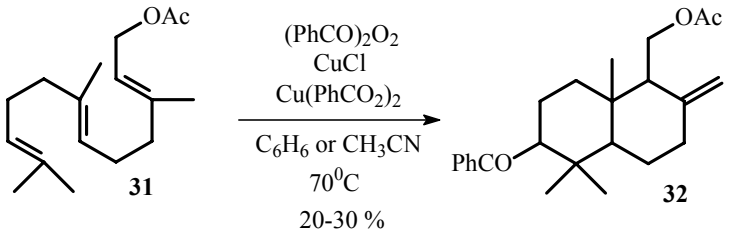

Scheme 7: Radical cyclization of farnesyl acetate **31** according to *Breslow*[13].

Further cyclizations of polyalkene terpenoids were successfully performed by *Zoretic*[14] (Scheme 8), *Pattenden*[15] (Scheme 9) and *Snider*[16].

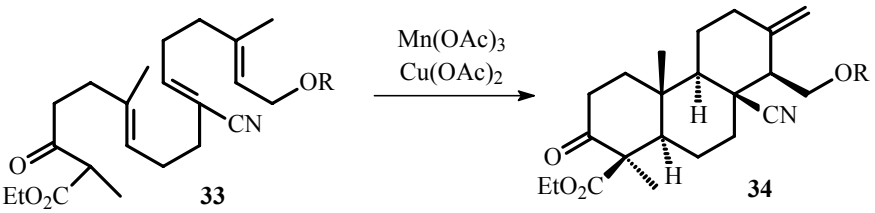

Scheme 8: $Mn(OAc)_3$ - induced free radical cyclization done by *Zoretic*[14].

Especially interesting is the radical cyclization performed by *Pattenden* toward the basic taxane skeleton (Scheme 9).

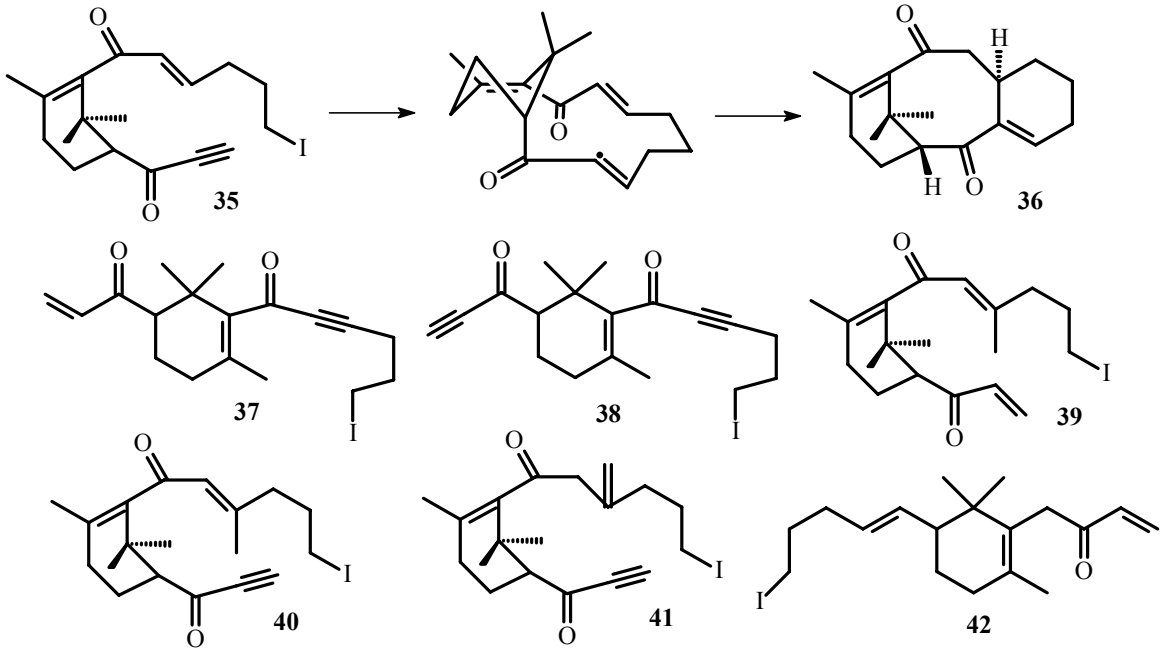

Scheme 9: Radical cyclization towards the basic taxane skeleton by *Pattenden*[15].

From the seven similar substrates (**35**, **37**-**42**, see Scheme 9) probed for the cyclization, only one (**35**) did undergo a cascade cyclization and gave the basic taxane skeleton **36**. In the six other cases the only product was the exchange of halogen for hydrogen.

Another exciting field of the biomimetic approaches under intensive investigation in the past two decades are photoelectron transfer cyclizations. Although the reactive intermediate in this type of reactions is the cation-radical, the cyclization proceeds only after cation trapping, suggesting a pure radical mechanism. The most successful investigations were achieved by the *Gassman*[17], *Mattay*[18] and *Demuth*[19] groups. This topic will be discussed in the following chapter in more detail.

2.2 Theoretical aspects of photochemically-induced electron transfer (PET) in biomimetic cyclizations

Recently, the oxidative photo-induced electron transfer (PET) reactions became a simple and versatile method for the conversion of acyclic polyalkene terpenoids into cyclic and polycyclic products with high stereo- and regioselectivity. This is usually achieved through the enhanced redox reactivity of the acceptor or donor upon photoexcitation (Figure 3).

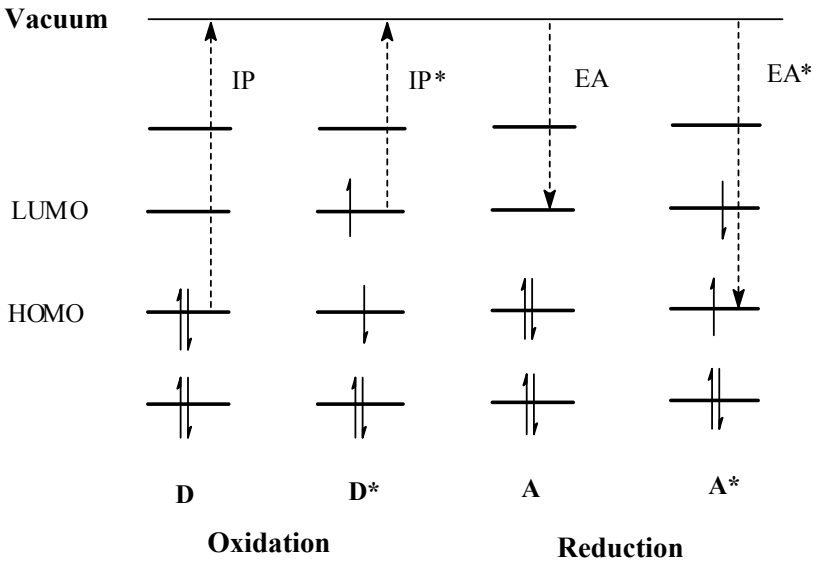

Figure 3: Enhanced redox reactivity of donor and acceptor upon irradiation.

A large number of methodologies for oxidative PET-initiated cyclizations was developed and it is possible now to perform reactions diastereoselectively and enantioselectively in homogenous solutions or in heterogenous micellar medias. Most of these reactions use photoexcitation of the acceptor, leading to electron transfer from the donor in its ground state to the photochemically excited acceptor. Alternatively, electron transfer can also take place from the excited donor to the acceptor in its ground state as depicted in Figure 4.

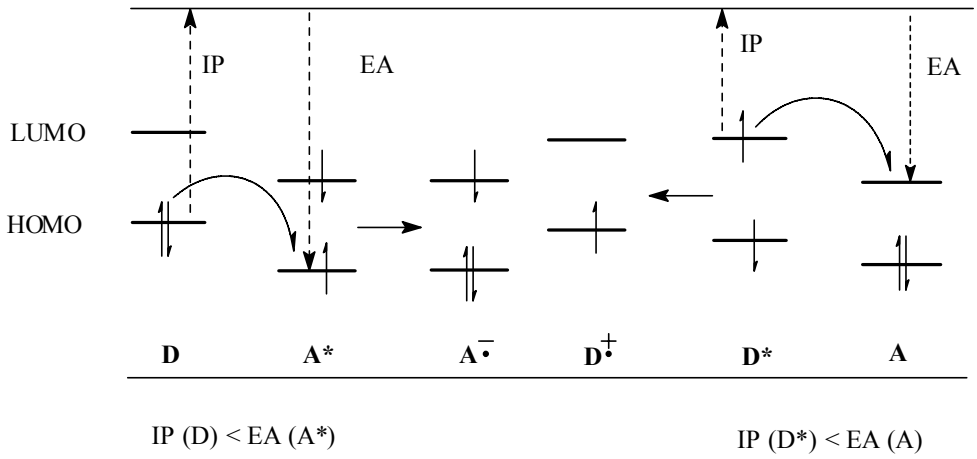

Figure 4: Electron transfer between donor (**D**) in the ground state and the photochemically excited acceptor (A*) *vs* excited donor (D*) and acceptor A (ground state).

Whichever pathway is taking place the intermediates are the cation-radicals of the donor and the anion-radicals of the acceptor. The electron transfer process, in general, depends on relative energies of donor and acceptor and photochemical properties of the substrates, such as redox potentials and absorption maxima.

Recent developments show the possibility to carry out such reactions not only upon artificial irradiation with lamps but also using the daylight as photon source. This methodology is extremely interesting and very relevant for an industrial applications as environmentally friendly process with free sun energy and low-cost equipment[20].

The big attraction of the photo-induced electron transfer is the possibility to perform reactions under mild and/or neutral conditions, thus, a big number of functional groups can be tolerated. Another advantage is that the PET-cyclizations are mostly regio- and stereoselective. Due to this a number of stereocenters can be formed in a single step upon radical cyclization, which is much more difficult to achieve using common preparative methods.

One of the most impressive photo-induced oxidative cyclization of enantiomerically pure geranylgeranylmethyldioxinon (**43**) was performed by *Heinemann*[21]. In this case the formation of eight stereocenters in one step was achieved. Furthermore, out of 254 possible diastereomeric products only 2 were obtained. After removal of the chiral auxiliary (-)-menthone, a tetracyclic terpene was ultimately obtained in enantiomerically pure form.

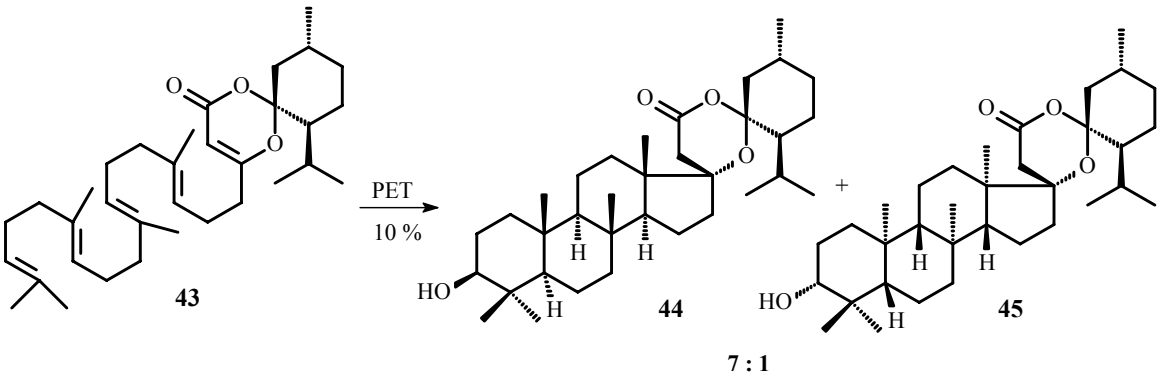

Scheme 10: Tetracyclization of geranylgeranylmethyldioxinon **43**[21].

Due to the formation of the cation-radical during the photochemically initiated oxidative process, it is typical for the oxidative PET-triggered cyclization reactions to have the nucleophile, such as water, methanol, ethanol, isopropanol or acids (acetic acid) and cyanide as external nucleophile in the reaction mixture. However, there are some examples in the literature where the intramolecular functionalities were used as a nucleophile[17, 22].

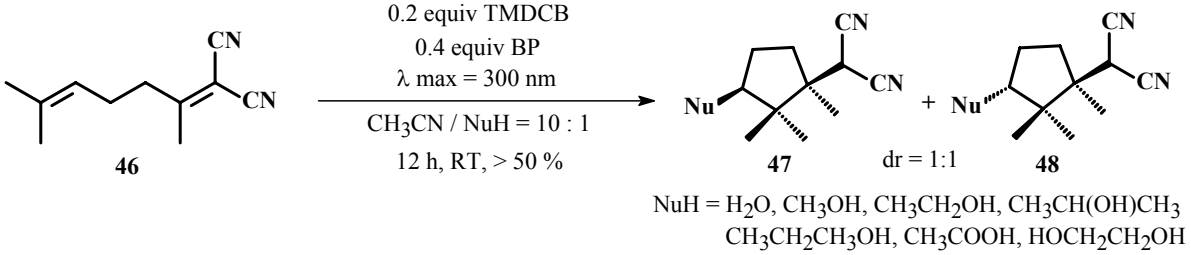

Scheme 11: PET cyclization of 2,6-dimethyl-1,5-heptadiene-1,1-dicarbonitrile (**46**)[23].

The example of *Gassmann*[17] represents the application of an unsaturated acid as a substrate and nucleophile at the same time. In all cases the products of *anti*-Markovnikov addition of the nucleophile is predominant.

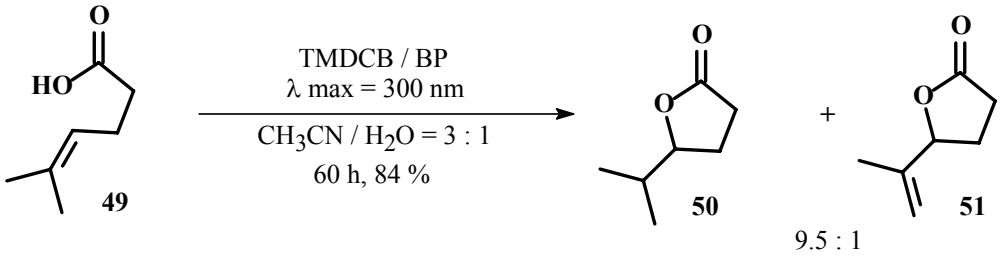

Scheme 12: *Anti*-Markovnikov lactonisation of **49** according to *Gassman*.

There are also some examples of PET-cyclizations known without an external nucleophile present in the reaction solution (*Roth* and co-workers[22], Scheme 13).

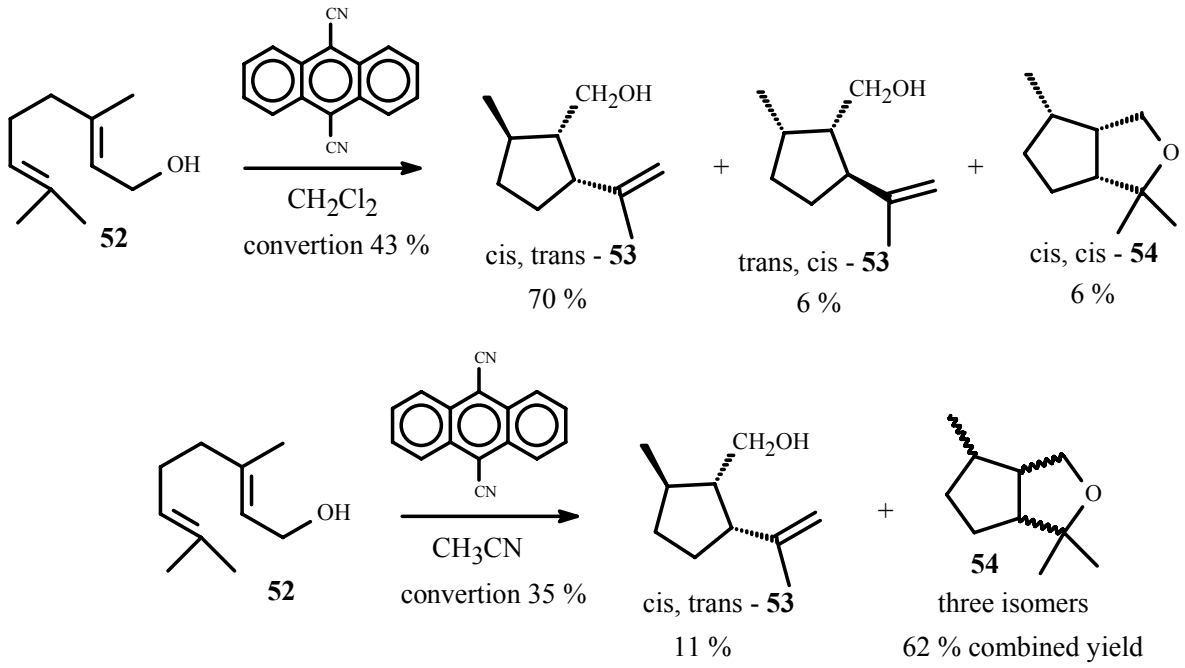

Scheme 13: Cyclization of geraniol in absence of an external nucleophile in polar and unpolar solvents.

Earlier investigations considered as the most probable process that after the cation-radical formation, the trapping of the nucleophile occurs prior to the radical cyclization[24]. The formation of a cyclic space-separated cation-radical *via* either cationic or radical cyclization seems to be inefficient according to the previous studies. According to this, it seems to be favourable for the cation-radical intermediate to undergo the elimination prior to the radical cyclization (see Scheme 13). It should be noticed that the reaction proceeds only until a certain conversion rate and than stops even in spite of extended reaction times. We anticipate that in this case the hydroxyl group plays an important role for the stabilization of an intermediate tertiary cation of the space-separated cation-radical. The radical cyclization is initiated by the secondary radical formed on place of the terminal double bond, followed and terminated by the elimination process. The monocyclic product **53** of radical cyclization and elimination is dominating in case of unpolar solvents, while the product of further cation trapping by the hydroxyl group (→ **54**) is predominant in a polar solvent.

The biggest problem for the efficiency of the photo-electron transfer is back electron transfer (BET) in the contact ion pair which is formed after excitation and primary electron transfer. The BET is highly dependent on reaction exothermicity[25], *i.e.* it is more efficient

under highly exotermic conditions. Accordingly, use of a strong donor with a strong acceptor to induce a reaction based on electron transfer is likely to be inefficient because of the fast back electron transfer. Upon photochemical excitation the exciplex (EXC) is formed. The critical step is the formation of the contact ion pair (CIP) followed by the formation of the solvent separated ion pair (SSIP). The final step of this transformation should be formation of the free ions (FI). The systems, where the ET and formation of FI is the less exothermic process, keep all energy in ion pairs and thus undergoe the BET very slowly[25]. If the formation of SSIP and FI is slow or inefficient due to unsatisfactory solvatation, the BET proceeds preferentially[26].

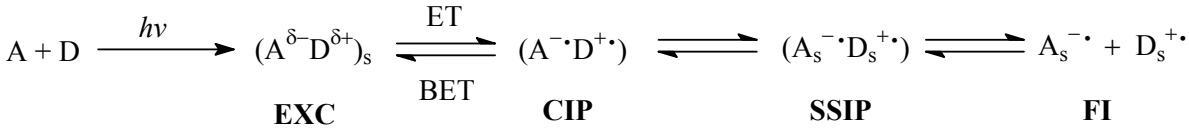

The polar solvents usually speed up the formation of SSIP and of the free ions, thus slowing down the BET. Furthermore, the use of acceptors with sterical hindrance plays an additional role in minimizing BET[17, 27].

Another aspect that resulted in positively influencing the reaction course and efficiency was the use of 1,1'-biphenyl (BP) as an electron co-acceptor[26, 28]. The biphenyl acts as a catalyst having a high oxidation potential and is used as a primary electron donor. Due to this additional charge delocalization slows down the BET process giving higher quantum yields of free ion-radical formation. If the substrate, *i.e.* a terpenoid polyalkene, is present in the mixture with low concentration, the secondary ET from the substrate to the cation-radical of biphenyl with formation of the cation-radical of the substrate proceeds even more efficiently than by the so-called direct way shown on the left side of Figure 5. In this case BP plays the electron acceptor role. Moreover, in the presence of BP the yields are drastically increased[24]. There are also some examples in literature, when using BP, the products were obtained with acceptable or even higher yields in contrast with analogous cases without co-acceptor, where no products were obtained[26, 28]. Another big advantage of this experimental set-up was the noticeable shortening of the reaction time.

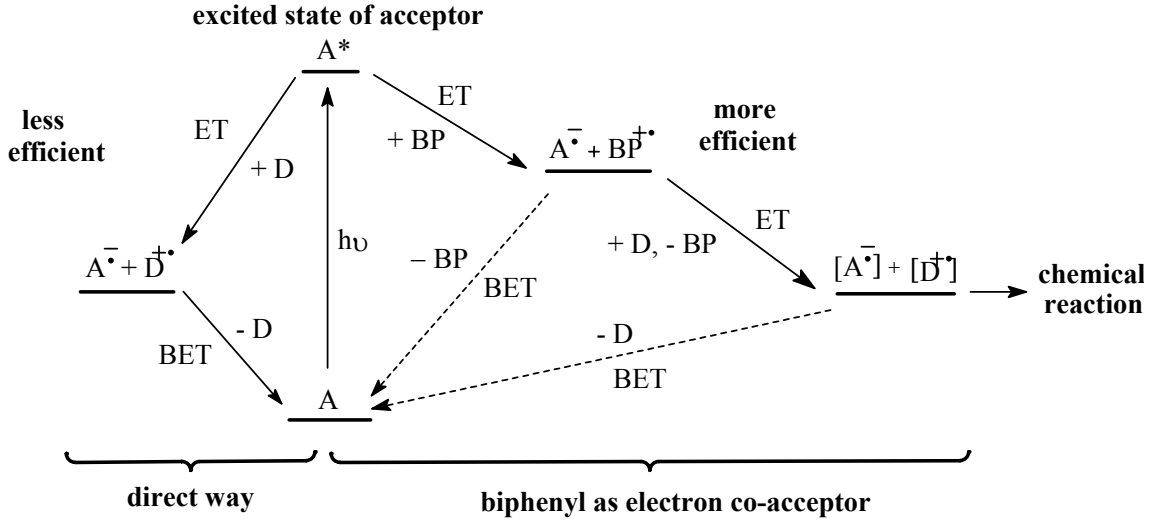

Figure 5: Energy diagram for PET-triggered reactions. Reactions with BP and without electron co-acceptor are on the left and right, respectively[25].

One should mention that the direct process is in general rather slow in contrast to the BET process. Another possibility to improve the yields by minimizing the BET was the idea to speed up the target ET leading to reactive ion-radicals in such way that the BET process will be comparably quick or even slower. This idea was realized in reactions where chloranil (2,3,5,6-tetrachlor-1,4-benzochinone) was used as acceptor[29]. The PET-reaction was quick enough to compete with the BET giving good yields of products.

According to recent investigations on the mechanism of the PET-triggered cyclization, the milestone steps can be formulated as follows:

- For efficient reaction and suppression of the BET the presence of an electron co-acceptor is necessary (see Figure 5).
- If a neutral electron acceptor together with a co-acceptor is used, polar solvents should be employed for successfully stabilizing the intermediate ion pair.

The overall mechanism is depicted below.

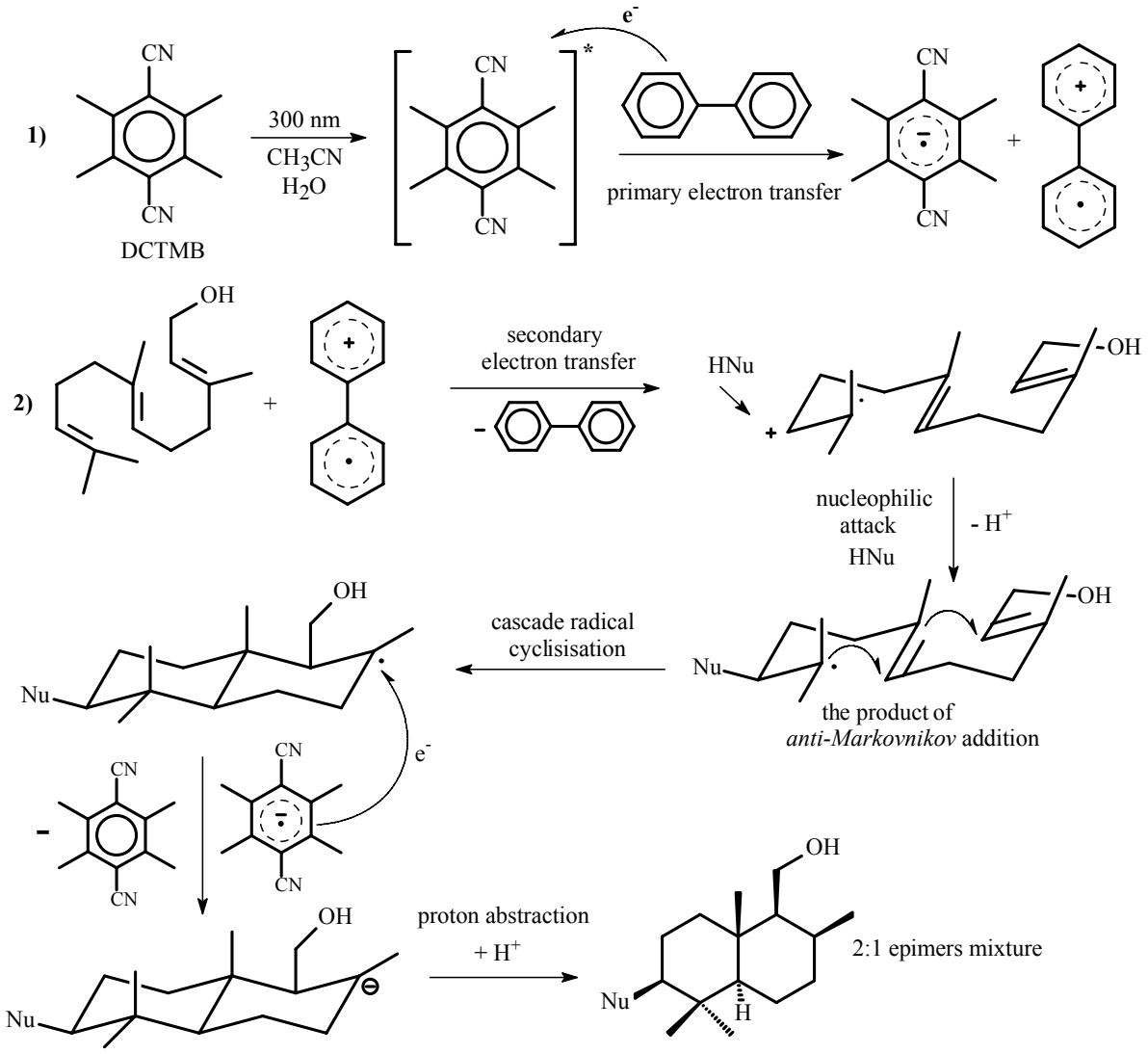

Scheme 14: Postulated mechanism of the oxidative PET-initiated cyclization[24, 30].

Upon irradiation the acceptor is promoted to the excited state and the primary electron transfer happens from the co-acceptor biphenyl (BP) to the excited acceptor DCTMB. At this stage the anion-radical of the acceptor and cation-radical of co-acceptor are formed. The secondary electron transfer proceeds upon oxidation of the polyalkene terpenoids by the cation-radical of BP. Free BP is released and the cation-radical of the alkene is trapped by a nucleophile. According to the literature and calculations[23, 24] the resulting radical performs a cascade cyclization from its previously adopted pre-folded conformation. The reduction of the final radical by the anion-radical of the acceptor is proposed as most probable termination. The released acceptor, being again neutral, closes the catalytic cycle. Finally, the resulting anion of the alkene is protonated by the solvent.

Recently a new and improved methodology for the PET-initiated cyclization was developed by *Demuth* and co-workers[31]. This methodology involves the use of cationic-types of acceptors, *e.g.* the N-methylquinolinium salt. The advantage of this acceptor is the formation of a neutral species – the N-methylquinolinium radical – upon primary electron transfer. This allows the use of unpolar solvents in the reaction because the charge separation is not necessary anymore. In the published results the quantum yields for the formation of separated cation-radicals upon irradiation of comparable acridinum salts were moderate[32] in polar solvents and high in unpolar solvents; the best result was achieved in dichloromethane[32].

2.3. Previous attempts of the synthesis of the basic taxane skeleton and total synthesis of taxol

Since its isolation in 1967[33] and structural determination four years later[33] the clinical tests showed high cytological activity of taxol (paclitaxel) against several types of cancer[34].

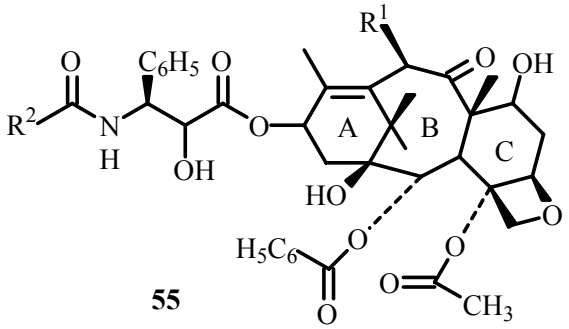

55

Taxol: R^1= OAc, R^2= Ph Taxotere: R^1= OH, R^2= tBuO

Figure 6: Structure of taxol and its closest analogue taxotere.

More intensive investigations later confirmed successful application of taxol in the therapy of mammal cancer[34]. Unfortunately, the natural source of taxol is insufficient and the current isolation process implies the irreversible utilization of many trees. For example, to obtain 1 kg of taxol one should process up to 10000 kg of the bark of the relatively rare Californian yew-tree. On the other hand, for a successful cure of one patient one needs 1 to 2 grams of taxol.

Other problems discovered during the clinical tests were the low solubility of taxol in water (about 25 mg/l) and the rather high toxity of taxol. Nevertheless, taxol remains an

important medicine in cancer therapy and a sufficient source of taxol is still a challenging problem for preparative organic chemistry.

In last past four decades a large number of attempts toward the total synthesis of taxol (paclitaxel) were undertaken[35]. However, only few of them were successful but involving too numerous steps in view of practical applications. Some of the attempt are depicted below.

The first one was performed by *Holton* and co-workers[36]. In this synthetic strategy the fragmentation of tricyclic epoxy alcohol **57** to obtain the rings A and B of the basic taxane skeleton **58** was used (Scheme 15).

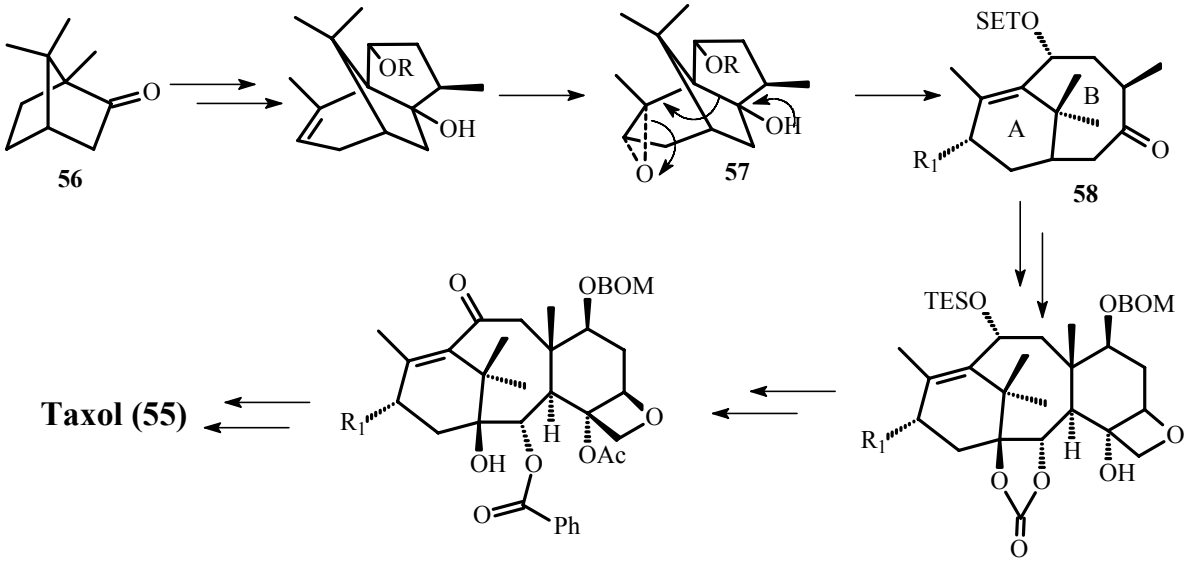

Scheme 15: Total synthesis of taxol according to the *Holton* procedure[36].

The synthetic procedure proposed by *Nicolaou*[37] includes the separate construction of building blocks corresponding to the rings A (**59**) and C (**60**) (Scheme 16), followed by their coupling. Formation of ring B and of the whole basic taxane skeleton (**61**) was achieved *via McMurry* coupling.

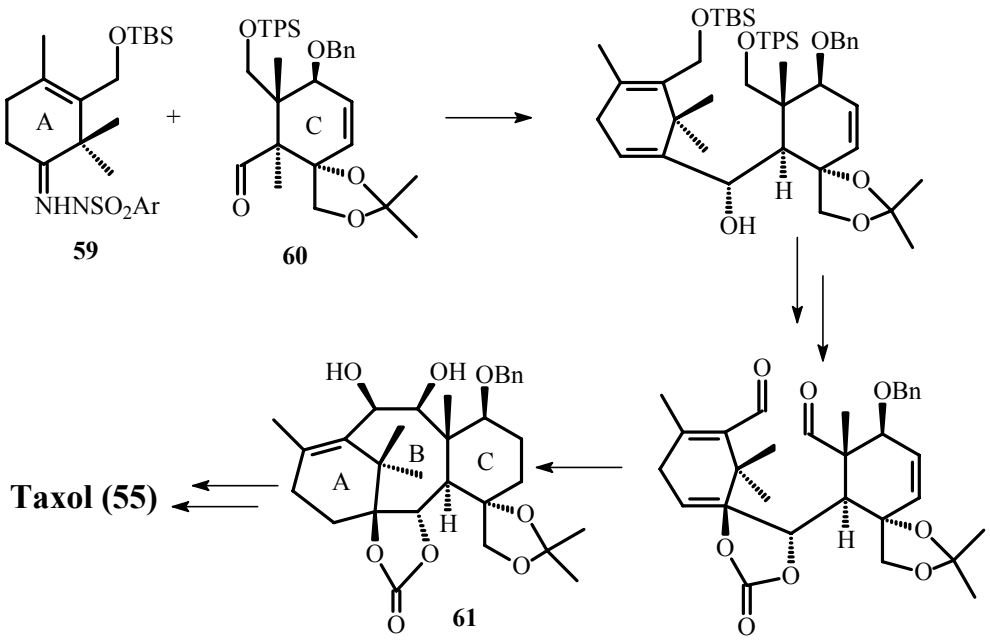

Scheme 16: The synthesis of taxol by *Nicolaou*[37].

An analogous principle of the separate enantioselective construction of rings A (**62**) and B (**63**) was also utilized by *Danishefski*[38] (Scheme 17). Unlike the previous case, the final cyclization towards the basic taxane skeleton, together with ring B formation, was performed using the *Heck* cyclization (→ **64**).

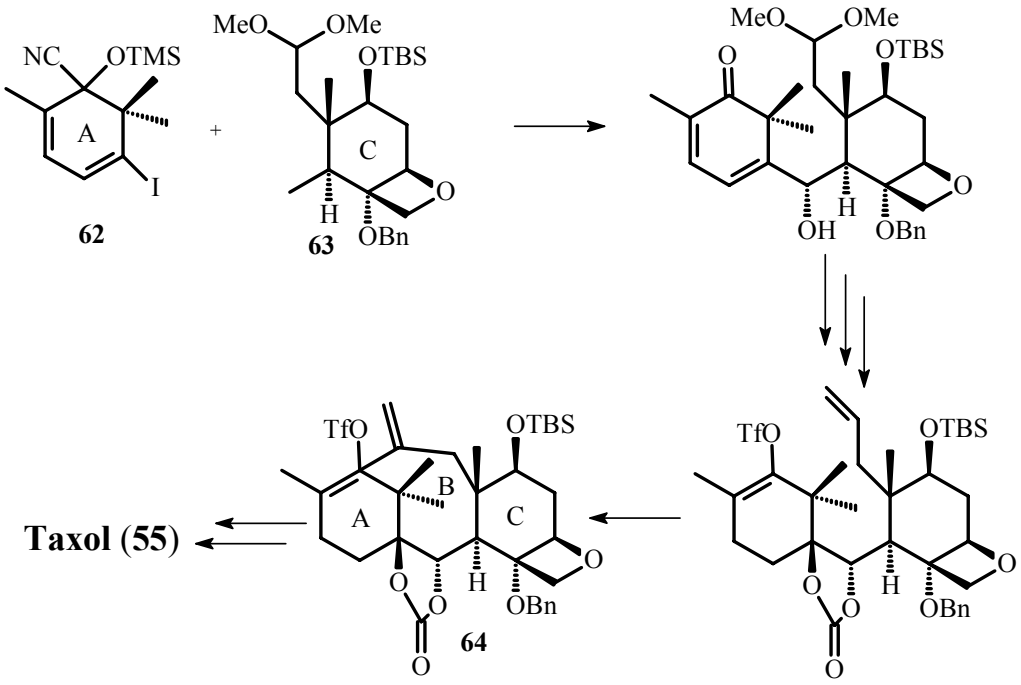

Scheme 17: The synthesis of taxol by *Danishefski*[38].

The shortest synthetic procedure was developed by *Wender*[39]; the total synthesis was performed in 37 steps. As the starting material he used the α-pinene **65** and for the ring B formation the fragmentation of the epoxide **66**.

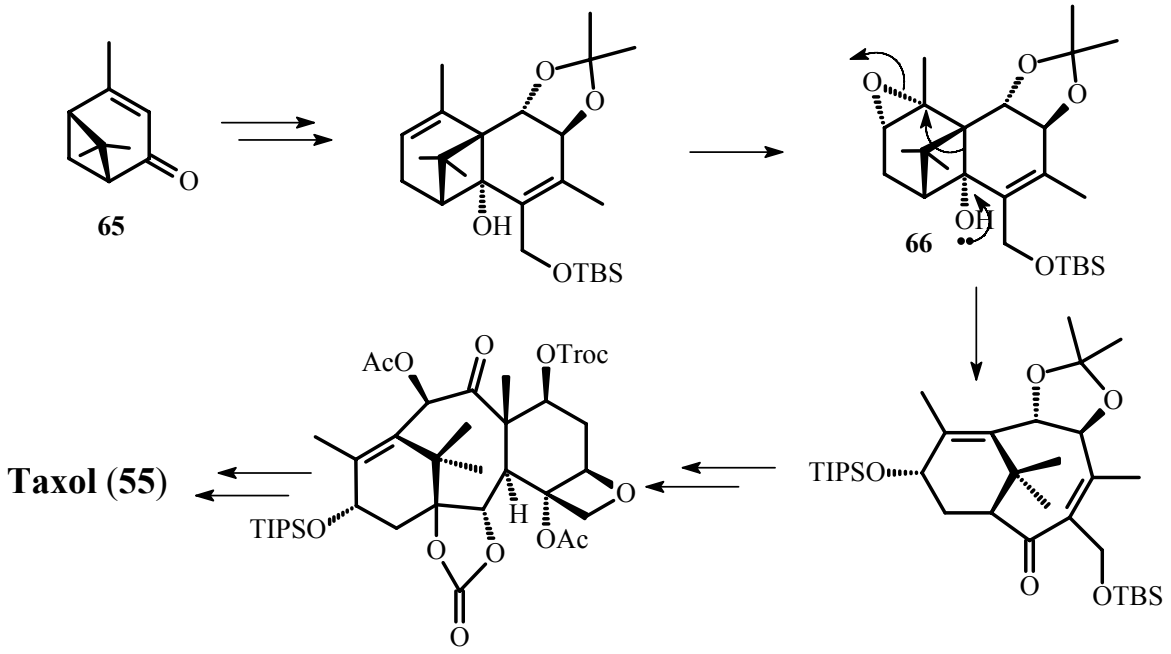

Scheme 18: The shortest synthesis of taxol performed by *Wender*.

While the synthetic strategies of *Holton* and *Wender* were linear, the *Nicolaou* and *Danishefski* approaches are convergent. There are many more synthetic strategies but they are not covered here since they do not lead to a properly functionalized skeleton.

Unfortunately, these successful synthetic procedures, even the best one, still could not be applied by the industry due to the low total yields, expensive chemicals and complicated experimental procedures. Some success was achieved in a so called semi-synthesis of taxol[40]. Few years ago half-products of taxol – baccatin III and 10-desacetylbaccetin III were found in the leaves of european trees. Now this method is applied for the industrial synthesis of taxol.

Due to taxol toxity and bad solubility in water the searching process for some taxol derivatives without these properties is still going on. Within the scope of interest are all compounds with the basic and conveniently substituted taxane skeleton. The taxol itself is a polyoxygenated complex molecule with a large number of substituents and fixed stereocentres. The importance of each substituent and pre-defined chirality on each stereocentre for anti-cancer activity was and still is unclear. There are only very few activities in this field, however, they are mostly concentrated on the role of substituents[41]. Therefore, the question concerning the importance of preserving the basic taxane skeleton is until now not answered. On the other

side resolving of this issue could simplify and support the experimental search for new, potentially more simple and maybe more powerful anti-cancer drugs.

In spite of relative progress in the synthesis of basic taxane skeleton, the elegant, short and cheap synthetic pathway is still a viable and challenging topic in actual synthetic organic chemistry. The problem could be formulated as follows: Firstly, a simple synthesis of a large number of polysubstituted pro-taxoid structures with possible application towards the total synthesis and secondly, combinatorial search for more simple structures with high biological activity should be achieved. It is also necessary to create a database of the molecules defining importance of the functional groups, increasing the solubility in water and possibly developing stronger and more universal drugs.

The work in this field started in our work group recently, first by *Straeubig* and *Eiblmeier*. In Scheme 19 [2+2] photocycloaddition, followed by opening of the cyclobutane in the [2+2] cycloadduct by a retroaldol reaction was assigned as the key step (**67→68**). The following work (Scheme 20) focused on application of the recently developed methodology involving the photochemical oxa-di-π-methane rearrangement (**70→71**). Unfortunately, both of the approaches were unsuccessful.

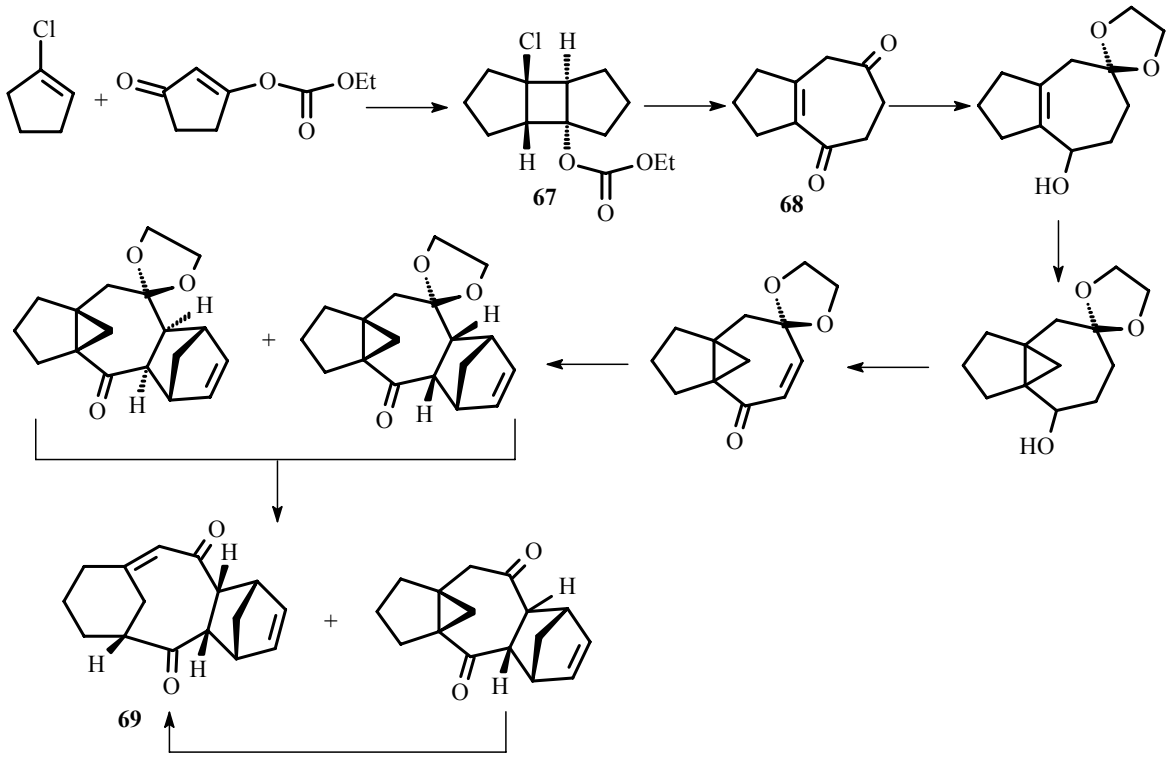

Scheme 19: The *Straeubig's* synthetic strategy[42].

Although, in the first case a product with a skeletal arrangement being similar to the basic taxane skeleton (**69**) was obtained, the further derivatization of the product and the examination of biological activity were not undertaken. The second attempt failed to produce a taxane-like skeleton. It should be noted, however, that enantioselectivity was achieved successfully and for the first time in the initial *Michael* addition with a 1,3-cyclopentadion-2-carboxylate.

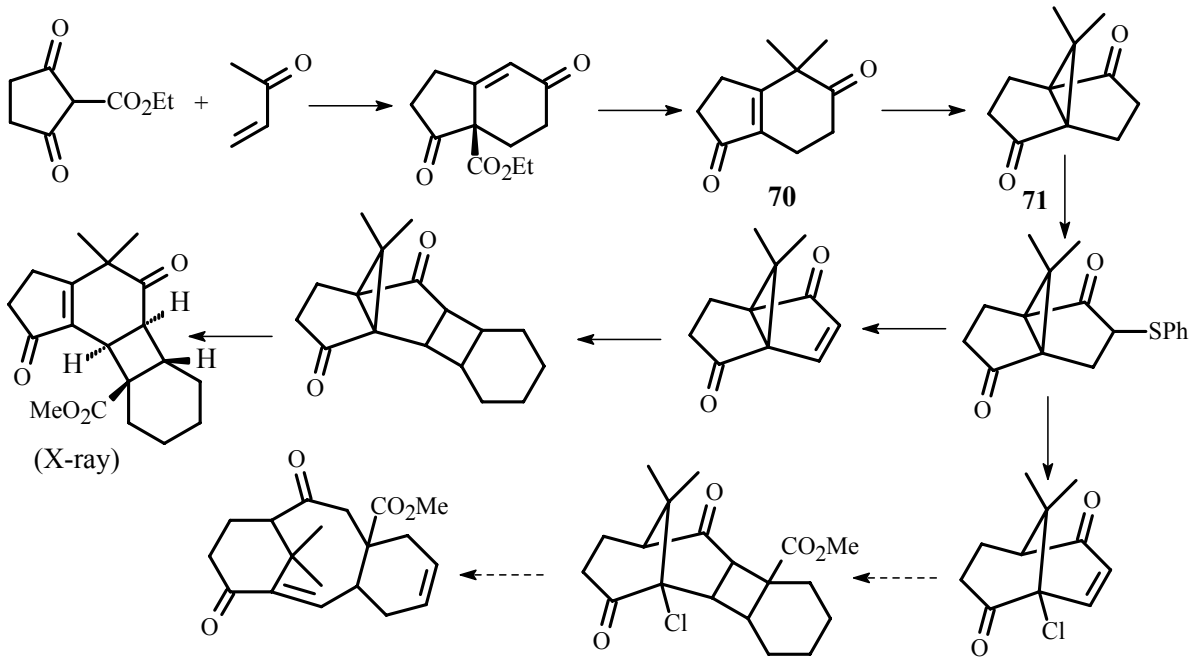

Scheme 20: Synthetic strategy of *Eiblmaier*[43].

More recent work has been established by *Goeller*[30] (Scheme 21). In this case the synthetic procedure implies a linear construction of the precursor **72** for two planned cyclizations, a PET-initiated and a Lewis-acid-induced cationic cascade cyclization.

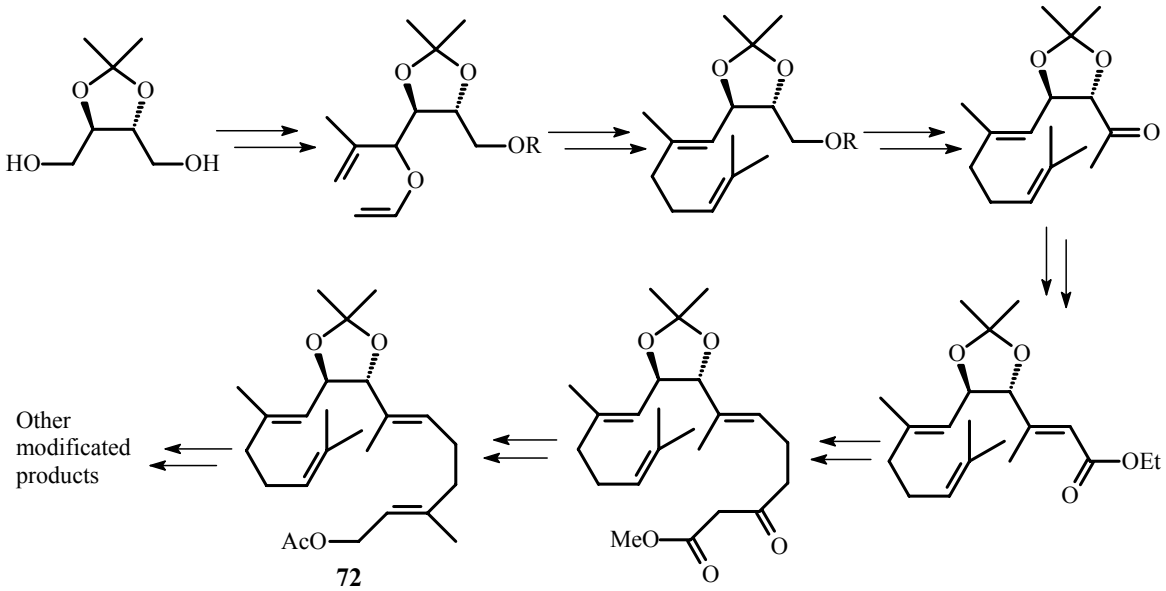

Scheme 21: *Goeller's* synthetic strategy toward the basic taxane skeleton.

Although the project was designed in a linear fashion and not convergent, which is not optimal from a the retrosynthetic point of view, the undisputable advantage of this approach was the introduction of two fixed chiral centres at the beginning of the synthetic pathway. This work was unfortunately stopped at the cyclization stage.

We can anticipate that the substrate **72** would most likely arrange, in non-folded conformation, even in polar solvents, due to the cyclic acetale protecting group giving rise to a biomimetic conformational folding of the chain (Scheme 21). However, no attempts to perform the conformational analysis of this substrate were yet undertaken. The linear synthetic strategy (about 15 steps) is also not an optimal solution for the synthesis of the crucial precursor **72** for the biomimetic-type cyclization(s).

The project initiated by *Goeller* was taken as a principal line for the present work. In the following chapters the improvement of the synthetic and methodological approach including challenges in cyclization attempts will be discussed.

3. Results and discussions

3.1 Our own synthetic, biomimetic approach toward the basic taxane skeleton

The previous attempts using well studied PET-induced cyclization have failed and investigations in this field were stopped for some time as was mentioned before. In order to solve the problem with the substrate construction, the work initially concentrated on the development of the new and simple pathway to the desired substrates for final cyclization to complete the basic taxane structure. In the following chapters the general concept of the substrate construction for cyclizations toward the basic taxane skeleton will be described. Furthermore, a synthetic strategy using new synthetic methodologies will be discussed, including computational calculations of minimized conformations of **73**.

3.1.1 General concept for the synthesis of substrates of type 73

According to the general principles of retrosynthetic analysis[44], the synthesis of the target molecule must be as simple as possible. Furthermore, it should be efficient and cheap. During the construction of big and complex molecules the synthetic strategy must be neither sequential or linear, but branched within reasonable limits.

Because of the fully sequential synthesis of the previously studied and described substrate for biomimetic cyclization toward the taxane skeleton, it was decided to change completely the synthetic strategy too. The retrosynthetic reflections are depicted in Scheme 22.

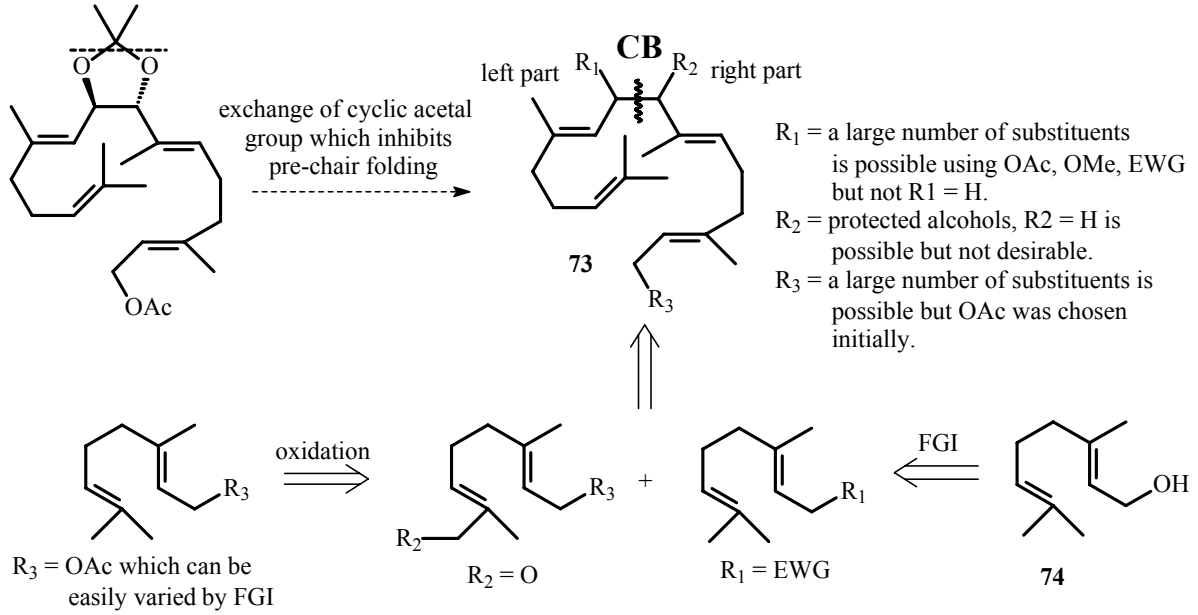

Scheme 22: General retrosynthetic concept toward the basic taxane skeleton.

The synthesis of the target intermediate **73** is now branched and can be obtained using geraniol (**74**) as a starting material. For both parts of the target molecule numerous variations of R_1 and R_3 are possible, this being possible before and after combination. Chirality control is also possible during combination of both geranyl derivatives to **73** or after that. In the first case it can be done by means of chiral metal complexes in catalytic or stoichiometric amount or using chiral auxiliaries. In the second variation it can be achieved by the oxidation of alcohol **73**, followed by enantioselective reduction. The EWG-group R_1 can also be transformed into other groups in enantiomeric pure form by means of common chemical transformation.

The most important problem in this strategy concerns the control of conformation in the substituted geranylgeraniol substrate **73** prior to cyclization(s). This can be achieved by the size and bulkyness of R_1 and R_2. Bulky R_1 and R_2 groups will favor biomimetic pre-taxane conformations, such as the one represented by **73**. If however, one of these substituents is smaller, free rotation around the central σ-bond (**CB**, Scheme 22) becomes more important and all-chair pre-folded conformations will predominate rendering the desired pre-taxane arrangement **73** unlikely. To learn more about these conformational aspects and requirements quantum mechanical calculations have been performed (see Chapter 3.4).

The R_3 group was initially chosen to be an acetate in order to reproduce previous work with similar substrates. Depending on the purpose, this group can be changed to an EWG or an electron donating group. This aspect will be discussed later.

3.1.2 The choice of protecting groups R_1, R_2, R_3

Some promising protecting groups which we planned to introduce are discussed. To prove the correct choice of such groups in terms of photochemical reactivity, a few model compounds were synthesized (**78**-**84**) and tested toward the desired photochemical oxidation of the terminal double bond[45].

The choice of the protecting group R_1 is discussed in the first place. It was decided to use the sulfone group due to the simple and efficient synthesis of such derivatives together with sufficient electronegativity of the sulfone for the following alkylation step. Furthermore, the sulfone group can be easily altered into a variety of other protections. The most attractive property of this group is its easy removal by reductive elimination or nucleophilic substitution[46].

As group R_2 an aldehyde was chosen. The reason was the ease of synthesis of such an aldehyde **79** from commercially available geraniol (**74**) or geranyl acetate (**77**). Another advantage of the aldehyde group is the formation of the corresponding alcohol **78** after alkylation. This gives the possibility to convert the alcohol into other functional groups or protect it to give a large number of derivatives. Functionality at this position as well as at the neighbor position R_1 is of extreme importance for the stabilization of the pre-taxane conformation **73** as discussed before. Another important task of the substituent R_2 is to control the photoreactivity of the neighboring double bond. It is important first to prevent this bond from photooxidation and, after formation of rings A and B of the basic taxane skeleton, to reactivate it easily. For this purpose several oxygenated geranyl acetate derivatives were synthesized including **78**-**84** and the model compounds **75**-**77** were purchased to check their reactivity toward photochemical oxidation in presence of with DCTMB/BP or NMQ·PF6/BP[31]. This research was accompanied by CV measurements.

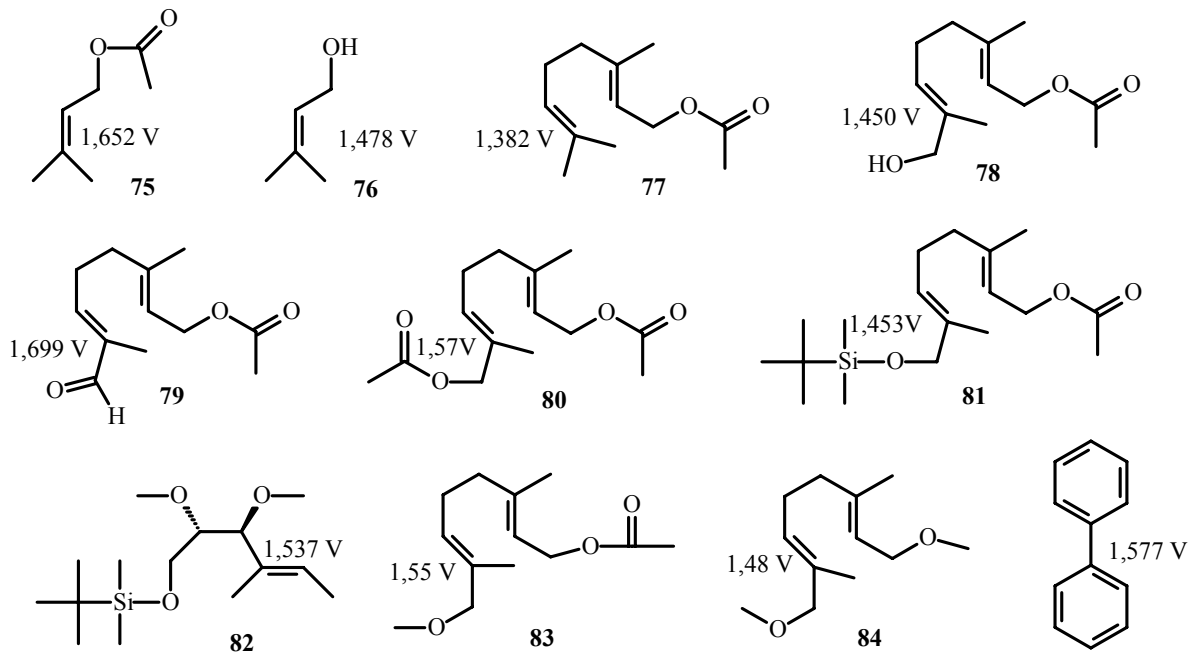

Figure 7: Oxidation potentials of test molecules **75-84** *vs* ferrocen[45].

These test compounds (**75-84**), exhibiting oxidation potential lower than BP, were successfully oxidized by DCTMB/BP as electron acceptor pair. Compounds with oxidation potentials higher than biphenyl were inert toward photooxidation. This study shows the relative tendency in changes of the oxidation potential depending on neighboring groups hence allowing in the future to use such arrangements of functionalities as protecting groups against photochemical electron transfer-triggered oxidation.

The third group R_3 we considered here to use initially as an acetate derivative. This group is the most common one for substrates for PET-induced cyclizations studied before. An allylic acetyl group deactivates the neighboring double bond completely towards photooxidation (see for example compounds **77** and **78**). Furthermore, with allylic acetate in hand one could conveniently study the cationic type of cyclization of substrates based on **73** (see Scheme 22) for an access to the taxane skeleton (for detailed discussion of the strategy, see chapter 3.1.5, Scheme 31).

In principle it is possible to introduce a number of electron withdrawing groups at position R_3 (compound **73**, Scheme 22). The presence of an EWG-group at this position together with the introduction of an epoxy group at the terminal double bond (left part of **73**) makes it possible to investigate also anionic-types of cyclizations (for detailed discussion of the strategy, see chapter 3.1.5, Scheme 32).

3.1.3 Synthesis of potential pro-taxoid substrates for cationic cyclization

According to the proposed synthetic strategy, presented and discussed before (see the chapter 3.1.1), the synthesis of test compounds for biomimetic cyclizations was realized. We started from geraniol (**74**) for the left part of **73** and with geranyl acetate (**77**) for the right part of **73** (Scheme 22). Both starting materials are cheap and commercially available.

3.1.3.1 Synthesis of geranylphenyl sulfone 86

The synthesis of the building block **86** from **74**, representing the **left part** of **precursor 73**, is outlined below (Scheme 23). It was performed with 70 % yield in 2 steps. Bromide **85**, synthesized from geraniol (**74**), was not purified and directly used for the next step (**85** is also commercially available). However, since **85** is very unstable its fresh preparation and use without purification is recommended. Its transformation to **86** is achieved with sodiumbenzene sulfinate at room temperature for 24h in the dark.

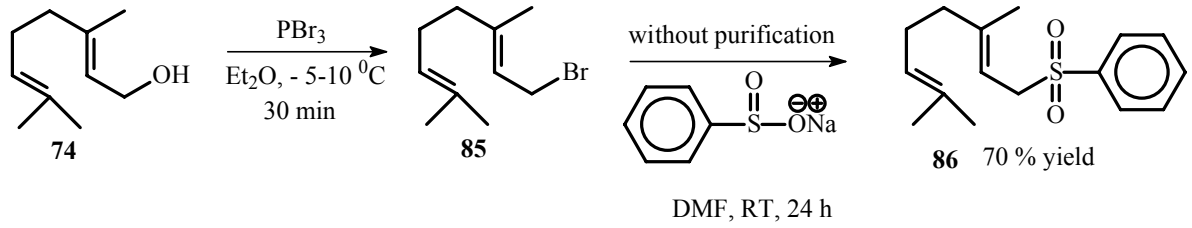

Scheme 23: Synthesis of geranylphenyl sulfone **86**[47].

3.1.3.2 Synthesis of aldehyde 79

The aldehyde **79**, representing the **right part** of **precursor 73**, was synthesized by allylic oxidation of **77** with selenium dioxide in 95 % in refluxing ethanol. In this case the conversion is about 60 % and the ratio of alcohol **78** and aldehyde **79** is 1 to 1.8.

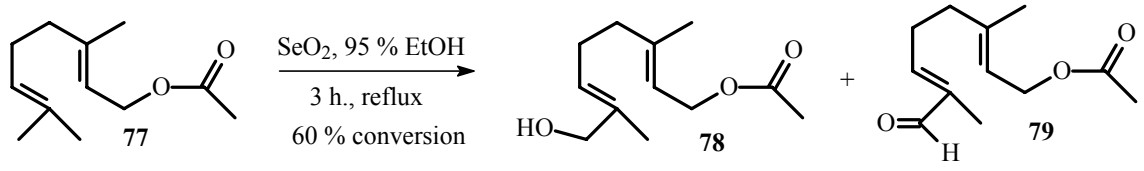

Scheme 24: Synthesis of aldehyde **79**.

It should be noticed that during this reaction some selenious by-products are formed and were present in small quantities even after purification by chromatography. Additionally the alcohol **78** can be oxidized to an aldehyde **79** by a number of procedures with nearly quantitative yield. However, this has not been done in this work. The alcohol was used for other purposes, like the synthesis of previously described model compounds (Chapter 3.1.2, Figure 7).

3.1.3.3 Coupling of geranylphenyl sulfone 86 with aldehyde 79 to give alcohol 87

The coupling of **86** with **79** was carried out using *n*-BuLi as a base in absolute THF as solvent. This reaction proceeds smoothly with about 80 % yield. After quenching of the reaction with saturated NH_4Cl solution, two diastereomeric alcohols resulted in a ratio of 3.5:1 (*R,R* : *R,S* according to the literature data[48]). All attempts to improve the yield by using complexing agents for anion stabilization, like DABCO, led to improvements of 3-5 % only[49]. Taking the more difficult product isolation and costs of the chemicals into account, such efforts are unsatisfactory and all other attempts to improve the yield were stopped too. For characterization purposes the alcohols were isolated. It is also possible to quench the reaction with different halides or chloranhydrides to obtain "*in situ*" protected alcohols[48].

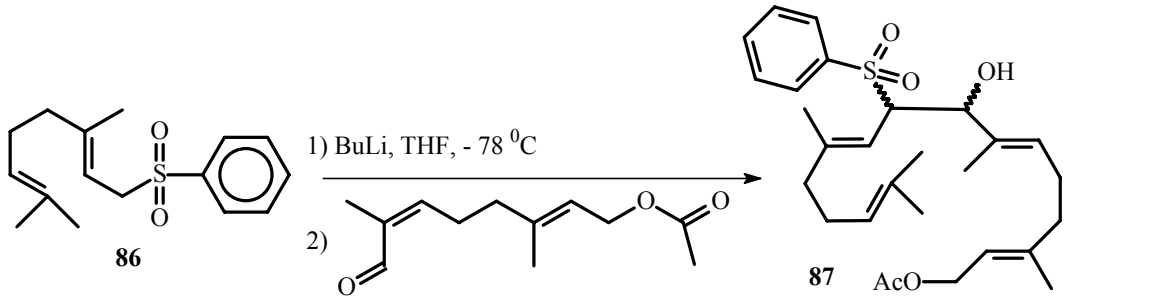

Scheme 25: Synthesis of alcohol **87**.

3.1.3.4 Protection of alcohol 87 with a benzoyl group

Finally, the alcohol **87** was protected. As was previously discussed, the protecting group must be bulky to prevent conformational rotation around the central σ-bond. The benzoyl group was initially tested as the most straightforward approach. Using benzoyl chloride it is possible to introduce this group "*in situ*" during the coupling reaction. In the present case, for

analytical purposes, the reaction was performed using alcohol **87**, benzoyl chloride and pyridine in dry dichloromethane. Nearly quantitative yield (95 %) of benzoyl-protected alcohol **88**, as a mixture of two diastereomers, was achieved (Scheme 26).

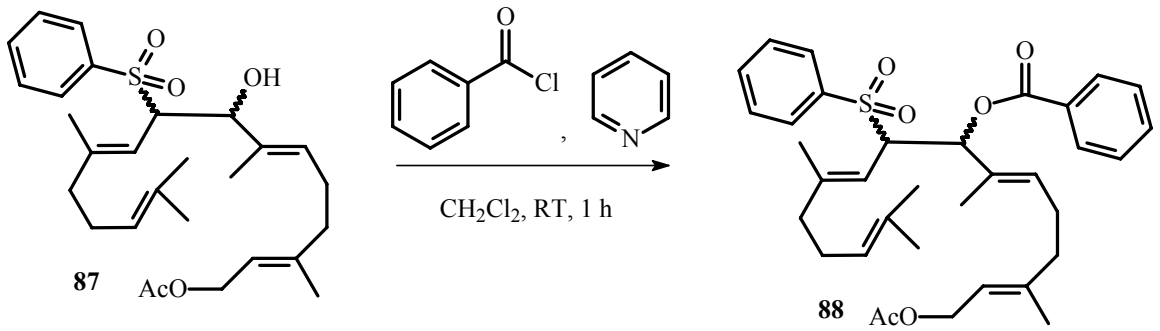

Scheme 26: Synthesis of benzoyl-protected alcohol **88**.

This sequence of reactions results in very similar products, in comparison to precursors previously synthesized by Goeller[30]. Notably, it would be possible to introduce chirality at this stage of the synthesis using cheap materials and in a few steps only.

3.1.3.5 Protection of alcohol 87 with a *tert*-butyl group (→87a)

Quantum mechanical calculations provided important information about stabilizing of non all-chair pre-folded conformation of acyclic substrates for ionic cyclization to the taxane skeleton in presence of *tert*-butyl ethers (see Abstract, Chapter 3.4, Chapter 5.7). In order to test the practical availability of such *tert*-butyl protected alcohols, the alcohol **87** was derivatized using trichloroacetimidate and a catalytic amount of boron trifluoride etherate in cyclohexane/dichloromethane mixture. The method works well for primary, but usually less efficient for secondary alcohols. The target ether **87a** was isolated in a yield of 45 % which is compared with other examples more than satisfactory.

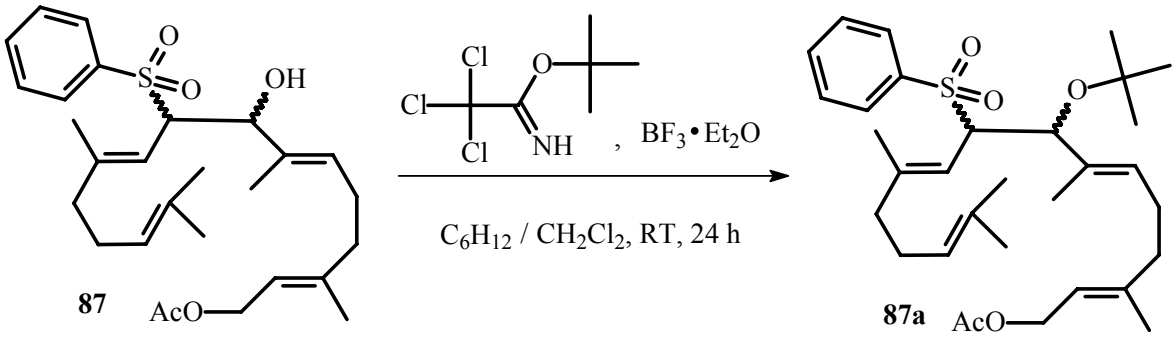

Scheme 26a: Protection of alcohol **87** with a *tert*-butyl group.

3.1.4 Synthesis of potential pro-taxoid substrates for anionic cyclizations

Using an identical experimental approach, as described in chapter 3.1.3, a similar slightly modified procedure was applied for the synthesis of acyclic precursors of type **73** for anionic cyclization to the taxane skeleton.

3.1.4.1 Synthesis of aldehyde 89

The synthetic pathway includes the synthesis of previously described sulfone **86**. One part of the product was then oxidized by selenium dioxide to the aldehyde **89** (Scheme 27). The synthesis was carried out according to the modified Sharpless procedure and results in even better yield[50] than previously described. The oxidation of geranylphenyl sulfone **86**, using 5 mol % of SeO_2, 10 mol % of 4-hydroxybenzoic acid and 3.6 equiv. of *tert*-butyl peroxide in dichloromethane results up to 80 % of aldehyde **89**. In the present case the corresponding alcohol was present in very little amounts and was not isolated. An alternative way to the product was proposed employing the allylic oxidation of TBDMS-protected geraniol with subsequent deprotection and introduction of an EWG-group. Unfortunately, attempts to perform allylic oxidation according to old and modified procedures of either geraniol or TBDMS-protected geraniol have failed and have resulted in a very complex inseparable mixture of many products and a low yield of the target substance only.

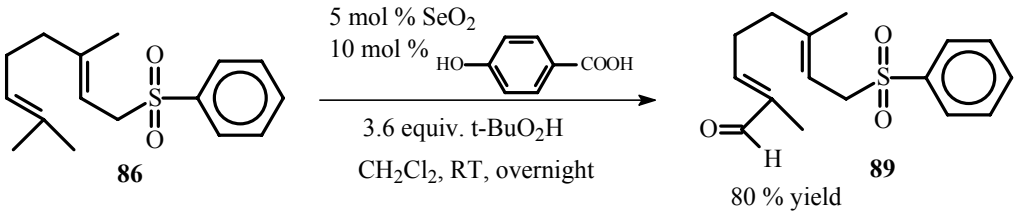

Scheme 27: Synthesis of oxygenated sulfone **89**[50].

3.1.4.2 Alkylation of geranylphenylsulphone 86 with aldehyde 89 to alcohol 90

The following alkylation step was similar to the above described coupling of **86** in chapter 3.1.3.3. The reaction was done in absolute THF using *n*-BuLi as a base and results a combined yield of 80 % of alcohol **90**, being a mixture of two diastereomers.

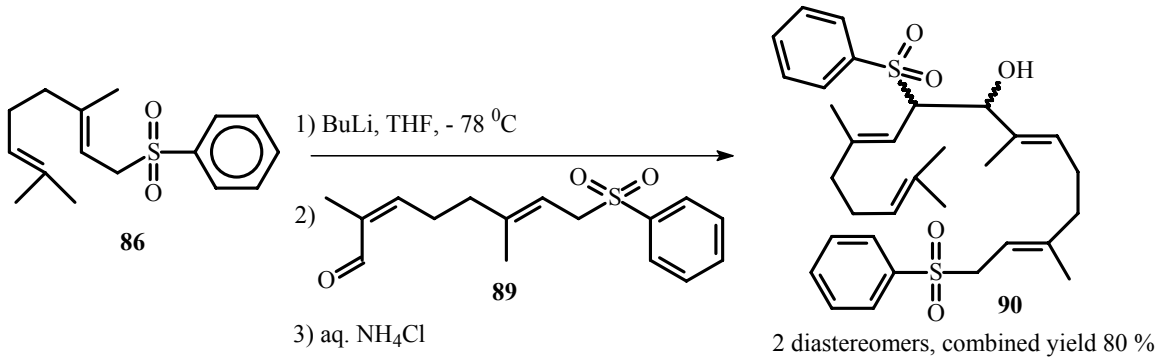

Scheme 28: Synthesis of the precursor to the taxane skeleton for anionic cyclization.

3.1.4.3 Protection of alcohol 90 with a benzoyl group

The following step, protection of the alcohol **90**, was identical to the previously described one in chapter 3.1.3.4 and proceeds nearly quantitatively with benzoyl chloride as a protection group (Scheme 29). As was shown in chapter 3.1.2 the presence of ester groups in allylic position to the double bond leads to the deactivation of this double bond toward the PET-initiated oxidation. In contrary, the presence of alcohols in the same position slightly increases the oxidation potential of the corresponding double bond. Such protection groups are easy to introduce and easy to remove. This was an additional reason for the choice of a benzoyl protecting group.

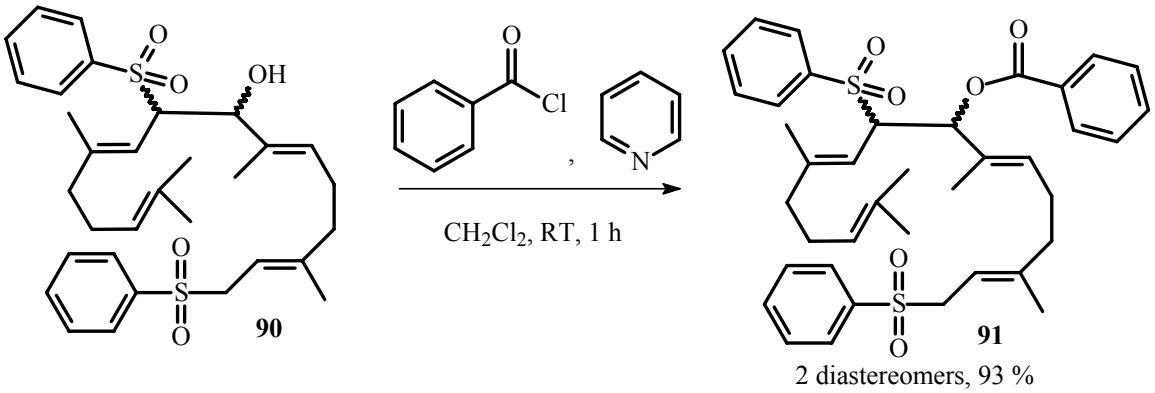

Scheme 29: Synthesis of protected alcohol **91**.

3.1.4.4 Epoxidation of 91

The final step in this synthetic sequence is the selective epoxidation of the terminal double bond. The reaction was performed using *m*-chlorperbenzoic acid (MCPBA) in dichloromethane and it results in selective epoxidation of terminal double bond of **91** (→ **92**) with a yield of 90 %. In spite of the presence of three additional double bonds, only the terminal one is reactive toward the oxidation and no other by-products were detected.

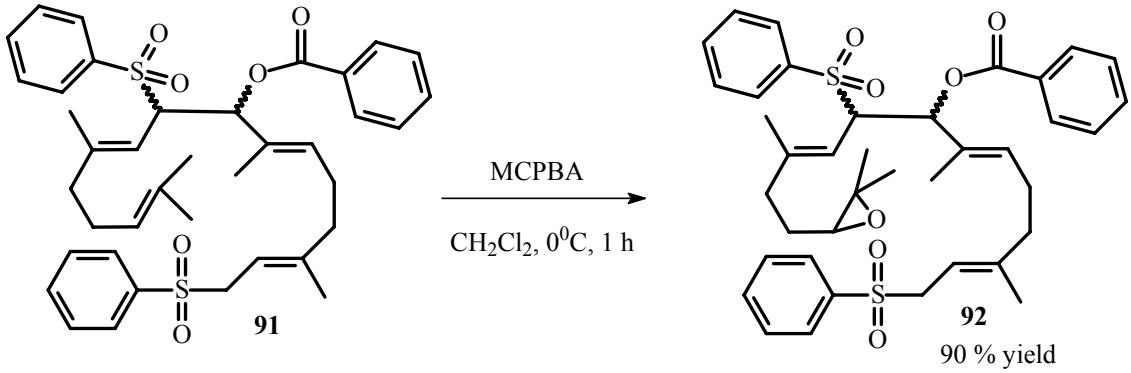

Scheme 30: Synthesis of epoxide **92**.

The strategy for the application of the acyclic precursors to the taxane skeleton in cationic, anionic and PET-initiated cyclizations will be discussed in the following chapters.

3.1.5 Unsuccessful attempts toward cationic and anionic macrocyclization

In this chapter the general concept for the planned cationic and anionic cyclizations will be discussed. Both concepts include macrocyclization with formation of ring A and macrocyclic precursor for rings B and C of the target skeleton. As was already formulated above for the cationic cyclization attempts, the first step should be the heterolytic substitution of the acetate group or other good leaving groups R_1 (see Scheme 31) like tosylate or mesylate, forming an allylic cation. Next would be the two-step cascade cationic cyclization which starts by ring A formation. It is anticipated that the resulting tertiary cation in ring A undergoes elimination or nucleophile (Nu_1) addition. For the formation of the rings B and C we propose to use the deprotected allylic alcohol having R_2=H to decrease the oxidation potential of the double bond of this moiety. Finally, the oxidative PET-induced cyclization should form rings B and C and hence the basic taxane skeleton **93** including addition of another nucleophile (Nu_2).

For the anionic cyclization (see Scheme 32) it is important to have an acceptor group R_1 in order to facilitate the stabilization of an adjacent anion which then will electrophilically attack the epoxide at the tri-substituted position to yield a tetrasubstituted alkoxide intermediate[51]. The alkoxide will be used after protonation as a leaving group to give rise to ring A formation together with the macrocyclic rings B/C precursor. Rings B and C will then be formed as previously described for the cationic pathway (Scheme 31).

For both, the cationic and anionic pathways, the conformational control on the stage of the macrocycle formation is most important deciding on a positive outcome of these two strategies based on the use of nearly the same precursors.

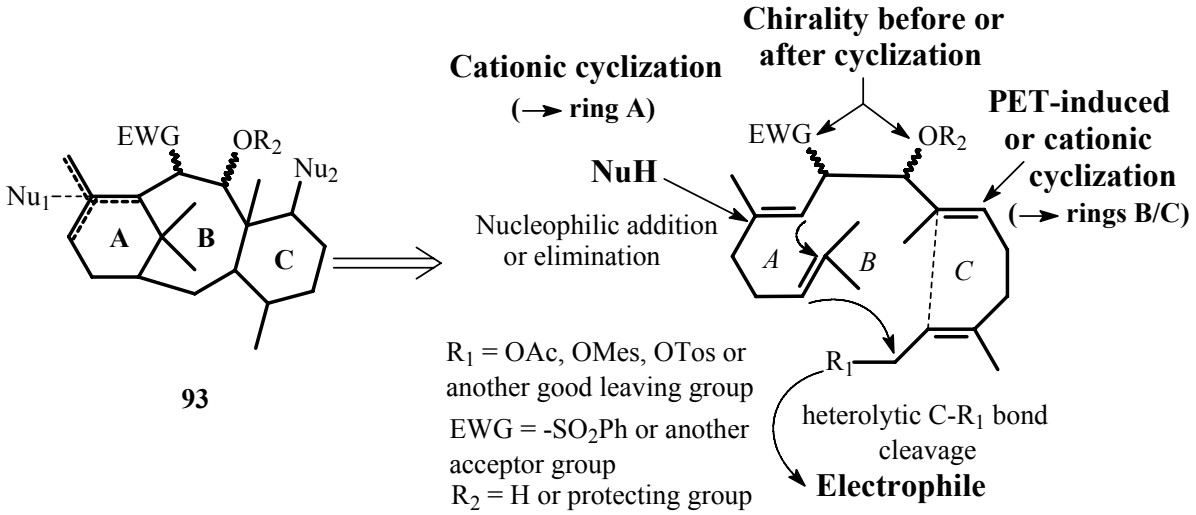

Scheme 31: Proposed strategy for the cationic pathway to the taxane skeleton.

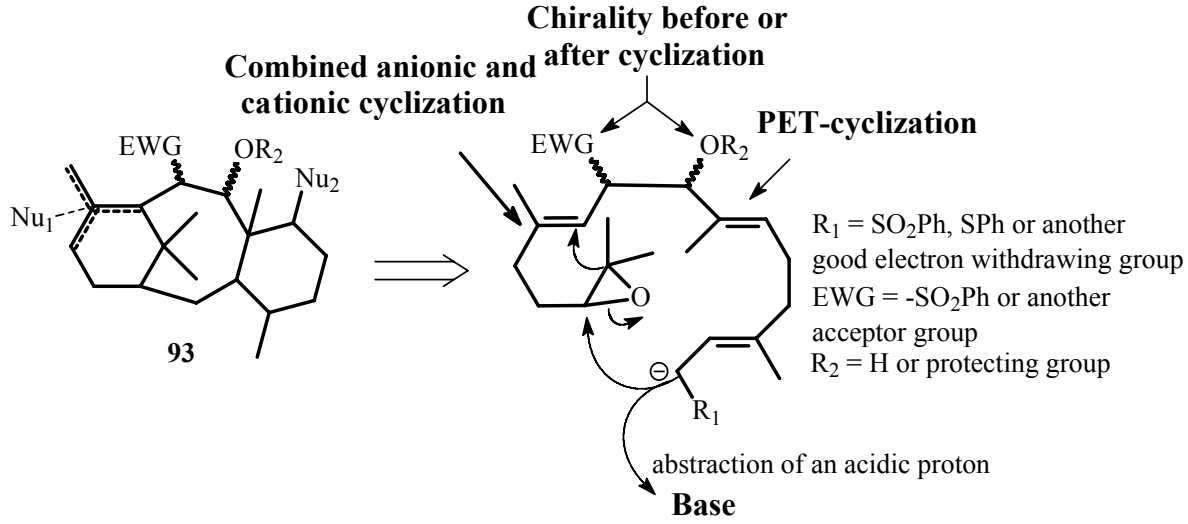

Scheme 32: Proposed strategy for the anionic pathway to the taxane skeleton.

3.1.5.1 Cyclization attempt using BuLi and LDA

First attempts aimed at the anionic synthetic strategy. For this purposes the synthesized substrate **92** was submitted to potential anionic cyclization conditions using both LDA and BuLi[51]. Both reactions were performed at –78 ^{0}C which must be sufficient for the anion stabilization and minimization of conformational rotation. Unfortunately, the only products obtained were the products of substrate decomposition depicted below (Scheme 33). It seems that the terminal benzenesulfonyl group is acidic enough. However, it also well stabilizes the anion and makes it much less reactive. Another problem is that the CH-group close to benzoyl-protected alcohol seems to be attacked during this reaction which leads to the decomposition of the substrate.

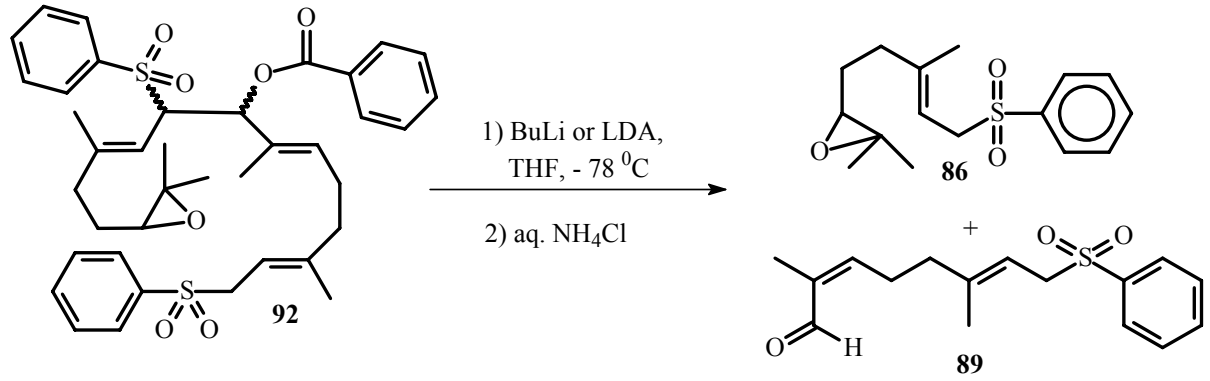

Scheme 33: Decomposition of the substrate **92** during cyclization attempts.

A possible solution for this problem could be substitution of the benzoyl group by a bulky group, such as *tert*-butyl, which could therefore be inert to bases. Another improvement can be the reduction of the benzenesulfonyl group in the right side chain to the corresponding thioether before coupling. Although the thioether has lower acidity in comparison with the benzenesulfonyl group, it has a higher reactivity which is needed for this reaction.

Finally, before synthesizing more substrates for the crucial cyclization to the taxane skeleton, a conformational analysis should be performed (see chapter 4).

In the following attempts to perform cationic-type of cyclizations, the substrate **88** was chosen for this purpose. Additionally, BF_3-etherate and trifluoroacetic acid were taken as (Lewis) acid agents to initiate macrocyclization.

3.1.5.2 Cyclization attempt using CF_3CO_2H

In order to diminish the side reactions and allylic rearrangements, the reaction was initially performed in CH_2Cl_2 at low temperature; the –78 to –40 ^{0}C temperature range turned out useless for this purpose since crystallization of trifluoroacetic acid was observed. The optimal balance between crystallization of trifluoroacetic acid and low temperature was achieved at –20^{0}C. Unfortunately, no reaction was observed even after 6 hours.

In further attempts the mixture was warmed up and finally was allowed to be refluxed for 6 hours. In all cases only two products were isolated with varying yields, this being temperature dependent. However, no cyclic or polycyclic products were detected in the mixture. Isolated products derived from the addition of CF_3COOH to the terminal double bond (→ **93**) which is also accompanied by a product derived from acetate cleavage upon work up (see **94,** Experimental part).

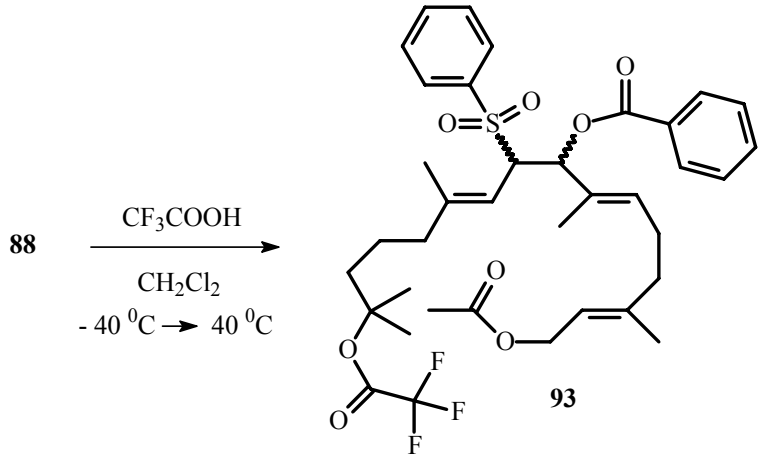

Scheme 34: Attempt to cyclize **88** using trifluoroacetic acid (→ **93**).

3.1.5.3 Attempt to cyclize 88 with $BF_3{\cdot}Et_2O$

For the work described below the same logic as before was used. Namely that the low temperature should stabilize the formed cation and decrease the conformational rotations of the substrate preventing undesired side products.

The reaction was initially tested using the same substrate **88** as in the previous case and nearly equimolar amount of $BF_3{\cdot}Et_2O$ in dichloromethane at –78^{0}C. Unfortunately, according to the TLC control, no changes in the reaction mixture were detected even after 5 hours. Slowly increasing the temperature up to –40^{0}C shows changes and formation of products (TLC

control). Quenching of the reaction and isolation of the products shows the absence of any cyclic or polycyclic products. Attempts to investigate the structure of the product(s) failed. We only learned that cleavage of the acetate group through the $BF_3 \cdot Et_2O$ occurs followed by rearrangements without formation of cyclic products.

The following reasons could be responsible for the failure of the attempted macrocyclization: The correct conformation(s), required for successful macrocyclization is (are) seemingly present in solution in a too low concentration only which may derive from temperature and solvent polarity effects. Furthermore, the substituent pattern of the acyclic substrate may be of crucial importance and has to be investigated in more details in the future.

A further topic in this field concerns the use of mild and catalytic reaction conditions which should beneficially lead to enantioselective processes. Our approach in this direction is outlined in the following chapter 3.2.

3.2 PET-induced cyclizations in presence of Cu(II)-acetate

3.2.1 Use and role of Cu(II)-acetate in PET-induced cyclizations

The previous investigations that include as the key step macrocyclization of an acyclic precursor of the type **72**, synthesized by *Goeller*[30], raised several questions and the major problems remain still unsolved, such as the adjustment of proper conformations of the acyclic precursors in decent concentration enabling successful macrocyclization.

As was discussed above, a further possible reason for unsuccessful cyclizations of **72** and analogous test molecules are likely sterical problems concerning the termination step. In Figure 8 the proposed termination step of the cyclization of geranyl acetate (**77**) and analogues thereof is outlined: In case of geranyl acetate (**77**), the transfer of an electron from the acceptor radical anion to the tertiary radical centre in **A** is likely inhibited from the top by 1,3-interaction with an axial methyl group as depicted. The analogous termination step from the bottom side of **A** (→ **B**, Figure 8) is according to spectral evaluation of the product preferred[24]. In case of the cyclization attempts with an analogue carrying a cyclic acetal function, the major product derives from reduction of the radical centre in **C**, followed by protonation of the resulting anion thereof. Mechanistically there are two options feasible. Either the cyclization step **C**→ **D** is inhibited at all by severe steric interactions between the geminal dimethyl and the cyclic acetal group. Or the cyclization occurs (→ **D**), but the

termination step (reduction/protonation in **D**) is unsuccessful because of sterically inhibited electron transfer to **D** from the top as well as from the bottom side of this cyclic radical intermediate as depicted in Figure 8.

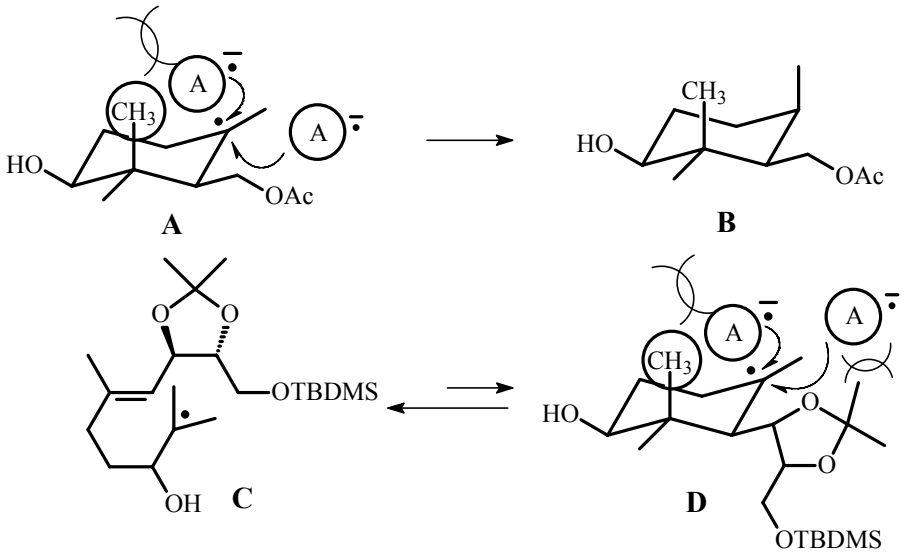

Figure 8: The proposed reactivity of mechanism for the termination steps **A→ B**, **C→ D**.

In case **C→D** the termination step should be reconsidered. The idea is to use metal salts with anions of low nucleophilicity as mild co-reductants or co-oxidants. In comparison with the large anion radical of DCTMB, the metal ions are much smaller and the steric inhibition in the termination step could be minimized.

The reductive pathway includes formation of the anion **96** (Scheme 35) by mean of a metal salt with reductive properties. The termination step in this case should be the protonation of the resulting tertiary cyclic anion **96**. The oxidized form of reductant should then react with the anion-radical of the acceptor DCTMB to re-form the neutral acceptor DCTMB and the reductant completing the catalytic cycle.

In the alternative oxidative pathway (Scheme 35, bottom), which will also be probed, the general idea to use a mild metallic co-oxidant could also be very valuable to form a cation **97** from radical **95** will also be helpful. Mild oxidation to **97** should increase the selectivity of this process and the use of counterions with little nucleophilicity should disfavour trapping of **97** and favour the cyclization process starting from this intermediate. The cyclization cascade is terminated in this case by elimination of a proton.

It is anticipated that the use of metal salts as a co-oxidant will not only lead to the cyclic products in case **C→D** but can also improve the yield in case **A→B** (Figure 8).

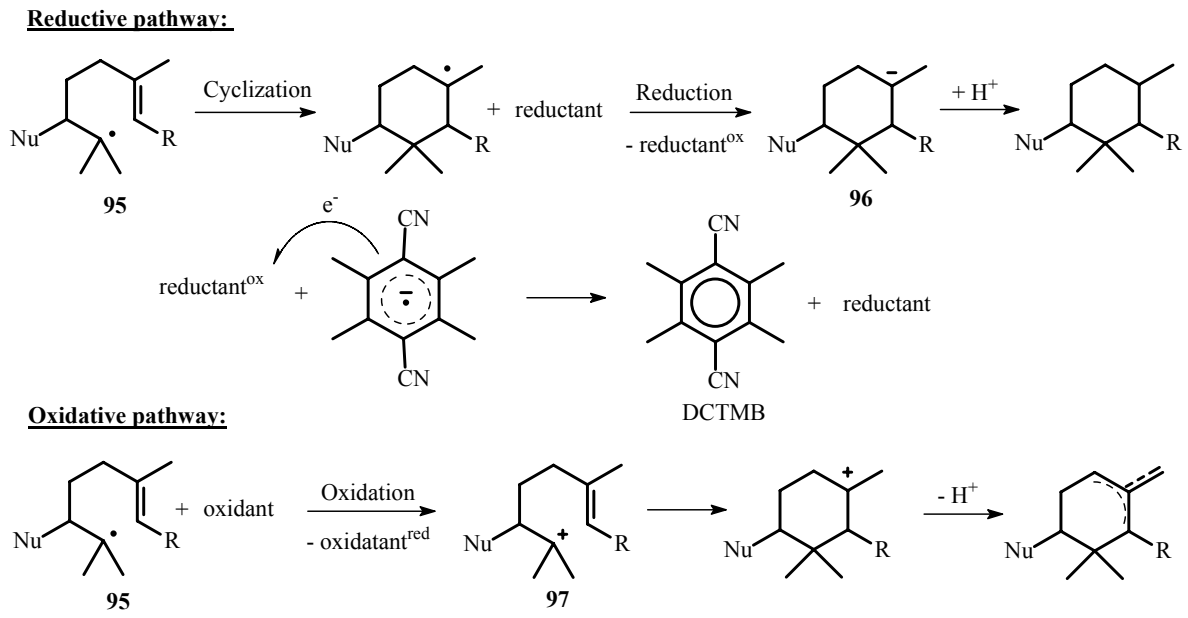

Scheme 35: Proposal for the reductive termination step of the PET-induced cyclization (top) and mechanism of cationic cyclization cascade (bottom).

Cyclovoltammetric measurements of the oxidation potentials of model compounds (see Figure 7, Chapter 3.1.2) suggest the possibility of oxidation of **78** and **81** and an improbable oxidation of **79**, **80** and **83**, due to the high oxidation potentials. In summary, in spite of the positive aspects of previous synthetic strategies the cyclic acetal group does not allow to perform the desired cyclization. At this point, not only the cyclization step but also the synthetic strategy should be reconsidered. Naturally, the absence of substituents at the marked positions (see pictures in Abstract and Table 2 and 3) will lead to both, a decrease of the oxidation potential of the neighbouring double bond and to less sterical hindrance at the same double bond. On the other hand, the removal of substituents at these positions should direct the substrate into a all-chair pre-folded conformation, especially in polar solvents. As was described in Section 2.1.2 the pro-chair conformation of the substrate for biomimetic synthesis of the basic taxane skeleton is however not desirable.

Conformational analysis and geometry optimization of the previously synthesized precursor **72** is therefore still is in the range of our interest. The results represent the most probable non-folded conformations. One of the most preferable and likely conformations is depicted in the Abstract, Cartesian coordinates and relative energies are presented in the Experimental part. In this sense substituents at marked/starred positions are definitely important for the steering of further possible cyclizations, either involving squalene-like or taxadiene-like folding. Their nature and relative strereochemistry is very important for the whole synthetic strategy, including the attempted macrocyclization.

In the following we decided to use the ability of the Cu^{2+}-salts to oxidize the radicals to cations and to reinvestigate the use and reactivity of Cu^{2+}-salts in PET-initiated cyclizations. This important property of Cu^{2+}-salts was discovered by *Heiba* and *Dessau*[52]; then it was extensively used for the Mn(III)-acetate-induced radical cyclizations, where Cu(II)-acetate plays the role of a mild co-oxidant[16]. From the literature it is known that the Mn^{3+}-salts have the ability to form radicals from alkyldicarboxilates, β-ketoesters, β-dicarbonyl compounds etc[16, 53]. The Mn^{3+}-salts posses the ability to oxidize the tertiary radicals to the corresponding cations efficiently. Primary and secondary radicals, on the other hand, are nearly unreactive. In contrast, the Cu^{2+}-salts have not the ability to form radicals but they are able to oxidize primary and secondary radicals in about 350 times faster than Mn^{3+}. Tertiary radicals are oxidized by Cu(II)-acetate almost as well as by Mn(III)-acetate. In terms of stability of the oxidant, its costs and in order to suppress side reactions it was decided to use the Cu(II)-acetate. Previous investigations of the mechanism of PET-induced cyclizations, using $CuCl_2$, were performed by *Xing*[24] and revealed the formation of an isomeric mixture of the chlorhydrins **98** and **99** as the major products besides the product of isomerization of the double bond (→**100**, see Scheme 36). A cyclic product was found in less than 1 %.

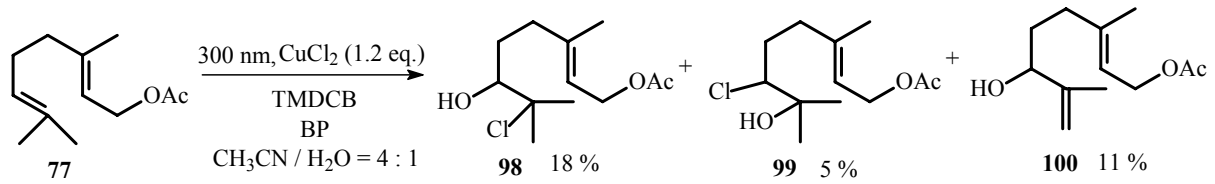

77 **98** 18 % **99** 5 % **100** 11 %

Scheme 36: Cyclization attempt in the presence of $CuCl_2$.

Literature provided the following important informations:

- Nucleophilic addition to the cation radical of the substrate promotes the oxidation of the residual radical mediated by a Cu^{2+} ion
- Oxidation of the radical intermediate has to be faster than the cyclization
- To perform cyclizations the Cu(II)-salt with non nucleophilic or at least with low nucleophilic anions should be used.

Out of this reasons Cu(II)-acetate was chosen as co-oxidant for the PET-induced cyclizations.

3.2.2 Cu(II)-acetate as oxidant in PET-induced cyclizations with water as nucleophile

Initially, the PET-cyclization reactions of different polyalkene terpenoids were tested in an acetonitrile-water mixture of 10 : 1. The reactions were performed in the presence of an

acceptor/co-acceptor pair such as DCTMB (0.2 equiv) and BP(0.9 equiv) at –20^{0}C. As substrates for the cyclization attempts geranyl acetate (**77**), geraniol (**74**) and other commercially available substrates were chosen. By changing of only one parameter in comparison with usual PET-induced cyclization procedures yields and reactivity were investigated. Another aim was to investigate the influence of temperature, solvents, solvent proportion and different types of substrates *i.e.* not only polyalkenes with terminal double bonds but also substrates with an allylic substituted terminal double bond (for a detailed description of the tested substrates see Chapter 3.1.2).

3.2.2.1 Oxidation of geranyl acetate (77)

Initial irradiation of geranyl acetate (**77**) was performed at 300 nm and has resulted in epoxide formation at the terminal double bond giving the major product **101** with a yield of 35 % (Scheme 37). However, some of the starting material has not reacted and could be recovered. The expected cyclic product **102** was also present, but in minor amounts only, much less than was usually obtained by PET-triggered reactions without a Cu(II)-salt. Two other by-products were typical for PET-reactions, the product of Markovnikov-type nucleophile addition (**103**) and the product with the *exo*-double bond (**100**).

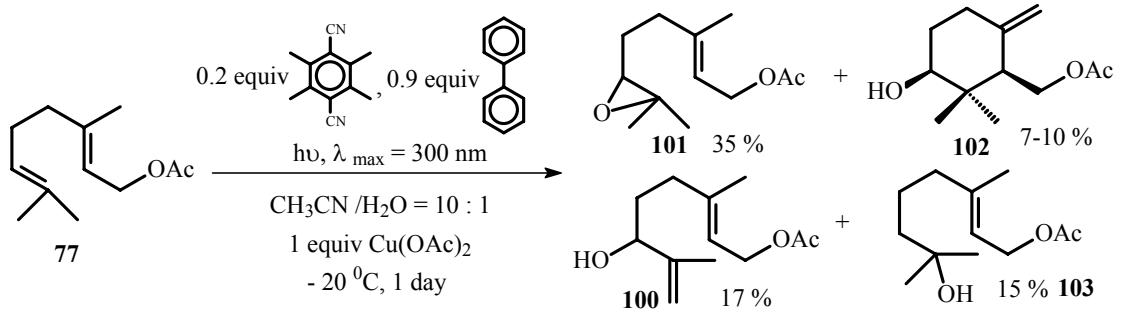

Scheme 37: Oxidation of geranyl acetate (**77**) in the presence of water as nucleophile.

Formation of the epoxide **101** is atypical for oxidative PET-reactions and was never obtained before. In terms of reactivity of a metal salt the first attempt was successful, however the yield of the target cyclic product **102** was moderate and has to be improved. Formation of the epoxide **101** was undesired. In general the product pattern and yields are in good agreement with previous results of PET-induced cyclizations without the metal salt[24].

3.2.2.2 Oxidation of the allylic alcohol 78 and of the TBDMS-protected alcohol 81

The oxidations were attempted with the allylic alcohol **78** and the TBDMS derivative **81** thereof. We also planned to investigate the possibility of intramolecular cation trapping of the cation-radical formed upon photochemical oxidation, by the allylic alcohol or the TBDMS-protected derivative to form an oxo-cyclobutane in the absence of an external nucleophile. Cyclization of substrates **78** and **81** and also 4-endo intramolecular cyclization processes have never being observed before, but would be of general interest especially with respect to a taxane synthesis.

The reactions performed under the same conditions as described in Chapter 3.2.2.1 gave the epoxides **104a, 104b** and **105** with low yields only, lower than in the case of geranyl acetate (**77**).

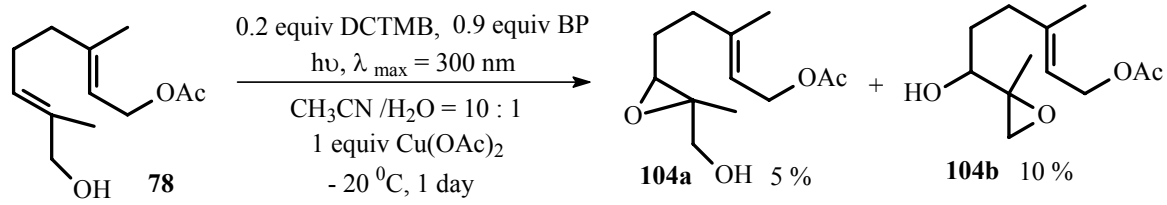

Scheme 38. Oxidation of the allylic alcohol **78**.

The cyclic product was present only in trace amounts, similarly to the case described in Chapter 3.2.2.1. The lower yield can be explained by the higher oxidation potentials of the terminal double bonds in **78** and **81** as compared to **77** (Figure 7). Furthermore, the oxidation of the same substrates in absence of a nucleophile, *i.e.* in pure acetonitrile, gives no oxo-cyclobutane products of intramolecular cation trapping by either the alcohol or the TBDMS-protected alcohol.

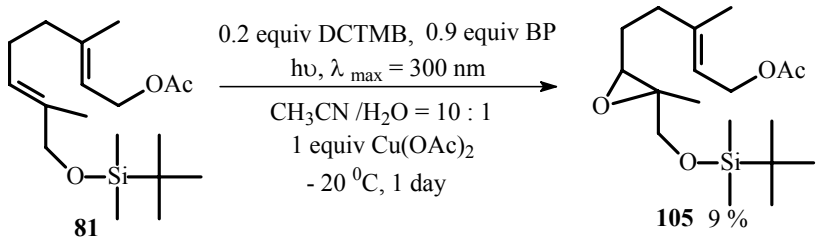

Scheme 39: Oxidation of the TBDMS-protected allylic alcohol **81**.

During these reactions the following problem appeared. The reaction vessel was completely covered with a Cu-mirror after prolonged irradiation. This actually is in good

agreement with the initial hypothesis that the Cu(II)-acetate acts twofold. Firstly with the anion radical of the acceptor and then with the radical of the oxidized substrate. However, this mirror shields the vessel from the UV-light, effectively stopping the reaction and resulting in only partial conversion. Now the problem is not only to direct the reaction to the cyclic products, but also to reduce the formation of a Cu-mirror.

3.2.2.3 Oxidation of all-*trans*-farnesol (106) in the presence of water as nucleophile and Cu(II)/Mn(III)-acetates as oxidant mixture

To solve the Cu-mirror problem the use of BSTFA, for coating the walls of the reaction vessel, was initially proposed. This strategy proved unsuccessful. In order to explore the application of this reaction and to reduce the Cu-mirror formation we decided to perform reactions in the presence of Mn(III)-acetate. A mixture of Cu(II)/Mn(III)-acetate was successfully applied in a number of reactions. In the literature examples, however concerning different reactions[16] the Cu(II)-acetate acts catalytically. It is reduced during the reaction from Cu^{2+} to Cu^{+} and than readily oxidized again by Mn(III)-acetate. During this process the Cu^{2+} and Mn^{2+} ions are formed. Cu(II)-acetate acts twofold, therefore 2 equivalents of Mn(III)-acetate are essential for solving the problem with the Cu-mirror. Furthermore, Mn(III)-acetate is able to oxidize the tertiary radical exactly as well as Cu(II)-acetate and it should therefore enhance the reaction. However, Mn(III)-acetate can participate in some side reactions, which lead to the undesired oxidations. In summary, the choice of Mn(III)-acetate for solving the Cu-mirror problem is not optimal.

Theoretically, according to the oxidation potential values, it can be any metal with an oxidation potential higher than the one for the reaction $Cu^{+} - e^{-} = Cu^{2+}$. In order to test this hypothesis, the photochemical oxidative cyclization of farnesol (**106**) in presence of 1 equivalent of Cu(II)-acetate and 2 equivalents of Mn(III)-acetate was carried out in acetonitrile-water mixture. Like the previous cases the corresponding epoxide **107** was formed. Surprisingly, the epoxide **107** was only a minor product with a yield of 6 %. The major product was the bicyclic compound **108** with a yield of 10 %. The combined yield of both products was also in good agreement with previously done usual PET-initiated cyclizations and represents the normal reactivity of the terminal double bond toward photochemical oxidation.

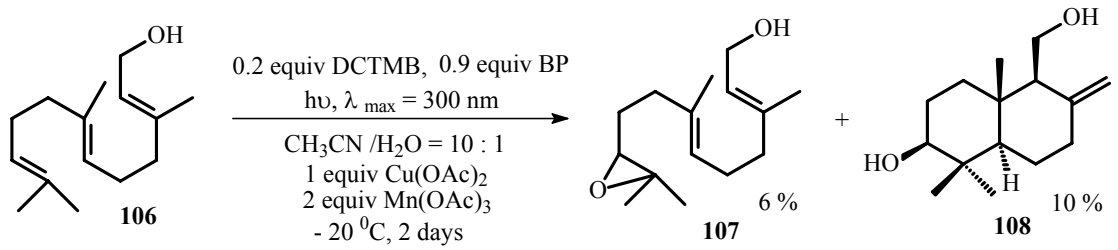

Scheme 40: Oxidation of all-*trans*-farnesol (**106** → **107**, **108**).

During this reaction the formation of a Cu-mirror was not observed. Mn(III)-acetate does the re-oxidation of Cu^{+}-ion. During the reaction the precipitation was observed, which was identified according to analysis as the Mn(II)-acetate. The failure of the modified procedure based on the fact, that after dissolving of Mn(III)-acetate, the solution turns into a dark brown colour and seems to be nearly untransparent for the UV-light. This makes the reaction time two times longer. Taking into account that some of the natural polyalkenes are not very stable, it can result in lower yields due to decomposition of starting materials.

3.2.3 Cu(II)-acetate-mediated PET-initiated cyclizations with methanol as nucleophile

The epoxide formation implies the reactivity of the terminal double bond, even being allylically substituted. This is in agreement with the initial anticipation that the Cu-mediated oxidation is a quicker process than the radical cyclization and the epoxide is formed after the cation formation. But achievement of cyclic products with a higher number of reactive centers is still a challenging target. The problem of the Cu-mirror formation was herewith solved. However, the second important problem concerning the formation of epoxides *vs.* cyclic products required a proper solution. The use of methanol as a co-solvent, instead of water, was proposed. In this case the epoxide formation could be excluded. The low freezing point of methanol makes the use of higher concentration of methanol possible keeping the temperature low. In case of water, the use of higher concentration was problematic because of the high freezing point. Logically, the higher concentration of nucleophile should result in higher yields of the product giving rise to the expectation of improvement. As was mentioned in the previous Chapter 3.2.2, the PET-initiated reaction, with methanol as a nucleophile, was tested initially with commercially available geraniol (**74**) and geranyl acetate (**77**). Later this approach was extended to all-*trans*-farnesol (**106**) and all-*trans*-farnesyl acetate (**118**).

3.2.3.1 Oxidative cyclization of geranyl acetate (77) with methanol as nucleophile

For this reaction the modified procedure is used (see Chapter 3.2.2.3) with similar conditions as was described before. The only difference is that the solvent proportion of acetonitrile / methanol is 4:1.

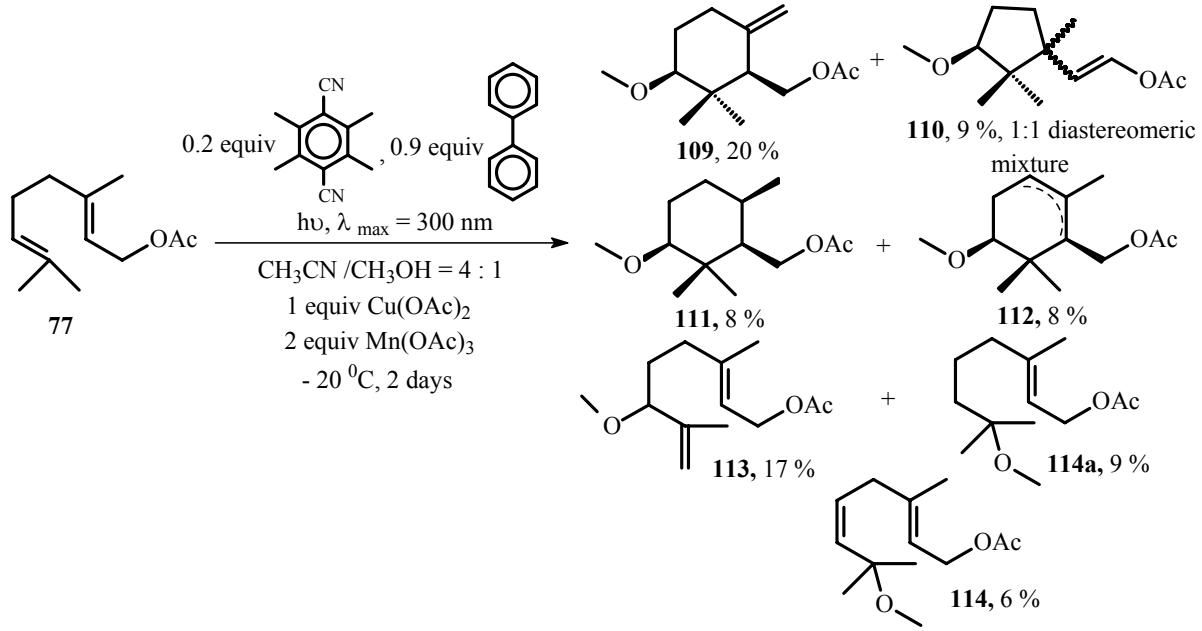

Scheme 41: Oxidation of geranyl acetate (**77**) with methanol as nucleophile.

As was expected, the cyclic products are dominating and no epoxides, even in traces, were detected. Surprising was the formation of **111** in small amount - the product of normal PET-initiated cyclization. Seemingly Cu-mediated oxidation of the intermediate radical competes efficiently with radical cyclization. Increasing of the temperature should speed up the Cu-mediated oxidation and decrease the formation of this product (mechanistic studies will be discussed in the following chapter).

Another surprise was the formation of the cyclic product **110**. The presence of this product speaks clearly for the cationic way of cyclization. It is only possible if the cationic intermediate is stabilized by the carboxyl group in pro-chair conformation in solution *via* a five- or six-member cyclic intermediate. Thermodynamically, the formation of the cyclohexane derivative **109** is more preferable and in fact it is the major one as compared to the kinetically controlled formation of the cyclopentane derivative **110**. As the next step a cyclization of geraniol (**74**) was investigated. In this case no stabilization of the intermediate cation through the hydroxyl group is possible and the cyclohexane derivatives should dominate as products.

3.2.3.2 Cyclization of geraniol (74) with methanol as nucleophile

The reaction was carried out under the same conditions as was described in Chapter 3.2.3.1 and proceeds smoothly with formation of two main products.

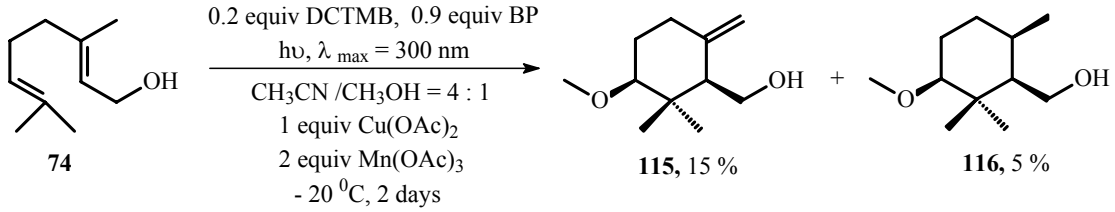

74 **115,** 15 % **116,** 5 %

Scheme 42: Oxidation of geraniol (**74**) with methanol as nucleophile.

The major product is, as expected, the cyclohexane derivative **115** and no traces of cyclopentane derivatives were detected. The minor product **116** is the typical product of PET-induced cyclization without a metal salt and appears due to a similar reason as described in Chapter 3.2.3.1. The cyclization of geraniol (**74**) using the standard PET-induced cyclization was unsuccessful until now. The use of Cu(II)-acetate as a mild co-oxidant allows to cyclize this substrate for the first time.

This experiment shows that the Cu-mediated oxidative cyclization happens *via* the cationic pathway and that the acetate group participates in the stabilization of an intermediate cyclic cation. The presence of the acetate substituent increases the yield of the target cyclic products including the conversion. However, it also increases the number of side products, thus making the separation of these difficult.

3.2.3.3 Cyclization of farnesol (106)

This reaction was performed in order to prove the mechanism and to check the validity of the methodology toward the cyclization of long-chain natural polyalkenes. The reaction was carried out under the same conditions as described above. It results in the bicyclic compound **117** as the only product with a yield of 22%.

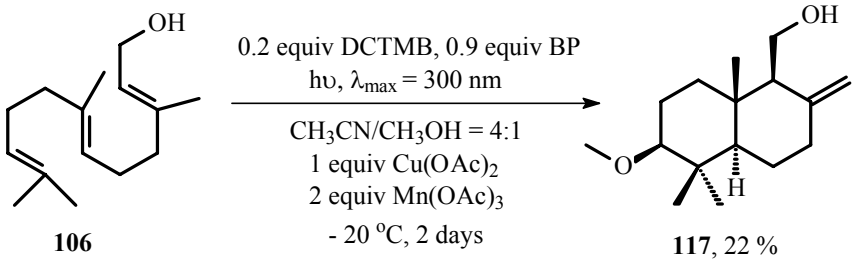

Scheme 43: Oxydation of all-*trans*-farnesol (**106**) with methanol as nucleophile.

Interestingly, the product of usual PET-initiated cyclization was present only in traces. Another important point is that the reaction proceeds *via* the cascade synchronic process. No other diastereomers were detected and isolated, which would be the case if the reaction was proceed *via* a stepwise cascade cyclization.

3.2.3.4 Cyclization of farnesyl acetate (118)

In order to achieve higher yield of the target bicyclic products the farnesyl acetate (**118**) was cyclized by a modified procedure using metal salts as co-oxidants. It was anticipated that in analogy to the geranyl method, the acetyl group will stabilize the cationic intermediate and will lead to a higher yield of the desired bicyclic products.

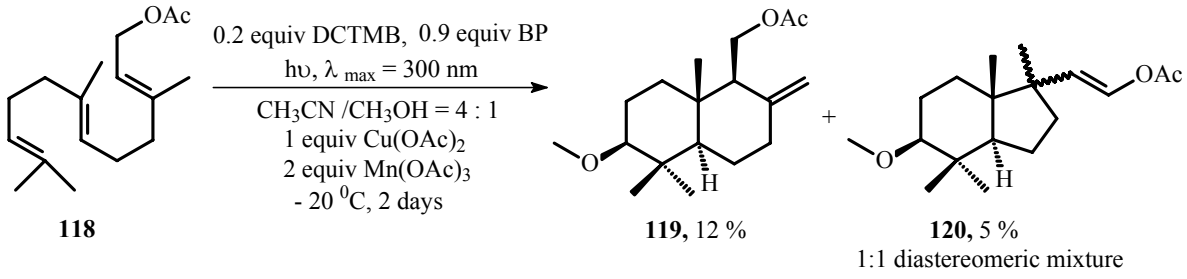

Scheme 44: Oxidation of all-*trans*-farnesyl acetate (**118**) with methanol as a nucleophile.

The reaction in Scheme 44 results in the formation of two bicyclic products: **119** (12 %) and about 5% of **120**. The last one is obtained due to the same reasons as described in Chapter 3.2.3.1. in case of geranyl acetate (**77→110**). The reaction proceeds with formation of many products and it was impossible to isolate and characterize all of them. The natural polyalkene terpenoid acetates are less stable upon irradiation than the corresponding alcohols. This is noticeable even in case of geranyl acetate (**77**) and with longer chain the instability increases.

Due to the above mentioned reasons and because of high costs of substrates, this investigations were not extended to longer chain analogues.

3.2.4 Proposed reaction mechanism and experiments for mechanistic studies

Compiling information from the previous investigations and our own experimental results, the following reaction mechanism can be proposed.

DCTMB is excited under 300-nm irradiation (*Rayonet*) (for a general graphical representation see Figures 3 and 4), leading to a primary electron transfer from BP to DCTMB (Step 1, Scheme 45). On this stage two charged particles, the anion-radical of DCTMB and the cation-radical of BP are formed. Then, the anion-radical of DCTMB should be oxidized either by a Cu^{2+}, or by Mn^{3+} if present. This leads to the formation of the neutral DCTMB and of the Cu^{+} (Step 2). If Mn^{3+}-ions are present, then Cu^{+} should be immediately oxidized by Mn^{3+} back to Cu^{2+}, accompanied by reduction of Mn^{3+} to the insoluble Mn^{2+}. The cation-radical of BP reacts further with the polyalkene substrate upon a secondary electron transfer to form the cation-radical of the substrate and neutral BP (Step 3) terminating the catalytic cycle. The cation-radical of the substrate is, as found earlier for photochemical electron transfer processes in absence of metal ions, trapped by a nucleophile to form mainly *anti*-Markovnikov products (→ **A**, Scheme 45). The remaining radical (**B**) is proposed to be rapidly oxidized by either Cu^{+} or by recovered Cu^{2+} or even by Mn^{3+} to give a tertiary cation (**C**) of the substrate and either Cu^{0}, Cu^{+} and/or Mn^{2+}. This mechanistic sequence would forcingly explain why the photoreaction, if carried out without Mn^{3+}-ions, leads to the formation of a Cu-mirror.

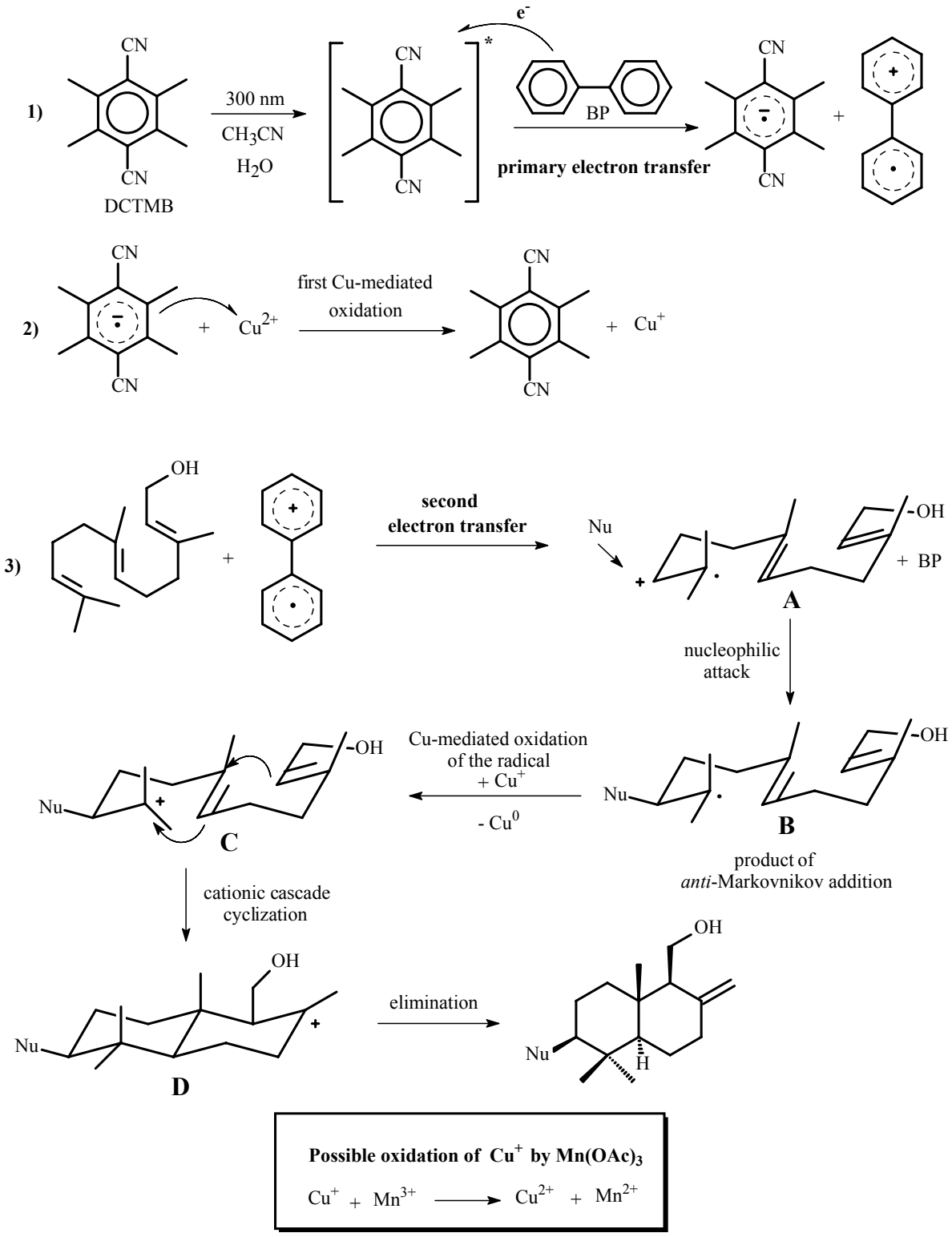

Scheme 45: Possible mechanism for the Cu(II)-acetate-mediated photocyclizations.

The tertiary cation (**C**) triggers the cascade cyclization giving the cyclic cation **D**. The most probable termination step from **D** is then elimination of a proton that leads predominantly

to the product with exo-double bond, although a minor amount of products with endo-double bond is formed too.

Now the role of Cu(II)-acetate in this reaction is clear although some questions remain concerning the mechanism of cyclization. Is the cyclization really synchronic or stepwise? On which stage is the cation formed?

We have performed some mechanistic investigation to resolve these issues. The pattern of the products of PET-induced cyclization with a) water as a nucleophile without a metal salt (Scheme 46), and b) with methanol as a nucleophile and in the presence of Cu(II)-acetate (Scheme 47). Noticeable differences are found.

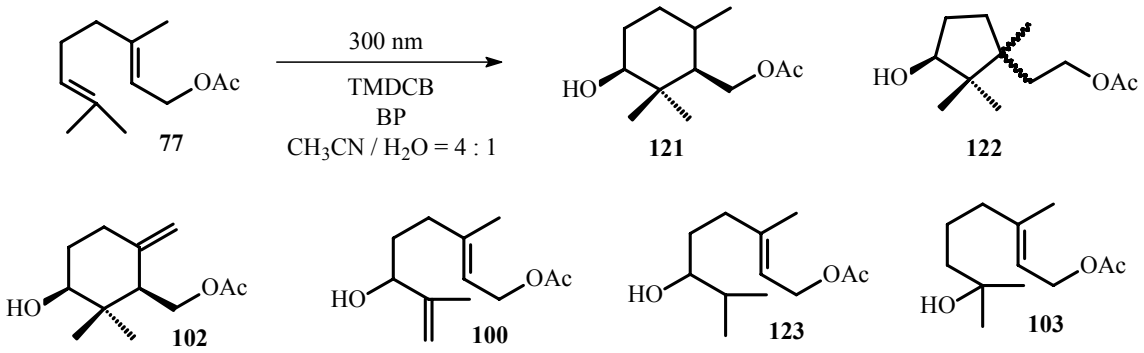

Compound	**121**	**122**	**102**	**100**	**123**	**103**
Yield, %	35	15	7	3	5	19

Scheme 46: Products and yield of photochemical cyclization of geranyl acetate (**77**)[24].

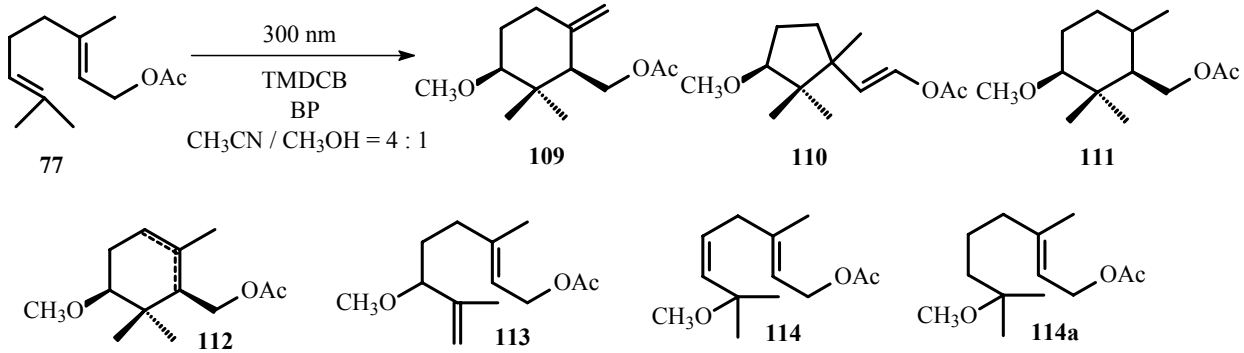

Compound	**109**	**110**	**112**	**111**	**113**	**114**	**114a**
Yield, %	20.4	9	7.8	7.8	17	5.8	9.3

Scheme 47: Products and yields of Cu-mediated photochemical cyclization of geranyl acetate (**77**).

The differences concern the formation of the products **110**, **112** and **114** which were never obtained as products of PET-induced cyclization without metal ions. The products **109** and **113** are formed under the new conditions in much higher yield and the products **111** and **114a** in a much lower yield. All these results confirm clearly the role of Cu(II)-ions as a co-oxidant in PET-induced cyclizations. Another conclusion is that the cyclization proceeds *via* cationic pathway. Formation of the product **100** in a yield of 3 % (Scheme 46) *vs.* 17 % of **113** (Scheme 47) speaks for the formation of a tertiary cation (like **B**→**C**, Scheme 45) giving rise to either cyclic products (**109**, **110** and **112**) or elimination (→**113**). Formation of the product **114** could be explained *via Markovnikov*-type trapping of the cation followed by an oxidation of the secondary radical center and elimination. Products **111** and **114a** are seemingly formed due to the same reason which is discussed in chapter 3.2.3.1.

Further experiments were done in order to clarify the influence of such parameters like temperature, solvent and solvent proportion (amount of nucleophile) on the course of reaction. Results of these investigations are depicted in Scheme 47 and summarized in Table 1.

	Parameters changed (reaction Scheme 47)		
	Solvent proportion: from 10/1 to 4/1	**Temperature:** from -15^0- -20^{0}C to RT	**Solvent changed:** from CH_3CN/CH_3OH 4/1 to DMF/CH_3OH 4/1
Yield, % (cyclic products)	**Changed** from 25 % to 45 % (total)	**Changed** from 45 % to 25 %	**Changed** from 45 % to traces
Yield, qualitative (acyclic products)	Nearly the same	Increased proportionally	Increased enormously

Table 1: Influence of temperature, solvent and solvent proportion on the course of reaction.

We have noticed strong dependence of Cu-mediated oxidations on the temperature. With higher temperature the oxidation ability of Cu^{2+}-ions grows and this should minimize at least the yield of products **111** and **114a**. This was found. However, increase of the temperature destabilizes the intermediate cation which seemingly undergoes more readily elimination rather than performing cyclization with elimination.

By changing the solvent from methanol to DMF we failed to produce the cyclic products. Instead of it, the products **113**, **114** and **114a** were dominant. Further insights into these aspects are provided by the results of theoretical investigations in the field of exothermicity of cationic

cascade polycyclizations and the mechanism of the lanosterol biosynthesis, performed by Joergensen[54]. According to these results the cationic cyclization is a highly exothermic process (about 20 kcal/mol) and proceeds in vacuum without activation barrier. In solution an activation barrier for the desolvatation is found which is about 3-4 kcal/mol at a separation of 5-6 Å. Such values were obtained for dichloromethane, tetrahydrofuran and methanol. For much more polar solvents, such as DMF, this desolvatation barrier should be higher and elimination should be preferred.

The last point for investigation was the stereochemical aspect of the cyclization. Is the Cu-mediated cyclization proceeds like the natural process? The relative stereochemical configuration of product **117** was investigated with NOESY experiments. The enhancements are depicted in Figure 9 and the results are in good agreement with the natural relative configuration[55].

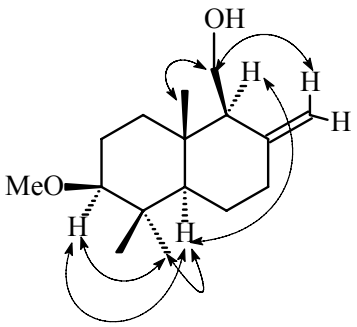

Figure 9: Relative stereochemistry of **117** according to NOESY experiments.

3.2.5 Experimental approach toward cyclizations including intramolecular or combined intra- and intermolecular trapping

To find more applications of the newly developed methodology of PET-induced cyclization with Cu(II)-acetate as a co-oxidant, the cyclization of a substrate with an internal nucleophile (**126**) was investigated.

The general idea was to use the hydroxy group as the internal nucleophile to trap the cyclic cation and to synthesize the bicyclic compound **127** (Scheme 48). The photochemical oxidation of the terminal double bond to the cation-radical is expected to occur according to the common mechanism of PET-induced cyclizations and also to the newly developed mechanism of PET-cyclizations with Cu(II)-acetate as a co-oxidant (→**A**). Further nucleophilic attack by an external nucleophile, such as methanol, should result in the tertiary radical **B**

which in turn should be oxidized by Cu(II)-acetate to the corresponding cation **C**. The cationic cyclization from **C** should result in the formation of **127**.

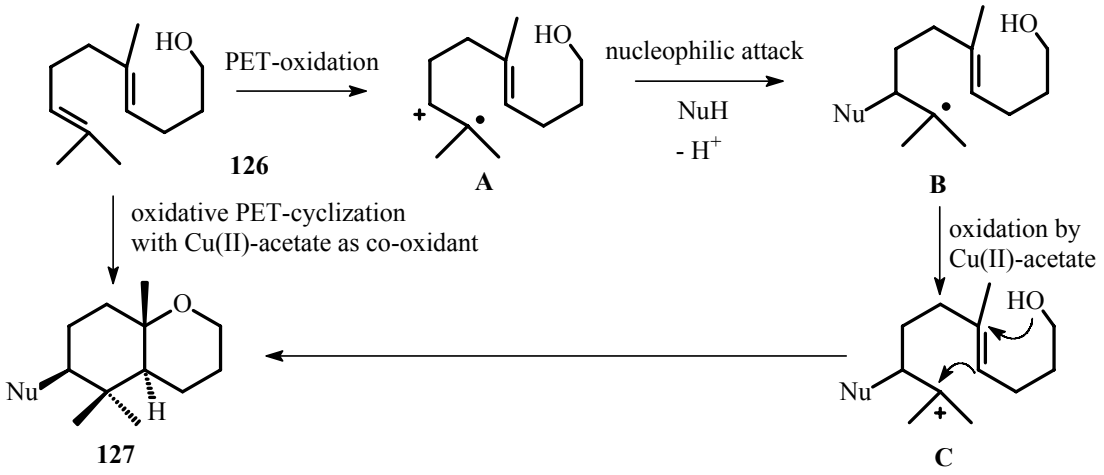

Scheme 48: Synthetic proposal toward the bicyclization of bis-homogeraniol (**126**).

3.2.5.1 The synthesis of geranyl diethylmalonate (124)

The synthesis of geranyl diethylmalonate (**124**) was accomplished in two steps starting from the commercially available geraniol (**74**). Firstly, the geraniol was brominated with phosphorus tribromide (PBr_3) in ether and used in the next step without purification. The use of commercially available geranylbromide (**85**) is not recommended due to its high instability.

The second step involved alkylation of diethylmalonate with **85** using NaH as base in dry THF to give geranyl diethylmalonate (**124**) in 78 % yield over the two steps.

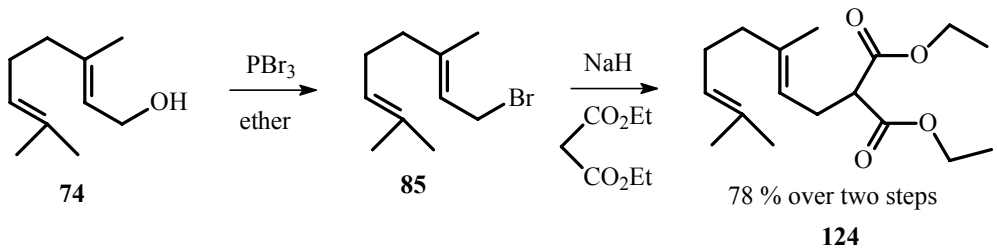

Scheme 49: Synthesis of geranyldiethylmalonate **124**.

3.2.5.2 Decarbethoxilation of gerahyl diethylmalonate. Synthesis of bis-homogeranic acid ethylester. Reduction of bis-homogeranic acid to bis-homogeraniol

The ethyl bis-homogeranate (**125**) was obtained using the LiCl in DMSO[56]. As compared with other possibilities, like deesterification-decarboxilation, this reaction saves one

synthetic step and results in a higher yield. According to this procedure the bis-homogeranic acid ethylester (**125**) was obtained with a yield of 90 %.

The next step was to perform reduction of the ethyl bis-homogeranate to the bis-homogeraniol (**125→126**, Scheme 50). This was achieved using $LiAlH_4$ in ether. The quenching and work-up of the reaction mixture was done with water, then concentrated KOH solution and finally washing with water again. This prevents difficult isolation of the products from the fine suspension of $Al(OH)_3$. Bis-homogeraniol (**126**) resulted in a yield of 95 %.

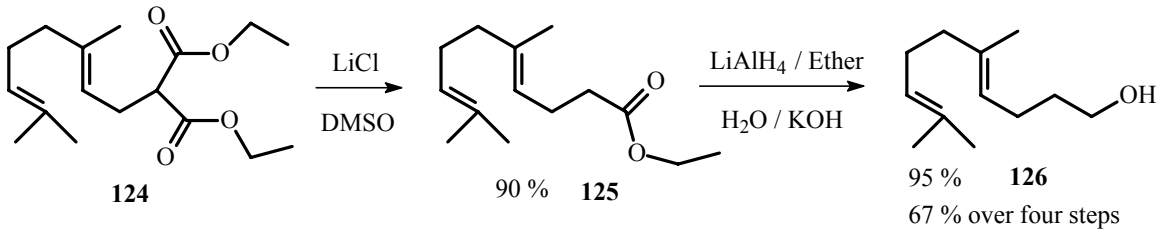

Scheme 50: Synthesis of bis-homogeraniol (**126**).

3.2.5.3 Irradiation of bis-homogeraniol with Cu(II)-acetate as co-oxidant

The irradiation of the bis-homogeraniol was performed at 300 nm using the DCTMB/BP acceptor pair with 1 equivalent of Cu(II)-acetate and 2 equivalents of Mn(III)-acetate in acetonitrile-methanol mixture 4/1 for 1 day.

Unfortunately, the bicyclic product **127** was not found. Instead, five different products, three of them (**128**, **130** and **131**) which are the products of monocyclization, were isolated. The methylenecyclohexane derivative **128** is the product of terminal double bond oxidation. The α-substituted tetrahydrofurans **130** and **131** are the products of internal double bond oxidation. In the latter case the hydroxyl group have played the role of an internal nucleophile. The intramolecular cation trapping seems to be quick enough to completely exclude methanol from the reaction (products **130** and **131**), thus no product of further methanol addition was found in case of cyclization. Methanol addition occurred in the acyclic cases (**129**, **129a**) only.

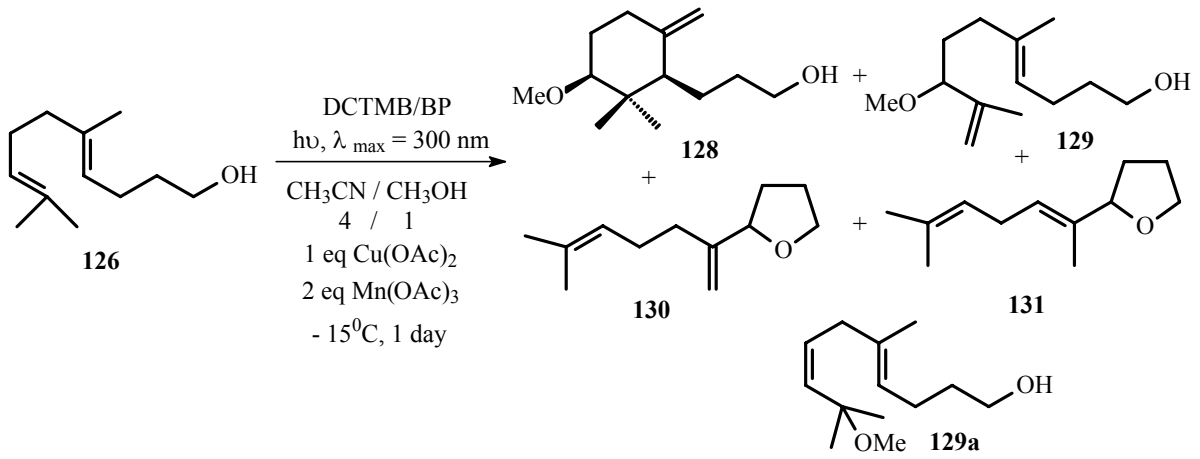

Scheme 51: Products of the irradiation of bis-homogeraniol (**126**).

The explanation of this phenomenon can be the low potential of the internal double bond of compound **126**. In comparison with previous cases, such as oxidative cyclization of geraniol (**74**) or geranyl acetate (**77**), the hydroxyl or acetate groups are two carbons closer to the inner double bond increasing the oxidation potential thereof, thus "protecting" it from photochemical oxidation. In contrast, these functional groups are in the present case distant from the inner double bond hence not providing sufficient "protection" from photooxidation.

Although the target bicyclic product **127** was not obtained, the present reaction gives important information about the photooxidation of substrates with internal nucleophile and about the influence of functional groups in proximity of an alkene.

A possible extension of this methodology could be an approach towards the synthesis of (±)-ambrox (**30**), an important natural fragrance, starting from homofarnesol (**29**).

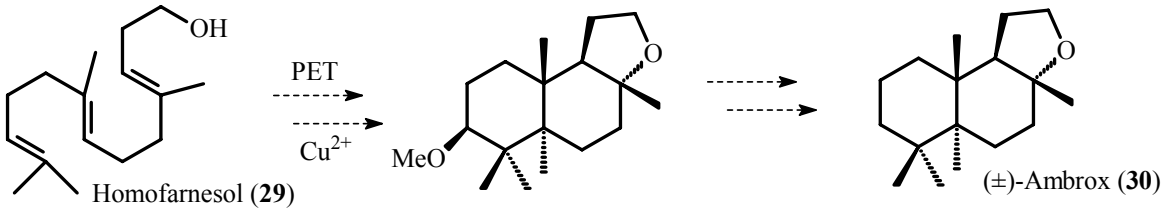

Scheme 52: Synthetic proposal toward the synthesis of (±)-ambrox.

3.3 Photochemistry of the Cu(II)-complexes and experiments for asymmetric induction

Enantioselective photochemical transformations are a very challenging topic in preparative photochemistry. With some exceptions[21], most synthesises result in racemic mixtures of the products. Catalytic enantioselective photochemical transformations are still unknown. However, chiral complexes of transition metals constitute in our opinion a great potential for such purposes. Especially efficient were in the past the combinations of Lewis acids and chiral Brønsted acids in the application for ground state reactions[57]. The photoreactions of such metal complexes are still unexplored. We decided to investigate the photochemistry and reactivity of chiral metal complexes, as potential substrates for biomimetic asymmetric cyclizations and especially in view of applications of previously designed synthetic procedures, such as Cu-mediated PET-cyclizations.

The desired photochemical enantioselective cyclizations could be performed if the substrate in complex is either much more reactive than in uncomplexed form or is reactive within the complex only. Such constellations should minimize reactions outside of the complex which will lead to a loss of induction and hence enantioselectivity. Proper unsymmetrical shielding of the reactive site by the chiral ligand and absence or minimized side reactions should be taken into account.

A major possibility is to reach the substrate reactivity only, or mostly, in complex meaning that the absorption maximum of the complex should be shifted to different wavelengths than the absorption(s) of the uncompexed substrate to facilitate excitation of complexed material. Graphically this is shown in Figure 10 (left). On the other hand the position of the absorption maximum of the complex could remain, but an increase of its intensity should be reached in order to favor predominantly photochemical transformation of the complex (right).

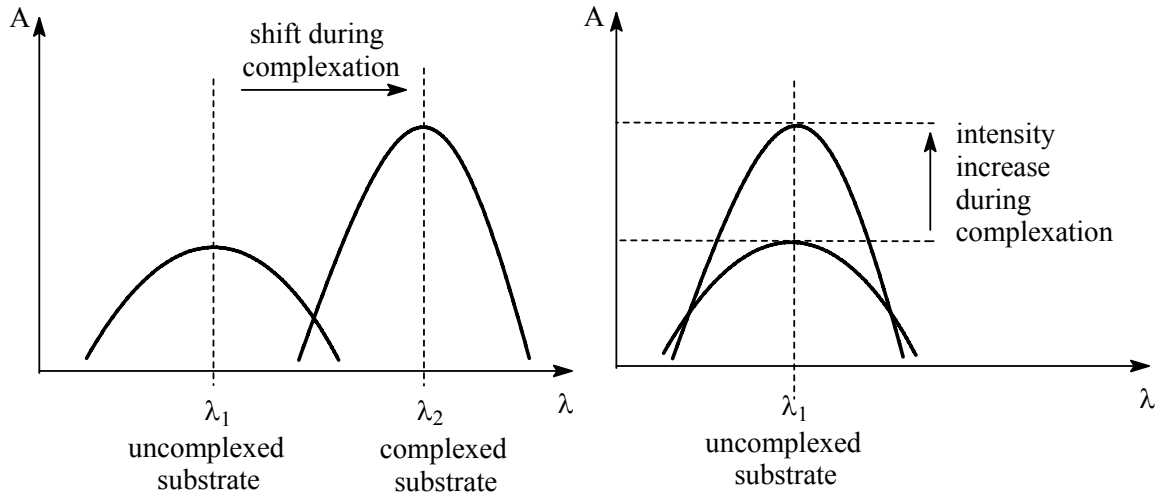

Figure 10: Desired absorption and intensity shifts during complexation.

3.3.1 Considerations on substrate, chiral ligand and complex formation

We analyzed which kind of organometallic complexes could be suitable for the desired photochemical transformations. One can suggest either σ,π-complexes or π,π-complexes independent of other conditions. The σ,π-complexes are more stable during the reaction. The metal-ligand bond lengths are shorter here which should improve the chirality transfer. However, the catalytic course of the reaction becomes more problematic due to a higher complex stability and slow decomplexation of the reacted substrate being strongly dependent on the metal used. The π,π-complexes promise more flexibility for complexation and decomplexation of substrates during reaction. This would facilitate a catalytic course of the reaction. The stability of π,π-complexes during photoreaction, especially in polar, well coordinating solvents like acetonitrile or water, is low due to the possible ligand exchange with the solvent.

In this work we investigated the photochemistry of organometallic σ, π - complexes with the aim to achieve enantioselectivity including the possibility to conduct such reactions also catalytically. It was decided to use β-ketoesters, such as **132**-**134** (Figure 11), as complexing materials. This choice we prefer due to the simple, cheap and effectively short synthesis of such ketoesters. Another advantage of these substrates is the high acidity of hydrogens between ketone and ester group, making enolization easy and, according to literature[58], allows the effective complex formation with metals such as Cu^{2+}, Ni^{2+}, Co^{2+} and Zn^{2+}.

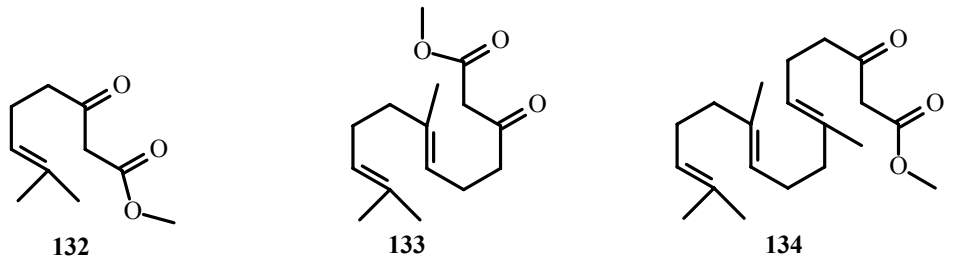

132 **133** **134**

Figure 11: Potential complexes for photochemical transformations in metal complexes.

The cyclization of polyalkene terpenoids *via* radical and cationic processes proceed as cascade processes. In case of substrate **132** the cyclization is possible only after formation of an enolate complex. In case of substrates **133** and **134** the cyclization should proceed through involvement of all double bonds including the enolic one which will be again formed upon complexation.

For the choice of chiral ligands the same logic as described above should apply. The chiral ligand should also give relatively strong σ,π-bonds with the metal and must be inert toward side reactions, especially photodecomposition. During the last decade a number of chiral ligands for homogeneous catalysis were developed. Especially widely applied and successful were the C-2 symmetrical bis-oxazalidinon ligands (alkyl-BOX-ligands)[59].

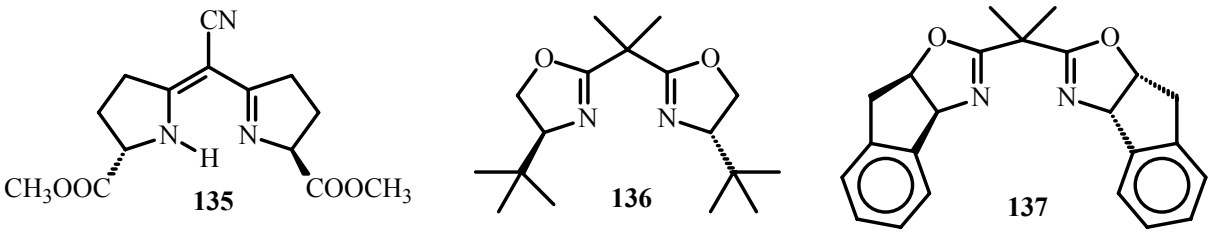

135 **136** **137**

Figure 12: Choice of chiral ligands for the photochemical transformations in metal complexes.

In spite of the noticeable advantages in synthesis, stability and price of alkyl-BOX-ligands (**136**, **137**) including the stability of the final complexes makes these ligands unattractive. However, the C-2 symmetrical ligand, named semicorrin **135**, was already described in literature[60] for its use in ground state reactions[61]. This ligand can give the desired σ,π-complexes. Although, the semicorrin is commercially available, the high price makes it again unattractive. On the other hand, the synthesis of semicorrin, starting from pyroglutamic acid seems to be not complicated and allows a preparation in multigram

quantities. The synthetic procedure is represented in Scheme 53 according to which we synthesized **135** on a 9-g scale.

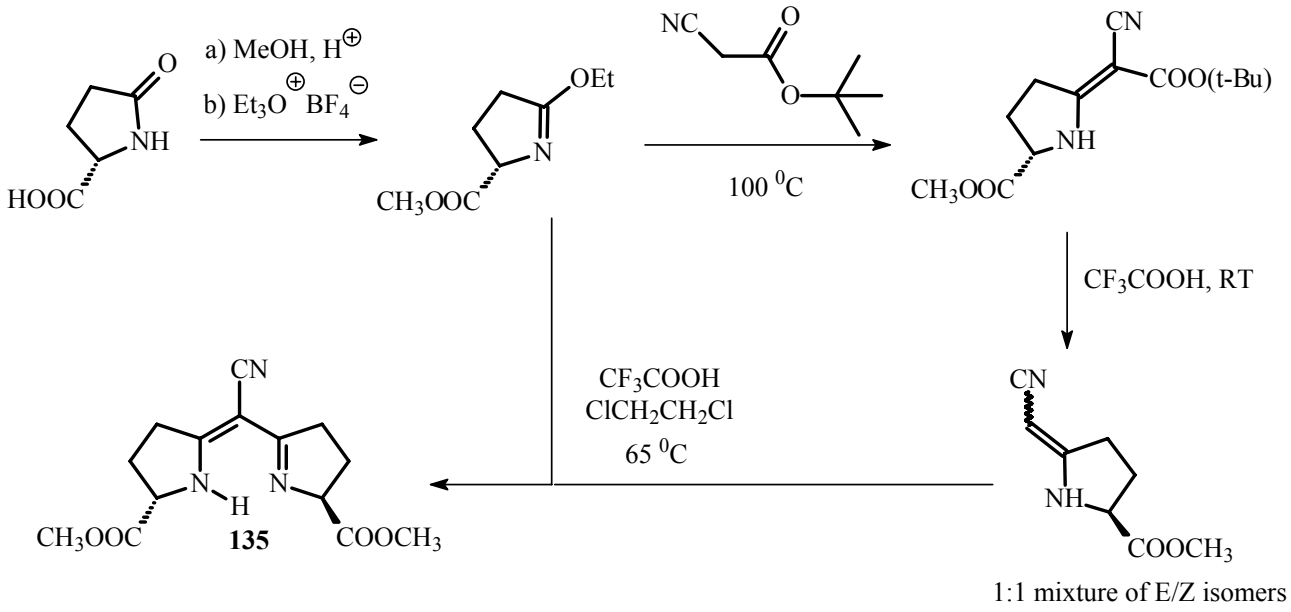

Scheme 53. Synthesis of the semicorrin **135**[60].

3.3.2 Synthesis of the β-ketoesters 132-134

The desired β-ketoester could be obtained in two ways. One is the γ-alkylation of methylacetoacetate. For this synthesis either excess of two differently strong bases (NaH and BuLi) or two equivalents of the lithium diisopropylamid (LDA) could be used, giving yields of 40-50 %. Even the use of additional anion stabilizer, DABCO, can not improve the yield.

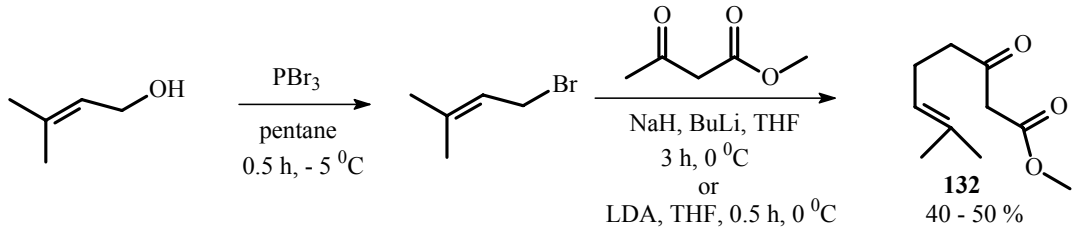

Scheme 54. Synthesis of β-ketoester **132**

Another possibility is to alkylate dimethyl carbonate with commercially available prenylacetone using sodium hydride in ether or tetrahydrofuran (THF). The reaction usually works better in THF than in ether. The yield of the target β-ketoester **132** is 70 – 80 %. This

method was chosen for the synthesis of homologues of the β-ketoester **132**. However, for the higher homologues of prenylacetone (geranyl- and farnesylacetone) ether as a solvent gives no alkylation, but the use of the THF results in up to 90 – 95 % yield of products.

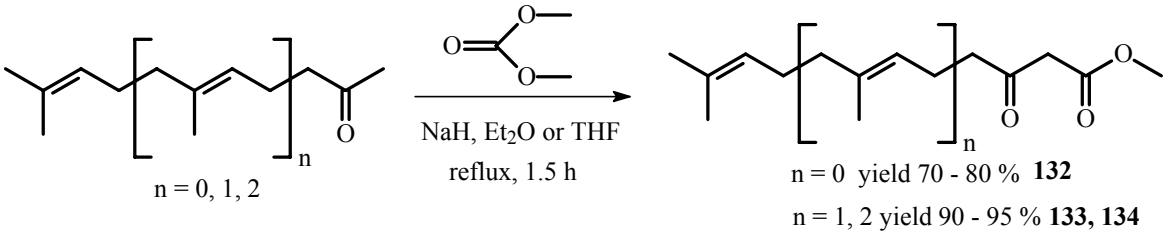

Scheme 55: Synthesis of β-ketoesters *via* alkylation of dimethylcarbonate.

3.3.3 Synthesis of bis(methyl 7-methyl-3-oxo-oct-6-enoato)copper(II) (138)

First we attempted the synthesis of bis(methyl 3-oxobutanoato)copper(II)[58] and extended then the methodology to a synthesis of the complex **138**. The use of triethylamine as a base works fine for methyl 3-oxobutanoate but for the substrate **132** complex formation was much lower (20-25%). It seems that due to reduced acidity of the CH_2-group stronger base is required. Indeed, the use of sodium hydroxide results in complex formation with 40-50 % yield. The isolation procedure was slightly different from a procedure described in literature[58] and an attempt to adopt previously described procedures failed. The complex precipitated from the solution as blue flakes. Filtration and washing with ice-cold methanol resulted in a blue powder which was taken in ether to remove all inorganic materials and crystallized by slow addition of ice-cold methanol.

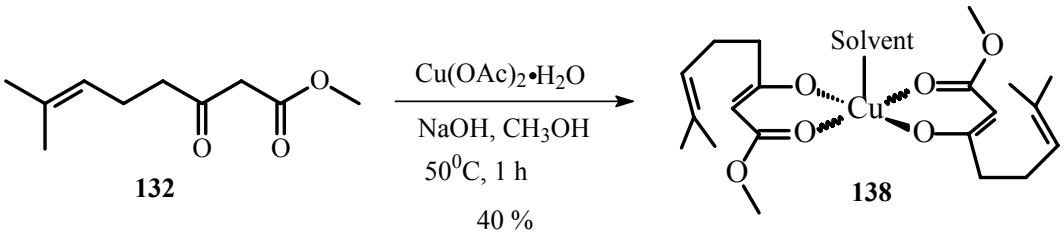

Scheme 56: Synthesis of symmetrical Cu(II)-complex **138**.

3.3.4 Irradiation of bis(methyl 7-methyl-3-oxo-oct-6-enoato)copper(II) (138)

The symmetrical Cu(II)-complex **138** was irradiated in acetonitrile – methanol solution 4:1, using DCTMB as acceptor and BP as a co-acceptor. The Cu(II)-acetate was also present in

the mixture (1 equiv) as a co-oxidant. The idea was to try to reproduce the cyclization of polyalkene terpenoids like geranyl acetate, but in complex.

Our first attempt to cyclize the β-ketoester **132** (→**138**) in complex under usual conditions resulted in two products in a ratio of about 1 : 1 (Scheme 57). The first is the substituted cyclopentanone **139** as a single diastereomer and the second one is the product of usual PET-initiated oxidation of the terminal double bond (**139a**). Quite remarkable is the absence of the methanol addition product in **139**. This led us to the conclusion that the presence of a nucleophile, such as methanol, in not necessary for the cyclization.

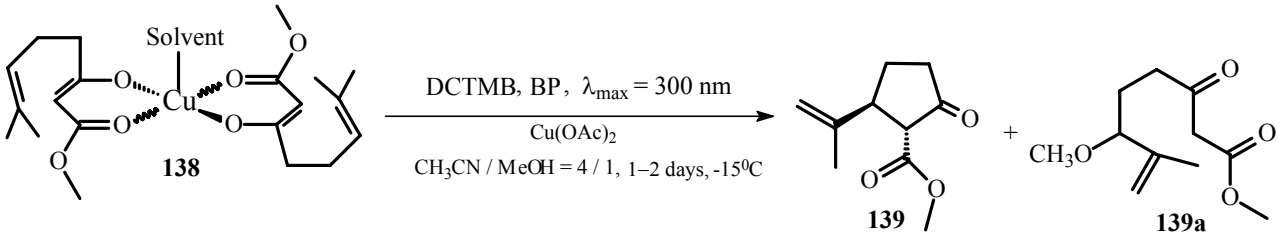

Scheme 57: Cyclization of the Cu-complex **138** with DCTMB-BP in acetonitrile – methanol mixture.

Polar solvents can promote exchange reactions in the complex and disturb the intended cyclizations. The presence of the nucleophilic co-solvent causes the side reaction to **139a** which is the product of the simple PET-initiated/Cu-mediated oxidation of the terminal double bond.

An important conclusion is, that the solution must be as unpolar as possible and no nucleophile is necessary for the cyclization reaction. It was also shown that the DCTMB-BP acceptor/co-acceptor pair does not work in unpolar solutions, because of insufficient separation of the contact ion pairs. A recently developed methodology by *Demuth* and co-workers[31] allows to perform PET-initiated cyclizations in solvents of low polarity, such as dichloromethane, with a minimal amount of nucleophile. This methodology involves the use of $NMQ{\cdot}PF_6$ – BP as acceptor/co-acceptor pair.

Aiming to improve the yield of cyclic product and to exclude the formation of the usual product of PET-triggered oxidation of **139a**, we decided to use the $NMQ{\cdot}PF_6$-methodology for the oxidation of the Cu-complex **138**. In order to perform this reaction some amount of acetonitrile was added to dissolve the Cu(II)-acetate and the acceptors. As expected, the product of the cyclization was the cyclopentanone **139**, which appears as a single diastereomer (Scheme 58).

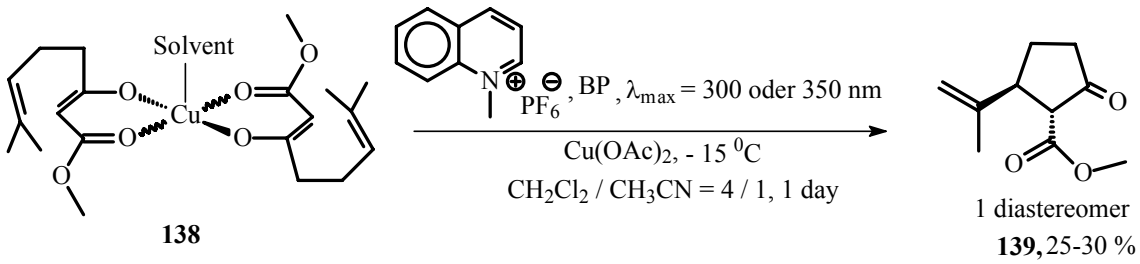

138 **139,** 25-30 %

Scheme 58: PET-induced oxidation of the Cu-complex **138** in a low polarity solvent mixture.

3.3.5 Proposed reaction mechanism and experiments for mechanistic considerations

After successfully performing cyclization, we were mainly interested in an investigation of the reaction mechanism. The major questions concerned the position at which the oxidation takes place and how the cyclization is going on. Therefore we measured the oxidation potential of a Cu-complex (Figure 13, left) and the commercially available Cu(II)-acetylacetonate (center of Figure 13) for comparison.

The oxidation of the synthesized complex **138**, as well as of all previously cyclized terpenoids, show irreversibility and therefore, although the molecules have more than one double bond, only the first value obtained can be assigned to the double bond with the lowest oxidation potential. However, these measurements provide no information regarding the position of this double bond. This however, could be figured out by the position of nucleophile addition, as was done in the previous work, but which is not applicable in the present case because of the lack of a nucleophile.

As was measured before, the oxidation potential of the terminal double bond, where the oxidation starts is in the range of +1.31 to +1.43 V (see Figures 7 and 13). The measurements depicted in Figure 13 clearly show that oxidation of the Cu-complex could start from the enolic double bond.

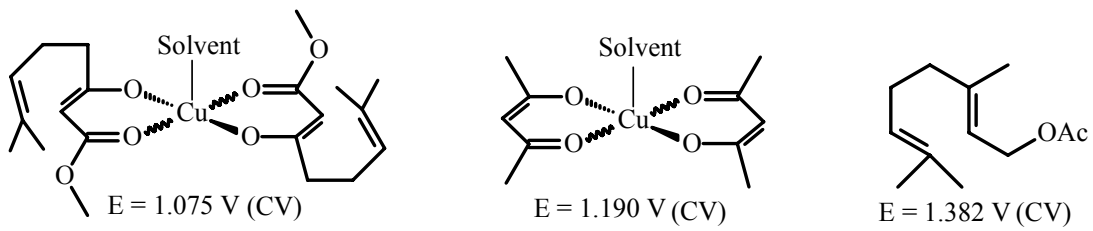

138 **77**

Figure 13: Oxidation potentials measured by CV.

Our results, however, could not exclude the possible oxidation of the terminal double bond in these complexes. To further investigate this point, additional experiments are necessary with substrates with more than one isoprene unit. If in this reaction both mechanisms are present and oxidation of both double bonds takes place, two main products should be formed (Scheme 59). If only one product appears in the reaction mixture then the double bond, where oxidation occurs, should have the oxidation potential measured above (Figure 13).

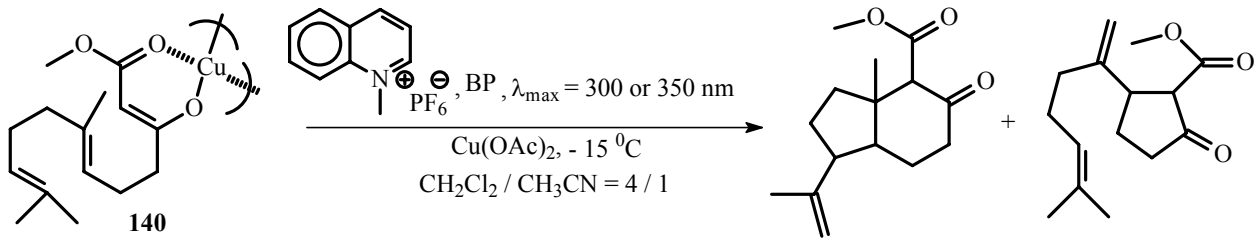

Scheme 59: Evaluation of the oxidation site in **140**.

The first product depicted in Scheme 59 should derive from oxidation of the terminal double bond forming typically bicyclic products. The second product would be characteristic for oxidation of the enolic double bond. In this case bicyclization is unprobable because of the less stabilized secondary radical formed after the first cyclization step. The monocyclization, on the other hand, should result in a tertiary radical as an intermediate. The following oxidation and elimination should finally give rise to the *exo*-double bond. The experiment with bis(Substrate)-Cu(II)-complexes (e.g. **140**) as substrates resulted exclusively in the isomeric mixture of *exo*/*endo*-double bond isomers (1:5.3 and 1:3.8, correspondingly) of products derived from enolic double bond oxidation.

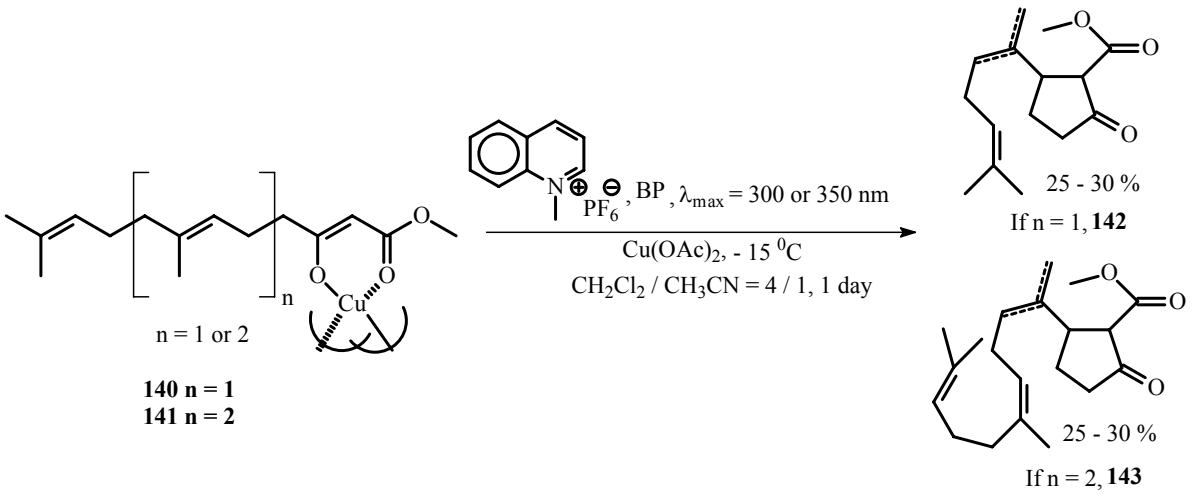

Scheme 60: Products of irradiation of Cu(II)-complexes.

These results, together with the oxidation potential measurements and with the obtained products allow us to propose the reaction mechanism that is represented in Scheme 61.

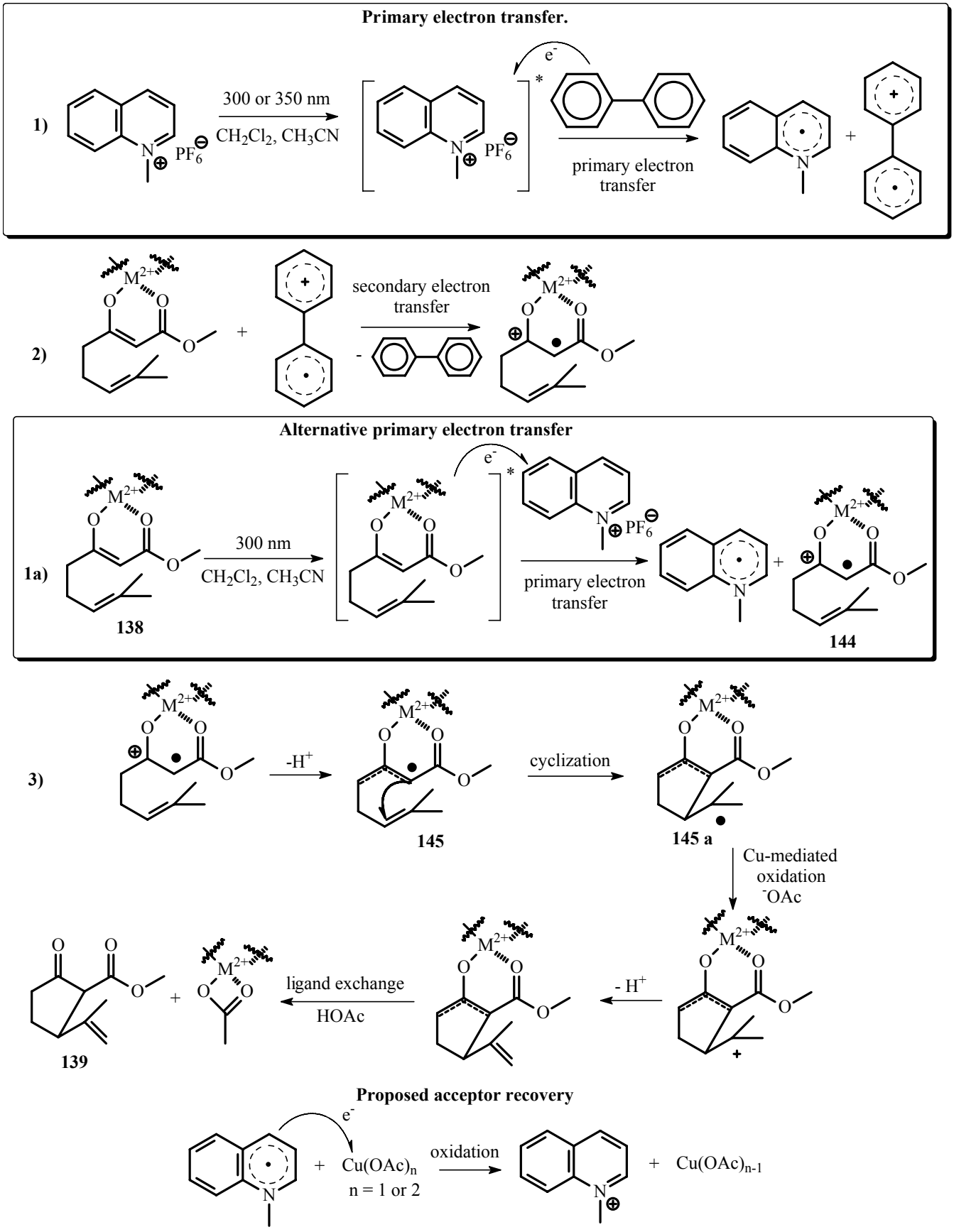

Scheme 61: Proposed mechanism for oxidative photochemical cyclization in Cu(II)-complexes.

In the first step, upon irradiation at 300 or 350 nm, the photoelectron transfer between the excited acceptor NMQ·PF_6 and biphenyl takes place. This step is actually similar to the process happening upon irradiation with DCTMB and BP. The difference is, that in the present reaction a neutral radical (of NMQ) and the cation-radical of BP are formed. The polar solvent for the transformation of a contact ion pair into the corresponding solvent separated ion pair is not necessary anymore. The next step should be the secondary electron transfer from complex **138** to the cation-radical of BP (step 2), with formation of neutral BP and the cation-radical of complex **144**. At this point must be noticed that the excitation of complex **138** upon irradiation cannot be excluded and an alternative way of oxidation could be proposed (step 1a). The electron transfer could proceed from the exited complex (substrate) to the unexcited acceptor NMQ·PF_6 without participation of BP. In case of reactions triggered by the DCTMB/BP acceptor/co-acceptor pair such direct oxidation of the substrate by DCTMB is much more exothermic as the corresponding stepwise oxidation of BP (see Figure 5). Reaction without BP results in much lower yields of products, because of efficient back electron transfer and not sufficient charge separation of the anion-radical of DCTMB and the cation-radical of the substrate. In case of the neutral NMQ-radical this aspect does not play a role and electron transfer from donor (complex) to acceptor (NMQ·PF_6) is possible. Unfortunately, the investigation of the primary electron transfer pathway (steps 1 and 2 *vs.* 1a, Scheme 61) could not be done here.

The cation-radical of complex **144** is formed. In the next step stabilization of the intermediate is achieved by proton abstraction/elimination (step 3), and the resulting radical **145** undergoes radical cyclization to form the tertiary radical **145a**. This is rapidly oxidized to the corresponding cation by Cu(II)-acetate which upon elimination renders the double bond.

Some amount of acetonitrile in the reaction mixture is necessary for better solubility of Cu(II)-acetate and NMQ·PF_6. However, acetonitrile promotes the ligand exchange and releases the cyclic product **139** from the complex. The most controversal question is the further transformation of the cation-radical **144** of the substrate. The substrate in the complex, prior to oxidation, possesses 6 π-electrons on 5 atoms, hence having the equivalent electronic configuration of cyclopentadienyl anion which is aromatic according to the Hueckel-rule. The metal ion has no π-electrons, therefore it is not participating in conjugation; however, the intramolecular-interannular electronic effects can be transferred over to the metal ion[62]. Accordingly we can conclude that the substrate in the starting complex is not exactly aromatic but has close similarity with an aromatic system, *i.e.* is quasi aromatic. Formation of the cation-radical leads to the loss of pseudo aromacity and is the destabilizing factor. The reaction

sequence that follows is still unclear. Probably the stabilization occurs by means of proton abstraction/elimination with subsequent radical cyclization, although the radical cyclization, followed by proton abstraction/elimination cannot be excluded. By proton abstraction/elimination the system becomes again pseudo aromatic, accompanied by a considerable gain in energy.

Acids make a big influence on the stability of complexes. Strong mineral acids destroy the complexes rapidly[62]. Here acetic acid is formed during reaction, creating an additional factor of uncertainty with regard to the stability of the complexes, together with acetonitrile, both factors being able to provide decomposition of the complex or giving rise to ligand exchange.

3.3.6 Attempts toward enantioselective cyclizations with Cu(II)-complexes

A still unexplored point concerns the investigation of the preparation and enantioselective photocyclization of chiral Cu(II)-complexes.

As was mentioned above, the chiral ligand semicorrin **135**, was chosen for preliminary experiments. In the literature there were some reports regarding the exchange reactions of semicorrin[60]. The semicorrin reacts successfully with Cu(II)-acetylacetonate in dichloromethane and replaces one molecule of acetylacetone in quantitative yield. Oppositely the reaction of Cu(II)-acetate with semicorrin leads to the unstable (semicorrinato-monoacetate)-Cu(II)-complex and then rapidly decomposes to the bis-(semicorrinato)-Cu(II)-complex. The last one is stable toward further ligand exchange.

The reaction of one equivalent of complex and semicorrin performed in dichloromethane according to previously described conditions, results in formation of an other complex. According to spectral properties and our own observation the structure could be assigned as mono-(semicorrinato-ketoester)-Cu(II)-complex (**146**).

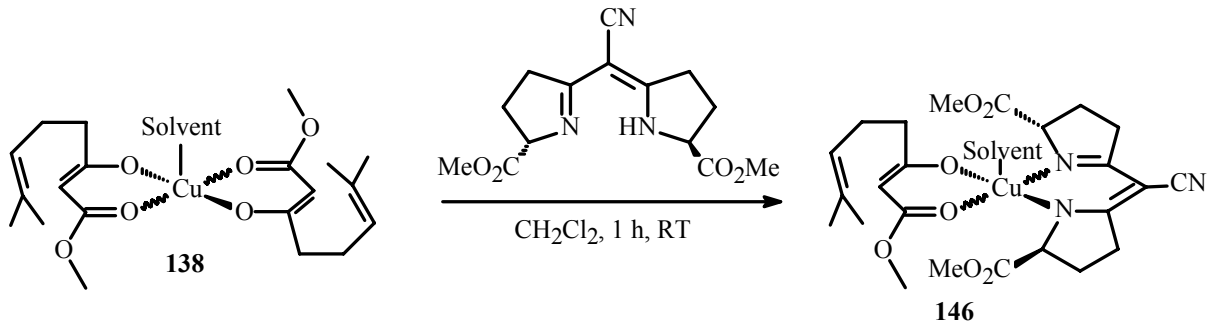

Scheme 62: Anticipated product of ligand exchange with semicorrin.

The complex was crystalline only at low temperature and tar-like at room temperature. The only spectroscopic way to confirm the complex formation (→**146**, Scheme 62) was UV/VIS spectroscopy; another possibility was to perform further photochemical oxidation of complex **146** (see Chapter 3.3.4, Scheme 58) and analyze an enantiomeric excess in the product obtained (**146→139**). The successful detection of an enantiomeric excess should indicate not only the formation of complex **146** but also should confirm the right choice of the chiral ligand in terms of sufficient shielding of the reactive site.

The reaction was performed under two different conditions a) and b)(Scheme 63). In the first case the cyclic product **139** was isolated in a yield of 30 % but no enantioselectivity could be detected (see Scheme 64). In the second case the product **139** was isolated with a lower yield (25 %) due to the prolonged irradiation time being necessary but notably, some low enantioselectivity was achieved.

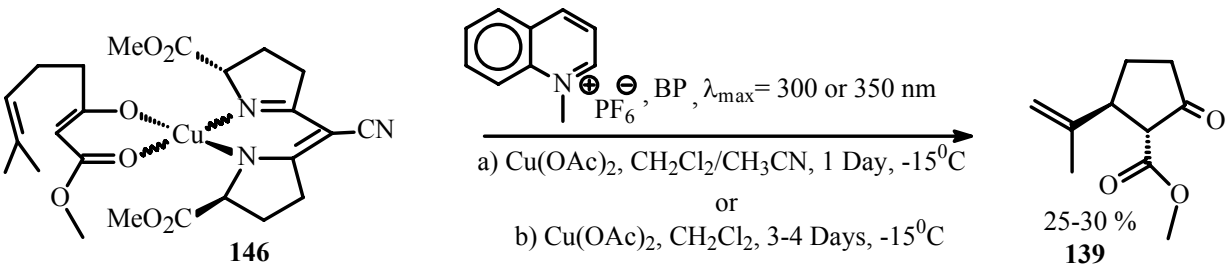

Scheme 63: Irradiation of chiral complex **146**.

The enantioselectivity achieved in this reaction was measured upon derivatization of the product **139** using enantiomerically pure phenylethylamine[63] by GC-analysis of the resulting diastereomeric enamine **147**. Other methods, such as chiral GC or NMR-experiments with chiral shifting reagents, have failed.

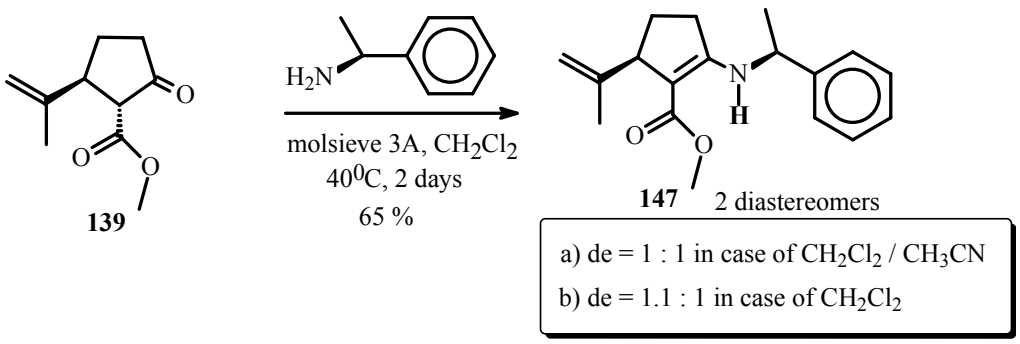

Scheme 64: The confirmation of the enantioselectivity in the reaction.

The loss of chirality in case a) (Schemes 63 and 64) was seemingly due to a quick ligand exchange which is typically promoted by polar protic or aprotic well coordinating solvents, such as acetonitrile or methanol. Alternatively (case b), Schemes 63 and 64), the reaction was performed in unpolar poorly coordinating solvent, such as pure dichloromethane, with an aim to suppress the ligand exchange. On the other hand, a lower solubility of the Cu(II)-acetate and $NMQ \cdot PF_6$ in this unpolar solvent contributes to the prolonged (up to 4 days) reaction time.

The low enantiomeric excess (about 10 %) was the next question to tackle. To solve it a possible structure of the chiral complex **146** was examined using quantum mechanical calculations performed using combined MM-DFT method (resulted structures are depicted in the Abstract, for Cartesian coordinates and heats of formation see also Chapter 5.7).

Calculated structure shows that the chiral ligand **135** does not provide the substrate with sufficient shielding of the reactive site making only some sterical hindrances resulting in a low enantioselectivity. A partial decomposition of the complex **146** leading most probably to the symmetrical bis-(semicorrinato)-Cu(II)- and bis-(ketoester)-Cu(II)-complexes over prolonged reaction time and results in a formation of the racemic product **139** (*via* **138**→**139**, Scheme 58) hence decreasing the enantioselectivity of the reaction.

The structure of the chiral Cu(II)-complex **146** obtained from the calculation shows, that it has the distorted square-planar conformation with distortion angle about 48^0 which is in a good agreement with literature data[64]. On the other hand, further calculations showed that in case of tetrahedral complexes better shielding of the reactive site can be achieved using semicorrin (**135**). Literature provides information that for Zn(II)-complexes most common is the tetrahedral arrangement[64]. Calculations performed with analogous to **146** Zn(II)-complex result in a typical tetrahedral structure (see Abstract and Chapter 5.7.2) with a distortion angle about 85^0. In this case the shielding seems to be sufficient to achieve higher enantioselectivity. Unfortunately, all attempts to synthesize analogous to **138** Zn(II)-complex, with an aim to synthesize a chiral Zn(II)-complex with semicorrin (**135**) and substrate (**132**) using applied for synthesis of Cu(II)-complexes methodology failed.

3.4 Quantum mechanical calculations to establish the viability of the crucial macrocyclization

In support of the future synthetic project (see Outlook, Chapter 4.1), quantum mechanical calculations (conformational analysis and geometry optimization) of potential substrates (analogs of **148**) for the macrocyclization in Cu(II)-complexes were performed. These calculations are expected to provide the information regarding connection between substituents at key positions and non all-chair pre-folded conformations. Initial calculations have shown that the alcohol group without protection (**148a**) has to be avoided (Table 2). The *tert*-butyl protected alcohol (**148b**), which is a good conformational anchor, provides the necessary pro-taxol conformation (Table 3).

During the conformational analysis the following assumptions were made: The energy barrier for conformational rotation is about 4-6 kcal/mol; the molecule is not absorbing energy from outside and hence the assumed barrier for conformational rotation should not be overcome. The calculations were performed for room temperature conditions; thus for reactions at lower temperature these assumptions should also be valid.

Finally, all calculations were performed for molecules in vacuum and the substrate-solvent interactions were not taken into account. On the other hand, well described substrate-solvent interactions exist for water, cyclohexane and decane. But all of them are not exactly reflecting the authentic reaction conditions, namely the reactions performed in dichloromethane. Polar solvents, such as water, turn substrates into all-chair pre-folded conformations and are not suitable for this approach. In terms of polarity, decane and cyclohexane are closer to dichloromethane. However, the use of this solvents for the calculation will drastically increase the calculation time but will only marginally improve the results.

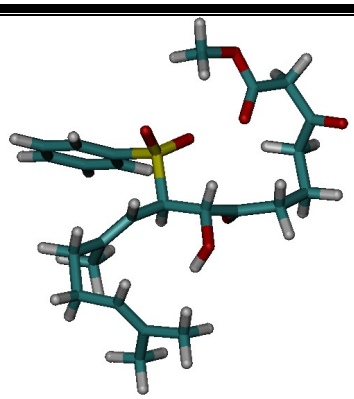	**77.4390299 kcal/mol**
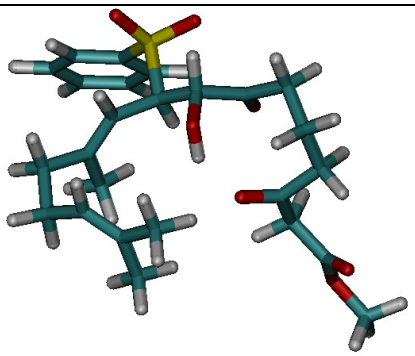	**77.5485209 kcal/mol**
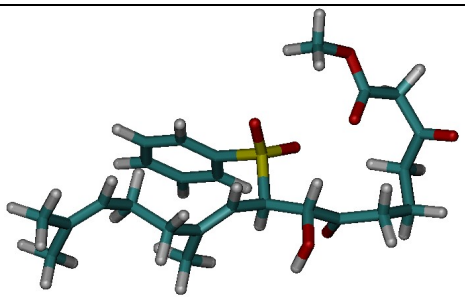	**77.8992429 kcal/mol**
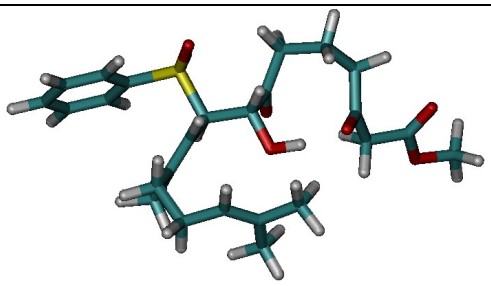	**77.9585099 kcal/mol**

Table 2: Calculated structures and energies of the unprotected alcohol (**148a**).

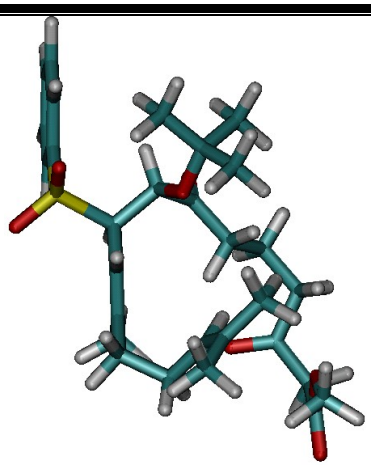	**100.683408 kcal/mol**
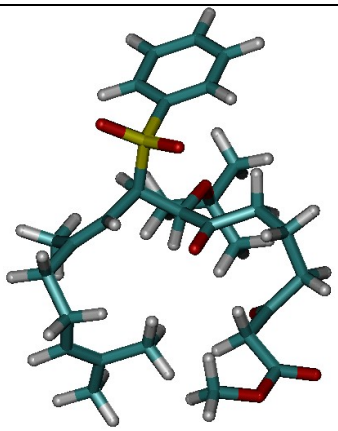	**104.477332 kcal/mol**
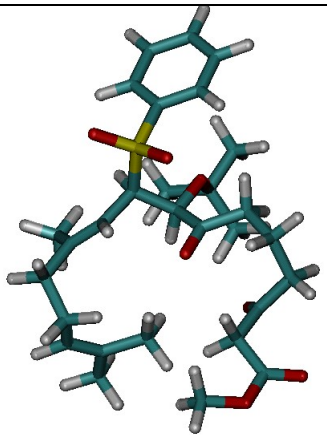	**104.477332 kcal/mol**
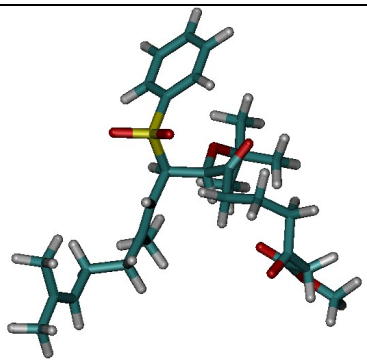	**104.933582 kcal/mol**

Table 3: Calculated structures and energies of the *tert*-Bu-protected alcohol (**148b**).

As one can see, the substrate **148a** is conformationally very flexible due to the absence of the bulky substitutents at the key positions (starred positions, see Abstract). The difference in energy for the most favorable conformers is minimal (Table 2).

A different result is obtained in case of the *tert*-butyl-protected alcohol **148b** (Table 3). The *tert*-butyl group makes the conformational rotation around the central bond much more difficult. The energy difference between first and second energetically favorable conformers is already at nearly 4 kcal/mol and is on the edge of the conformational rotation energy. This fact leaves the hope for successful accomplishment of the key step involving macrocyclization which could beneficially include the further cyclization steps required to establish the taxane skeleton.

Not only the *tert*-butyl group, but a number of other bulky protecting groups could be used, for example the isopropyl group. Prior to applications of such groups quantum mechanical calculations prior to the synthesis are urgently recommended.

4. Outlook

4.1 Cu(II)-mediated processes

In general, Cu(II)-mediated processes should be looked at in more detail. Some considerations based on previously obtained results are summarized below.

- In the cyclization in Cu(II)-complexes one should avoid a competition between possible formation of a 5-membered ring, which is not desirable (right path in the picture), and macrocyclization (left path in the picture) being dependent on the substrate conformation in complex.

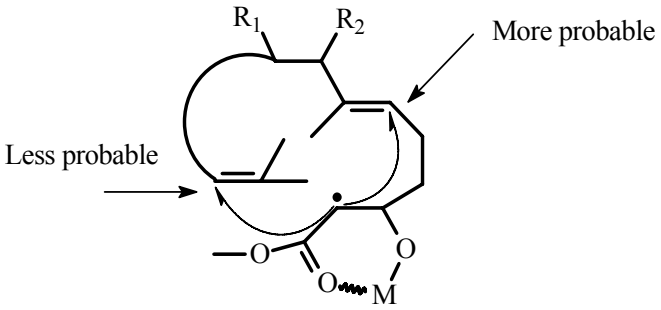

- The choice of wavelengths for irradiation should not interfere with the absorption of the substrate (complex) but will only lead to excitation of the acceptor(s). Otherwise, it could cause conformational changes which finally will lead to undesired products.
- Due to use of free Cu(II)-acetate as a co-oxidant in macrocyclization the low temperature which is usually preferable for enantioselective processes is not necessary because the Cu(II) oxidative activity drops at low temperature. High temperature should also be avoided, due to possible conformational changes.

Finally a new (retrosynthetic) access to the general precursor for the macrocyclization *via* Cu(II)-complexes is depicted below.

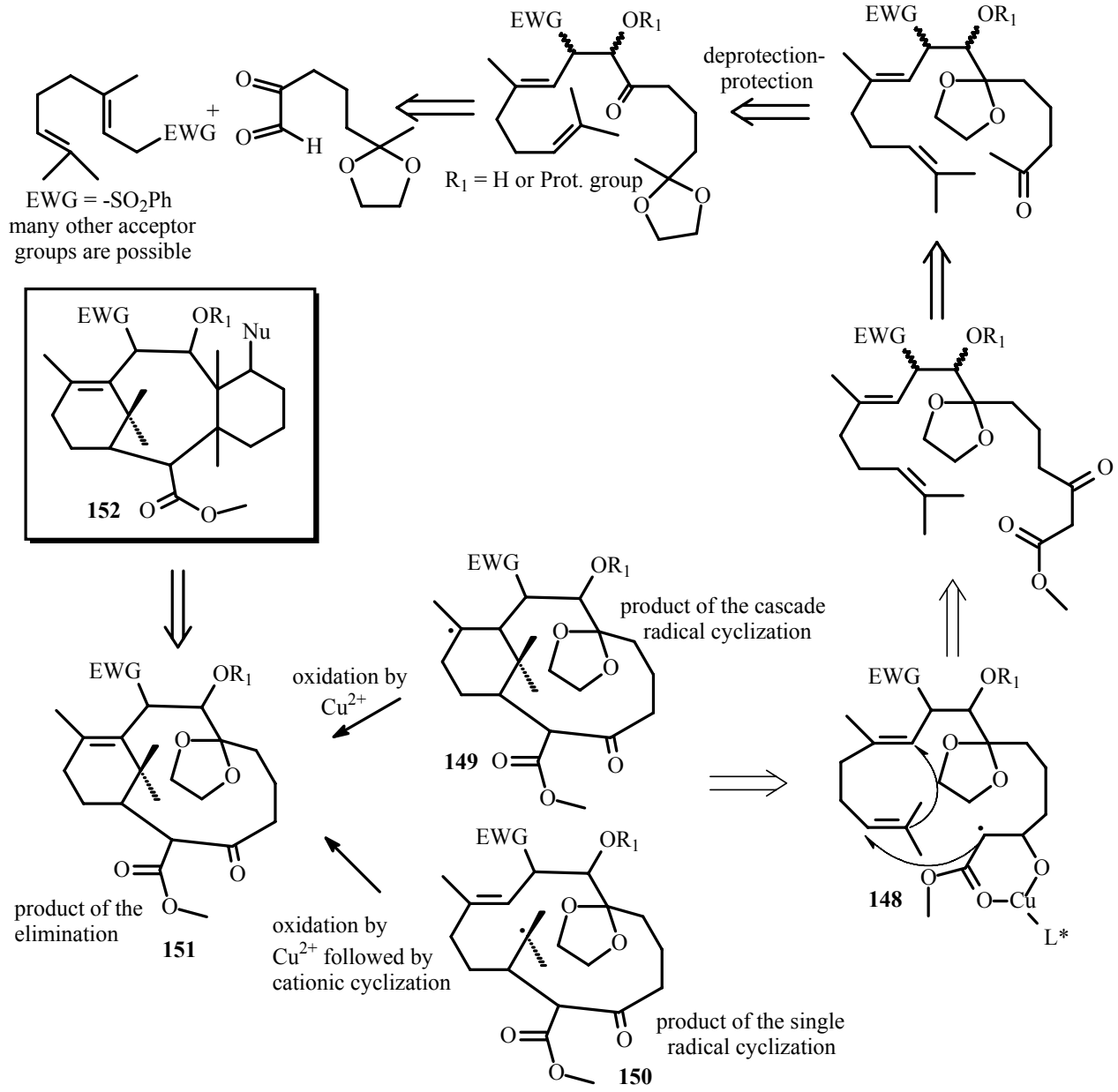

Scheme 65: Retrosynthetically presented synthetic strategy to the basic taxane skeleton.

In this strategy the radical macrocyclization in Cu(II)-complex **148 (→149** or **150**) is the key step and is the most challenging. According to the proposed reaction mechanism the enolic double bond should be oxidized selectively. It is difficult to predict which type of cyclization (cascade radical or only radical monocyclization) will take place to form either **149** or **150**. In the first case the free Cu(II)-acetate should oxidize the radical **149** to the cation and then lead

to elimination forming **151**. The second variant involves oxidation of the tertiary radical **150** and cationic cyclization, followed by elimination (→**151**).

Another crucial point is the formation of cycles B and C of the basic taxane skeleton (**151→152**). It is planned to achieve this goal *via* ring enlargement.

This synthetic strategy combines advantages of selective oxidation of enolic double bonds, connected to the metal center, and the use of free Cu(II)-acetate in combination with efficient synthesis of acyclic and differently substituted geranylgeranyl derivatives.

4.2 Ionic cyclizations

Besides the Cu(II)-mediated processes still further attempts should be made in the fields of cationic- and anionic-type cyclizations en route, *e.g.* to the basic taxane skeleton.

4.3 Calculations

All ionic approaches as well as radical-mediated macrocyclizations (see Chapter 4.1) should be accompanied by computational analysis.

4.4 Biochemical approach

Major attempts should involve enzymatic processes for the macrocyclization step, including further cyclizations to the A/B/C rings of the taxane/taxadiene skeleton. For this purpose the reaction properties of taxadiene cyclase[65] should be tested.

Taxadiene synthase plasmide + *E. coli* ⟶ Overproduction of *Taxadiene synthase*

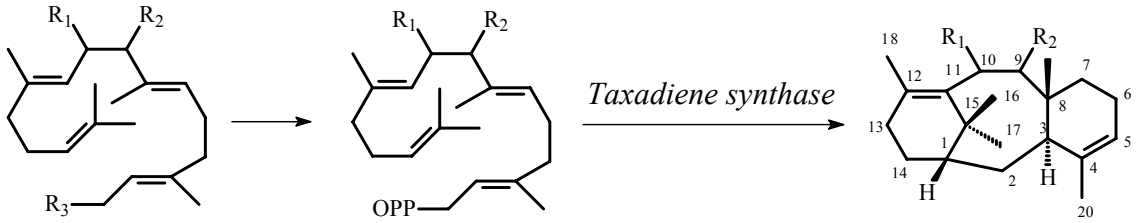

In case of unsuccesfull cyclization ⟶ Selective mutation of the active site environment

5. Experimental section

At this point I would like to thank the following co-workers of the Max Planck Institute for Bioinorganic Chemistry and the Max Planck Institute for Coal Research (Mülheim an der Ruhr) for their most valuable services: Mrs. K. Sand, Mr. J. Bitter (NMR spectra); Mr. W. Schmoeller and Mr. W. Joppek (MS spectra); Mrs. G. Schmitz, Mrs. U. Westhoff and Mrs. M. Trinoga (GC and HPLC analysis); Mr. E. Bothe (CV measurements). My appreciation is also extended to all the members of the administration, library staff and technical staff of the Max Planck Institute for Bioinorganic Chemistry, whose assistance has made the completion of this work both possible and enjoyable.

5.1 Instruments, methods and materials

Infrared spectra (IR):

Recorded with KBr-pressed plates using *Brucker IFS 66* (FT-IR-Spectrometer) or *Perkin-Elmer 1600* spectrometer. Frequency values are given in cm^{-1}. The symbols s (strong), m (medium) and w (weak) characterize the relative band intensities.

Ultraviolet absorption spectra (UV):

Recorded on Cary 17 or Bruins Omega-10 spectrometers. λ_{max} values are given in nm; ε values are given in parentheses.

Mass spectra (MS):

Recorded on *Finnigan MAT 311A* or *MAT 95* (HRMS) instrument at 70 eV ionisation energy. Data are presented in m/z values. When required, molecular ion peaks were ascertained by chemical ionisation (CI), electron ionisation (EI) or fast atom bombardment (FAB) techniques.

Nuclear Magnetic Resonance spectra (NMR):

Recorded in *Fourier* Transform mode on the following *Brucker* instruments: a DRX-500 (500 MHz for ^{1}H, 125.8 MHz for ^{13}C), an AM-400 (400 MHz for ^{1}H, 100.6 MHz for ^{13}C), or a ARX-250 (250 MHz for ^{1}H, 62.9 MHz for ^{13}C) with dilute solutions in deuteriochloroform ($CDCl_3$) at 300 K unless stated otherwise. Chemical shift values are given in δ units (parts per million, ppm). All coupling constants, *J*, are reported in Hz. The multiplicity of a signal is

designated by one of the following abbreviations: s (singlet), d (doublet), t (triplet), q (quartet), m (multiplet) and br (broad). NOE: abbreviations: s (strong), m (medium) and w (weak).

Gas chromatographic analysis (GC):

Chromatograms were recorded on *Hewlett-Packard HP 5890* and *HP 6890* instruments equipped with a flame ionisation detector (FID) and capillary columns 15 m RTX-65TG S-56 and 30 m RTX-65 S-57, respectively. Hydrogen was used as a carrier gas. Conditions are given in the following sequence: type of the column, the length of the column, starting temperature [^{0}C], heating rate [^{0}C /min], final temperature [^{0}C]. Unless stated otherwise, the standard chromatography runs involved an initial column temperature of 60 ^{0}C or 80 ^{0}C with 6 ^{0}C or 8 ^{0}C/min increments, an injector temperature of 230 ^{0}C and a detector temperature of 250 ^{0}C.

Thin layer chromatography (TLC):

Performed on *Merck* silica gel 60 F_{254} precoated aluminium plates. Solution containing 30 g vanillin, 5 ml conc. H_2SO_4, and 1000 ml ethanol or 2 g $KMnO_4$, 5 g K_2CO_3 and 100 ml water was used as a development reagent. The plates were visualized with UV light and then were thermally developed.

Column chromatography:

Gravimetric columns or high pressure variant on self-packed *Kronlab Sepakron-FPGC* glass columns of different sizes on *Merck* silica gel 60 (0.063-0.20 or 0.04-0.063 mm) with pressure pumps *Buechi 688* or *Besta E-100* and pressure 1-10 bar were used. All solvents were distilled before use.

Cyclovoltammographic measurements:

Oxidation potentials were measured on the Princeton Applied Research 273 A instrument. The graphite electrode (∅ = 2 mm) was used as a stationary electrode. $Ag/AgNO_3$ electrode was used as a reference electrode and platinum as a counter electrode was used. Tetra-*n*-butylammoniumhexafluorophosphat (TBAF) was used as a conducting salt and a Ferrocene was used as an internal standard. All measurements were performed in acetonitrile solution.

Irradiations:

All samples were stirred and flushed with argon prior to irradiation. Cylindrical *Pyrex* reaction vessels equipped with cooling finger (*i*-PrOH or H_2O coolant) were used. *Rayonet* reactors

(RPR-100-System, Southern New England Ultraviolet company) with sixteen 300 or 350 nm (λ_{max}) lamps (8 Watt/lamp) were employed.

Solvents:

Purchased from *Merck*, *Aldrich* or *Fluka* and used directly or purified by a standard procedures. Absolute solvents were purchased from *Fluka* and kept under molecular sieves. If necessary, the absolution was performed using the standard methods[66].

Reagents:

The chemical name, abbreviated molecular formula (within parentheses, if appropriate), quality, purification procedure and company of purchase are listed below:

Ammonium chloride: 99 %, *Merck*.

Benzoyl chloride: 99 %, *Merck*

Biphenyl (BP): 99 %, *Fluka*.

Boron trifluoride ethyl etherate ($BF_3 \cdot Et_2O$): BF_3-contetnt of 46.5-49.5 %, *Fluka*.

***tert*-Butyldimethylsilyl chloride (TBDMSCl):** > 97 %, *Fluka*.

n-Butyllithium (n-BuLi): 15 % solution (ca. 1.6 M) in hexane, *Aldrich*.

***tert*-Butyl-2,2,2-trichloroacetimidate:** 96 %, *Aldrich*.

Chloroform-d1 (Deuterochloroform): Deuteration > 99.5 %, *Deutero GmbH*.

3-Chloroperbenzoic acid (MCPBA): 70 %, *Fluka.*

Copper(II) acetate monohydrate ($Cu(OAc)_2 \cdot H_2O$): 98 %, *Fluka*.

1,4-Dicyano-2,3,5,6-tetramethylbenzene (DCTMB): Prepared from 1,2,4,5-tetramethyl-benzene (durene) according to Suzuki procedure, with only a difference that the DMF instead of HMPT was used[24].

Diethyl malonate: 98 %, *Merck*.

Dimethyl carbonate: 99 %, *Fluka*.

6,10-Dimethyl-undeca-5,9-dien-2-one (*trans*-Geranylacetone): 98 %, *Fluka.*

all-*trans*-Farnesol: > 99 %, distilled from isomeric mixture (95 %, *Aldrich*) at b.p. 92-94 ^{0}C under 0.1 torr (Spaltrohrkolonne, Fa, Fischer).

all-*trans*-Farnesyl acetate: 98 %, *Aldrich*.

Ferrocene : 98 %, *Fluka*.

Geranyl acetate: 98 %, *Aldrich*.

Geraniol: 98 %, *Aldirch*.

Lithium aluminum hydride (LAH): 97 %, *Aldrich*.

Lithium chloride: 99 %, *Fluka*.

Lithium diisopropylamide (LDA): 2M solution in THF/ Heptane / Ethylbenzene, *Fluka*.

Methyl acetoacetate: 99 %, *Aldrich*.

R(+)-α-Methylbenzylamine (R(+)-1-Phenyl-ethylamin): 98 %, *Fluka*.

3-Methyl-but-2-en-1-ol (Prenol): 98 %, *Aldrich*.

6-Methyl-hept-5-en-2-one (Prenylacetone): 98 %, *Fluka*.

Methyl iodide: 99%, *Fluka*.

Mn(III) acetate dihydrate ($Mn(OAc)_3 \cdot 2H_2O$): 97 %, *Fluka*.

N-methylquinoliniumhexafluorophosphate (NMQ-PF_6): Prepared according to the literature procedure[67].

Phosphorus tribromide (PBr3): 99 %, *Fluka*.

Potassium hexafluorophosphate (KPF_6): 99%, *Aldrich*.

Quinolin: 97%, *Fluka*.

Selenium dioxide: 97 %, *Fluka*.

Sodium hydride (NaH): 55-60 % by wt. dispersion in mineral oil, *Fluka*.

Sodium hydroxide (NaOH): flakes, z. A. *Merck*.

Trifluoroacetic acid: 99 %, *Fluka*.

Quantum mechanical calculations: Performed on a Silicon Graphics O_2 workstation, using the Spartan program for calculations. The conformational analysis was performed using the MMFF94 force field with the following assumptions:

- The difference in energy for the whole number of conformers was assigned to be 10 kcal/mol. All conformers with energy difference values above were cutted off.
- The conformational rotation angle was assumed 120^0. At the most important positions it was compressed up to 60^0.

Geometry optimisation of the complexes was performed using MMFF94 force field for pre-optimisation and the DFT method with NLSDA/BP86/DN* as model was applied for final geometry optimisation.

5.2 Nomenclature and general synthetic procedures

Nomenclature: Compounds have been named according to the standard nomenclature rules (IUPAC) by means of the program *AUTONOM*. In some cases the numbering system was chosen differently in order to facilitate correlation with NMR signal assignments.

General synthetic procedures: A cooling bath of –20 ^{0}C to –78 ^{0}C consisted of a mixture of "dry ice" (CO_2) and acetone. Oxygen- or moisture-sensitive reactions were performed under an argon flow in either oven- or heat gun-dried glassware equipped with a rubber septum. Air- or moisture-sensitive liquids and solutions were transferred by a syringe; solids were transferred through the funnel under a rapid argon flow. "Concentration" involved drying the combined organic layers over anhydrous Na_2SO_4, filtration and removal of the solvent(s) by rotary evaporation and/or at high vacuum (10^{-1} - 10^{-3} torr).

5.2.1 General procedure for the PET-initiated reactions with $Cu(OAc)_2$ as a cooxidant

5.2.1.1 Typical procedure when water was used as the nucleophile

In a representative procedure, the substrate (1 equiv., about 0.005 mol), biphenyl (0.9 mol equiv.), DCTMB (0.25 mol equiv.) and $Cu(OAc)_2 \cdot H_2O$ (1 equiv.) were dissolved in MeCN/H_2O 10/1 (500 ml) and the resulting solution was stirred and degassed (argon) for 0.5 h inside the cylindrical *Pyrex* irradiation vessel equipped with a cooling finger (isopropanol as the coolant, -15 ^{0}C) prior to be placed in a *Rayonet* reactor (λ_{max} = 300 nm). Upon irradiation for about 12 h a copper mirror was formed. The reaction vessel was changed and the reaction mixture degassed again for additional 0.5 h before the irradiation was continued. In the next 12 h the reaction was completed (with a conversion of about 95 %, monitored by TLC). After evaporation of the solvent mixture, the residue was chromatographed on a silica gel column using pentane/ether mixtures as eluant.

If $Mn(OAc)_3$ was used, 2 equiv. of this reagent were added to the reaction mixture. The resulting dark brown reaction mixture was irradiated during 3 days and then filtered from the $Mn(OAc)_2$ precipitate and concentrated. Products were isolated by column chromatography (silica gel) using pentane/ether mixtures as eluant.

5.2.1.2 Typical procedure when methanol was used as the nucleophile

In a representative procedure, the irradiation wavelength, amount and proportion of acceptor/co-acceptor, temperature and the amount of Cu(II)-acetate were the same as described in chapter 5.2.1.1. The solvents and solvent proportions were changed from MeCN/H_2O 10/1 to MeCN/MeOH 4/1. 2 mol equivalents of Mn(III)-acetate were added to the reaction mixture in order to prevent formation of the Cu-mirror. The resulting dark brown mixture was stirred and degassed with argon for 0.5 h in a cylindrical *Pyrex* irradiation vessel prior to the transfer to a *Rayonet* reactor for irradiation. The irradiation was conducted up to 3 days (TLC control has shown nearly complete conversion after 3 days). During this time the colour of the reaction mixture changes from dark brown to transparent light green-blue. Additionally, light rose precipitation of Mn(II)-acetate was formed. The precipitation was removed by filtration and solvent was removed in vacuum resulting in a residue which was purified further by column chromatography (see previous chapter).

5.2.2 General procedure for the irradiation of Cu(II)-complexes

N-methylquinoliniumhexafluorophosphate (1.1 equiv.), biphenyl (0.9 equiv.) and Cu(II)-acetate (1 equiv.) were dissolved or suspended in 100 ml of dry dichloromethane or in 100 ml of 4/1 dichloromethane/acetonitrile mixture and the resulting reaction mixture was stirred and degassed under argon for 30 min in a cylindrical *Pyrex* irradiation vessel equipped with a cooling finger (isopropanol as a coolant, -15 ^{0}C or water at room temperature). This Cu(II)-complex (chiral or achiral) (1 equiv., about 1 mmol) was then added in 2-5 ml of degassed dry dichloromethane to reaction mixture. The mixture was irradiated in a *Rayonet* reactor (λ_{max} = 300 nm or λ_{max} = 350 nm) for 2-4 days (monitoring by TLC). During this time a Cu-mirror was formed. The reaction mixture was then transferred into a round bottom flask and the reaction vessel was washed twice with dichloromethane. The combined organic phases were concentrated. The resulting residue was dissolved or suspended in ether/dichloromethane 10/1 and was bubbled with H_2S for 1-2 min in order to precipitate Cu^{2+}-ions and remove all organic molecules from the complex. The resulting dark brown suspension was degassed (argon) for 30 min. and the precipitation was filtered off, washed twice on a filter with ether before concentration. The crude mixture was chromatographed on silica gel using n-pentane/ether mixtures as eluant.

5.3 Synthesis of pro-taxoid precursors and attempts toward their cyclization *via* cationic and anionic pathways

5.3.1 Synthesis of acetic acid 9-benzenesulfonyl-8-hydroxy-3,7,11,15-tetramethyl-hexadeca-2,6,10,14-tetraenyl ester (87)

2.5 M *n*-Butyllithium solution in hexane (5.6 ml, 14 mmol) was added dropwise to a stirred solution of (E)-geranyl phenyl sulphone[47] (3.54 g, 12.7 mmol) in absolute tetrahydrofuran (30 ml) at – 78 ^{0}C under an argon flow. After 20 min being stirred, the acetic acid 3,7-dimethyl-8-oxo-octa-2,6-dienyl ester (2.89 g, 13.7 mmol) in absolute tetrahydrofuran (15ml) was added dropwise. After additional 1 h of stirring at – 78 ^{0}C a saturated NH_4Cl solution in water was added dropwise (10 ml) and the mixture was allowed to warm to room temperature and was stirred at this temperature for 15 min. The mixture was diluted with ether and the organic layer washed with brine and dried over Na_2SO_4. After concentration and column chromatography using n-pentane/ether 3/1 $\rightarrow$ 1/1 a mixture of two diastereomers in a 1 : 3.5 proportion (5.16 g, combined yield of 83 %) was isolated as a light yellow oil.

Acetic acid 9-benzenesulfonyl-8-hydroxy-3,7,11,15-tetramethyl-hexadeca-2,6,10,14-tetraenyl ester (87):

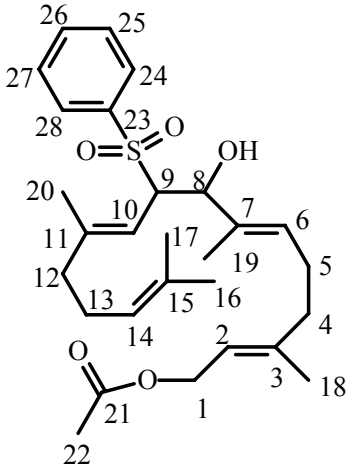

87

IR (KBr): υ_{max} 3488 s, 3063 m, 2925 s, 2731 w, 2443 w, 2219 w, 1974 w, 1902 w, 1735 s, 1663 s, 1585 m, 1448 s, 1384 s, 1296 m, 1141 m, 1083 m, 1023 m, 854 w, 715 w, 689 w, 620 w, 579 w, 541 w;

^{1}H NMR (400 MHz, ^{1}H-^{1}H-COSY, $CDCl_3$):

δ: 7.81 (d, J = 7.9 Hz, 2H, HC-**24**, HC-**28**); 7.58 (t, J = 6.2 Hz, 1H, HC-**26**); 7.47 (t, J = 7.9 Hz, 2H, HC-**25**, HC-**27**); 5.44 (t, J = 7.9 Hz, 1H, HC-**6**); 5.35 (d, J =

10.7 Hz, 1H, HC-**10**); 5.26 (t, J = 8.2 Hz, 1H, HC-**2**); 4.97 (br. s, 1H, HC-**14**); 4.93 (br. s, 1H, HC-**8**); 4.51 (d, J = 7.1 Hz, 2H, H_2C-**1**); 3.79 (dd, J = 1.8, 10.7 Hz, 1H, HC-**9**); 2.96 (d, J = 2.5, 1H, HO); 2.06 (m, 2H, H_2C-**5**); 1.99 (s, 3H, H_3C-**22**); 1.98 (m, 2H, H_2C-**4**); 1.90 (m, 4 H, H_2C-**13,** H_2C-**12**)1.63 (s, 6H, H_3C-**16**, H_3C-**17**); 1.54 (s, 3H, H_3C-**18**); 1.50 (s, 3H, H_3C-**19**); 1.10 (s, 3H, H_3C-**20**);

^{13}C NMR (100 MHz, BB, DEPT, ^{1}H-^{13}C-COSY, $CDCl_3$):

δ: 170.97 (Cq, C-**21**); 146.35 (Cq, C-**11**); 141.59 (Cq, C-**3**); 137.94 (Cq, C-**23**); 133.51 (Cq, C-**7**); 133.40 (CH, C-**26**); 131.85 (Cq, C-**15**); 129.05 (CH, C-**25**); 128.99 (CH, C-**27**); 128.68 (CH, C-**24**); 128.63 (CH, C-**28**); 126.48 (CH, C-**6**); 123.50 (CH, C-**14**); 118.47 (CH, C-**2**); 111.90 (CH, C-**10**); 72.25 (CH, C-**8**); 67.79 (CH, C-**9**); 61.21 (CH_2, C-**1**); 39.73 (CH_2, C-**12**); 38.83 (CH_2, C-**4**); 26.19 (CH_2, C-1**3**); 25.74 (CH_2, C-**5**); 25.55 (CH_3, C-**16**); 20.90 (CH_3, C-**22**); 17.56 (CH_3, C-**18**); 16.35 (CH_3, C-**20**); 16.32 (CH_3, C-**17**); 13.04 (CH_3, C-**19**)

MS (EI) m/z (rel. int.):

488 (M^+, $C_{28}H_{40}O_5S^+$)(0.4), 209 (32.2), 151 (13), 137 (51), 136 (27.4), 121 (20.7), 107 (9.1), 95 (13), 93 (26.8), 84 (9.8), 82 (8.4), 81 (44.7), 77 (11.4), 69 (100), 68 (8.7), 67 (17.5), 55 (17), 43 (45.5), 41 (37.9).

HRMS ESIpos : m/z calcd for $C_{28}H_{40}NaO_5S$ (M+Na) :

511.249417. Found: 511.24902.

5.3.2 Synthesis of acetic acid 9-benzenesulfonyl-8-benzoxy-3,7,11,15-tetramethyl-hexadeca-2,6,10,14-tetraenyl ester (88)

Alcohol **87** (1 g, 2 mmol) was dissolved in 1 ml of absolute dichloromethane. Benzoyl chloride (0.32 g, 2.25 mmol, 1.1 equiv.) was added dropwise, followed by rapid addition of 1 ml of dry pyridine. The mixture was allowed to stir overnight at room temperature, then diluted with ether and the precipitate of pyridinium hydrochloride was removed by filtration and washed twice with ether. The solvent was removed in vacuum and the product was purified by a column chromatography using *n*-pentane/ether 3/1 → 1/1 as eluant to give 1.15 g (95 % yield) of compound **88** in form of a light yellow oil.

Acetic acid 9-benzenesulfonyl-8-benzoxy-3,7,11,15-tetramethyl-hexadeca-2,6,10,14-tetraenyl ester (88):

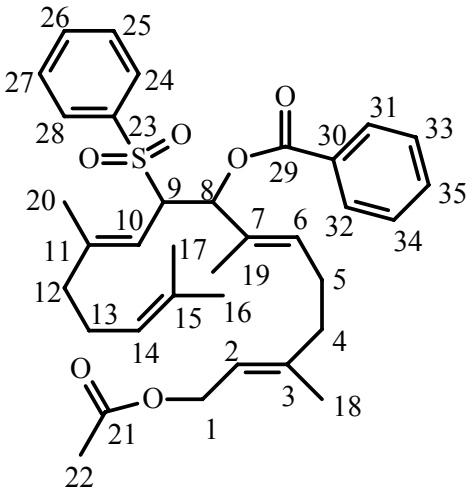

88

IR (KBr): υ_{max}, 3063 m, 2923 s, 2337 w, 2226 w, 1968 w, 1910 w, 1725 s, 1663 s, 1602 m, 1585 m, 1448 s, 1384 s, 1306 s, 1265 s, 1177 m, 1144 s, 1107 m, 1025 m, 954 m, 846 w, 804 w, 743 m, 712 m, 688 m, 585 m, 536 m;

^{1}H NMR (500 MHz, ^{1}H-^{1}H-COSY, $CDCl_3$):

δ: 7.83 (d, J = 8.2 Hz, 2H, HC-**31**, HC-**32**); 7.78 (d, J = 7.7 Hz, 2H, HC-**24**, HC-**28**); 7.47 (t, J = 7.3 Hz, 1H, HC-**26**); 7.32 (m, 5H, HC-**35**, HC-**33**, HC-**34**, HC-**25**, HC-**27**); 5.85 (d, J = 9.3 Hz, 1H, HC-**8**); 5.59 (t, J = 7.8 Hz, 1H, HC-**6**); 5.24 (t, J = 7 Hz, 1H, HC-**2**); 4.99 (br. s, 1H, HC-**14**); 4.87 (d, J = 10.8 Hz, 1H, HC-**10**); 4.48 (d, J = 7.1 Hz, 2H, H_2C-**1**); 4.35 (t, J = 9.4 Hz, 1H, HC-**9**); 2.05-1.99 (br. m, 4H, H_2C-**4**, H_2C-**12**); 1.98 (s, 3H, H_3C-**22**); 1.95 (br. s, 4H, H_2C-**5**, H_2C-**13**); 1.64 (s, 3H, H_3C-**16**); 1.61 (s, 3H, H_3C-**20**); 1.55 (s, 3H, H_3C-**17**); 1.50 (s, 3H, H_3C-**19**); 1.48 (s, 3H, H_3C-**18**);

^{13}C NMR (125 MHz, BB, DEPT, ^{1}H-^{13}C-COSY, $CDCl_3$):

δ: 170.96 (Cq, C-**21**); 164.78 (Cq, C-**29**); 146.34 (Cq, C-**11**); 141.27 (Cq, C-**3**); 139.38 (Cq, C-**30**); 133.15 (CH, C-**35**); 132.83 (CH, C-**26**); 132.14 (CH, C-**6**); 130.61 (Cq, C-**7**); 130.07 (Cq, C-**15**); 129.64 (CH, C-**31**, C-**32**); 129.16 (CH, C-**24**, C-**28**); 128.71 (CH, C-**33**, C-**34**); 128.27 (Cq, C-**23**); 128.12 (CH, C-**25**, C-**27**); 123.37 (CH, C-**14**); 118.76 (CH, C-**2**); 113.34 (CH, C-**10**); 77.50 (CH, C-**8**); 66.42 (CH, C-**9**); 61.17 (CH_2, C-**1**); 39.79 (CH_2, C-**12**); 38.61 (CH_2, C-**4**); 26.22 (CH_2, C-**5**); 25.83 (CH_2, C-1**3**); 25.66 (CH_3, C-**16**); 20.95 (CH_3, C-**22**); 17.66 (CH_3, C-**17**); 16.69 (CH_3, C-**18**); 16.35 (CH_3, C-**20**); 11.60 (CH_3, C-**19**)

MS **(EI) m/z (rel. int.):**

451 (6.1), 269 (7.1), 201 (7.5), 145 (2.8), 133 (5.2), 121 (4.9), 119 (3.4), 106 (7.6), 105 (100), 93 (4), 81 (3.7), 77 (7.7), 69 (15.1), 43 (5.8), 41 (4.6)

HRMS **ESIpos : m/z calcd for $C_{35}H_{44}NaO_6S$ (M+Na) :**

615.275632. Found: 615.27561.

5.3.3 Synthesis of 1,9-bis-benzenesulfonyl-3,7,11,15-tetramethyl-hexadeca-2,6,10,14-tetraen-8-ol (90)

Under argon flow 2.5 M *n*-Butyllithium solution in hexane (1.2 ml, 3.1 mmol) was added dropwise to a stirred solution of (E)-geranyl phenyl sulphone **86** (0.77 g, 2.8 mmol) in absolute tetrahydrofuran (7 ml) at – 78 ^{0}C. After 20 min stirring the aldehyde **89** (0.89 g, 3.1 mmol) in absolute tetrahydrofuran (3 ml) was added dropwise. After additional 1 h of stirring at – 78 ^{0}C the saturated NH_4Cl solution in water was added dropwise (5 ml) and the mixture was allowed to warm to room temperature and then stirred for 15 min. The mixture was diluted with ether and the organic layer was separated, washed with brine, dried over Na_2SO_4 and concentrated. Further column chromatography, using *n*-pentane/ether 3/1 → 1/1, resulted in 1.27 g of a light yellow oil **90** as a mixture of two diastereomers (proportion 1 : 3.5) in combined yield of 80 %.

1,9-Bis-benzenesulfonyl-3,7,11,15-tetra-methyl-hexadeca-2,6,10,14-tetraen-8-ol (90):

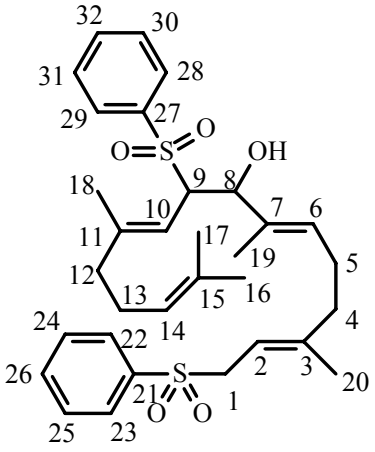

90

^{1}H NMR **(400 MHz, ^{1}H-^{1}H-COSY, $CDCl_3$):**

δ: 7.79 (d, J = 8.2 Hz, 4H, HC-**22**, HC-**23**, HC-**28**, HC-**29**); 7.58 (m, 2H, HC-**26**, HC-**32**); 7.48 (t, J = 8.1 Hz, 4H, HC-**24**, HC-**25**, HC-**30**, HC-**31**); 5.28 (t, J = 6.5

Hz, 1H, HC-**6**); 5.10 (t, J = 7.2 Hz, 1H, HC-**2**); 4.94 (t, J = 5.8 Hz, 1H, HC-**14**); 4.65 (d, J = 10.8 Hz, 1H, HC-**10**); 4.55 (d, J = 8.6 Hz, 1H, HC-**8**); 4.10 (d, J = 1.1 Hz, 1H, HO); 3.90 (dd, J = 9.1, 10.8 Hz, 1H, HC-**9**); 3.73 (d, J = 7.9 Hz, 2H, H_2C-**1**); 1.99-1.77 (br. m, 8H, H_2C-**4**, H_2C-**5**, H_2C-**12**, H_2C-**13**); 1.63 (s, 3H, H_3C-**16**); 1.52 (s, 3H, H_3C-**17**); 1.42 (s, 3H, H_3C-**19**); 1.27 (s, 3H, H_3C-**18**); 1.08 (s, 3H, H_3C-**20**)

^{13}C NMR (100 MHz, BB, DEPT, ^{1}H-^{13}C-COSY, $CDCl_3$):

δ: 145.62 (Cq, C-**3**); 144.43 (Cq, C-**11**); 138.70 (Cq, C-**21**); 137.45 (Cq, C-**27**); 133.78 (CH, C-**26**); 133.46 (CH, C-**32**); 131.94 (Cq, C-**7**); 129.29 (Cq, C-**15**); 129.17 (CH, C-**6**); 128.89 (CH, C-**22**, C-**23**); 128.75 (CH, C-**28**, C-**29**); 128.33 (CH, C-**24**, C-**25**); 128.33 (CH, C-**30**, C-**31**); 123.24 (CH, C-**14**); 114.22 (CH, C-**10**); 110.57 (CH, C-**2**); 76.31 (CH, C-**8**); 68.40 (CH, C-**9**); 55.91 (CH_2, C-**1**); 39.47 (CH_2, C-**12**); 38.86 (CH_2, C-**4**); 26.14 (CH_2, C-**13**); 25.55 (CH_2, C-**5**); 25.54 (CH_3, C-**16**); 17.53 (CH_3, C-1**7**); 16.03 (CH_3, C-**18**); 15.14 (CH_3, C-**20**); 10.52 (CH_3, C-**19**)

5.3.4 Synthesis of 1,9-bis-benzenesulfonyl-8-benzoxy-3,7,11,15-tetramethyl-hexadeca-2,6,10,14-tetraen (91)

In analogy to the synthesis described in chapter 5.3.2, the alcohol **90** (0.667 g, 1.17 mmol) was dissolved in 0.5 ml of dry dichloromethane. Benzoyl chloride (0.181 g, 1.28 mmol) was added, followed by addition of 0.5 ml of dry pyridine. The reaction was allowed to stir overnight. The formed precipitate was filtered off, washed twice with ether and the combined organic layers were concentrated under vacuum. Column chromatography using *n*-pentane/ether 5/1→ 1/1 gave 0.73 g (93 %) of **91** in form of a light yellow very viscous oil.

1,9-Bis-benzenesulfonyl-8-benzoxy-3,7,11,15-tetramethyl-hexadeca-2,6,10,14-tetraen (91):

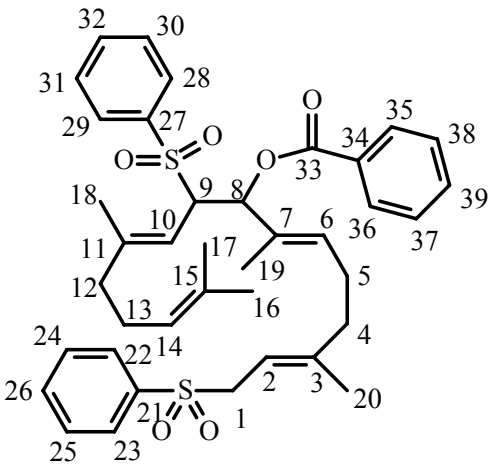

91

^{1}H NMR (400 MHz, ^{1}H-^{1}H-COSY, $CDCl_3$):

δ: 7.75 (m, 6H, HC-**22**, HC-**23**, HC-**28**, HC-**29**, HC-**35**, HC-**36**); 7.52-7.36 (br. m, 4H, HC-**39**, HC-**32**, HC-**37**, HC-**38**); 7.25 (m, 5H, HC-**24**, HC-**25**, HC-**26**, HC-**30**, HC-**31**); 5.83 (d, J = 9.3, 1H, HC-**8**); 5.46 (br. t, 1H, HC-**6**); 5.01 (t, J = 7.6 Hz, 1H, HC-**2**); 4.93 (m, 1H, HC-**14**); 4.81 (d, J = 10.7 Hz, 1H, HC-**10**); 4.33 (t, J = 9.9 Hz, 1H, HC-**9**); 3.63 (d, J = 7.8 Hz, 2H, H_2C-**1**); 1.87 (m, 8H, H_2C-**4**, H_2C-**5**, H_2C-**12**, H_2C-**13**); 1.56 (s, 3H, H_3C-**20**); 1.47 (s, 3H, H_3C-**19**); 1.41 (s, 6H, H_3C-**16**, H_3C-**18**); 1.13 (s, 3H, H_3C-**17**)

^{13}C NMR (62.5 MHz, BB, DEPT, ^{1}H-^{13}C-COSY, $CDCl_3$):

δ: 165.07 (Cq, C-**33**); 146.75 (Cq, C-**3**); 145.72 (Cq, C-**11**); 139.61 (Cq, C-**21**); 138.92 (Cq, C-**27**); 133.95 (CH, C-**26**); 133.60 (CH, C-**32**); 133.27 (CH, C-**39**); 132.20 (Cq, C-**7**); 132.00 (CH, C-**6**); 131.25 (Cq, C-**34**); 130.28 (Cq, C-**15**); 129.95 (CH, C-**22**, C-**23**); 129.34 (CH, C-**28**, C-**29**); 129.10 (CH, C-**35**, C-**36**); 129.05 (CH, C-**24**, C-**25**); 128.69 (CH, C-**30**, C-**31**); 128.51 (CH, C-**37**, C-**38**); 123.75(CH, C-**14**); 113.57 (CH, C-**10**); 111.21 (CH, C-**2**); 77.70 (CH, C-**8**); 66.55 (CH, C-**9**); 56.17 (CH_2, C-**1**); 40.04 (CH_2, C-**12**); 39.07 (CH_2, C-**4**); 26.52 (CH_2, C-**13**); 26.07 (CH_3, C-**16**); 25.99 (CH_2, C-**5**); 18.03 (CH_3, C-**17**); 16.99 (CH_3, C-**18**); 16.34 (CH_3, C-**20**); 11.92 (CH_3, C-**19**)

5.3.5 Synthesis of 1,9-bis-benzenesulfonyl-8-benzoxy-3,7,11,15-tetramethyl-14-oxiranyl-hexadeca-2,6,10-trien (92)

A stirred solution containing 0.65 g (0.96 mmol) of **91**, in 3 ml of dichloromethane, was cooled in an ice bath. A solution of 0.25 g (1.02 mmol) of 70 % m-chloroperoxybenzoic acid (MCPBA) in 2 ml of dichloromethane was added during 10 min, followed by addition of 0.084 g (1.023 mmol) of the anhydrous sodium acetate. The mixture was stirred at 5 ^{0}C for 1 h and then filtered, the liquid phase washed sequentially with aqueous $NaHCO_3$, water, brine and dried over Na_2SO_4. Solvent removal under reduced pressure gave an oil which was purified by column chromatography on silica using *n*-pentane/ether 2/1 → 1/2 as eluant to resulting in 0.6 g (90 %) of **92** as a light yellow oil.

1,9-Bis-benzenesulfonyl-8-benzoxy-3,7,11,15-tetramethyl-14-oxiranyl-hexadeca-2,6,10-trien (92):

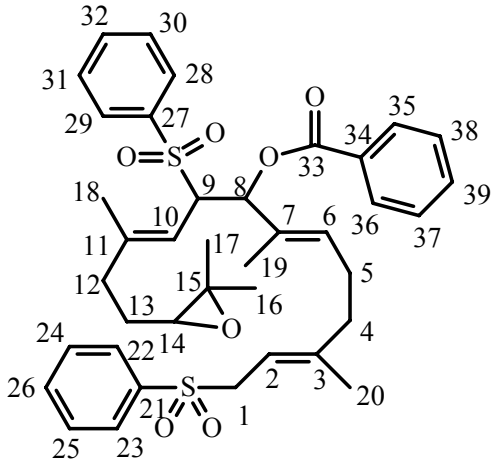

92

^{1}H NMR (400 MHz, ^{1}H-^{1}H-COSY, $CDCl_3$):

δ: 7.77 (m, 6H, HC-**22**, HC-**23**, HC-**28**, HC-**29**, HC-**35**, HC-**36**); 7.57 (t, J = 7.3 Hz, 1H, HC-**39**); 7.47 (m, 3H, HC-**32**, HC-**37**, HC-**38**); 7.31 (m, 5H, HC-**24**, HC-**25**, HC-**26**, HC-**30**, HC-**31**); 5.81 (dd, J = 9.3, 12.4 Hz, 1H, HC-**8**); 5.50 (br. t, J = 5.9 Hz, 1H, HC-**6**); 5.07 (t, J = 7.8 Hz, 1H, HC-**2**); 4.91 (d, J = 10.7 Hz, 1H, HC-**10**); 4.35 (t, J = 9 Hz, 1H, HC-**9**); 3.68 (d, J = 7.9 Hz, 2H, H_2C-**1**); 2.60 (dd, J = 7.1, 12.5 Hz, 1H, HC-**14**); 2.18-2.01 (br. m, 2H, H_2C-**12**); 1.92 (m, 4H, H_2C-**4**, H_2C-**5**); 1.54, 1.52 (2 s, 3H, H_3C-**20**); 1.51-1.37 (br. m, 2H, H_2C-**13**); 1.45 (s, 3H, H_3C-**19**); 1.25 (s, 3H, H_3C-**16**); 1.23 (s, 3H, H_3C-**18**); 1.20 (s, 3H, H_3C-**17**)

^{13}C NMR (100 MHz, BB, DEPT, ^{1}H-^{13}C-COSY, $CDCl_3$):

δ: 164.58 (Cq, C-**33**); 145.52 (Cq, C-**3**); 145.31 (Cq, C-**11**); 139.31 (Cq, C-**21**); 138.64 (Cq, C-**27**); 133.43 (CH, C-**26**); 133.11 (CH, C-**32**); 132.80 (CH, C-**39**); 131.73 (CH, C-**6**); 130.70 (Cq, C-**34**); 129.49 (Cq, C-**7**); 128.87 (CH, C-**22**, C-**23**); 128.67 (CH, C-**28**, C-**29**); 128.61 (CH, C-**35**, C-**36**); 128.59 (CH, C-**24**, C-**25**); 128.27 (CH, C-**30**, C-**31**); 128.04 (CH, C-**37**, C-**38**); 113.75 (CH, C-**10**); 110.75 (CH, C-**2**); 77.31 (CH, C-**8**); 66.26 (CH, C-**9**); 63.30 (CH, C-**14**); 58.16 (Cq, C-**15**); 55.81 (CH_2, C-**1**); 38.60 (CH_2, C-**4**); 36.51 (CH_2, C-**12**); 27.16 (CH_2, C-**13**); 25.62 (CH_2, C-**5**); 24.68 (CH_3, C-**16**); 18.58 (CH_3, C-**17**); 16.59 (CH_3, C-**20**); 15.11 (CH_3, C-**18**); 11.55 (CH_3, C-**19**)

5.3.6 An attempt to cyclize 88 with trifluoroacetic acid

88 (1.5 mmol, 0.89 g) was dissolved in 150 ml of dichloromethane, then it was cooled with dry ice-acetone coolant to –78 ^{0}C. Trifluoroacetic acid (0.14 mol, 15.9 g, 10.75 ml) was added at this temperature and the temperature was increased thereafter to avoid crystallization of trifluoroacetic acid. The course of reaction was monitored by TLC. Due to no reactivity of the substrate, the reaction mixture was refluxed for 3 h. Over this time the starting material disappeared nearly quantitatively. The reaction was quenched with triethylamine (10.74 ml) in 30 ml ethanol and then concentrated. The residue was dissolved in water and extracted with ether. The organic layer was washed with 10 % $NaHCO_3$, brine and concentrated to give a crude product mixture. It was separated by chromatography on silica using pentane-ether 20/1→5/1 as eluant and resulted in two products **93** and **94** in a combined yield of a 65 % (proportion about 1:1), both in form of white crystals accompanied by some amount of starting material.

Acetic acid 9-benzenesulfonyl-8-benzoxy-3,7,11,15-tetramethyl-15-trifluoroacetoxy hexadeca-2,6,10-trienyl ester (93):

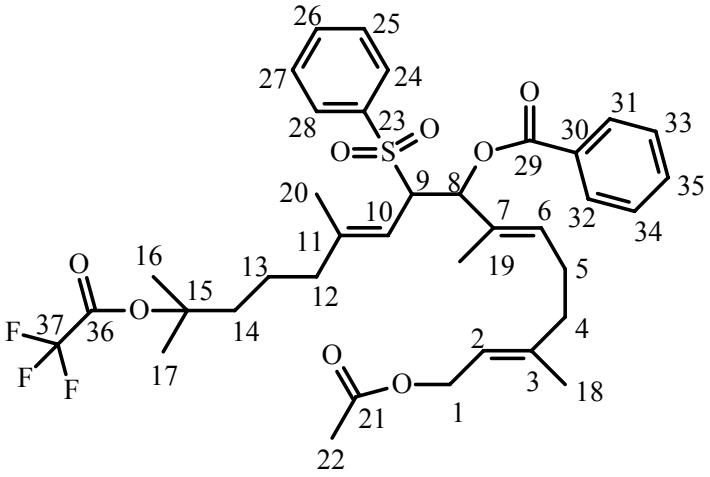

93

^{1}H NMR (400 MHz, ^{1}H-^{1}H-COSY, $CDCl_3$):

δ: 7.71 (m, 4H, HC-**24**, HC-**28**, HC-**31**, HC-**32**); 7.38 (t, J = 7.4 Hz, 1H, HC-**26**); 7.23 (m, 5H, HC-**25**, HC-**27**, HC-**33**, HC-**34**, HC-**35**); 5.80 (d, J = 9.3 Hz, 1H, HC-**8**); 5.53 (t, J = 6.3 Hz, 1H, HC-**6**); 5.18 (dt, J = 1.1, 7.1 Hz, 1H, HC-**2**); 4.83 (d, J = 10.8 Hz, 1H, HC-**10**); 4.40 (d, J = 7 Hz, 2H, H_2C-**1**); 4.32 (dd, J = 9.4, 10.8 Hz, 1H, HC-**9**); 1.98-1.91 (br. m, 8H, H_2C-**5**, H_2C-**12**, H_2C-**13**, H_2C-**14**); 1.89 (s, 3H, H_3C-**22**); 1.63 (m, 2H, H_2C-**4**); 1.53 (s, 3H, H_3C-**18**); 1.45 (s, 3H, H_3C-**20**); 1.41 (s, 9H, H_3C-**16**, H_3C-**17**, H_3C-**19**)

^{13}C NMR (100 MHz, BB, DEPT, ^{1}H-^{13}C-COSY, $CDCl_3$):

δ: 170.69 (Cq, C-**21**); 164.56 (Cq, C-**29**); 156.00 (q, Cq, C-**36**); 145.62 (Cq, C-**11**); 140.90 (Cq, C-**3**); 139.57 (Cq, C-**30**); 133.10 (CH, C-**35**); 132.78 (CH, C-**26**); 132.11 (CH, C-**6**); 130.57 (Cq, C-**7**); 129.94 (Cq, C-**23**); 129.51 (CH, C-**31**, C-**32**); 128.70 (CH, C-**24**, C-**28**); 128.56 (CH, C-**33**, C-**34**); 128.03 (CH, C-**25**, C-**27**); 118.95 (CH, C-**2**); 113.90 (CH, C-**10**); 88.86 (Cq, C-**15**); 77.46 (CH, C-**8**); 66.32 (CH, C-**9**); 60.98 (CH_2, C-**1**); 39.65 (CH_2, C-**12**); 39.48 (CH_2, C-**4**); 38.50 (CH_2, C-**14**); 25.66 (CH_2, C-**5**); 25.44 (CH_3, C-**16**); 25.25 (CH_3, C-**17**); 21.30 (CH_2, C-**13**); 20.72 (CH_3, C-**22**); 16.21 (CH_3, C-**20**); 16.14 (CH_3, C-**18**); 11.47 (CH_3, C-**19**)

9-Benzenesulfonyl-8-benzoxy-3,7,11,15-tetramethyl-15-trifluoroacetoxy hexadeca-2,6,10-trien-1-ol (94):

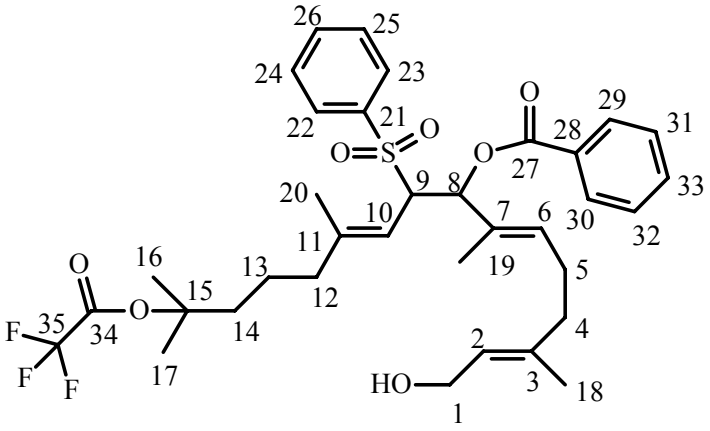

94

^{1}H NMR (400 MHz, ^{1}H-^{1}H-COSY, $CDCl_3$):

δ: 7.73 (m, 4H, HC-**22**, HC-**23**, HC-**29**, HC-**30**); 7.42 (m, 1H, HC-**26**); 7.26 (m, 5H, HC-**24**, HC-**25**, HC-**31**, HC-**32**, HC-**33**); 5.79 (d, J = 9.2 Hz, 1H, HC-**8**); 5.54 (m, 1H, HC-**6**); 5.26 (t, J = 6.7 Hz, 1H, HC-**2**); 4.86 (d, J = 10.8 Hz, 1H, HC-**10**); 4.34 (t, J = 10.3 Hz, 1H, HC-**9**); 3.98 (d, J = 6.7 Hz, 2H, H_2C-**1**); 2.16 (br. s, 1H, HO); 2.09-1.90 (br. m, 6H, H_2C-**4**, H_2C-**5**, H_2C-**12**, H_2C-**13**); 1.65 (m, 2H, H_2C-**14**); 1.49 (s, 6H, H_3C-**18**, H_3C-**20**); 1.44 (s, 9H, H_3C-**16**, H_3C-**17**, H_3C-**19**)

^{13}C NMR (100 MHz, BB, DEPT, ^{1}H-^{13}C-COSY, $CDCl_3$):

δ: 164.87 (Cq, C-**27**); 156.00 (q, Cq, C-**34**); 145.75 (Cq, C-**11**); 139.54 (Cq, C-**3**); 137.54 (Cq, C-**28**); 133.15 (CH, C-**33**); 132.92 (CH, C-**26**); 132.68 (CH, C-**6**); 130.12 (Cq, C-**7**); 129.80 (Cq, C-**21**); 129.55 (CH, C-**29**, C-**30**); 128.75 (CH, C-**22**, C-**23**); 128.58 (CH, C-**31**, C-**32**); 128.11 (CH, C-**24**, C-**25**); 124.64 (CH, C-**2**); 113.80 (CH, C-**10**); 88.94 (Cq, C-**15**); 77.84 (CH, C-**8**); 66.36 (CH, C-**9**); 59.01 (CH_2, C-**1**); 39.66 (CH_2, C-**12**); 39.50 (CH_2, C-**4**); 38.45 (CH_2, C-**14**); 25.51 (CH_2, C-**5**); 25.40 (CH_3, C-**16**); 25.32 (CH_3, C-**17**); 21.31 (CH_2, C-**13**); 16.30 (CH_3, C-**20**); 15.78 (CH_3, C-**18**); 11.42 (CH_3, C-**19**)

5.3.7 Synthesis of acetic acid 9-benzenesulfonyl-8-*tert*-butoxy-3,7,11,15-tetramethyl-hexadeca-2,6,10,14-tetraenyl ester (87a)[68]

The secondary alcohol **87** (3.43 mmol, 1.67 g) was dissolved in a mixture of 7 ml of cyclohexane and 3.5 ml of dichloromethane. Then it was transferred into a 3-neck round-bottom flask. The mixture was treated with 2 equiv. of trichloroacetimidate (6.86 mmol, 1.5 g, 1.23 ml) and a catalytic amount of boron trifluoride etherate. The reaction mixture was stirred under argon at room temperature for 24 h. Following this solid $NaHCO_3$ was added. This mixture was then filtered through a short plug of silica in order to completely remove trichloroacetamide, formed during reaction. The silica was washed twice with pentane and the combined organic layer was concentrated to give a crude product which was submitted for further purification to column chromatography on silica with pentane-ether 50/1 → 3/1 as eluant to give 0.84 g (45 % yield) of pure product as a light yellow viscous oil.

Acetic acid 9-benzenesulfonyl-8-*tert*-butoxy-3,7,11,15-tetramethyl-hexadeca-2,6,10,14-tetraenyl ester (87a):

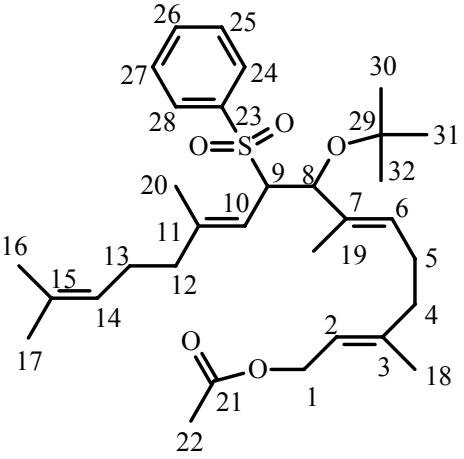

87a

^{1}H NMR (250 MHz, ^{1}H-^{1}H-COSY, $CDCl_3$):

δ: 7.75 (d, J = 8.2 Hz, 2H, HC-**24**, HC-**28**); 7.49-7.34 (m, 3H, HC-**25**, HC-**26**, HC-**27**); 5.27 (m, 2H, HC-**2**, HC-**6**); 4.86 (m, 1H, HC-**14**); 4.73 (d, J = 11.3 Hz, 1H, HC-**10**); 4.63 (d, J = 8.4 Hz, 1H, HC-**8**); 4.49 (d, J = 7.1 Hz, 2H, H_2C-**1**); 3.99 (dd, J = 8.5, 10.2 Hz, 1H, HC-**9**); 2.05-1.93 (br. m, 4H, H_2C-**4**, H_2C-**12**); 1.97 (s, 3H, H_3C-**22**); 1.69 (m, 4H, H_2C-**5**, H_2C-**13**); 1.60 (s, 3H, H_3C-**18**); 1.58 (s, 3H, H_3C-**20**); 1.48 (s, 3H, H_3C-**16**); 1.40 (s, 3H, H_3C-**17**); 1.13 (s, 9H, H_3C-**30**, H_3C-**31**, H_3C-**32**); 1.06 (s, 3H, H_3C-**19**)

^{13}C NMR (62.5 MHz, BB, DEPT, ^{1}H-^{13}C-COSY, $CDCl_3$):

δ: 171.32 (Cq, C-**21**); 144.29 (Cq, C-**11**); 141.82 (Cq, C-**3**); 140.82 (Cq, C-**7**); 136.20 (CH, C-**15**); 133.04 (CH, C-**26**); 132.10 (Cq, C-**23**); 129.04 (CH, C-**24**, C-**28**); 128.83 (CH, C-**6**); 128.66 (CH, C-**25**, C-**27**); 123.92 (CH, C-**14**); 119.01 (CH, C-**2**); 116.12 (CH, C-**10**); 77.38 (CH, C-**8**); 75.73 (Cq, C-**29**); 68.69 (CH, C-**9**); 61.56 (CH_2, C-**1**); 39.85 (CH_2, C-**12**); 38.95 (CH_2, C-**4**); 28.78 (CH_3, C-**30**, C-**31**, C-**32**); 26.53 (CH_2, C-**13**); 25.98 (CH_3, C-**16**); 25.95 (CH_2, C-**5**); 21.32 (CH_3, C-**22**); 17.95 (CH_3, C-**18**); 16.62 (CH_3, C-**17**); 16.47 (CH_3, C-**20**); 11.74 (CH_3, C-**19**)

5.4 Photochemical oxidations with water as nucleophile and $Cu(OAc)_2$ as a co-oxidant

5.4.1 Irradiation of geranyl acetate (77) (→ 100, 101, 102, 103)

According to the general synthetic procedure discussed in chapter 5.2.1.1 geranyl acetate (1 g, 5.1 mmol), biphenyl (0.72 g, 4.7 mmol), DCTMB (0.22 g, 1.21 mmol) and $Cu(OAc)_2$ (1.02 g, 5.1 mmol) were dissolved in 440 ml of a 10/1 CH_3CN/H_2O mixture and subjected to irradiation. The irradiation was continued for 1 day. During this time the reaction vessel was once changed due to formation of a Cu-mirror. After concentration of the resulting light green solution, the residue was purified by chromatography using *n*-pentane-ether 20/1 → 2/1 as eluant to give 0.38 g (35 %) of epoxide **101**, 86.5 mg (8 %) of **102**, 0.18 g (17 %) of **100** and 0.16 g (15 %) of **103**. All of them have the same spectral properties as already described[24].

5.4.2 Oxidation of the allylic alcohol 78 (→ 104a, 104b)

For this reaction (see general procedure in chapter 5.2.1.1) 1.1 g (5.2 mmol) of alcohol **78**, 0.74 g (4.8 mmol) of biphenyl, 0.227 g (1.2 mmol) of DCTMB and 1.04 g (5.2 mmol) of $Cu(OAc)_2 \cdot H_2O$ were dissolved in 440 ml of an acetonitrile/water 10:1 mixture. After degassing (argon) for 0.5 h, the reaction mixture was subjected to irradiation at 300 nm for 1 day. The resulting solution was concentrated and the products were purified by silica gel chromatography using pentane/ether 50/1→ 2/1 as eluant. This resulted in 60 mg (5 %) of racemic (*S,S*/*R,R*) epoxide **104 a** and 120 mg (10 %) of epoxide **104 b**, both in form of a yellow oil.

Acetic acid 5-(3'-hydroxymethyl-3'-methyl-oxiranyl)-3-methyl-pent-2-enyl ester (104a):

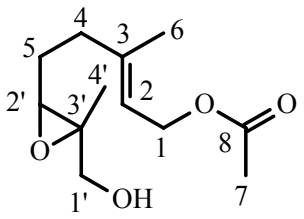

104 a

^{1}H NMR (400 MHz, ^{1}H-^{1}H-COSY, $CDCl_3$):

δ: 5.34 (t, J = 7.1 Hz, 1H, HC-**2**); 4.54 (d, J = 7 Hz, 2H, H_2C-**1**); 3.62 (s, 2H, H_2C-**1'**); 2.78 (dt, J = 1.5, 6.4 Hz, 1H, HC-**2'**); 2.16 (m, 2H, H_2C-**4**); 2.00 (s, 3H, H_3C-**7**); 1.72 (m, 2H, H_2C-**5**); 1.68 (s, 3H, H_3C-**6**); 1.33 (s, 3H, H_3C-**4'**)

^{13}C NMR (100 MHz, BB, DEPT, ^{1}H-^{13}C-COSY, $CDCl_3$):

δ: 171.08 (Cq, C-**8**); 140.99 (Cq, C-**3**); 119.16 (CH, C-**2**); 64.29 (CH, C-**2'**); 63.85 (CH_2, C-**1'**); 61.19 (CH_2, C-**1**); 60.96 (Cq, C-**3'**); 36.24 (CH_2, C-**4**); 26.29 (CH_2, C-**5**); 20.97 (CH_3, C-**7**); 20.06 (CH_3, C-**4'**); 16.40 (CH_3, C-**6**)

Acetic acid 6-hydroxy-3-methyl-6-(2'-methyl-oxiranyl)-hex-2-enyl ester (104b):

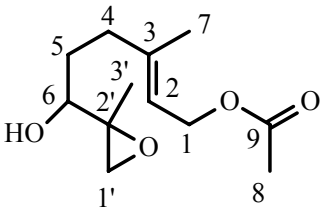

104 b

^{1}H NMR (400 MHz, ^{1}H-^{1}H-COSY, $CDCl_3$):

δ: 5.30 (ddd, J = 1.2, 2.7, 7.0 Hz, 1H, HC-**2**); 4.50 (d, J = 7.1 Hz, 2H, H_2C-**1**); 3.56 (d, J = 12.2 Hz, 1H, *H*HC-**1'**); 3.46 (d, J = 12.2 Hz, 1H, H*H*C-**1'**); 2.91 (t, J = 6.2 Hz, 1H, HC-**6**); 2.45 (br. s, 1H, OH); 2.10 (m, 2H, H_2C-**4**); 1.96 (s, 3H, H_3C-**8**); 1.64 (s, 3H, H_3C-**7**); 1.61 (m, 2H, H_2C-**5**); 1.19 (s, 3H, H_3C-**3'**)

^{13}C NMR (100 MHz, BB, DEPT, ^{1}H-^{13}C-COSY, $CDCl_3$):

δ: 170.95 (Cq, C-**9**); 140.80 (Cq, C-**3**); 118.94 (CH, C-**2**); 65.42 (CH_2, C-**1'**); 61.06 (CH_2, C-**1**); 61.00 (Cq, C-**2'**); 59.66 (CH, C-**6**); 35.93 (CH_2, C-**4**); 26.20 (CH_2, C-**5**); 20.79 (CH_3, C-**8**); 16.25 (CH_3, C-**7**); 14.03 (CH_3, C-**3'**)

5.4.3 Oxidation of TBDMS-protected allylic alcohol 81 (→ 105)

For the reaction (see general procedure in chapter 5.2.1.1) 1.1 g (3.4 mmol) of TBDMS-protected alcohol **81**, 0.48 g (3.12 mmol) of biphenyl, 0.148 g (0.8 mmol) of DCTMB and 0.676 g (3.4 mmol) of $Cu(OAc)_2 \cdot H_2O$ were dissolved in 440 ml of an acetonitrile/water mixture (10:1) and subjected to irradiation for 1 day. The resulting solution was concentrated and the residue was purified by silica gel chromatography using pentane/ether 50/1→ 10/1 as eluant to give 105 mg (9%) of **105** in form of a yellow oil.

acetic acid 5-[3'-(tert-butyl-dimethyl-silanyloxymethyl)-3'-methyl-oxiranyl]-3-methyl-pent-2-enyl ester (105):

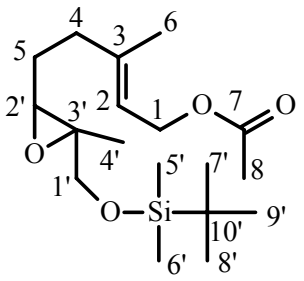

105

^{1}H NMR (500 MHz, ^{1}H-^{1}H-COSY, $CDCl_3$):

δ: 5.34 (t, J = 6.9 Hz, 1H, HC-**2**); 4.52 (d, J = 7.3 Hz, 2H, H_2C-**1**); 3.52 (s, 2H, H_2C-**1'**); 2.80 (t, J = 6.4 Hz, 1H, HC-**2'**); 2.14 (m, 2H, H_2C-**4**); 2.00 (s, 3H, H_3C-**8**); 1.68 (s, 3H, H_3C-**6**); 1.63 (m, 2H, H_2C-**5**); 1.22 (s, 3H, H_3C-**4'**); 0.85 (s, 9H, H_3C-**7'**, H_3C-**8'**, H_3C-**9'**); 0.01 (s, 3H, H_3C-**5'**); 0.00 (s, 3H, H_3C-**6'**);

^{13}C NMR (125 MHz, BB, DEPT, ^{1}H-^{13}C-COSY, $CDCl_3$):

δ: 170.91 (Cq, C-**7**); 141.03 (Cq, C-**3**); 118.91 (CH, C-**2**); 67.68 (CH_2, C-**1'**); 61.14 (CH_2, C-**1**); 60.92 (Cq, C-**3'**); 60.28 (CH, C-**2'**); 36.09 (CH_2, C-**4**); 26.52 (CH_2, C-**5**); 25.76 (3xCH_3, C-**7'**, C-**8'**, C-**9'**); 20.90 (CH_3, C-**8**); 18.22 (Cq, C-**10'**); 16.38 (CH_3, C-**6**); 14.07 (CH_3, C-**4'**); -5.46 (2x CH_3, C-**5'**, C-**6'**).

5.4.4 Irradiation of all-*trans*-farnesol (106) (→ 107, 108)

According to the general synthetic procedure, described in chapter 5.2.1.1, 1 g (4.5 mmol) of all-*trans*-farnesol (**106**), 0.64 g (4.15 mmol) of biphenyl, 0.198 g (1.07 mmol) of DCTMB, 0.9 g (4.5 mmol) of $Cu(OAc)_2 \cdot H_2O$ and 2.4 g (9 mmol) of $Mn(OAc)_3 \cdot 2H_2O$ were dissolved in 440 ml of an acetonitrile/water mixture (10:1) and the resulting dark brown

solution was subjected to irradiation for 3 days (TLC control shows nearly completed conversion after 2.5 days). The resulting slightly green solution was filtered in order to remove insoluble Mn(II)-acetate and then concentrated. The residue was chromatographed on silica using pentane/ether 10/1→ 1/2 as eluant to give 64 mg (6%) of epoxide **107** together with 110 mg (10 %) of the cyclic diol **108**[55]. Both products are light yellow oils.

3,7,11-Trimethyl-10-oxido-dodeca-2(E),6(E)-dien-1-ol (107):

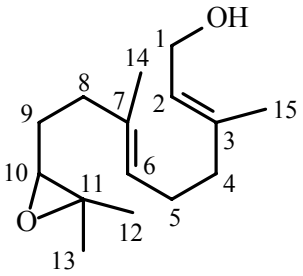

107

^{1}H NMR (500 MHz, ^{1}H-^{1}H-COSY, $CDCl_3$):

δ: 5.36 (t, 1H, J = 6.8 Hz, HC-**2**); 5.12 (t, 1H, J = 6.4 Hz, HC-**6**); 4.09 (d, 2H, J = 6.9 Hz, H_2C-**1**); 2.66 (t, 1H, J = 6.2 Hz, HC-**10**); 2.14-2.03 (m, 6H, H_2C-**4**, H_2C-**5**, H_2C-**8**); 1.63 (s, 3H, H_3C-**15**); 1.59 (m, 2H, H_2C-**9**); 1.58 (s, 3H, H_3C-**14**); 1.26 (s, 3H, H_3C-**13**); 1.22 (s, 3H, H_3C-**12**)

^{13}C NMR (125 MHz, BB, DEPT, ^{1}H-^{13}C-COSY, $CDCl_3$):

δ: 139.17 (Cq, C-**3**); 134.25 (Cq, C-**7**); 124.47 (CH, C-**6**); 123.54 (CH, C-**2**); 64.16 (CH_2, C-**1**); 59.58 (CH, C-**10**); 58.44 (Cq, C-**11**); 39.32 (CH_2, C-**4**); 36.24 (CH_2, C-**8**); 27.19 (CH_2, C-**9**); 26.09 (CH_2, C-**5**); 24.76 (CH_3, C-**13**); 18.68 (CH_3, C-**12**); 16.14 (CH_3, C-**15**); 15.89 (CH_3, C-**14**)

5-Hydroxymethyl-1,1,4a-trimethyl-6-methylene-decahydro-naphthalen-2-ol (108):

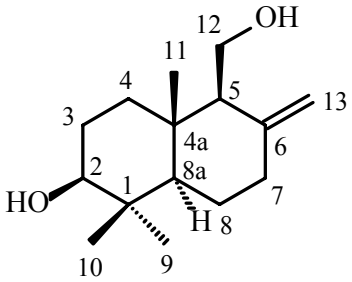

108

^{1}H NMR (250 MHz, ^{1}H-^{1}H-COSY, $CDCl_3$):

δ: 4.85 (s, 1H, *H*HC-**13**); 4.57 (s, 1H, H*H*C-**13**); 4.05 (d, 2H, J = 6.8 Hz, H_2C-**12**); 3.80 (br. s, 2H, OH); 3.18 (dd, 1H, J = 4.2, 11.1 Hz, HC-**2**); 2.34 (ddd, 1H, J = 2.3, 3.6, 13.0 Hz, H*H*C-**7**); 1.92 (m, 1H, *H*HC-**7**); 1.83 (dd, 1H, J = 2.8, 8.7 Hz, HC-**5**); 1.59-1.46 (m, 3H, H*H*C-**3**, H*H*C-**4**, H*H*C-**8**); 1.24-1.17 (m, 3H, *H*HC-**3**, *H*HC-**4**, *H*HC-**8**); 1.07 (dd, 1H, J = 2.8, 12.8 Hz, HC-**8a**); 0.91 (s, 3H, H_3C-**10**); 0.68 (s, 3H, H_3C-**9**); 0.63 (s, 3H, H_3C-**11**)

^{13}C NMR (62.5 MHz, BB, DEPT, ^{1}H-^{13}C-COSY, $CDCl_3$):

δ: 146.98 (Cq, C-**6**); 106.75 (CH_2, C-**13**); 78.45 (CH, C-**2**); 58.51 (CH, C-**5**); 58.48 (CH_2, C-**12**); 57.27 (CH, C-**8a**); 38.99 (Cq, C-**1**); 38.53 (Cq, C-**4a**); 37.57 (CH_2, C-**7**); 36.90 (CH_2, C-**4**); 28.21 (CH_3, C-**10**); 27.48 (CH_2, C-**3**); 23.63 (CH_2, C-**8**); 15.43 (CH_3, C-**9**); 15.15 (CH_3, C-**11**)

5.5 Photochemical oxidations with methanol as nucleophile and $Cu(OAc)_2$ as a co-oxidant

5.5.1 Oxidative cyclization of geranyl acetate (77). Experiment for mechanistic studies

For detailed experimental procedure see chapter 5.2.1.2. Solution of 1 g (5.1 mmol, 1.09 ml) of geranyl acetate (**77**), 0.73 g (4.7 mmol) of biphenyl, 0.22 g (1.2 mmol) of DCTMB, 1.02 g (5.1 mmol) of $Cu(OAc)_2 \cdot H_2O$ and 2.73 g (10.2 mmol) of $Mn(OAc)_3 \cdot 2H_2O$ in 450 ml of a MeCN / MeOH 4/1 mixture was irradiated at λ_{max} = 300 nm for 2 days. Separation of resulting products was achieved by column chromatography, using pentane/ether 50/1 → 7/1 as eluant, to give 228 mg (20 %) of **109**, 104 mg (9 %) of **110** as a mixture of two diastereomers (about 1:1), 92 mg (8 %) of **111**, 93 mg (8 %) of **112** as an inseparable mixture of two double bond isomers (about 1:1), 195 mg (17 %) of **113** and 175 mg (15 %) of compounds **114** and **114a (**proportion 1:1.6). All products were isolated in form of yellow oils.

Acetic acid 3-methoxy-2,2-dimethyl-6-methylene-cyclohexylmethyl ester (109):

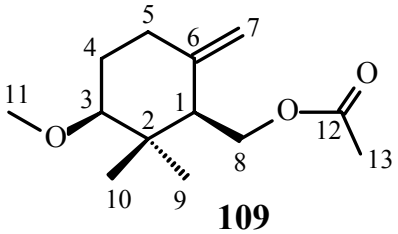

109

^{1}H NMR (250 MHz, ^{1}H-^{1}H-COSY, $CDCl_3$):

δ: 4.80 (s, 1H, HHC-**7**); 4.58 (s, 1H, HHC-**7**); 4.35 (dd, B part of ABX system, J = 10, 11.3 Hz, 1H, HHC-**8**); 4.24 (dd, A part of ABX system J = 4.1, 11.3 Hz, 1H, HHC-**8**); 3.28 (s, 3H, H_3C-**11**); 2.82 (dd, J = 3.3, 6.5 Hz, 1H, HC-**3**); 2.33 (m, 1H, HHC-**5**); 2.03 (m, 1H, HC-**1**); 1.98 (s, 3H, H_3C-**13**); 1.89 (m, 1H, HHC-**5**); 1.8-1.5 (br. m, 2H, H_2C-**4**); 0.87 (s, 3H, H_3C-**10**); 0.81 (s, 3H, H_3C-**9**)

^{13}C NMR (62 MHz, BB, DEPT, ^{1}H-^{13}C-COSY, $CDCl_3$):

δ: 171.08 (Cq, C-**12**); 146.08 (Cq, C-**6**); 110.08 (CH_2, C-**7**); 85.02 (CH, C-**3**); 62.92 (CH_2, C-**8**); 57.31 (CH_3, C-**11**); 51.78 (CH, C-**1**); 38.93 (Cq, C-**2**); 29.02 (CH_2, C-**5**); 26.67 (CH_3, C-**10**); 25.65 (CH_2, C-**4**); 21.02 (CH_3, C-**9**); 19.79 (CH_3, C-**13**);

MS (EI) m/z (rel. int.):

166 (22.9), 151 (18.4), 135 (20.5), 134 (100), 123 (92.4), 121 (72.9), 120 (21.9), 119 (81.8), 109 (18.6), 108 (20.4), 107 (31), 106 (15.2), 105 (20.4), 93 (56.9), 91 (31.6), 81 (14.7), 79 (30.2), 77 (15.4), 67 (24), 55 (19.7), 45 (14.3), 43 (94.1), 41 (29.8).

Acetic acid 2-(3'-methoxy-1',2',2'-trimethyl-cyclopentyl)-vinyl ester (110):

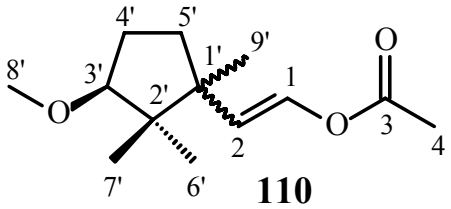

110

^{1}H NMR (250 MHz, ^{1}H-^{1}H-COSY, $CDCl_3$) in parentheses the values for the second diastereomer:

δ: 6.99 (6.97) (d, J = 12.6 Hz, 1H, HC-**1**); 5.45 (5.55) (d, J = 12.6 Hz, 1H, HC-**2**); 3.34 [(3.47) dd, J = 6.5, 8.5 Hz] (dd, J = 5.9, 8.4 Hz, 1H, HC-**3'**); 3.26 (s, 3H, H_3C-**8'**); 2.1-1.5 (br. m, 4H, H_2C-**4'**, H_2C-**5'**); 2.08 (s, 3H, H_3C-**4**); 0.99 (s, 3H, H_3C-**7'**); 0.97 (s, 6H, H_3C-**6'**, H_3C-**9'**)

^{13}C NMR (62 MHz, BB, DEPT, ^{1}H-^{13}C-COSY, $CDCl_3$):

δ: 168.05 (Cq, C-**3**); 134.12 (CH, C-**1**); 122.12 (CH, C-**2**); 89.63 (CH, C-**3'**); 57.73 (CH_3, C-**8'**); 46.79 (Cq, C-**1'**); 45.68 (Cq, C-**2'**); 33.90 (CH_2, C-**4'**); 27.24 (CH_2, C-**5'**); 23.39 (CH_3, C-**7'**); 21.57 (CH_3, C-**6'**); 20.70 (CH_3, C-**4**); 17.36 (CH_3, C-**9'**)

MS **(EI) m/z (rel. int.):**

184 (27.4), 152 (14.9), 143 (17.5), 134 (16.5), 126 (21.8), 123 (25.6), 109 (21), 101 (72.5), 97 (23), 87 (71.6), 86 (24.8), 85 (44.3), 84 (100), 83 (29.5), 81 (18.1), 80 (30.1), 71 (22.9), 69 (30.1), 55 (27.8), 43 (83.8), 41 (38.6)

Acetic acid 3-methoxy-2,2,6-trimethyl-cyclohexylmethyl ester (111):

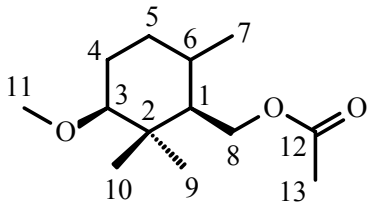

111

^{1}H NMR **(250 MHz, ^{1}H-^{1}H-COSY, $CDCl_3$):**

δ: 4.22 (dd, J = 4.5, 12.8 Hz, 1H, HHC-**8**); 4.08 (dd, J = 4.1, 12 Hz, 1H, HHC-**8**); 3.32 (s, 3H, H_3C-**11**); 2.62 (dd, J = 3.8, 7 Hz, 1H, HC-**3**); 2.00 (s, 3H, H_3C-**13**); 1.75-1.43 (br. m, 5 H, H_2C-**4**, H_2C-**5**, HC-**6**); 1.04 (s, 3H, H_3C-**10**); 0.91 (m, 1H, HC-**1**); 0.84 (d, J = 5.2 Hz, 3H, H_3C-**7**); 0.76 (s, 3H, H_3C-**9**)

^{13}C NMR **(62 MHz, BB, DEPT, ^{1}H-^{13}C-COSY, $CDCl_3$):**

δ: 170.94 (Cq, C-**12**); 87.18 (CH, C-**3**); 63.56 (CH_2, C-**8**); 57.47 (CH_3, C-**11**); 51.50 (CH, C-**1**); 38.60 (Cq, C-**2**); 33.19 (CH_2, C-**4**); 30.17 (CH, C-**6**); 25.62 (CH_3, C-**10**); 25.52 (CH_2, C-**5**); 20.88 (CH_3, C-**13**); 19.95 (CH_3, C-**7**); 14.65 (CH_3, C-**9**)

MS **(EI) m/z (rel. int.):**

157 (9.3), 136 (14), 121 (52.8), 109 (11.1), 98 (13.2), 97 (100), 96 (24.1), 95 (29.7), 93 (16.4), 87 (21), 86 (14.2), 85 (34.5), 84 (15.1), 83 (16.1), 81 (16.9), 72 (33.8), 71 (52.5), 69 (20.9), 67 (16.7), 58 (16.5), 55 (45.7), 43 (48.5), 41 (25.4).

Acetic acid 6-methoxy-3,7-dimethyl-octa-2,7-dienyl ester (113):

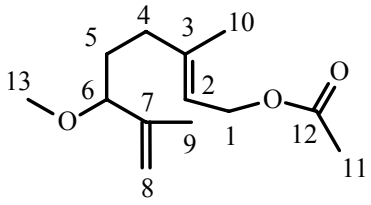

113

^{1}H NMR (400 MHz, ^{1}H-^{1}H-COSY, $CDCl_3$):

δ: 5.29 (t, J = 7.1 Hz, 1H, HC-**2**); 4.87 (d, J = 1.5 Hz, 1H, HHC-**8**); 4.83 (s, 1H, HHC-**8**); 4.52 (d, J = 7 Hz, 2H, H_2C-**1**); 3.40 (t, J = 6.7, 1H, HC-**6**); 3.13 (s, 3H, H_3C-**13**); 2.07-1.98 (m, 2H, H_2C-**4**); 1.98 (s, 3H, H_3C-**11**); 1.71-1.45 (br. m, 2H, H_2C-**5**); 1.64 (s, 3H, H_3C-**9**); 1.58 (s, 3H, H_3C-**10**)

^{13}C NMR (100 MHz, BB, DEPT, ^{1}H-^{13}C-COSY, $CDCl_3$):

δ: 170.87 (Cq, C-**12**); 144.16 (Cq, C-**7**); 141.70 (Cq, C-**3**); 118.44 (CH, C-**2**); 113.54 (CH_2, C-**8**); 85.01 (CH, C-**6**); 61.19 (CH_2, C-**1**); 55.86 (CH_3, C-**13**); 35.47 (CH_2, C-**4**); 31.44 (CH_2, C-**5**); 20.87 (CH_3, C-**11**); 16.30 (CH_3, C-**9**); 16.22 (CH_3, C-**10**)

Acetic acid 7-methoxy-3,7-dimethyl-octa-2,5-dienyl ester (114):

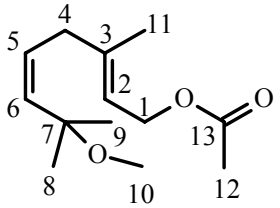

114

^{1}H NMR (250 MHz, ^{1}H-^{1}H-COSY, $CDCl_3$):

δ: 5.36 (m, 2H, HC-**5**, HC-**6**); 5.21 (m, 1H, HC-**2**); 4.43 (d, J = 7.1 Hz, 2H, H_2C-**1**); 3.00 (s, 3H, H_3C-**10**); 2.62 (d, J = 5.3, 2H, H_2C-**4**); 1.89 (s, 3H, H_3C-**12**); 1.55 (s, 3H, H_3C-**11**); 1.11 (s, 3H, H_3C-**8**); 0.99 (s, 3H, H_3C-**9**)

^{13}C NMR (62.5 MHz, BB, DEPT, ^{1}H-^{13}C-COSY, $CDCl_3$):

δ: 170.54 (Cq, C-**13**); 141.78 (Cq, C-**3**); 137.43 (CH, C-**6**); 126.75 (CH, C-**5**); 119.04 (CH, C-**2**); 74.33 (Cq, C-**7**); 60.94 (CH_2, C-**1**); 49.86 (CH_3, C-**10**); 42.13 (CH_2, C-**4**); 25.49 (CH_3, C-**8**); 24.61 (CH_3, C-**9**); 20.61 (CH_3, C-**12**); 16.10 (CH_3, C-**11**)

Acetic acid 7-methoxy-3,7-dimethyl-oct-2-enyl ester (114a):

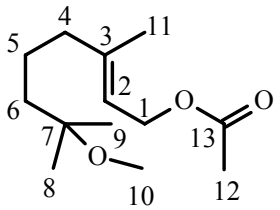

114a

^{1}H NMR (250 MHz, ^{1}H-^{1}H-COSY, $CDCl_3$):

δ: 5.21 (m, 1H, H<u>C</u>-**2**); 4.41 (d, J = 7.1 Hz, 2H, H_2<u>C</u>-**1**); 3.01 (s, 3H, H_3<u>C</u>-**10**); 1.93-1.84 (m, 2H, H_2<u>C</u>-**4**); 1.90 (s, 3H, H_3<u>C</u>-**12**); 1.55 (s, 3H, H_3<u>C</u>-**11**); 1.28 (m, 4H, H_2<u>C</u>-**5**, H_2<u>C</u>-**6**); 1.11 (s, 3H, H_3<u>C</u>-**8**); 0.99 (s, 3H, H_3<u>C</u>-**9**)

^{13}C NMR (62.5 MHz, BB, DEPT, ^{1}H-^{13}C-COSY, $CDCl_3$):

δ: 170.51 (Cq, C-**13**); 140.35 (Cq, C-**3**); 118.17 (CH, C-**2**); 74.05 (Cq, C-**7**); 60.89 (CH_2, C-**1**); 48.68 (CH_3, C-**10**); 39.56 (CH_2, C-**4**); 39.05 (CH_2, C-**6**); 25.49 (CH_3, C-**8**); 24.61 (CH_3, C-**9**); 21.44 (CH_2, C-**5**); 20.61 (CH_3, C-**12**); 15.95 (CH_3, C-**11**)

5.5.2 Irradiation of geraniol (74) (→ 115, 116)

According to the general synthetic procedure described in chapter 5.2.1.2, a solution of 1 g (6.5 mmol) of geraniol (**74**), 0.925 g (6 mmol) of biphenyl, 0.285 g (1.55 mmol) of DCTMB, 1.3 g (6.5 mmol) of $Cu(OAc)_2 \cdot H_2O$ and 3.49 g (13 mmol) of $Mn(OAc)_3 \cdot 2H_2O$ in 450 ml of acetonitrile/methanol 4:1 was subjected to irradiation for 3 days. Filtration followed by concentration results in a crude product mixture, which was subjected directly to further purification by column chromatography. Separation, using pentane/ether 10/1→ 1/1, resulted in 180 mg (15 %) of **115** and 60 mg (5%) of **116**, both as nearly colourless oils.

(3-Methoxy-2,2-dimethyl-6-methylene-cyclohexyl)-methanol (115):

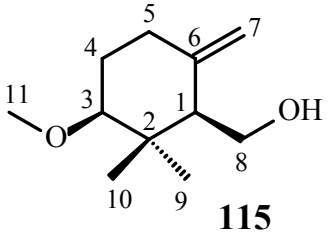

115

IR (KBr): υ_{max} 3422 s (br), 2938 s, 1743 s, 1647 m, 1516 w, 1464 s, 1385 m, 1161 m, 1094 s, 1025 m, 979 m, 917 w, 892 w, 661 w;

^{1}H NMR (250 MHz, ^{1}H-^{1}H-COSY, $CDCl_3$):

δ: 4.84 (s, 1H, HHC-**7**); 4.66 (s, 1H, HHC-**7**); 3.80 (dd, B part of ABX system, J_{ab} = 11.1 Hz, J_{bx} = 7.3 Hz, 1H, HHC-**8**); 3.53 (dd, A part of ABX system, J_{ab} = 11.1 Hz, J_{ax} = 3.7 Hz, 1H, HHC-**8**); 3.28 (s, 3H, H_3C-**11**); 2.84 (dd, J = 4, 9.6 Hz, 1H, HC-**3**); 2.59 (br. s, 1H, OH); 2.35 (m, 1H, HHC-**5**); 1.97 (m, 1H, HHC-**5**); 1.89 (m, 1H, HC-**1**); 1.80-1.50 (br. m, 2H, H_2C-**4**); 0.91 (s, 3H, H_3C-**10**); 0.90 (s, 3H, H_3C-**9**);

^{13}C NMR (62 MHz, BB, DEPT, ^{1}H-^{13}C-COSY, $CDCl_3$):

δ: 147.48 (Cq, C-**6**); 110.57 (CH_2, C-**7**); 84.06 (CH, C-**3**); 61.90 (CH_2, C-**8**); 56.92 (CH_3, C-**11**); 55.41 (CH, C-**1**); 38.28 (Cq, C-**2**); 28.14 (CH_2, C-**5**); 27.65 (CH_3, C-**10**); 24.79 (CH_2, C-**4**); 21.56 (CH_3, C-**9**)

MS (EI) m/z (rel. int.):

123 (22.6), 122 (100), 121 (39.9), 109 (13.6), 107 (72.6), 96 (32.7), 93 (27.7), 91 (20.48), 81 (29.8), 79 (28.9), 67 (17.64), 55 (15.6), 41 (23.4).

HRMS: ESIpos m/z calcd for $C_{11}H_{20}NaO_2$ (M+Na):

207.136099. Found: 207.13636 (M+Na).

(3-Methoxy-2,2,6-trimethyl-cyclohexyl)-methanol (116):

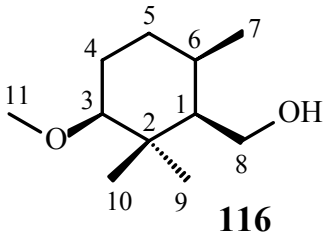

116

IR (KBr): υ_{max} 3428 s, 2929 s, 2868 m, 1707 m, 1462 s, 1362 m, 1082 s;

^{1}H NMR (250 MHz, $CDCl_3$):

δ: 3.64 (m, 2H, H_2C-**8**); 3.34 (s, 3H, H_3C-**11**); 2.82 (t, J = 2.5 Hz, 1H, HC-**3**); 2.00 (m, 2H, H_2C-**4**); 1.80 (m, 1H, HHC-**5**); 1.60 (br m, 2H, HHC-**5** and OH); 1.25 (m, 1H, HC-**6**); 1.10 (m, 1H, HC-**1**); 1.05 (s, 3H, H_3C-**10**); 1.03 (s, 3H, H_3C-**9**); 1.01 (d, 3H, HC-**7**);

^{13}C NMR (62 MHz, BB, DEPT, ^{1}H-^{13}C-COSY, $CDCl_3$):

δ: 83.51 (CH, C-**3**); 59.16 (CH_2, C-**8**); 56.53 (CH_3, C-**11**); 49.16 (CH, C-**1**); 37.71 (Cq, C-**2**); 29.17 (CH, C-**6**); 28.38 (CH_3, C-**10**); 26.41 (CH_2, C-**4**); 25.07 (CH_3, C-**7**); 23.33 (CH_2, C-**5**); 19.26 (CH_3, C-**9**);

MS (EI) m/z (rel. int.):

186 (M^+, $C_{11}H_{22}O_2^+$)(0.75), 124 (31.5), 123 (18.7), 121 (19.5), 109 (20.1), 95 (18.2), 82 (22.8), 81 (32.5), 72 (17.6), 71 (100), 69 (18.5), 67 (18), 58 (18.1), 55 (28.7), 43 (18.3), 41 (29.4).

HRMS: ESIpos m/z calcd for $C_{11}H_{22}NaO_2$ (M+Na):

209.151749. Found: 209.15193 (M+Na).

5.5.3 Irradiation of all-*trans*-farnesol (106) (→ 117)

1 g (4.5 mmol) of all-*trans*-farnesol (**106**), 0.64 g (4.15 mmol) of biphenyl, 0.20 g (1.07 mmol) of DCTMB, 0.9 g (4.5 mmol) of $Cu(OAc)_2 \cdot H_2O$ and 2.4 g (8.95 mmol) of $Mn(OAc)_3 \cdot 2H_2O$ were dissolved in a 450 ml acetonitrile/methanol 4:1 mixture and the resulting dark brown solution was subjected to irradiation for 2 days (for detailed synthetic procedure see chapter 5.2.1.2). The reaction was concentrated and purified by column chromatography using *n*-pentane/ether 10/1→ 1/1 as eluant to give 259 mg (22 %) of pure **117** as a light yellow oil.

(6-Methoxy-5,5,8a-trimethyl-2-methylene-decahydro-naphthalen-1-yl)-methanol (117):

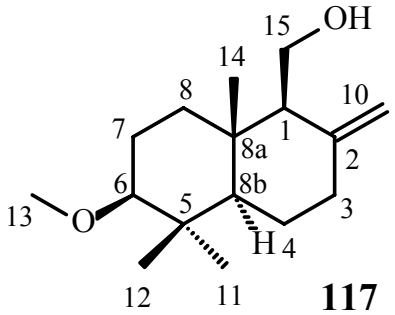

117

IR (KBr): υ_{max} 3440 (OH), 2926 (CH, aliphatic), 1734, 1646, 1457, 1385, 1260, 1180, 1104, 1030, 888, 798, 555;

^{1}H NMR (500 MHz, ^{1}H-^{1}H-COSY, $CDCl_3$):

δ: 4.93 (d, J = 1,4 Hz, 1H, HHC-**10**); 4.63 (d, J = 1,4 Hz, 1H, HHC-**10**); 3.78 (dd, J = 3.8, 11 Hz, 1H, HHC-**15**); 3.76 (dd, J = 9.3, 11 Hz, 1H, HHC-**15**); 3.34 (s, 3H, H_3C-**13**); 2.68 (dd, J = 4.2, 11.9 Hz, 1H, HC-**6**); 2.41 (ddd, J = 2.3, 4.2, 12.9 Hz, 1H, HHC-**3**); 2.01 (m, 1H, HHC-**3**); 1.90 (dd, J = 3.2, 9.2 Hz, 1H, HC-**1**); 1.85 (m, 1H, HHC-**7**); 1.71 (m, 3H, H_2C-**4**, HHC-**8**); 1.38 (m, 1H, HHC-**7**); 1.26 (m, 1H, HHC-**8**); 1.08 (dd, J = 2.8, 12.4 Hz, 1H, HC-**8b**); 0.96 (s, 3H, H_3C-**12**); 0.73 (s, 3H, H_3C-**11**); 0.70 (s, 3H, H_3C-**14**);

^{13}C NMR (125 MHz, BB, DEPT, ^{1}H-^{13}C-COSY, $CDCl_3$):

δ: 147.35 (Cq, C-**2**); 106.59 (CH_2, C-**10**); 88.27 (CH, C-**6**); 58.88 (CH, C-**1**); 58.75 (CH_2, C-**15**); 57.54 (CH_3, C-**13**); 54.89 (CH, C-**8b**); 39.03 (Cq, C-**5**); 38.68 (Cq, C-**8a**); 37.69 (CH_2, C-**3**); 36.84 (CH_2, C-**8**); 28.28 (CH_3, C-**12**); 23.62 (CH_2, C-**4**); 22.53 (CH_2, C-**7**); 16.17 (CH_3, C-**11**); 15.23 (CH_3, C-**14**)

NOE (400 MHz, $CDCl_3$, saturation → enhancement):

2.67 (CH) → 3,34 (s, OMe) and 1.08 (dd, 1H) and 0,96 (s, 3H); 1.90 (CH) → 3.79 (d, H*H*C) and 2.7 (dd, 1H) and 1.08 (dd, 1H); 1.08 (CH) → 2.7 (dd, 1H) and 1.90 (dd, 1H) and 0,96 (s, 3H); 0.96 (s, 3H) → 2.7 (dd, 1H) and 1.08 (dd, 1H) and 0.73 (s, 3H)

MS (EI) m/z (rel. int.):

252 (M^+, $C_{16}H_{28}O_2^+$)(14.5), 220 (21.5), 202 (31.8), 187 (19.1), 167 (20.1), 166 (55.6), 153 (20.7), 149 (30.3), 135 (100), 134 (27.1), 133 (20.3), 121 (27.4), 119 (25.8), 107 (47.2), 105 (21.2), 95 (19.6), 93 (41.6), 91 (24), 85 (41), 81 (29.8), 79 (25.2), 71 (24.4), 69 (25.3), 67 (25.4), 55 (33.9), 43 (33.1), 41 (46.3)

HRMS: m/z calcd for $C_{16}H_{28}O_2$:

252.2089. Found: 252.2091.

5.5.4 Irradiation of all-*trans*-farnesyl acetate (118) (→ 119)

According to the general synthetic procedure (see chapter 5.2.1.2), 1 g (3.8 mmol) of all-*trans*-farnesyl acetate (**118**), 0.54 g (3.5 mmol) of biphenyl, 0.16 g (0.87 mmol) of DCTMB, 0.75 g (3.8 mmol) of $Cu(OAc)_2 \cdot H_2O$ and 2.04 g (7.6 mmol) of $Mn(OAc)_3 \cdot 2H_2O$ were dissolved in a 450 ml acetonitrile/methanol 4:1 mixture and the resulting dark brown solution was subjected to irradiation for 2 days. The residue obtained after evaporation of the solvent was purified by column chromatography using pentane/ether 20/1→ 5/1 as eluant. 134 mg (12 %) of pure **119** and 56 mg (5 %) of **120** were isolated in form of light yellow oils.

Acetic acid 6-methoxy-5,5,8a-trimethyl-2-methylene-decahydro-naphthalen-1-yl-methyl ester (119):

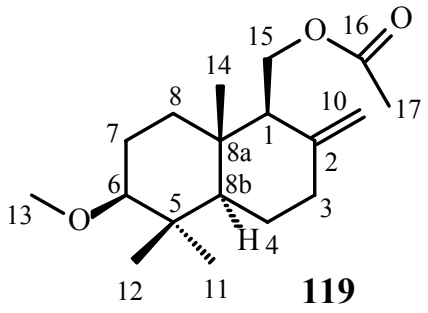

119

IR (KBr): υ_{max} 3082 w, 2938 s, 1740 s, 1646 m, 1463 s, 1386 s, 1367 s, 1232 s, 1182 m, 1102 s, 1030 m, 979 m, 890 m, 679 w, 649 w, 605 w, 579 w, 528 w, 463 w;

^{1}H NMR (400 MHz, ^{1}H-^{1}H-COSY, $CDCl_3$):

δ: 4.82 (s, 1H, HHC-**10**); 4.49 (s, 1H, HHC-**10**); 4.28 (dd, J = 3.8, 11.3 Hz, 1H, HHC-**15**); 4.14 (dd, J = 9, 11.1 Hz, 1H, HHC-**15**); 3.32 (s, 3H, H_3C-**13**); 2.66 (dd, J = 4, 11.1 Hz, 1H, HC-**6**); 2.37 (ddd, J = 2.5, 4, 13.2 Hz, 1H, HHC-**3**); 2.03-1.92 (br. m, 2H, HHC-**3**, HC-**1**); 1.98 (s, 3H, H_3C-**17**); 1.89-1.60 (br. m, 4H, HHC-**4**, H_2C-**7**, HHC-**8**); 1.40-1.20 (br. m, 2 H, HHC-**4**, HHC-**8**); 1.07 (dd, J = 2.7, 12.6 Hz, 1H, HC-**8b**); 0.94 (s, 3H, H_3C-**12**); 0.72 (s, 6H, H_3C-**11**, H_3C-**14**)

^{13}C NMR (100 MHz, BB, DEPT, ^{1}H-^{13}C-COSY, $CDCl_3$):

δ: 171.28 (Cq, C-**16**); 146.23 (Cq, C-**2**); 107.43 (CH_2, C-**10**); 88.10 (CH, C-**6**); 61.43 (CH_2, C-**15**); 57.42 (CH_3, C-**13**); 54.71 (CH, C-**8b**); 54.40 (CH, C-**1**); 38.97 (Cq, C-**5**); 38.62 (Cq, C-**8a**); 37.35 (CH_2, C-**3**); 36.76 (CH_2, C-**8**); 28.24 (CH_3, C-

12); 23.27 (CH_2, C-**4**); 22.38 (CH_2, C-**7**); 21.05 (CH_3, C-**17**); 16.12 (CH_3, C-**11**); 14.99 (CH_3, C-**14**)

MS **(EI) m/z (rel. int.):**

202 (55.9), 187 (41.3), 166 (25.3), 159 (41.9), 153 (31.6), 148 (20), 135 (83.5), 134 (26.8), 133 (27.4), 121 (21.8), 119 (26.2), 107 (44.6), 105 (25), 93 (36.1), 91 (31.2), 85 (24.3), 79 (23.4), 71 (24.5), 55 (28.7), 43 (100), 41 (56.6);

HRMS **CI (DE) *i*-butane: m/z calcd. for $C_{18}H_{31}O_3$:**

295.227320 (M+H). Found: 295.227005.

5.5.5 Experiments toward intramolecular or combined intramolecular and intermolecular cyclizations including trapping

5.5.5.1 Synthesis of geranyldiethylmalonate (2-Ethylcarboxylate-5,9-dimethyl-deca-4,8-dienoic acid ethyl ester) (124)

5 g (32.4 mmol, 5.62 ml) of geraniol (**74**) was dissolved in 120 ml of absolute diethyl ether under argon, the solution was cooled to 0 ^{0}C and 3.4 ml (35.6 mmol, 9.65 g) of phosphorus tribromide was added dropwise over a 15 min period at this temperature. The reaction was then allowed to stir for 45 min at 0 ^{0}C and then warmed up to the room temperature. After quenching with an excess of water, the organic layer was separated, washed twice with water, again once with diluted $NaHCO_3$ solution and once with brine. The ethereal solution was dried and concentrated in vacuum at 30 ^{0}C and the resulting light yellow oil was tested by express NMR analysis which showed nearly complete conversion to geranyl bromide. This bromide was used for the next step without further purification.

NaH 1.3 g (32.4 mmol, 60 % in mineral oil) was placed in three-neck flame-dried flask and was washed twice with pentane under argon. In the following step pentane was decanted and 20 ml of dry DME were added. The flask was cooled to 0 ^{0}C and a solution of 4.95 ml diethylmalonate (32.4 mmol, 5.19 g) in 20 ml of dry DME was added dropwise over a 20 min period. The mixture was allowed to stir for further 15 min without cooling. The geranyl bromide in 10 ml of dry DME was then added dropwise over 15 min and the reaction allowed to stir overnight at room temperature before finally quenching with water. Ether was added and the organic layer was separated, washed with water and brine and dried over Na_2SO_4. The

organic layer was concentrated, resulting in a residue which was purified by column chromatography using pentane/ether 10/1→2/1 as eluant. 7.61 g (78 %) of pure geranyldiethylmalonate (**124**) were isolated as a light yellow oil.

2-Ethylcarboxylate-5,9-dimethyl-deca-4,8-dienoic acid ethyl ester (124):

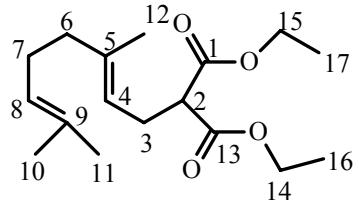

124

^{1}H NMR (250 MHz, ^{1}H-^{1}H-COSY, $CDCl_3$):

δ: 5.01 (m, 2H, HC-**4**, HC-**8**); 4.12 (q, J = 7.1 Hz, 4H, H_2C-**14**, H_2C-**15**); 3.28 (t, J = 7.7 Hz, 1H, HC-**2**); 2.55 (t, J = 7.4 Hz, 2H, H_2C-**3**); 2.03-1.86 (br. m, 4H, H_2C-**6**, H_2C-**7**); 1.62 (s, 3H, H_3C-**10**); 1.58 (s, 3H, H_3C-**11**); 1.53 (s, 3H, H_3C-**12**); 1.20 (t, J = 7.1 Hz, 6H, H_3C-**16**, H_3C-**17**)

^{13}C NMR (62.5 MHz, BB, DEPT, ^{1}H-^{13}C-COSY, $CDCl_3$):

δ: 168.93 (Cq, C-**1**, C-**13**); 138.08 (Cq, C-**5**); 131.13 (Cq, C-**9**); 123.75 (CH, C-**4**); 119.36 (CH, C-**8**); 60.93 (CH_2, C-**14**, C-**15**); 51.97 (CH, C-**2**); 39.39 (CH_2, C-**3**); 27.18 (CH_2, C-**6**); 26.26 (CH_2, C-**7**); 25.34 (CH_3, C-**10**); 17.35 (CH_3, C-**11**); 15.78 (CH_3, C-**12**); 13.79 (CH_3, C-**16**, C-**17**)

5.5.5.2 Synthesis of 5,9-Dimethyl-deca-4,8-dienoic acid ethyl ester (bis-homogeranic acid ethyl ester) (125)

Geranyldiethylmalonate (7.6 g, 25.7 mmol), LiCl (3.27 g, 77.1 mmol) and H_2O (0.46 g, 25.7 mmol) were placed in 100 ml two-neck round bottom flask and 43 ml of DMSO was added. The reaction mixture was stirred and refluxed for a 5 h period. In the next step reaction mixture was cooled to the room temperature and solvent was removed in vacuum. To the resulting products water and ether were added and the water layer was extracted twice with ether. Combined organic layer was washed with water and brine, dried over Na_2SO_4 and concentrated in vacuum. The crude product was purified by a column chromatography, using pentane / ether 20/1→5/1 as eluant. 5.18 g (90 %) of pure bis-homogeranic acid ethyl ester **125** were isolated as a light yellow oil.

5,9-Dimethyl-deca-4,8-dienoic acid ethyl ester (125):

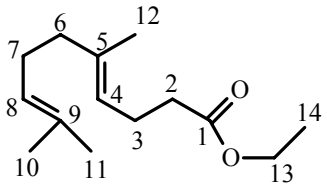

125

^{1}H NMR (250 MHz, ^{1}H-^{1}H-COSY, $CDCl_3$):

δ: 5.02 (m, 2H, HC-**4**, HC-**8**); 4.06 (q, J = 7.1 Hz, 2H, H_2C-**13**); 2.25 (m, 4H, H_2C-**2**, H_2C-**3**); 2.03-1.87 (br. m, 4H, H_2C-**6**, H_2C-**7**); 1.61 (s, 3H, H_3C-**10**); 1.56 (s, 3H, H_3C-**11**); 1.53 (s, 3H, H_3C-**12**); 1.19 (t, J = 7.1 Hz, 3H, H_3C-**14**)

^{13}C NMR (62.5 MHz, BB, DEPT, ^{1}H-^{13}C-COSY, $CDCl_3$):

δ: 173.02 (Cq, C-**1**); 136.21 (Cq, C-**5**); 130.98 (Cq, C-**9**); 123.90 (CH, C-**4**); 122.08 (CH, C-**8**); 59.84 (CH_2, C-**13**); 39.35 (CH_2, C-**2**); 34.21 (CH_2, C-**3**); 26.32 (CH_2, C-**6**); 25.33 (CH_3, C-**10**); 23.27 (CH_2, C-**7**); 17.32 (CH_3, C-**11**); 15.64 (CH_3, C-**12**); 13.93 (CH_3, C-**14**)

5.5.5.3 Synthesis of 5,9-Dimethyl-deca-4,8-dien-1-ol (bis-homogeraniol) (126)

1 g (powder 95%, 25.2 mmol) of $LiAlH_4$ was dispersed in 25 ml of absolute ether at 0^0C and a solution of ethyl bis-homogeranate (4.7 g, 21 mmol) in 25 ml of absolute ether was added dropwise. The reaction mixture was stirred at this temperature for 2 h and was finally quenched by a slow addition of 1 ml of water and then of 1 ml of 15 % NaOH. Additional 3 ml of water were added and the precipitate was removed by filtration. The layers were separated and the organic one was washed with water and brine, dried over Na_2SO_4 and concentrated in vacuum. The crude product was subjected to purification by column chromatography, using pentane/ether 5/1→1/2 as eluant. 3.63 g (95 %) of pure bis-homogeraniol (**126**), as a light yellow oil, were isolated.

5,9-Dimethyl-deca-4,8-dien-1-ol (126):

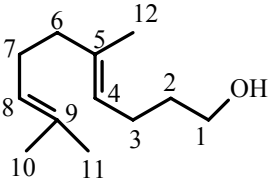

126

IR (KBr): υ_{max} 3384 s (br), 2926 s, 2730 w, 1669 m, 1649 m, 1448 s, 1377 s, 1225 w, 1153 w, 1107 m, 1058 s, 986 m, 918 w, 886 m, 830 m, 740 w, 595 w;

^{1}H NMR (500 MHz, ^{1}H-^{1}H-COSY, $CDCl_3$):

δ: 5.08 (t, J = 7.2 Hz, 1H, HC-**8**); 5.03 (t, J = 6.8, 1H, HC-**4**); 3.54 (dt, J = 1.1, 6.6 Hz, 2H, H_2C-**1**); 2.62 (br. s, 1H, HO); 2.00 (m, 4H, H_2C-**2**, H_2C-**7**); 1.91 (m, 2H, H_2C-**6**); 1.62 (s, 3H, H_3C-**10**); 1.53 (m, 8H, H_3C-**11**, H_3C-**12**, H_2C-**3**);

^{13}C NMR (125 MHz, BB, DEPT, ^{1}H-^{13}C-COSY, $CDCl_3$):

δ: 135.43 (Cq, C-**9**); 131.11 (Cq, C-**5**); 124.57 (CH, C-**8**); 123.69 (CH, C-**4**); 62.20 (CH_2, C-**1**); 39.57 (CH_2, C-**6**); 32.58 (CH_2, C-**3**); 26.53 (CH_2, C-**7**); 25.47 (CH_3, C-**10**); 24.01 (CH_2, C-**2**); 17.46 (CH_3, C-**11**); 15.75 (CH_3, C-**12**)

MS (EI) m/z (rel. int.):

182 (M^+, $C_{12}H_{22}O^+$) (4.3), 140 (4.9), 139 (38), 123 (16.5), 109 (7.4), 107 (4.3), 96 (15.5), 95 (74.4), 93 (14.1), 91 (4.6), 83 (4.3), 82 (8.8), 81 (14.6), 80 (3.7), 79 (8.1), 70 (11.4), 69 (100), 68 (12.1), 67 (32), 57 (7.5), 55 (24), 53 (12.9), 43 (13.2), 41 (63.5), 39 (9.8), 29 (9.5), 27 (7.1)

HRMS CI (FE) *i*-butane : m/z calcd. for $C_{12}H_{23}O_1$ (M+H):

183.174890. Found: 183.175033.

5.5.5.4 Irradiation of bis-homogeraniol (126) (→ 128, 129, 129a, 130, 131)

Irradiation of bis-homogeraniol (**126**) was performed according to the modified procedure, using $Cu(OAc)_2$ and $Mn(OAc)_3$ as co-oxidants. A solution of bis-homogeraniol (**126**) (5.49 mmol, 1 g), biphenyl (5 mmol, 0.77 g), DCTMB (1.31 mmol, 0.24 g), $Cu(OAc)_2$ (5.5 mmol, 1.1 g) and $Mn(OAc)_3$ (11 mmol, 2.94 g) in 500 ml of CH_3CN/CH_3OH 4/1 was irradiated at 300 nm in a *Rayonet* reactor at -15^0C for 2 days (the course of reaction was controlled by TLC). The resulting solution was concentrated in vacuum and the reaction products were separated by the column chromatography, using pentane/ether 30/1→5/1 as eluant. The order of elution was **130**, **131**, **128**, **129**, **129a**. Five main products **128** (120 mg, 10

%), **129** (116 mg, 10 %), **129a** (59 mg, 5 %), **130** (68 mg, 6 %) and **131** (72 mg, 6 %), all in form of light yellow oils, were isolated.

2-(5-Methyl-1-methylene-hex-4-enyl)-tetrahydrofuran (130):

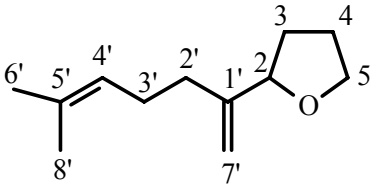

130

^{1}H NMR (500 MHz, ^{1}H-^{1}H-COSY, $CDCl_3$):

δ: 5.16 (t, J = 6.9 Hz, 1H, HC-**4'**); 5.08 (s, 1H, HHC-**7'**); 4.85 (s, 1H, HHC-**7'**); 4.31 (t, J = 7.1, 1H, HC-**2**); 3.95 (q, J = 7.1 Hz, 1H, HHC-**5**); 3.82 (dd, J = 7.8, 14 Hz, 1H, HHC-**5**); 2.19 (m, 2H, H_2C-**3'**); 2.05 (m, 4H, H_2C-**3**, H_2C-**4**); 1.91 (m, 2H, H_2C-**2'**); 1.72 (s, 3H, H_3C-**6'**); 1.64 (s, 3H, H_3C-**8'**)

^{13}C NMR (125 MHz, BB, DEPT, ^{1}H-^{13}C-COSY, $CDCl_3$):

δ: 149.84 (Cq, C-**1'**); 131.58 (Cq, C-**5'**); 124.15 (CH, C-**4'**); 108.29 (CH_2, C-**7'**); 81.55 (CH, C-**2**); 68.19 (CH_2, C-**5**); 32.02 (CH_2, C-**3'**); 31.13 (CH_2, C-**2'**); 26.50 (CH_2, C-**3**); 25.76 (CH_2, C-**4**); 25.62 (CH_3, C-**6'**); 17.65 (CH_3, C-**8'**)

2-(1,5-Dimethyl-hexa-1,4-dienyl)-tetra-hydrofuran (131):

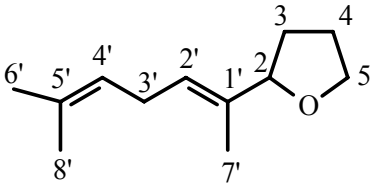

131

^{1}H NMR (500 MHz, ^{1}H-^{1}H-COSY, $CDCl_3$):

δ: 5.37 (dt, J = 1.2, 7.2 Hz, 1H, HC-**2'**); 5.08 (dt, J = 1.3, 7.2 Hz, 1H, HC-**4'**); 4.16 (t, J = 7.1 Hz, 1H, HC-**2**); 3.89 (m, 1H, HHC-**5**); 3.74 (m, 1H, HHC-**5**); 2.69 (t, J = 7.1 Hz, 2H, H_2C-**3'**); 1.93-1.85 (br. m, 4H, H_2C-**3**, H_2C-**4**); 1.66 (s, 3H, H_3C-**6'**); 1.60 (s, 3H, H_3C-**8'**); 1.57 (s, 3H, H_3C-**7'**)

^{13}C NMR (125 MHz, BB, DEPT, ^{1}H-^{13}C-COSY, $CDCl_3$):

δ: 134.88 (Cq, C-**1'**); 131.58 (Cq, C-**5'**); 124.58 (CH, C-**2'**); 122.75 (CH, C-**4'**); 83.97 (CH, C-**2**); 68.32 (CH_2, C-**5**); 30.32 (CH_2, C-**3**); 26.68 (CH_2, C-**3'**); 26.11 (CH_2, C-**4**); 25.86 (CH_3, C-**6'**); 17.66 (CH_3, C-**8'**); 11.83 (CH_3, C-**7'**)

3-(3-Methoxy-2,2-dimethyl-6-methylene-cyclohexyl)-propan-1-ol (128):

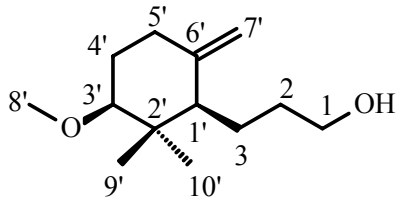

128

^{1}H NMR (500 MHz, ^{1}H-^{1}H-COSY, $CDCl_3$):

δ: 4.79 (s, 1H, HHC-**7'**); 4.52 (s, 1H, HHC-**7'**); 3.57 (dt, J = 1.5, 6.2 Hz, 2H, H_2C-**1**); 3.28 (s, 3H, H_3C-**8'**); 3.05-2.90 (br. s, 1H, HO); 2.79 (dd, J = 3.7, 8.8 Hz, 1H, HC-**3'**); 2.24 (m, 2H, H_2C-**3**); 1.90-1.45 (br. m, 7H, H_2C-**2**, H_2C-**4'**, H_2C-**5'**, HC-**1'**); 0.95 (s, 3H, H_3C-**9'**); 0.72 (s, 3H, H_3C-**10'**)

^{13}C NMR (125 MHz, BB, DEPT, ^{1}H-^{13}C-COSY, $CDCl_3$):

δ: 147.76 (Cq, C-**6'**); 108.42 (CH_2, C-**7'**); 86.48 (CH, C-**3'**); 63.07 (CH_2, C-**1**); 57.54 (CH_3, C-**8'**); 52.42 (CH, C-**1'**); 40.30 (Cq, C-**2'**); 31.91 (CH_2, C-**3**); 26.82 (CH_2, C-**5'**); 26.43 (CH_3, C-**9'**); 24.17 (CH_2, C-**4'**); 21.90 (CH_2, C-**2**); 17.53 (CH_3, C-**10'**)

8-Methoxy-5,9-dimethyl-deca-4,9-dien-1-ol (129):

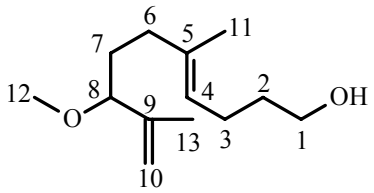

129

^{1}H NMR (500 MHz, ^{1}H-^{1}H-COSY, $CDCl_3$):

δ: 5.10 (t, J = 7.2 Hz, 1H, HC-**4**); 4.89 (s, 1H, HHC-**10**); 4.84 (s, 1H, HHC-**10**); 3.58 (dt, J = 1.5, 6.6 Hz, 2H, H_2C-**1**); 3.42 (t, J = 6.7 Hz, 1H, HC-**8**); 3.15 (s, 3H, H_3C-**12**); 2.03 (q, J = 7.3 Hz, 2H, H_2C-**7**); 1.97-1.89 (br. m, 2H, H_2C-**3**); 1.70-1.56 (br. m, 4H, H_2C-**2**, H_2C-**6**); 1.60 (s, 3H, H_3C-**11**); 1.56 (s, 3H, H_3C-**13**)

^{13}C NMR (125 MHz, BB, DEPT, ^{1}H-^{13}C-COSY, $CDCl_3$):

δ: 144.33 (Cq, C-**9**); 135.27 (Cq, C-**5**); 123.93 (CH, C-**4**); 113.54 (CH_2, C-**10**); 85.28 (CH, C-**8**); 62.51 (CH_2, C-**1**); 55.90 (CH_3, C-**12**); 35.64 (CH_2, C-**3**); 32.71 (CH_2, C-**6**); 31.87 (CH_2, C-**2**); 24.18 (CH_2, C-**7**); 16.27 (CH_3, C-**13**); 15.90 (CH_3, C-**11**)

9-Methoxy-5,9-dimethyl-deca-4,7-dien-1-ol (129a):

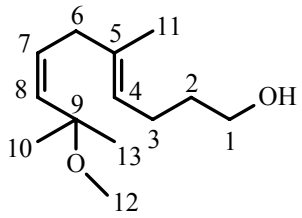

129a

^{1}H NMR (400 MHz, ^{1}H-^{1}H-COSY, $CDCl_3$):

δ: 5.45 (m, 1H, HC-**7**); 5.36 (d, J = 16.7 Hz, 1H, HC-**8**); 5.12 (t, J = 7.1 Hz, 1H, HC-**4**); 3.56 (m, 2H, H_2C-**1**); 3.08 (s, 3H, H_3C-**12**); 2.65 (d, J = 6.3 Hz, 2H, H_2C-**6**); 2.14-1.88 (br. m, 4H, H_2C-**2**, H_2C-**3**) 1.62 (s, 3H, H_3C-**11**); 1.19 (s, 6H, H_3C-**10**, H_3C-**13**)

^{13}C NMR (100 MHz, BB, DEPT, ^{1}H-^{13}C-COSY, $CDCl_3$):

δ: 136.50 (CH, C-**8**); 131.54 (Cq, C-**5**); 128.34 (CH, C-**7**); 124.75 (CH, C-**4**); 74.75 (Cq, C-**9**); 62.30 (CH_2, C-**1**); 50.06 (CH_3, C-**12**); 42.57 (CH_2, C-**6**); 30.85 (CH_2, C-**3**); 26.12 (CH_2, C-**2**); 25.73 (2xCH_3, C-**10**, C-**13**); 25.53 (CH_3, C-**11**)

5.6 Photochemistry of the metal complexes

5.6.1 Synthesis of methyl 7-methyl-3-oxo-oct-6-enoat (132)[69]

Dimethyl carbonate (0.158 mol, 14.23 g) was added to NaH (60 %, dispersion in mineral oil; 0.158 mol, 6.32 g) in dry ether (25 ml). After 10 min refluxing a solution of prenylacetone (0.079 mol, 9.97 g) in ether (5 ml) was added dropwise over a period of 1 h. After refluxing for 2 h, the mixture was cooled and the reaction quenched with MeOH (15 ml) in ether (75 ml). The suspension was poured onto ice and acidified with concentrated HCl until an acidic pH was reached. The reaction mixture was extracted with ether (3 times) and washed with concentrated $NaHCO_3$ until neutrality. The combined organic layers were dried over Na_2SO_4

and concentrated resulting in a red oil. Further purification by column chromatography on silica gel, using n-pentane/ether 5/1 as eluant, gave pure **132** with a yield of 75 % (10.9g).

5.6.2 Synthesis of bis(methyl 7-methyl-3-oxo-oct-6-enoato) copper(II) (138)

Cu(OAc)•H_2O (0.415 g, 2.08 mmol) was dissolved under argon in 23 ml of warm (about 45-50 °C) absolute methanol. A solution of β-ketoester **132** (0.765 g, 4.16 mmol) in 8 ml of absolute methanol was added, followed by immediate addition of a solution of NaOH (0.166 g, 4.16 mmol) in 10 ml of absolute methanol. The water bath was removed and the reaction mixture was stirred for 1 h at room temperature. The resulting blue precipitate was separated by filtration and washed twice on a filter with ice-cold methanol. This achieved complete removal of starting β-ketoester. Precipitated reaction products were dissolved in ether, all inorganic particles we removed by filtration and the ether was then removed under reduced pressure. Complex **138** was isolated in form of a dark-blue wax. The complex was recristallized from ether by slow addition of ice-cold methanol resulting in 0.45 g (50 %) of the complex **138** as a light-blue powder.

UV (CH_2Cl_2)**:** λ = 268 nm (ε = 9800)

IR (KBr): υ_{max} 2967 s, 2926 s, 1616 s, 1528 s, 1457 m, 1416 w, 1375 w, 1332 m, 1287 s, 1245 m, 1192 w, 1171 m, 1060 s, 1033 m, 982 w, 922 w, 833 w, 776 m, 740 w, 560 w, 457 w

HRMS ESIpos : m/z calcd for $C_{20}H_{30}NaO_6Cu$ (M+Na) and $C_{20}H_{30}KO_6Cu$ (M+K): 452.08, 468.04, 484.09 (small amount of solvated complex with 1 molecule of methanol)

5.6.3 Synthesis of the chiral Cu(II)-complex 146

bis-(Methyl 7-methyl-3-oxo-oct-6-enoato) Cu(II) (**138)** (0.147 g, 0.34 mmol) and semi-corrin **135** (0.1 g, 0.34 mmol) were dissolved in 10 ml of absolute dichloromethane and stirred for 1 h at room temperature. UV/VIS measurements done directly after mixing and after 1 h stirring show no significant differences. The resulting intensive green solution was concentra-

ted, washed several times with pentane with effective scraching. The complex crystallized as a green powder only at – 10^0C and lower temperature. Upon warming up it turns back to form a wax and cannot be isolated in crystalline form. This complex was subjected to irradiation without further purification. The curves below represent the UV/VIS measurements during this reaction.

UV (CH_2Cl_2)**:** λ = 269 nm (ε = 29900), 316 nm (sh)

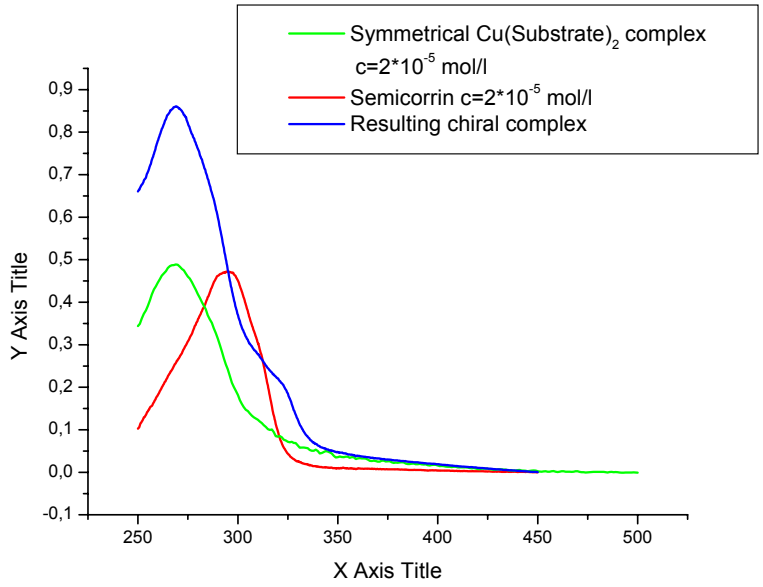

5.6.4 Irradiation of the achiral Cu(II)-complex 132

According to the general synthetic procedure, described in the chapter 5.2.2, complex **132** (0.213 g, 0.5 mmol), NMQ·PF_6(0.158 g, 0.55 mmol), BP (0.077 g, 0.5 mmol) and $Cu(OAc)_2 \cdot H_2O$ (0.2 g, 1 mmol) were dissolved or suspended in 100 ml of dichloromethane and subjected to a 3 days' irradiation at –15 ^{0}C. The work-up procedure, described in chapter 5.2.2, gave the crude product which was purified by column chromatography, using pentane/ether 10/1→5/1 as eluant. 55 mg (30 % yield) of the 2-(carbomethoxy)-3-isopropenylcyclopentanone (**139**[69]) were isolated as a light yellow oil.

2-(Carbomethoxy)-3-isopropenylcyclopentanone (139):

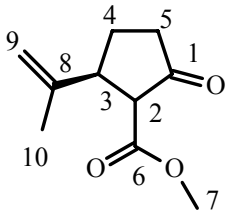

139

^{1}H NMR (400 MHz, ^{1}H-^{1}H-COSY, $CDCl_3$):

δ: 4.80 (d, J = 14.2, 2H, $\underline{H}_2$C-**9**); 3.72 (s, 3H, $\underline{H}_3$C-**7**); 3.16 (m, 2H, $\underline{H}$C-**2,** $\underline{H}$C-**3**); 2.44-2.33 (br. m, 2H, $\underline{H}_2$C-**5**); 2.23 (m, 1H, $\underline{H}_b$-C-**4**); 1.69 (m, 1H, $\underline{H}_a$-C-**4**); 1.74 (s, 3H, $\underline{H}_3$C-**10**)

^{13}C NMR (100 MHz, BB, DEPT, ^{1}H-^{13}C-COSY, $CDCl_3$):

δ: 210.97 (Cq, C-**1**); 169.53 (Cq, C-**6**); 144.17 (Cq, C-**8**); 111.12 (CH_2, C-**9**); 59.69 (CH, C-**2**); 52.42 (CH_3, C-**7**); 47.70 (CH, C-**3**); 38.31 (CH_2, C-**5**); 26.33 (CH_2, C-**4**); 20.35 (CH_3, C-**10**)

5.6.5 Irradiation of the chiral Cu(II)-complex 146

The irradiation of the chiral complex **146** was performed similar to the general synthetic procedure described in chapter 5.2.2 for the achiral symmetrical Cu(II)-complexes. For this reaction 0.184 g (0.34 mmol) of the complex **146**, 0.12 g (0.41 mmol)of NMQ·PF_6, 0.05 g (0.31 mmol) of BP and 0.069 g (0.34 mmol) of $Cu(OAc)_2 \cdot H_2O$ were dissolved or suspended in 100 ml of dry dichloromethane and the mixture was stirred and degassed with argon for 0.5 h. The mixture was then subjected to a 3 days' irradiation at 350 nm (λ_{max}, *Rayonet* reactor). Afterwards, the light green solution was filtered, the vessel and filter were washed twice with 5 ml of dichloromethane and the combined organic phases were concentrated. The resulting product mixture was dissolved or suspended in 60 ml of 1:1 ether/dichloromethane and treated with H_2S by bubbling for 1-2 min. The resulting dark brown suspension was degassed with argon for 0.5 h, filtered and concentrated. The crude products were then purified by column chromatography on silica, using pentane/ether 10/1→5/1 as eluant. 19 mg (30 %) of the cyclic ketoester **139**, and 92 mg (> 90 %) of the semicorrin **136** were isolated. The ketoester **139** was then subjected to racemic splitting.

Owing to the failed attempts to determine the enantiomeric excess using such methods as NMR with chiral shift reagents and chiral GC, the enantiomeric splitting using enantiomerically pure (S)-1-phenylethylamine was used to determine the enantiomeric excess of the products of cyclization.

3 Å molecular sieves (0.1 g) was placed in heat-dried two-neck flask. A solution of 19 mg (0.104 mmol) of the cyclic ketoester **139** in dry dichloromethane (5 ml) was transferred *via* syringe into the flask; this was followed by the addition of (S)-1-phenylethylamine (42 mg, 0.345 mmol). The reaction mixture was heated and refluxed under argon for 2 days. During

this time 2-3 ml of dry dichloromethane were added. After 2 days, the reaction mixture was cooled and the solution was removed from the flask by syringe. The molecular sieves were washed twice with dichloromethane. The combined solution was concentrated and purified by column chromatography on silica gel using *n*-pentane/ether 5/1→2/1 as eluant to give the enamine **147** as a light yellow oil in a yield of 65 % (20 mg) as a mixture of two diastereomers in 1.1:1 proportion. The characteristic ^{1}H spectral data of the minor diastereomer are given in brackets.

5-Isopropenyl-2-(1-phenyl-ethylamino)-cyclopent-1-enecarboxylic acid methyl ester (147):

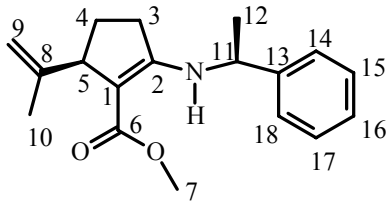

147

IR (KBr): υ_{max} 3404 s, 2963 s, 1734 s, 1653 s, 1457 s, 1384 m, 1367 s, 1262 m, 1123 m, 1045 m, 912 w, 763 w, 701 w, 540 w;

^{1}H NMR (400 MHz, ^{1}H-^{1}H-COSY, $CDCl_3$):

δ: 7.96 (d, J = 6.9 Hz, 1H, HN); 7.30 (m, 2H, HC-**15**, **17**); 7.22 (m, 3H, HC-**14**, **16, 18**); 4.62 (d, J = 7.6 Hz, 2H, H_2C-**9**); 4.55 (m, 1H, HC-**11**); 3.65 (s, 3H, OCH_3-**7**); 3.42 (m, 1H, HC-**5**); 2.58-2.12 (br. m, 2H, H_2C-**4**); 2.03-1.81 (br. m, 2H, H_2C-**3**); 1.66 (s, 3H, H_3C-**10** [major diastereomer]); 1.57 (s, 3H, H_3C-**10** [minor diastereomer]); 1.50 (d, J = 1.1 Hz, 3H, H_3C-**12** [major diastereomer]); 1.48 (d, J = 1.1 Hz, 3H, H_3C-**12** [minor diastereomer]);

^{13}C NMR (100 MHz, BB, DEPT, ^{1}H-^{13}C-COSY, $CDCl_3$):

δ: 169.00 (Cq, C-**6**); 165.17 (Cq, C-**1**); 149.23 (Cq, C-**8**); 145.03 (Cq, C-**13**); 128.70 (CH, C-**15**, C-**17**); 127.00 (CH, C-**16**); 125.37 (CH, C-**14**, C-**18**); 108.28 (CH_2, C-**9**); 95.98 (Cq, C-**2**); 54.20 (CH, C-**11**); 50.05 (CH_3, C-**7**); 48.90 (CH, C-**5**); 30.74 (CH_2, C-**3**); 27.76 (CH_2, C-**4**); 24.87 (CH_3, C-**12**); 20.11 (CH_3, C-**10**);

MS (EI) m/z (rel. int.):

285 (M^+, $C_{18}H_{23}NO_2^{+}$) (43.3), 270 (4.2), 245 (18), 244 (100), 238 (3.8), 226 (4), 166 (4.6), 150 (3.2), 140 (69.3), 122 (5.7), 108 (14.4), 106 (14.5), 105 (87.6), 104 (4.4), 103 (8.9), 91 (3.9), 80 (4.9), 79 (16.2), 77 (14), 53 (3.3);

HRMS EI (DE): m/z calcd for $C_{18}H_{23}NO_2$:
285.172879. Found: 285.172929.

5.6.6 Further experiments for mechanistic studies

Further experiments were performed in order to clarify the mechanism of cyclization in Cu(II)-complexes. For detailed discussion see chapter 3.3.5. Two homologues of prenylacetone (geranylacetone and farnesylacetone) were used for this purpose. The geranylacetone is commercially available in isomerically pure form and farnesylacetone is available only in form of a *cis-trans* isomeric mixture. For our purpose this mixture could be used for mechanistic studies. However, it can lead to decreased yields due to failure of application of PET in the cyclization of the *cis*-isomers of the natural terpenoids.

5.6.6.1 Synthesis of methyl 7,11-dimethyl-3-oxo-dodeca-6,10-dienoat (133)

Dimethyl carbonate (67 mmol, 6.04 g) was added to NaH (60 %, dispersion in mineral oil; 67 mmol, 2.68 g) in absolute THF (12 ml). After heating of the reaction mixture it was refluxed for 10 min. Then the geranylacetone (22 mmol, 4.35 g) in absolute THF (3 ml) was added dropwise during 20 min. After an additional 2 h refluxing, the reaction mixture was cooled and the reaction quenched by addition of concentrated HCl (6 ml) / water (35 ml). Extraction with ether (3 × 30 ml), washing with concentrated $NaHCO_3$, drying over Na_2SO_4 and concentration resulted in a crude product which was purified by column chromatography on silica gel, using *n*-pentane/ether 5/1 → 2/1 as eluant. Pure compound **133** was obtained as a yellow oil in 92 % yield.

Methyl 7,11-dimethyl-3-oxo-dodeca-6,10-dienoat (133):

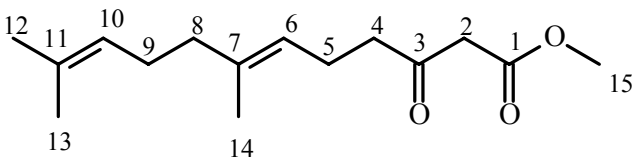

133

^{1}H NMR (250 MHz, ^{1}H-^{1}H-COSY, $CDCl_3$):

δ: 5.02 (m, 2H, HC-**6**, HC-**10**); 3.68 (s, 3H, H_3C-**15**); 3.40 (s, 2H, H_2C-**2**); 2.52 (t, J = 7.3 Hz, 2H, H_2C-**4**); 2.23 (q, J = 7.2 Hz, 2H, H_2C-**5**); 1.95 (m, 4H, H_2C-**8**, H_2C-**9**); 1.62 (s, 3H, H_3C-**12**); 1.56 (s, 3H, H_3C-**14**); 1.54 (s, 3H, H_3C-**13**)

^{13}C NMR (62.5 MHz, BB, DEPT, ^{1}H-^{13}C-COSY, $CDCl_3$):

δ: 202.36 (Cq, C-**3**); 167.55 (Cq, C-**1**); 136.67 (Cq, C-**7**); 131.33 (Cq, C-**11**); 124.07 (CH, C-**6**); 121.98 (CH, C-**10**); 59.19 (CH_3, C-**15**); 49.00 (CH_2, C-**2**); 42.97 (CH_2, C-**4**); 39.55 (CH_2, C-**5**); 26.51 (CH_2, C-**8**); 25.57 (CH_3, C-**12**); 22.08 (CH_3, C-**9**); 17.57 (CH_3, C-**14**); 15.89 (CH_3, C-**13**)

5.6.6.2 Synthesis and irradiation of bis(methyl 7,11-dimethyl-3-oxo-dodeca-6,10-dieno-ato) copper (II) (140)

The synthesis of **140** was performed similar to the procedure described in chapter 5.6.2. 0.79 g (3.96 mmol) of Cu(II)-acetate was dissolved in 20 ml of absolute and warm methanol under an argon flow. A solution of 2 g (7.9 mmol) of ketoester **133** in 10 ml of absolute methanol was added, followed by a rapid addition of a solution of 0.32 g (7.9 mmol) of NaOH in 15 ml of absolute methanol. The mixture was allowed to stir at room temperature for 1 h. During this time the colour of the mixture changed from dark blue to light green whereas dark blue drops of wax formed at the wall. The reaction mixture was concentrated and the resulting dark blue very viscous wax was three times washed and scratched extensively with ice-cold methanol (3 x 10 ml). The solvent was decanted and the rest of the solvent was removed in vacuum. The resulting wax was dissolved in 20 ml of ether. The solution was filtered in order to remove all inorganic particles and finally concentrated to give 1.19 g (53 %) of the target complex **140** as a dark blue wax. It was used for the irradiation step without further purification.

The irradiation was performed according to the general synthetic procedure, described in chapter 5.2.2. For this purpose 1.19 g (2.1 mmol) of complex **140**, 0.67 g (2.3 mmol, 1.1 equiv.) of NMQ·PF_6, 0.29 g (1.9 mmol) of BP and 0.84 g (4.21 mmol) of $Cu(OAc)_2 \cdot H_2O$ were dissolved in 125 ml of dichloromethane/acetonitrile 4:1. This reaction mixture was then irradiated for 1 day at 350 nm (λ_{max}, *Rayonet* reactor), thereafter concentrated, taken up in

dichloromethane/ether 1:1 prior to bubbling through the solution H_2S. Filtration and concentration resulted in a crude product mixture which was separated by column chromatography on silica gel using pentane/ether 20/1→ 3/1 as eluant. Two products, **142a** and **142b**, were isolated in a combined yield of 30 % (0.145 g, proportion 1 : 5.3), both in form of light yellow oils.

2-(5'-Methyl-1'-methylene-hex-4-enyl)-5-oxo-cyclopentanecarboxylic acid methyl ester (142a):

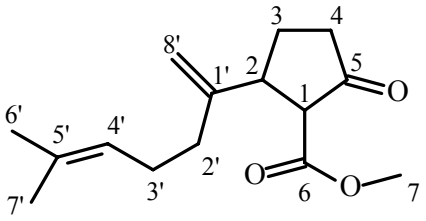

142 a

^{1}H NMR (400 MHz, ^{1}H-^{1}H-COSY, $CDCl_3$):

δ: 5.05 (t, 1H, J = 6.6 Hz, HC-**4**`); 4.81 (d, 2H, J = 5.7 Hz, $H_2$C-**8**`); 3.69 (s, 3H, H_3C-**7**); 3.16 (m, 2H, HC-**1**, HC-**2**); 2.56-2.48 (br. m, 2H, H_2C-**4**); 2.22 (m, 1H, *H*HC-**3**); 2.16-2.08 (br. m, 4H, H_2C-**2**`, $H_2$C-**3**`); 1.74 (m, 1H, H*H*C-**3**); 1.64 (s, 3H, H_3C-**7**`); 1.56 (s, 3H, $H_3$C-**6**`)

^{13}C NMR (100 MHz, BB, DEPT, ^{1}H-^{13}C-COSY, $CDCl_3$):

δ: 210.92 (Cq, C-**5**); 169.48 (Cq, C-**6**); 148.51 (Cq, C-**1**`); 131.92 (Cq, C-**5**`); 123.53 (CH, C-**4**`); 109.39 ($CH_2$, C-**8**`); 59.97 (CH, C-**1**); 52.33 (CH_3, C-**7**); 46.60 (CH, C-**2**); 38.27 (CH_2, C-**4**); 34.24 (CH_2, C-**2**`); 26.87 ($CH_2$, C-**3**`); 26.44 (CH_2, C-**3**); 25.53 (CH_3, C-**7**`); 17.54 ($CH_3$, C-**6**`)

2-(1',5'-Dimethyl-hexa-1',4'-dienyl)-5-oxo-cyclopentanecarboxylic acid methyl ester (142b):

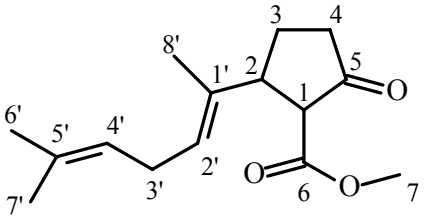

142 b

^{1}H NMR (400 MHz, ^{1}H-^{1}H-COSY, $CDCl_3$):

δ: 5.21 (t, 1H, J = 6.9 Hz, HC-**2**`); 5.00 (dt, 1H, J = 1.3, 7.1 Hz, HC-**4**`); 3.68 (s, 3H, H_3C-**7**); 3.11 (m, 2H, HC-**1**, HC-**2**); 2.65 (t, 1H, J = 7 Hz, H_2C-**3**`); 2.44-2.30

(br. m, 2H, $\underline{H}_2$C-**4**); 2.26 (m, 1H, *H*HC-**3**); 1.70 (m, 1H, H*H*C-**3**); 1.64 (s, 3H, $\underline{H}_3$C-**7`**); 1.61 (s, 3H, $\underline{H}_3$C-**8`**); 1.56 (s, 3H, $\underline{H}_3$C-**6`**)

^{13}C NMR (100 MHz, BB, DEPT, ^{1}H-^{13}C-COSY, $CDCl_3$):

δ: 211.29 (Cq, C-**5**); 169.63 (Cq, C-**6**); 133.05 (Cq, C-**1`**); 131.82 (Cq, C-**5`**); 124.97 (CH, C-**2`**); 122.43 (CH, C-**4`**); 59.48 (CH, C-**1**); 52.22 (CH_3, C-**7**); 49.47 (CH, C-**2**); 38.19 (CH_2, C-**4**); 26.83 (CH_2, C-**3`**); 26.17 ($CH_2$, C-**3**); 25.53 ($CH_3$, C-**7`**); 17.62 (CH_3, C-**6`**); 13.63 ($CH_3$, C-**8`**)

5.6.6.3 Synthesis of 7,11,15-trimethyl-3-oxo-hexadeca-6,10,14-trienoic acid methyl ester (134)

According to the synthetic procedure described above, the 7,11,15-Trimethyl-3-oxo-hexadeca-6,10,14-trienoic acid methyl ester (**134**) was prepared using dimethyl carbonate (3.1 g, 34.3 mmol, 2.9 ml) and 1.37 g NaH (60 %, dispersion in mineral oil; 34.3 mmol) dissolved and dispersed in 8 ml of absolute THF. 3 g of farnesylacetone (mixture of isomers, 11.4 mmol) were added dropwise to the boiling reaction mixture over a 20 min period and refluxed for additional 2 h. After cooling of the reaction in an ice-bath HCl (12 ml) and water (70 ml) were added. Extraction with ether (3 × 30 ml), washing with concentrated $NaHCO_3$ and brine, drying over Na_2SO_4 and concentration gave the crude product which was further purified by column chromatography on silica, using *n*-pentane/ether 10/1 → 5/1. The target product **134** was isolated as a mixture of isomers in form of yellow oils in combined yield of 90 %.

7,11,15-Trimethyl-3-oxo-hexadeca-6,10,14-trienoic acid methyl ester (134):

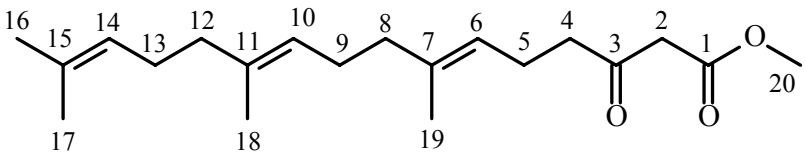

134

The values of the isomers are given in brakets.

^{1}H NMR (250 MHz, ^{1}H-^{1}H-COSY, $CDCl_3$):

δ: 5.04 (m, 3H, HC-**6**, HC-**10**, HC-**14**); 3.66 (s, 3H, H_3C-**20**); 3.39 (s, 2H, H_2C-**2**); 2.50 (m, 2H, H_2C-**4**); 2.23 (q, J = 7.3 Hz, 2H, H_2C-**5**); 1.97 (m, 8H, H_2C-**8**, H_2C-**9**, H_2C-**12**, H_2C-**13**); 1.62 (s, 6H, H_3C-**18**, H_3C-**19**); 1.55 (s, 6H, H_3C-**16**, H_3C-**17**)

^{13}C NMR (62 MHz, BB, DEPT, ^{1}H-^{13}C-COSY, $CDCl_3$):

δ: 202.28 [202.20] (Cq, C-**3**); 167.51 (Cq, C-**1**); 136.80 [136.68] (Cq, C-**7**); 134.96 [135.10, 135.22, 135.34] (Cq, C-**11**); 131.11 [131.37] (Cq, C-**15**); 124.26 [124.75] (CH, C-**6**); 123.95 [123.84] (CH, C-**10**); 121.99 [122.01] (CH, C-**14**); 52.17 (CH_3, C-**20**); 48.98 (CH_2, C-**2**); 42.97 [43.19] (CH_2, C-**4**); 39.65 [39.55, 39.84] (CH_2, C-**5**); 31.86 [31.78] (CH_2, C-**8**); 26.56 [26.53] (CH_3, C-**12**); 26.33 [26.44] (CH_2, C-**9**); 25.59 (CH_3, C-**17**); 23.28 (CH_3, C-**18**); 21.89 (CH_2, C-**13**); 17.57 (CH_3, C-**16**); 15.89 (CH_3, C-**19**);

5.6.6.4 Synthesis and irradiation of bis(methyl 7,11,15-trimethyl-3-oxo-hexadeca-6,10,14-trienoato)copper(II) (141)

The synthesis and isolation of **141** was performed according to the synthetic procedure described in chapter 5.6.6.2 using 0.91 g (4.55 mmol) of Cu(II)-acetate, dissolved in 20 ml of absolute methanol, 2.9 g (9.1 mmol) of the ketoester **134**, dissolved in 10 ml of absolute methanol and a solution of 0.36 g (9.1 mmol) of NaOH in 15 ml of methanol. The described work-up resulted in 1.9 g (60 %) of the dark blue waxy complex **141** which was directly used for the irradiation step without further purification.

The irradiation was conducted according to the general synthetic procedure described in chapter 5.2.2 using 1 g (1.4 mmol) of complex **141**, 0.45 g (1.57 mmol, 1.1 equiv.) of NMQ·PF_6, 0.22 g (1.4 mmol) of BP and 0.57 g (2.85 mmol) of $Cu(OAc)_2 \cdot H_2O$. These components were dissolved in 100 ml of dichloromethane/acetonitrile 4:1 and irradiated for 1 day at 350 nm (λ_{max}, *Rayonet* reactor). The reaction mixture was then concentrated, taken up in dichloromethane/ether mixture and bubbled with H_2S. Filtration and concentration resulted in a crude products mixture which was separated by a column chromatography, using pentane/ether 20/1→ 3/1 as eluant. Two products **143a** and **143b** were isolated in a combined yield of 19 % (0.091 g) in a proportion of 1 : 3.8, both in form of light yellow oils.

2-(5,9-Dimethyl-1-methylene-deca-4,8-dien-yl)-5-oxo-cyclopentanecarboxylic acid methyl ester (143a):

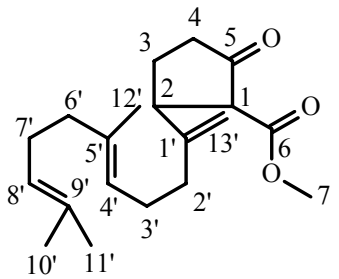

143 a

^{1}H NMR (250 MHz, ^{1}H-^{1}H-COSY, $CDCl_3$):

δ: 4.97 (m, 2H, HC-**4`**, HC-**8`**); 4.75 (d, J = 4.8 Hz, 2H, H_2C-**13`**); 3.64 (s, 3H, $H_3$C-**7**); 3.10 (m, 2H, HC-**1**, HC-**2**); 2.48-2.41 (m, 2H, $H_2$C-**4**); 2.15 (m, 1H, *H*HC-**3**); 2.07-1.80 (m, 9H, $H_2$C-**2`**, H_2C-**3`**, $H_2$C-**6`**, H_2C-**7`**, H*H*C-**3**); 1.57 (s, 3H, $H_3$C-**10`**); 1.49 (s, 6H, H_3C-**11`**, $H_3$C-**12`**)

^{13}C NMR (62.5 MHz, BB, DEPT, ^{1}H-^{13}C-COSY, $CDCl_3$):

δ: 211.04 (Cq, C-**5**); 169.51 (Cq, C-**6**); 148.49 (Cq, C-**1`**); 135.72 (Cq, C-**5`**); 131.58 (Cq, C-**9`**); 124.13 (CH, C-**4`**); 122.30 (CH, C-**8`**); 109.45 ($CH_2$, C-**13`**); 60.01 (CH, C-**1**); 52.41 (CH_3, C-**7**); 46.60 (CH, C-**2**); 39.60 (CH_2, C-**4**); 38.33 (CH_2, C-**3**); 26.92 (CH_2, C-**2`**); 26.76 ($CH_2$, C-**6`**); 26.49 (CH_2, C-**7`**); 26.33 ($CH_2$, C-**3`**); 25.63 (CH_3, C-**10`**); 17.54 ($CH_3$, C-**11`**); 16.03 (CH_3, C-**12`**)

2-Oxo-5-(1,5,9-trimethyl-deca-1,4,8-trien-yl)-cyclopentanecarboxylic acid methyl ester (143b):

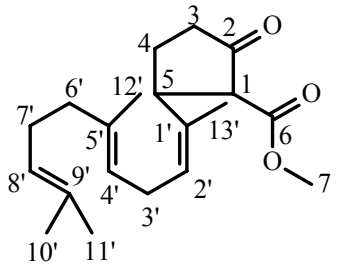

143 b

^{1}H NMR (400 MHz, ^{1}H-^{1}H-COSY, $CDCl_3$):

δ: 5.13 (m, 1H, HC-**2`**); 4.97 (m, 2H, HC-**4`**, HC-**8`**); 3.62 (s, 3H, $H_3$C-**7**); 3.07 (m, 2H, HC-**1**, HC-**5**); 2.60 (t, J = 7.1 Hz, 2H, $H_2$C-**3`**); 2.38-2.27 (m, 2H, H_2C-**3**); 2.22 (m, 1H, *H*HC-**4**); 2.02-1.86 (m, 5H, H_2C-**6`**, $H_2$C-**7`**, H*H*C-**4**); 1.57 (s, 3H, H_3C-**10`**); 1.54 (s, 3H, $H_3$C-**13`**); 1.49 (s, 6H, H_3C-**11`**, $H_3$C-**12`**)

^{13}C NMR (100 MHz, BB, DEPT, ^{1}H-^{13}C-COSY, $CDCl_3$):

δ: 211.42 (Cq, C-**2**); 169.66 (Cq, C-**6**); 133.09 (Cq, C-**1`**); 132.57 (Cq, C-**5`**); 131.32 (Cq, C-**9`**); 125.08 (CH, C-**2`**); 124.17 (CH, C-**4`**); 123.06 (CH, C-**8`**); 59.51 (CH, C-**1**); 52.31 (CH_3, C-**7**); 49.50 (CH, C-**5**); 39.60 (CH_2, C-**3**); 38.25 (CH_2, C-**4**); 31.95 (CH_2, C-**3`**); 26.62 ($CH_2$, C-**6`**); 26.21 (CH_2, C-**7`**); 25.63 ($CH_3$, C-**10`**); 23.33 (CH_3, C-**12`**); 17.62 ($CH_3$, C-**11`**); 13.70 (CH_3, C-**13`**)

5.7 Quantum mechanical calculations

In the following the Cartesian coordinates of calculated molecules and heats of formation are depicted. In case of small molecules DFT calculation were applied. In case of larger molecules the UHF/PM3 method with H…H correction was used. The results, obtained by UHF/PM3 (PM3 H...H correction), are in good agreement with the results of the DFT method. In contrast to DFT, the UHF/PM3 method is much quicker to perform.

5.7.1 Data for the Cu(II)-complex 146

```
run type:                    OPT
 model:           NLSDA/BP86/DN*
 number of shells:            276
  169 S shells
   71 P shells
   36 D shells
 number of valence orbitals: 562
 point group symmetry used:   C1
 spin multiplicity:            2
stoichiometry:     CuO7N3C24H31

 molecular charge             0.0
 number of electrons        281.0
```

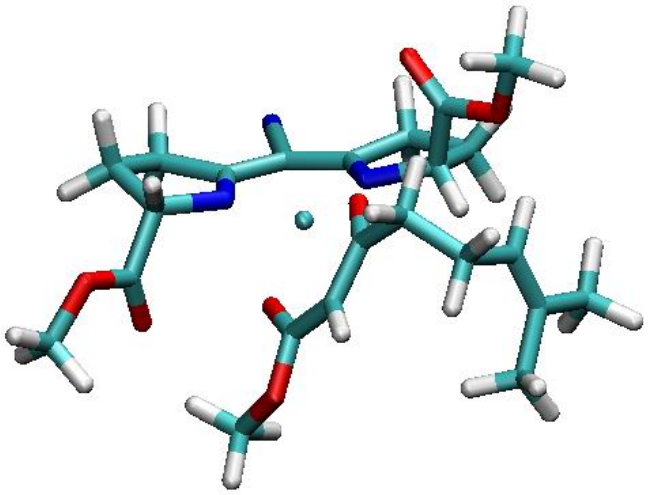

cartesian coordinates (angstroms)

atom		x	y	z
H1	1	-2.9512768	-1.5378908	-4.0174543
Cu1	2	-0.1789721	-0.1543619	-0.4360797
C1	3	2.5965951	-2.4504457	1.7813411
N1	4	-1.4876201	0.4490081	0.9042088
O1	5	1.4098586	0.4519950	-1.4308315
C2	6	-2.6469611	0.9927727	0.5874382
C3	7	-3.4074325	1.4887002	1.7951940
C4	8	-3.1788471	1.0883277	-0.7271893
C5	9	-2.4301798	1.2584135	2.9628820
H2	10	-4.3443297	0.9211281	1.9036661
H3	11	-3.6858043	2.5457669	1.6713385
C6	12	-1.3227272	0.3393377	2.3598801

H4	13	-2.9187273	0.7994059	3.8347186
H5	14	-1.9746892	2.2016523	3.2942929
C7	15	-1.4997319	-1.1031966	2.8500883
H6	16	-0.3109071	0.6602310	2.6448930
C8	17	-2.5999738	0.5237647	-1.8976465
C9	18	-4.4336970	1.7357636	-0.8708861
N2	19	-5.4652053	2.2834266	-0.9857457
N3	20	-1.3989029	-0.0182920	-1.9727349
C10	21	-3.3593601	0.4490322	-3.2003696
C11	22	-0.1346515	0.2578345	-4.1541753
H7	23	-0.7413287	-1.5731224	-3.2335171
C12	24	-2.5203821	-0.5275034	-4.0408779
H8	25	-3.4289856	1.4495765	-3.6546192
H9	26	-4.3880537	0.0964267	-3.0364041
C13	27	-1.1349635	-0.5495265	-3.3206596
H10	28	-2.4387872	-0.2221747	-5.0940942
C14	29	2.5845399	0.1351153	-1.0749420
O2	30	3.6267494	0.7491295	-1.7005877
C15	31	2.9648119	-0.8075241	-0.0904202
C16	32	3.2673208	1.8306331	-2.5955589
H11	33	4.2152000	2.2162337	-2.9870990
H12	34	2.7301433	2.6139510	-2.0464062
H13	35	2.6234492	1.4764338	-3.4059620
O3	36	0.7911210	-1.2660461	0.8165019
H14	37	4.0315931	-1.0128605	0.0087840
C17	38	2.0687316	-1.4499088	0.7656627
C18	39	3.5127873	-1.8083398	2.8431009
H15	40	3.1344019	-3.2582124	1.2577320
H16	41	1.7212149	-2.8977060	2.2720221
C19	42	2.7837340	-0.8137054	3.6980888
H17	43	4.3726983	-1.3364376	2.3471019
H18	44	3.9254422	-2.6181574	3.4740177
C20	45	3.1495484	0.4617201	3.9170480
H19	46	1.8551003	-1.1704404	4.1577669
C21	47	4.3930509	1.0755864	3.3106641
C22	48	2.3363363	1.3700646	4.7982190
H20	49	5.3045397	0.5362779	3.6097782
H21	50	4.5130896	2.1204038	3.6293422
H22	51	4.3544517	1.0701372	2.2102426
H23	52	2.9275109	1.7163821	5.6623590
H24	53	1.4348427	0.8743335	5.1822836
H25	54	2.0242379	2.2784717	4.2566771
O4	55	-2.2611334	-1.9278660	2.3872410
O5	56	-0.6971740	-1.3126419	3.9403488
C23	57	-0.7017528	-2.6579193	4.4787677
H26	58	-1.7060095	-2.9505087	4.8116151
H27	59	-0.0108048	-2.6344578	5.3290279
H28	60	-0.3459399	-3.3615426	3.7159305
O6	61	-0.0071918	1.4650039	-4.1737845
O7	62	0.5446676	-0.6083152	-4.9724561
C24	63	1.4213940	-0.0048426	-5.9563589
H29	64	0.8684089	0.6994030	-6.5912451
H30	65	1.8072812	-0.8382924	-6.5544027
H31	66	2.2509281	0.5145644	-5.4619771

<S*S> = 0.752

E(DFT) = -3265.56430 BP86

5.7.2 Data for the Zn(II)-analogue of complex 146

```
run type:                    OPT
 model:           NLSDA/BP86/DN*
 number of shells:            276
  169 S shells
   71 P shells
   36 D shells
 number of valence orbitals: 562
 point group symmetry used:   C1
 spin multiplicity:            1
stoichiometry:     ZnO7N3C24H31

 molecular charge             0.0
 number of electrons        282.0
```

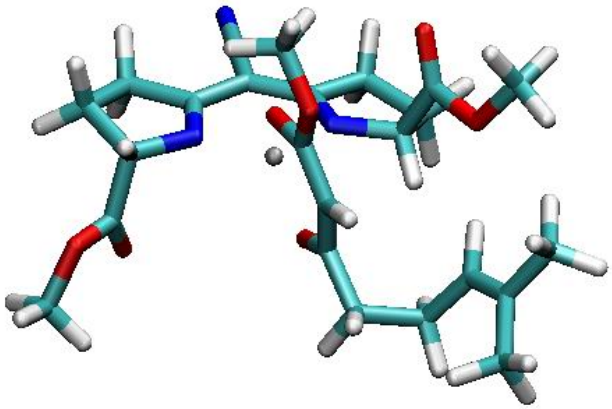

cartesian coordinates (angstroms)

atom		x	y	z
O1	1	0.6099662	-1.9345003	-0.4634196
Zn1	2	-0.0064919	-0.0215176	-0.6937117
O2	3	1.3858347	0.7518500	0.4562470
H1	4	-4.2095051	1.0614582	2.1715114
N1	5	-0.3867448	0.3784629	-2.6004136
C1	6	-1.6155918	0.6507748	-3.0194596
C2	7	-1.7139096	0.6969919	-4.5288617
C3	8	-2.7513325	0.8901839	-2.1989223
C4	9	-3.9674966	1.2042948	-2.8675560
C5	10	-2.7838999	0.8935561	-0.7742662
N2	11	-1.7907348	0.5288904	0.0154638
C6	12	-4.0039701	1.3497071	-0.0055275
N3	13	-4.9711231	1.4590347	-3.4207085
C7	14	-2.3134900	-0.7018581	2.0987614
H2	15	-1.3560668	1.2113408	1.9612015
C8	16	-0.3526064	0.1477811	-4.9856932
H3	17	-1.8863553	1.7366060	-4.8514350
H4	18	-2.5626974	0.0920998	-4.8851108
H5	19	0.0410405	0.6722429	-5.8647466
H6	20	-0.4354070	-0.9166706	-5.2379783
C9	21	0.5483294	0.2962051	-3.7283784
H7	22	1.2169833	-0.5644806	-3.5992501
C10	23	1.4205597	1.5515447	-3.8526344
H8	24	-4.3795206	2.3095497	-0.3949225
C11	25	-3.4909382	1.4531736	1.4412463
H9	26	-4.8106165	0.6078543	-0.1199271
H10	27	-3.2909176	2.5000930	1.6986066
C12	28	-2.1489290	0.6667125	1.4313684
O3	29	1.0476651	2.7000552	-3.7178237
O4	30	2.6754726	1.1835774	-4.2297156
C13	31	3.5706171	2.2656667	-4.5826337
H11	32	3.1751510	2.8038348	-5.4497622
H12	33	4.5175828	1.7807356	-4.8332792
H13	34	3.6932628	2.9589649	-3.7458062
O5	35	-2.9878404	-1.6205735	1.6743885
O6	36	-1.6462250	-0.7194026	3.2839550
C14	37	-1.9022373	-1.8701721	4.1249356
H14	38	-2.9453992	-1.8487067	4.4573015
H15	39	-1.2300433	-1.7563762	4.9782232
H16	40	-1.7084807	-2.8000513	3.5843454

C15	41	3.0616336	0.8348674	2.1241262
C16	42	2.2352852	-1.3591335	1.2315341
C17	43	1.4623215	-2.2355390	0.4308918
O7	44	1.6932435	-3.5530548	0.6726854
C18	45	0.9525178	-4.4775290	-0.1573132
H17	46	1.2892838	-5.4721261	0.1496218
H18	47	1.1808851	-4.3052147	-1.2148604
H19	48	-0.1254046	-4.3670306	0.0055072
H20	49	2.9243786	-1.8282154	1.9312918
C19	50	2.1715443	0.0358133	1.1985443
C20	51	2.3465667	1.2757111	3.4307525
H21	52	3.3739810	1.7385780	1.5829576
H22	53	3.9649643	0.2646791	2.3726323
C21	54	1.9408951	0.1373401	4.3259918
H23	55	1.4499932	1.8449106	3.1416426
H24	56	3.0139481	1.9761282	3.9584864
H25	57	0.9672756	-0.3156509	4.1092436
C22	58	2.6665468	-0.3590879	5.3444316
C23	59	2.1891764	-1.5273720	6.1608939
C24	60	4.0141160	0.2043169	5.7355289
H26	61	4.6701559	0.3254616	4.8627543
H27	62	4.5290991	-0.4537848	6.4504291
H28	63	3.9109154	1.1922892	6.2121916
H29	64	2.8897159	-2.3728277	6.0588282
H30	65	1.1964630	-1.8741889	5.8450813
H31	66	2.1449564	-1.2826191	7.2359346

E(DFT) = -3404.47060 BP86

5.7.3 Data for compound 72

```
Run type: Geometry optimization
  Model: UHF/6-31G*
  Number of shells: 196
   109 S shells
    58 SP shells
    29 6D shells
  Number of basis functions: 515
  Number of electrons: 222
  Use of molecular symmetry disabled
  Molecular charge:   0
  Spin multiplicity:  1
Point Group = C1 Order = 1 Nsymop = 1
This system has 201 degrees of freedom
Coordinates read from pre-optimization
```

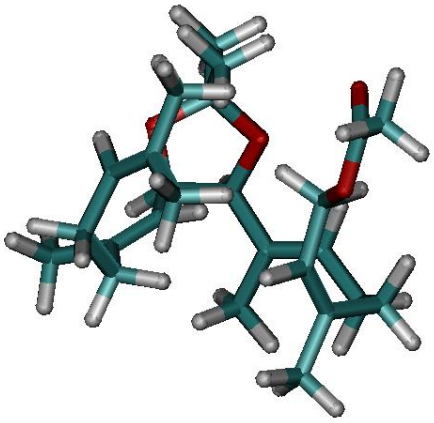

Cartesian Coordinates (Angstroms)

Atom	Label	X	Y	Z
H	H14	1.3844565	-3.9241298	-3.8444519
O	O1	2.0329404	-2.2591856	-1.9032953
C	C2	2.4868728	-0.9738286	-1.5243960
C	C3	1.9210018	-0.1174360	-2.6727219
H	H9	2.0276085	-2.4412297	-4.5342401
C	C5	0.8955290	-2.1521371	-2.7251206
H	H13	0.3116756	-2.8098117	-4.6927180
H	H3	3.5657268	-0.9966583	-1.5571225

C	C1	1.9941671	-0.5781646	-0.1554876
C	C15	1.7296756	1.3607429	-2.4199124
H	H6	2.5933572	-0.2235366	-3.5243848
H	H12	-1.2181995	-2.5502789	-2.6256569
O	O2	0.7172469	-0.7771981	-2.9495277
C	C7	1.1707317	-2.8782353	-4.0345675
C	C6	-0.3341660	-2.6910949	-2.0142236
H	H10	-0.4740420	-2.1724297	-1.0748841
H	H11	-0.2135055	-3.7494386	-1.8126291
H	H1	1.0521904	-0.0581157	-0.1402115
C	C4	2.5906862	-0.8227653	1.0028985
C	C10	3.8990394	-1.5629011	1.1542086
C	C8	1.9607293	-0.3545050	2.3001214
C	C9	1.3809008	-1.4744811	3.1913468
H	H4	1.1706565	0.3549369	2.0804722
H	H8	2.7129318	0.1798717	2.8789445
C	C11	0.2624008	-2.2503233	2.5414736
H	H15	1.0538457	-1.0235728	4.1202912
H	H16	2.1728775	-2.1679203	3.4629231
H	H7	4.6225230	-0.9513570	1.6886009
H	H17	4.3340313	-1.8562255	0.2091445
H	H18	3.7604897	-2.4693987	1.7367415
C	C13	-2.0230458	-3.0487078	2.0419519
H	H19	0.5818552	-2.9436512	1.7800811
C	C12	-1.0384610	-2.1772677	2.7878490
C	C14	-1.6832330	-1.2538571	3.7940574
H	H2	-2.5935013	-3.6636965	2.7350874
H	H20	-1.5259643	-3.7080228	1.3405653
H	H21	-2.7407876	-2.4480643	1.4887940
H	H22	-2.2591386	-1.8236050	4.5197135
H	H23	-2.3804019	-0.5842430	3.2953773
H	H24	-0.9747812	-0.6437604	4.3366722
C	C17	3.0274566	2.0853424	-2.1487339
C	C18	0.1572875	3.3664762	-2.3402454
C	C16	0.5301613	1.9151392	-2.4930674
H	H28	-0.2955252	1.2627776	-2.7178976
H	H5	3.7514279	1.8758591	-2.9328400
H	H25	3.4669972	1.7581070	-1.2103373
H	H26	2.9049400	3.1576860	-2.0999538
C	C19	-1.0485635	3.5828667	-1.4032963
H	H29	-0.1249510	3.7528708	-3.3183739
H	H30	0.9937755	3.9672247	-2.0093215
C	C20	-0.8018220	3.2359509	0.0501747
H	H31	-1.8945812	3.0337078	-1.7958141
H	H32	-1.3225748	4.6351135	-1.4497248
C	C21	-1.4176831	2.2738922	0.7230315
C	C23	-2.4122645	1.2740814	0.2177251
C	C22	0.2111244	4.1123332	0.7524465
H	H27	-1.1827225	2.1497497	1.7679247
H	H33	0.2413459	3.9113576	1.8164571
H	H34	-0.0263619	5.1640340	0.6129029
H	H35	1.2110485	3.9552915	0.3580218
H	H36	-2.0127689	0.2706432	0.2829058
H	H37	-2.7201285	1.4400808	-0.8015623
O	O3	-3.5613457	1.3571362	1.0664927
C	C24	-4.5378975	0.4884413	0.8550601
O	O4	-4.5010240	-0.3529248	0.0149121
C	C25	-5.6855239	0.7065788	1.8047780
H	H38	-6.4578232	-0.0235231	1.6140809
H	H39	-6.0808533	1.7074636	1.6746986
H	H40	-5.3380681	0.6219262	2.8277912

E(HF) = -1269.3994010 a.u.

5.7.4 Data for compound 87

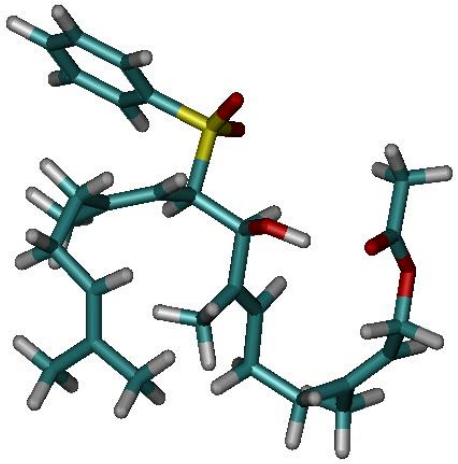

SPARTAN MECHANICS (MMFF94X) PROGRAM: SGI/R5K

Minimization performed under the following constraints:
Dihedral : C13 - C14 - C16 - C17 r= -115.893 sigma = 100.00
Constraint final values:

Dihedral : C13 C14 C16 C17 th = -119.881 (-115.893)

	Atom Label	FF Atom Type Symbol	#	chrg	Cartesian Coordinates (Angstroms) X	Y	Z	Charge
1	S1	SO2	18		-0.5289	-0.1616	3.1633	1.204
2	C1	CHR3	1		0.1395	-0.0712	1.4790	0.243
3	C13	CSP2	2		1.4173	0.7513	1.5070	-0.288
4	C2	CHR3	1		-0.9757	0.4629	0.5478	0.418
5	H4	HC	5		0.3305	-1.1174	1.2186	0.000
6	O3	OR	6		-0.9995	1.8894	0.5036	-0.680
7	H5	HC	5		-1.9511	0.1592	0.9455	0.000
8	C22	CSP2	2		-0.8556	-0.0581	-0.8817	-0.276
9	O1	O2S	32		-0.6905	1.1668	3.7264	-0.650
10	O2	O2S	32		-1.6544	-1.0839	3.1614	-0.650
11	C3	CB	37		0.7630	-0.9717	4.0923	-0.009
12	C4	CB	37		2.7578	-2.2427	5.5520	-0.150
13	C5	CB	37		1.6553	-0.2089	4.8507	-0.150
14	C6	CB	37		0.8440	-2.3675	4.0804	-0.150
15	C7	CB	37		1.8502	-3.0005	4.8096	-0.150
16	C8	CB	37		2.6589	-0.8502	5.5758	-0.150
17	H1	HC	5		1.5789	0.8759	4.8782	0.150
18	H7	HC	5		0.1309	-2.9644	3.5169	0.150
19	H8	HC	5		1.9234	-4.0854	4.8077	0.150
20	H9	HC	5		3.3611	-0.2651	6.1647	0.150
21	H10	HC	5		3.5388	-2.7392	6.1232	0.150
22	H47	HC	5		-6.0419	1.6122	1.6982	0.000
23	H46	HC	5		-3.8677	1.1153	-2.1617	0.000
24	H40	HC	5		-5.7817	-2.9508	-3.4371	0.000
25	H48	HC	5		-4.4209	2.0729	2.2539	0.000
26	C31	COO	3		-4.5295	1.5527	0.1942	0.659

27	O5	O=C	7	-3.6253	2.3001	-0.1561	-0.570
28	C32	CH3R	1	-4.9769	1.3819	1.6136	0.061
29	H41	HC	5	-4.1142	-3.5087	-3.2765	0.000
30	H42	HC	5	-4.6772	-2.8025	-4.8076	0.000
31	O4	OC=x	6	-5.2514	0.7441	-0.6230	-0.430
32	H50	HOR	21	-1.8490	2.1486	0.0845	0.400
33	H44	HC	5	-4.7753	0.3598	1.9438	0.000
34	H45	HC	5	-5.5641	1.5171	-2.5021	0.000
35	C14	CSP2	2	2.6891	0.3432	1.3112	-0.276
36	C15	CH3R	1	3.1074	-1.0757	1.0347	0.138
37	H20	HC	5	1.2417	1.8098	1.7158	0.150
38	C16	CH2R	1	3.8302	1.3429	1.4265	0.138
39	H19	HC	5	2.2970	-1.7978	1.1498	0.000
40	H21	HC	5	3.8993	-1.3772	1.7286	0.000
41	H22	HC	5	3.4873	-1.1696	0.0129	0.000
42	H2	HC	5	4.4897	1.0090	2.2386	0.000
43	H23	HC	5	3.4520	2.3243	1.7429	0.000
44	C17	CH2R	1	4.6787	1.5251	0.1572	0.138
45	H24	HC	5	5.5073	2.2023	0.4012	0.000
46	C18	CSP2	2	3.9184	2.1438	-0.9858	-0.288
47	H26	HC	5	5.1416	0.5731	-0.1134	0.000
48	C19	CSP2	2	3.8110	1.7017	-2.2545	-0.276
49	C21	CH3R	1	3.0135	2.4820	-3.2684	0.138
50	H28	HC	5	3.4148	3.0757	-0.7248	0.150
51	C20	CH3R	1	4.4378	0.4499	-2.8016	0.138
52	H25	HC	5	3.6594	-0.2335	-3.1573	0.000
53	H27	HC	5	5.0413	-0.0944	-2.0732	0.000
54	H29	HC	5	5.0918	0.6954	-3.6451	0.000
55	H30	HC	5	2.2241	1.8556	-3.6960	0.000
56	H31	HC	5	3.6645	2.8215	-4.0807	0.000
57	H32	HC	5	2.5354	3.3656	-2.8326	0.000
58	H37	HC	5	0.1561	0.3523	-2.7639	0.000
59	C23	CSP2	2	-1.7689	-0.9296	-1.3623	-0.288
60	C24	CH3R	1	0.3060	0.4628	-1.6867	0.138
61	H33	HC	5	-2.5861	-1.2438	-0.7114	0.150
62	H38	HC	5	1.2222	-0.0692	-1.4163	0.000
63	C25	CH2R	1	-1.8033	-1.5733	-2.7246	0.138
64	H34	HC	5	0.4589	1.5325	-1.5135	0.000
65	C26	CH2R	1	-2.8877	-0.9840	-3.6388	0.138
66	H35	HC	5	-1.9587	-2.6509	-2.5916	0.000
67	H36	HC	5	-0.8341	-1.4822	-3.2258	0.000
68	H6	HC	5	-2.7080	-1.3393	-4.6625	0.000
69	H39	HC	5	-2.7716	0.1041	-3.7001	0.000
70	C27	CSP2	2	-4.3054	-1.3654	-3.2534	-0.276
71	C28	CSP2	2	-5.1595	-0.5709	-2.5757	-0.288
72	C29	CH3R	1	-4.7459	-2.7313	-3.7172	0.138
73	H43	HC	5	-6.1648	-0.9406	-2.3758	0.150
74	C30	CH2R	1	-4.9014	0.7955	-2.0130	0.418
						Net Charge :	0.000

```
      Net Charge :    0.000
   Dipole Moment :    5.726 Debye
      components :    1.9005   -4.5066   -2.9780
```

```
Final Energy Calculation
             ---- Energy ----       |Gmax| ---   <|Gi|> ---
    Totals      103.44006870          1.2173e-3  285.5822e-6
```

5.7.5 Data for *tert*-butyl protected alcohol 87a

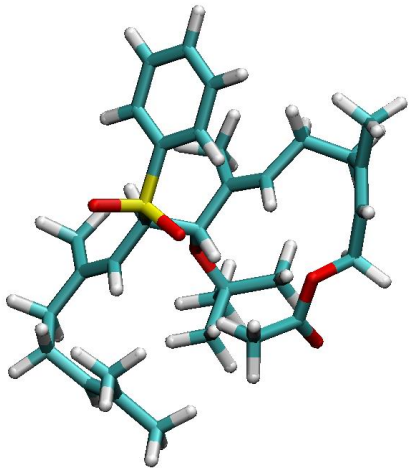

```
SPARTAN MECHANICS (MMFF94X) PROGRAM: SGI/R5K

Minimization performed under the following constraints:
    Dihedral   :   O1 -  S1 -  C1 - C13   r=  -46.481  sigma =  100.00
    Dihedral   :   C1 -  C2 -  O3 -  C9   r= -136.184  sigma =  100.00
    Dihedral   :   O1 -  S1 -  C3 -  C6   r=  118.613  sigma =  100.00
    Dihedral   :  C16 - C17 - C18 - C19   r=  133.016  sigma =  100.00
    Dihedral   :  C25 - C26 - C27 - C28   r=  103.209  sigma =  100.00
    Dihedral   :  C27 - C28 - C30 -  O4   r= -118.129  sigma =  100.00
    Dihedral   :  C28 - C30 -  O4 - C31   r=  174.969  sigma =  100.00
    Dihedral   :  C30 -  O4 - C31 -  O5   r=   -0.032  sigma =  100.00

Constraint final values:
    Dihedral   : O1   S1   C1   C13   th =  -46.481 ( -46.481)
    Dihedral   : C1   C2   O3   C9    th = -136.184 (-136.184)
    Dihedral   : O1   S1   C3   C6    th =  118.614 ( 118.613)
    Dihedral   : C16  C17  C18  C19   th =  133.017 ( 133.016)
    Dihedral   : C25  C26  C27  C28   th =  103.209 ( 103.209)
    Dihedral   : C27  C28  C30  O4    th = -118.129 (-118.129)
    Dihedral   : C28  C30  O4   C31   th =  174.969 ( 174.969)
    Dihedral   : C30  O4   C31  O5    th =   -0.032 (  -0.032)
```

		FF Atom Type		Cartesian Coordinates (Angstroms)			
	Atom Label	Symbol	#	chrg	X	Y	Z	Charge
1	S1	SO2	18		1.9819	-1.4411	-0.3655	1.204
2	C1	CHR3	1		0.9101	-0.5556	-1.5386	0.243
3	C13	CSP2	2		1.7172	0.6625	-2.0018	-0.288
4	C2	CHR3	1		-0.4361	-0.1535	-0.8860	0.418
5	H4	HC	5		0.7719	-1.2270	-2.3887	0.000
6	O3	OR	6		-1.1384	0.7304	-1.7852	-0.560
7	H5	HC	5		-0.2341	0.3635	0.0577	0.000
8	C22	CSP2	2		-1.3854	-1.3310	-0.6487	-0.276
9	O1	O2S	32		3.3169	-1.5594	-0.9301	-0.650
10	O2	O2S	32		1.8171	-0.8541	0.9549	-0.650
11	C3	CB	37		1.3819	-3.1150	-0.2921	-0.009
12	C4	CB	37		0.5114	-5.7544	-0.1793	-0.150
13	C5	CB	37		1.3108	-3.8706	-1.4666	-0.150
14	C6	CB	37		1.0524	-3.6823	0.9420	-0.150
15	C7	CB	37		0.6121	-5.0047	0.9935	-0.150
16	C8	CB	37		0.8645	-5.1907	-1.4065	-0.150
17	H1	HC	5		1.6187	-3.4542	-2.4224	0.150

18	H7	HC	5	1.1335	-3.1077	1.8622	0.150
19	H8	HC	5	0.3492	-5.4515	1.9493	0.150
20	H9	HC	5	0.8053	-5.7875	-2.3137	0.150
21	H10	HC	5	0.1704	-6.7861	-0.1348	0.150
22	C9	CR	1	-1.7713	1.9005	-1.2426	0.280
23	C10	CH3R	1	-2.7980	1.5696	-0.1543	0.000
24	C11	CH3R	1	-2.5104	2.5305	-2.4333	0.000
25	C12	CH3R	1	-0.7374	2.9085	-0.7281	0.000
26	H3	HC	5	-3.3646	2.4587	0.1432	0.000
27	H13	HC	5	-2.3172	1.1748	0.7447	0.000
28	H14	HC	5	-3.5079	0.8104	-0.5004	0.000
29	H11	HC	5	-3.0304	3.4517	-2.1500	0.000
30	H15	HC	5	-3.2459	1.8312	-2.8481	0.000
31	H16	HC	5	-1.8128	2.7629	-3.2467	0.000
32	H12	HC	5	-1.2143	3.8404	-0.4054	0.000
33	H17	HC	5	-0.0116	3.1508	-1.5105	0.000
34	H18	HC	5	-0.1692	2.5175	0.1208	0.000
35	C14	CSP2	2	1.8081	1.1620	-3.2529	-0.276
36	C15	CH3R	1	1.0202	0.6210	-4.4217	0.138
37	H20	HC	5	2.2876	1.1381	-1.2061	0.150
38	C16	CH2R	1	2.7018	2.3349	-3.6429	0.138
39	H19	HC	5	1.6963	0.1650	-5.1521	0.000
40	H21	HC	5	0.4755	1.4336	-4.9148	0.000
41	H22	HC	5	0.2763	-0.1276	-4.1403	0.000
42	H2	HC	5	2.0645	3.1323	-4.0482	0.000
43	H23	HC	5	3.3279	1.9896	-4.4775	0.000
44	C17	CH2R	1	3.6623	2.9427	-2.6019	0.138
45	H24	HC	5	4.2475	2.1453	-2.1363	0.000
46	C18	CSP2	2	2.9753	3.8329	-1.5981	-0.288
47	H26	HC	5	4.3807	3.5732	-3.1417	0.000
48	C19	CSP2	2	3.1159	3.8384	-0.2576	-0.276
49	C21	CH3R	1	2.3281	4.8057	0.5879	0.138
50	H28	HC	5	2.2924	4.5570	-2.0433	0.150
51	C20	CH3R	1	4.0312	2.9382	0.5264	0.138
52	H25	HC	5	4.6969	3.5372	1.1571	0.000
53	H27	HC	5	4.6668	2.3087	-0.0991	0.000
54	H29	HC	5	3.4458	2.2783	1.1740	0.000
55	H30	HC	5	1.6744	5.4472	-0.0124	0.000
56	H31	HC	5	3.0048	5.4558	1.1519	0.000
57	H32	HC	5	1.6962	4.2613	1.2963	0.000
58	H37	HC	5	-1.2775	-2.0732	-2.6736	0.000
59	C23	CSP2	2	-1.6673	-1.7376	0.6073	-0.288
60	C24	CH3R	1	-2.0149	-1.9419	-1.8765	0.138
61	H33	HC	5	-1.1371	-1.2595	1.4306	0.150
62	H38	HC	5	-2.8164	-1.2992	-2.2539	0.000
63	C25	CH2R	1	-2.6721	-2.7815	1.0262	0.138
64	H34	HC	5	-2.4327	-2.9343	-1.6866	0.000
65	C26	CH2R	1	-3.4495	-2.3902	2.2962	0.138
66	H35	HC	5	-2.1585	-3.7368	1.1723	0.000
67	H36	HC	5	-3.4129	-2.9341	0.2341	0.000
68	H6	HC	5	-4.3406	-3.0285	2.3667	0.000
69	H39	HC	5	-3.8432	-1.3731	2.1925	0.000
70	C27	CSP2	2	-2.6608	-2.5542	3.5827	-0.276
71	C28	CSP2	2	-2.0978	-1.5460	4.2801	-0.288
72	C29	CH3R	1	-2.5525	-3.9722	4.0868	0.138
73	H43	HC	5	-1.5634	-1.7876	5.1986	0.150
74	C30	CH2R	1	-2.0744	-0.0824	3.9532	0.418
75	H40	HC	5	-2.0095	-4.0352	5.0359	0.000
76	H41	HC	5	-2.0228	-4.5997	3.3638	0.000
77	H42	HC	5	-3.5497	-4.3940	4.2502	0.000
78	O4	OC=x	6	-0.6982	0.2763	3.7926	-0.430

```
     79 H45          HC      5        -2.5015     0.4795     4.7915   0.000
     80 H46          HC      5        -2.6309     0.1541     3.0431   0.000
     81 C31          COO     3        -0.4968     1.5555     3.3850   0.659
     82 O5           O=C     7        -1.3767     2.3752     3.1587  -0.570
     83 C32          CH3R    1         0.9655     1.8229     3.2050   0.061
     84 H44          HC      5         1.2545     1.5846     2.1800   0.000
     85 H47          HC      5         1.5538     1.2273     3.9086   0.000
     86 H48          HC      5         1.1665     2.8771     3.4137   0.000
                                                        Net Charge :    0.000
          Net Charge :    0.000
       Dipole Moment :    4.593 Debye
          components :   -3.2704   -3.1439   -0.7210

Final Energy Calculation
               ---- Energy ----       |Gmax| ---   <|Gi|> ---
    Totals      123.86514155        215.9653e-6   52.5474e-6
```

5.7.6 Data for molecules for the synthetic proposal

In the next chapters the data for the molecules **148a** and **148b** are presented, which are similar to the key substrates for the synthetic proposal discussed in the chapter 4. These molecules were not synthesized, but their geometry was optimised in order to check the tendency in conformational changes depending on the substituents. As was expected the unprotected alcohol took the most preferable pre-folded conformation, which we believe is not useful for the desired macrocyclization. The second structure – *tert*-butyl protected alcohol was in the good agreement with previously obtained results. The non-folded conformation was preferable. Moreover, the energy difference between closest conformers is big, due to the *tert*-butyl group – the conformational anker.

5.7.6.1 Data for unprotected alcohol 148a for the synthetic proposal

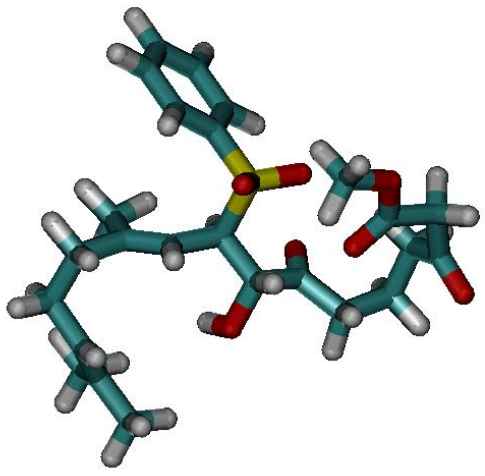

SPARTAN MECHANICS (MMFF94X) PROGRAM: SGI/R5K Release 5.1.3

Minimization performed under the following constraints:
Dihedral : C15 - C23 - C24 - C25 r= 54.673 sigma = 100.00

Constraint final values:
Dihedral : C15 C23 C24 C25 th = 68.506 (54.673)

	Atom Label	FF Atom Type Symbol	#	Cartesian Coordinates (Angstroms) chrg	X	Y	Z	Charge
1	C13	CSP2	2		0.7032	-1.1443	-0.9715	-0.288
2	C1	CHR3	1		-0.0913	-0.0319	-0.3061	0.243
3	H2	HC	5		-0.3001	0.7699	-1.0177	0.000
4	C2	CHR3	1		0.6302	0.5421	0.9275	0.341
5	S1	SO2	18		-1.7007	-0.6998	0.2005	1.204
6	H3	HC	5		0.5271	-0.1253	1.7876	0.000
7	C15	C=OR	3		0.0757	1.9220	1.2919	0.448
8	O1	OR	6		2.0364	0.7292	0.6955	-0.680
9	H38	HC	5		-2.3125	2.4569	2.6113	0.000
10	O2	O2S	32		-1.5213	-2.0260	0.7673	-0.650
11	O3	O2S	32		-2.4512	0.2979	0.9429	-0.650
12	C3	CB	37		-2.5567	-0.9029	-1.3508	-0.009
13	C4	CB	37		-3.9031	-1.1995	-3.7626	-0.150
14	C5	CB	37		-3.1823	0.2044	-1.9319	-0.150
15	C6	CB	37		-2.6177	-2.1613	-1.9547	-0.150
16	C7	CB	37		-3.2898	-2.3041	-3.1681	-0.150
17	C8	CB	37		-3.8527	0.0516	-3.1448	-0.150
18	H4	HC	5		-3.1544	1.1798	-1.4498	0.150
19	H7	HC	5		-2.1461	-3.0267	-1.4948	0.150
20	H8	HC	5		-3.3408	-3.2778	-3.6496	0.150
21	H9	HC	5		-4.3421	0.9057	-3.6071	0.150
22	H10	HC	5		-4.4300	-1.3161	-4.7069	0.150
23	H37	HC	5		-3.8502	1.3335	4.1896	0.000
24	O7	OC=x	6		-3.2175	-1.2172	4.3477	-0.430
25	H40	HC	5		-1.7024	-2.5983	3.8420	0.000
26	H41	HC	5		-3.1757	-2.5921	2.8103	0.000
27	H42	HC	5		-3.2263	-3.2637	4.4497	0.000
28	C27	CH2R	1		-2.9481	1.0664	4.7489	0.122
29	O6	O=C	7		-1.2523	-0.2505	3.6386	-0.570
30	C29	CH3R	1		-2.7899	-2.4784	3.8260	0.280
31	O5	O=C	7		-1.3147	2.5136	5.7118	-0.570
32	H39	HC	5		-3.2283	0.8850	5.7923	0.000
33	C28	COO	3		-2.3482	-0.1820	4.1784	0.659
34	H6	HOR	21		2.1538	1.0837	-0.2054	0.400
35	C16	CH3R	1		0.6692	-0.2950	-3.3623	0.138
36	C14	CSP2	2		1.0671	-1.2484	-2.2669	-0.276
37	H20	HC	5		1.0471	-1.9141	-0.2762	0.150
38	C17	CH2R	1		1.9389	-2.4119	-2.7154	0.138
39	O4	O=C	7		-0.5504	2.5990	0.4715	-0.570
40	H34	HC	5		6.4544	0.5001	-0.8791	0.000
41	C23	CH2R	1		0.4360	2.4651	2.6662	0.061
42	H21	HC	5		0.2587	-0.8500	-4.2127	0.000
43	H23	HC	5		1.5360	0.2753	-3.7082	0.000
44	H24	HC	5		-0.0969	0.4205	-3.0582	0.000
45	H22	HC	5		1.4541	-2.9070	-3.5666	0.000
46	H25	HC	5		1.9959	-3.1747	-1.9272	0.000
47	C18	CH2R	1		3.3664	-2.0052	-3.1187	0.138
48	C19	CSP2	2		4.1429	-1.4009	-1.9775	-0.288
49	H27	HC	5		3.3301	-1.3496	-3.9924	0.000

```
     50 H28          HC      5          3.9018    -2.9059    -3.4448    0.000
     51 C22          CH3R    1          5.4143     0.2541    -0.6412    0.138
     52 H29          HC      5          4.2642    -2.0730    -1.1269    0.150
     53 C20          CSP2    2          4.6801    -0.1681    -1.8890   -0.276
     54 C21          CH3R    1          4.6211     0.8925    -2.9524    0.138
     55 H26          HC      5          4.1173     0.5711    -3.8655    0.000
     56 H30          HC      5          5.6343     1.1996    -3.2329    0.000
     57 H32          HC      5          4.0870     1.7711    -2.5755    0.000
     58 H31          HC      5          5.4242    -0.5304     0.1228    0.000
     59 H33          HC      5          4.9391     1.1376    -0.2026    0.000
     60 H1           HC      5          0.4632     1.6458     3.3892    0.000
     61 C24          CH2R    1         -0.5197     3.5629     3.1397    0.000
     62 H19          HC      5          1.4501     2.8739     2.5919    0.000
     63 C25          CH2R    1         -1.9273     3.0483     3.4463    0.061
     64 H35          HC      5         -0.5917     4.3433     2.3724    0.000
     65 H36          HC      5         -0.0933     4.0404     4.0299    0.000
     66 H5           HC      5         -2.6080     3.8963     3.5838    0.000
     67 C26          C=OR    3         -1.9919     2.2279     4.7225    0.448
                                                          Net Charge :    0.000 e

        Net Charge :    0.000
     Dipole Moment :    6.550 Debye
        components :   -1.4937   -1.5240   -6.1923

Final Energy Calculation
              ---- Energy ----       |Gmax| ---   <|Gi|> ---
    Totals       77.43903014         325.1746e-6  107.0135e-6
```

5.7.6.2 Data for *tert*-butyl protected alcohol 148b for the synthetic proposal

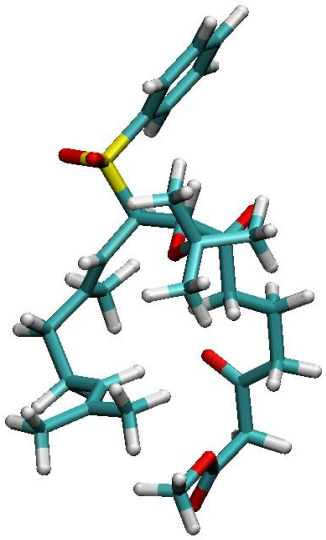

```
SPARTAN MECHANICS (MMFF94X) PROGRAM: SGI/R5K        Release 5.1.3

Minimization performed under the following constraints:
    Dihedral   :   S1 -  C1 -  C2 -  O1   r=   51.393  sigma =  100.00

Constraint final values:
    Dihedral   : S1   C1   C2   O1    th =  100.873 (  51.393)
```

FF Atom Type	Atom Label	Cartesian Coordinates (Angstroms) Symbol	#	chrg	X	Y	Z	Charge
1	C13	CSP2	2		-0.3237	-0.1586	2.0048	-0.288
2	C1	CHR3	1		-0.7131	-1.5203	1.4517	0.243
3	H2	HC	5		0.1398	-2.2049	1.4848	0.000
4	C2	CHR3	1		-1.3152	-1.4852	0.0291	0.341
5	S1	SO2	18		-1.8782	-2.2597	2.6256	1.204
6	H3	HC	5		-2.1011	-2.2362	-0.0791	0.000
7	C15	C=OR	3		-0.1986	-1.9040	-0.9326	0.448
8	O1	OR	6		-1.8238	-0.2001	-0.3297	-0.560
9	C9	CR	1		-2.9947	-0.1336	-1.1608	0.280
10	O2	O2S	32		-1.2242	-2.4271	3.9117	-0.650
11	O3	O2S	32		-3.1499	-1.5644	2.5379	-0.650
12	C3	CB	37		-2.1403	-3.9149	2.0146	-0.009
13	C4	CB	37		-2.5265	-6.4943	1.0556	-0.150
14	C5	CB	37		-3.4069	-4.3026	1.5686	-0.150
15	C6	CB	37		-1.0717	-4.8161	2.0101	-0.150
16	C7	CB	37		-1.2689	-6.1071	1.5218	-0.150
17	C8	CB	37		-3.5948	-5.5962	1.0834	-0.150
18	H4	HC	5		-4.2482	-3.6139	1.5985	0.150
19	H7	HC	5		-0.0935	-4.5313	2.3904	0.150
20	H8	HC	5		-0.4440	-6.8157	1.5084	0.150
21	H9	HC	5		-4.5751	-5.9086	0.7316	0.150
22	H10	HC	5		-2.6762	-7.5031	0.6777	0.150
23	C12	CH3R	1		-4.2421	-0.5626	-0.3811	0.000
24	C11	CH3R	1		-2.8586	-0.9438	-2.4562	0.000
25	C10	CH3R	1		-3.1360	1.3511	-1.5258	0.000
26	H12	HC	5		-4.0211	1.5375	-2.1431	0.000
27	H13	HC	5		-2.2538	1.6998	-2.0747	0.000
28	H14	HC	5		-3.2057	1.9703	-0.6239	0.000
29	H11	HC	5		-3.7144	-0.7781	-3.1198	0.000
30	H15	HC	5		-2.8016	-2.0191	-2.2588	0.000
31	H16	HC	5		-1.9479	-0.6691	-2.9989	0.000
32	H6	HC	5		-5.1557	-0.3824	-0.9579	0.000
33	H17	HC	5		-4.3178	-0.0136	0.5638	0.000
34	H18	HC	5		-4.2170	-1.6270	-0.1304	0.000
35	C16	CH3R	1		2.1551	-0.5483	2.3880	0.138
36	C14	CSP2	2		0.8925	0.2720	2.4005	-0.276
37	H20	HC	5		-1.1614	0.5396	2.0838	0.150
38	C17	CH2R	1		1.0535	1.6791	2.9566	0.138
39	O4	O=C	7		-0.0794	-3.0887	-1.2554	-0.570
40	H34	HC	5		-1.7642	4.2999	-0.4752	0.000
41	C23	CH2R	1		0.7718	-0.8323	-1.4104	0.061
42	H21	HC	5		2.9624	-0.0039	1.8904	0.000
43	H23	HC	5		2.0501	-1.5016	1.8667	0.000
44	H24	HC	5		2.4710	-0.7615	3.4145	0.000
45	H22	HC	5		1.6637	1.6221	3.8674	0.000
46	H25	HC	5		0.0826	2.0766	3.2815	0.000
47	C18	CH2R	1		1.7052	2.6729	1.9837	0.138
48	C19	CSP2	2		0.8370	2.9833	0.7920	-0.288
49	H27	HC	5		2.6625	2.2830	1.6173	0.000
50	H28	HC	5		1.9592	3.5861	2.5315	0.000
51	C22	CH3R	1		-0.6934	4.2443	-0.6963	0.138
52	H29	HC	5		0.8402	2.2035	0.0305	0.150
53	C20	CSP2	2		0.0962	4.0877	0.5762	-0.276
54	C21	CH3R	1		-0.0457	5.2355	1.5372	0.138
55	H26	HC	5		-1.1055	5.4417	1.7222	0.000
56	H30	HC	5		0.4122	6.1366	1.1167	0.000
57	H32	HC	5		0.4132	5.0464	2.5102	0.000
58	H31	HC	5		-0.5357	3.4097	-1.3871	0.000

59 H33	HC	5	-0.3965	5.1616	-1.2153	0.000
60 H1	HC	5	0.2042	-0.0453	-1.9168	0.000
61 C24	CH2R	1	1.8190	-1.3985	-2.3723	0.000
62 H19	HC	5	1.2555	-0.3983	-0.5332	0.000
63 C25	CH2R	1	2.8316	-0.3500	-2.8311	0.061
64 H35	HC	5	1.3038	-1.7967	-3.2558	0.000
65 H36	HC	5	2.3389	-2.2454	-1.9072	0.000
66 H5	HC	5	3.3682	-0.7480	-3.7003	0.000
67 C26	C=OR	3	3.8785	-0.0180	-1.7779	0.448
68 H38	HC	5	2.3226	0.5700	-3.1347	0.000
69 C27	CH2R	1	4.9984	0.8975	-2.1941	0.122
70 O5	O=C	7	3.8155	-0.4532	-0.6276	-0.570
71 H37	HC	5	5.1569	0.8290	-3.2747	0.000
72 H39	HC	5	5.9118	0.5393	-1.7057	0.000
73 C28	COO	3	4.7859	2.3315	-1.8233	0.659
74 O7	OC=x	6	3.4913	2.7086	-2.0045	-0.430
75 O6	O=C	7	5.6920	3.0823	-1.4845	-0.570
76 C29	CH3R	1	3.2417	4.0861	-1.7133	0.280
77 H40	HC	5	3.4236	4.2909	-0.6539	0.000
78 H41	HC	5	2.1923	4.2938	-1.9369	0.000
79 H42	HC	5	3.8600	4.7316	-2.3452	0.000
					Net Charge :	0.000 e

```
      Net Charge :    0.000
   Dipole Moment :    8.200 Debye
      components :   -0.4371    0.6310   -8.1641

Final Energy Calculation
              ---- Energy ----       |Gmax| ---   <|Gi|> ---
    Totals      100.68340764          1.0255e-3  365.0945e-6
```

6. References

[1] a) G. Stork, A.W. Burgstahler, *J. Am. Chem. Soc.* **1955**, *77*, 5086-5077.
b) A. Eschenmoser, L. Ruzicka, O. Jeger, D. Arigoni, *Helv. Chim. Acta* **1955**, *38*, 1890-1904.

[2] P. A. Bartlett in *Asymmetric Synthesis* (Hrsg.: J. D. Morrison), Academic Press, New York, 1984, Bd. 3B, pp. 341-409.

[3] a) K. U. Wendt, G. E. Schulz, E. J. Corey, D. R. Liu, *Angew. Chem. Int. Ed.* **2000**, *39*, 2812-2833.
b) I. Abe, M. Rohmer, G. D. Prestwich, *Chem. Rev.* **1993**, *93*, 2189-2206.
c) I. Abe, T. Dang, Y. F. Zheng, B. A. Madden, C. Fei, K. Poralla, G. D. Prestwich, *J. Am. Chem. Soc.* **1997**, *119*, 11333-11334.
d) E. Caspi, *Acc. Chem. Res.* **1980**, *13*, 97-104.

[4] a) E. J. Corey, W. E. Russey, P. R. Ortiz de Montellano, *J. Am. Chem. Soc.* **1966**, *88*, 4750-4751.
b) E. E. van Tamelen, J. D. Willet, R. B. Clayton, K. E. Lord, *J. Am. Chem. Soc.* **1966**, *88*, 4752-4754.
c) J. D. Willet, K. B. Sharpless, K. E. Lord, E. E. van Tamelen, R. B. Clayton, *J. Biol. Chem.* **1967**, *242*, 4182-4191.

[5] a) E. E. van Tamelen, *J. Am. Chem. Soc.* **1982**, *104*, 6480-6481.
b) E. J. Corey, S. C. Virgil, S. Sarshar, *J. Am. Chem. Soc.* **1991**, *113*, 8171-8172.
c) H. H. Rees, L. J. Goad, T. W. Goodwin, *Biochem. J.* **1968**, *107*, 417-426.

[6] D. A. Whittington, M. L. Wise, M. Urbansky, R. M. Coates, R. B Croteau, D. W. Christianson, *PNAS*, **2002**, *99*, 15375-15380.

[7] a) X. Lin, M. Hezari, A. E. Koepp, H. G. Floss, R. Croteau, *Biochemistry*, **1996**, *35*, 2968-2977.
b) S. Jennewein, R. Croteau, *Appl. Microbiol. Biotechnol.* **2001**, *57*, 13-19.

[8] T. Eguchi, Y. Dekishima, Y. Hamano, T. Dairi, H. Seto, K. Kakinuma, *J. Org. Chem.* **2003**, *68*, 5433-5438.

[9] a) E. E. van Tamelen, M. A. Schwartz, E. J. Hessler, A. Storni, *Chem. Comm.* **1966**, *13*, 409-411.
b) E. E. van Tamelen, E. J. Hessler, *Chem. Comm.* **1966**, *13*, 411-413.
c) E. E. van Tamelen, R. M. Coates, *Chem. Comm.* **1966**, *13*, 413-415.

[10] W. S. Johnson, R. A. Buchanan, W. R. Bartlett, F. S. Tham, R. K. Kullnig, *J. Am. Chem. Soc.* **1993**, *115*, 504-515.

[11] a) M. Nishizawa, H. Takenaka, H. Nishide, Y. Hayashi, *Tetrahedron Lett.* **1983**, *24*, 2581-2584.

b) M. Nishizawa, H. Takenaka, H. Nishide, Y. Hayashi, *J. Am. Chem. Soc.* **1985**, *107*, 522-523.

c) M. Nishizawa, H. Takao, Y. Iwamoto, H. Yamada, H. Imagawa, *Synlett* **1998**, 79-80.

[12] K. Ishihara, S. Nakamura, H. Yamamoto, *J. Am. Chem. Soc.* **1999**, *121*, 4906-4907.

[13] R. Breslow, S. S. Olin, J. T. Groves, *Tetrahedron Lett.* **1968**, *15*, 1837-1840.

[14] P. A. Zoretic, Y. Zhang, H. Fang, *J. Org. Chem.* **1998**, *63*, 1162-1167.

[15] S. A. Hitchcock, S. J. Houldsworth, G. Pattenden, D. C. Pryde, N. M. Thomson, A. J. Blake, *J. Chem. Soc., Perkin Trans. 1* **1998**, 3181-3206.

[16] a) B. Snider, *Chem. Rev.* **1996**, *96*, 339-363.

b) M. A. Dombrowski, S. A. Kates, B. B. Snider, *J. Am. Chem. Soc.* **1990**, *112*, 2759-2767.

[17] a) P. G. Gassman, K. J. Bottorff, *J. Am. Chem. Soc.* **1987**, *109*, 7547-7548.

b) P. G. Gassman, S. A. De Silva, *J. Am. Chem. Soc.* **1991**, *113*, 9870-9872.

[18] a) J. Mattay, *Angew. Chem.* **1987**, *99*, 849-870.

b) J. Mattay, *Synthesis*, **1989**, 233-252.

[19] a) U. Hoffmann, Y. Gao, B. Pandey, S. Klinge, K. -D. Warzecha, C. Krueger, H. D. Roth, M. Demuth, *J. Am. Chem. Soc.* **1993**, *115*, 10358-10359.

b) K.-D. Warzecha, X. Xing, M. Demuth, R. Goddard, M. Kessler, C. Krueger, *Helv. Chim. Acta* **1995**, *78*, 2065-2076.

c) K.-D. Warzecha, X. Xing, M. Demuth, *Pure Appl. Chem.* **1997**, *69*, 109-112.

d) X. Xing, M. Demuth, *Synlett*, **1999**, 987-990.

e) X. Xing, M. Demuth, *Eur. J. Org. Chem.* **2001**, 537-544.

[20] a) C. Heinemann, X. Xing, K.-D. Warzecha, P. Ritterskamp, H. Görner, M. Demuth, *Pure Appl. Chem.* **1998**, *70*, 2167-2176.

b) Patentanmeldung: Flachbettkollektor und Reaktor für solar photo- und thermochemische Synthese, M. Demuth und A. Ritter, WO 99/54032.

[21] C. Heinemann, M. Demuth, *J. Am. Chem. Soc.* **1997**, *119*, 1129-1130.

[22] a) H. D. Roth, *Top. Curr. Chem.* **1992**, *163*, 131-245.

b) H. Weng, C. Scarlata, H. D. Roth, *J. Am. Chem. Soc.* **1996**, *118*, 10947-10953.

[23] K.-D. Warzecha, PhD Thesis, Max-Planck-Institut für Strahlenchemie/University of Essen, **2002**.

[24] X. Xing, PhD Thesis, Max-Planck-Institut für Strahlenchemie/University of Essen, **1997**.

[25] I. R. Gould, D. Ege, J. E. Moser, S. Farid, *J. Am. Chem. Soc.* **1990**, *112*, 4290-4301.

[26] a) S. L. Mattes, S. Farid, *Organic Photochemistry*, A. Padwa, Ed., Marcel Dekker: New York, **1983**, Vol. 6, p. 233.

b) M. A. Fox, *Advances in Photochemistry*, D. H. Volman, G. S. Hammond, K. Gollnick, Eds., Wiley: New York, **1986**, Vol. 13, p. 237.

c) S. L. Mattes, S. Farid, *J. Chem. Soc. Chem. Commun.* **1980**, 126.

d) S. L. Mattes, S. Farid, *J. Am. Chem. Soc.* **1986**, *108*, 7356.

[27] I. R. Gould, J. E. Moser, D. Ege, S. Farid, *J. Am. Chem. Soc.* **1988**, *110*, 1991-1993.

[28] a) T. Majima, C. Pac, A. Nakasone, H. Sakurai, *J. Am. Chem. Soc.* **1981**, *103*, 4499-4508.

b) D. R. Arnold, X. Du, *J. Am. Chem. Soc.* **1989**, *111*, 7666-7667.

c) A. P. Schaap, S. Siddiqui, G. Prasad, E. Palomino, L. Lopez, *J. Photochem.* **1984**, *25*, 167.

[29] a) E. Baciocchi, T. Del Giacco, F. Elisei, O. Lanzalunga, *J. Am. Chem. Soc.* **1998**, *120*, 11800-11801.

b) E. Baciocchi, T. Del Giacco, F. Elisei, M. Ioele, *J. Org. Chem.* **1995**, *60*, 7974-7983.

[30] F. Göller, PhD Thesis, Max-Planck-Institut für Strahlenchemie/University of Essen, **2001**.

[31] M. E. Ozser, H. Icil, Y. Makhynya, M. Demuth, *Eur. J. Org. Chem.* **2004**, 3686-3692.

[32] W. P. Todd, J. P. Dinnocenzo, S. Farid, J. L. Goodman, I. R. Gould, *J. Am. Chem. Soc.* **1991**, *113*, 3601-3602.

[33] M. C. Wani, H. L. Taylor, M. E. Wall, *J. Am. Chem. Soc.* **1971**, *93*, 2325-2327.

[34] D. G. I. Kingston, *J. Nat. Prod.* **2000**, *63*, 726-734.

[35] G. Mehta, V. Singh, *Chem. Rev.* **1999**, *99*, 881-930.

[36] a) R. A. Holton, C. Somoza, H.-B. Kim et al., *J. Am. Chem. Soc.* **1994**, *116*, 1597.

b) R. A. Holton, H.-B. Kim, R. R. Juo et al., *J. Am. Chem. Soc.* **1988**, *110*, 6558.

[37] a) K. C. Nicolaou, Z. Yang, J. J. Liu et al., *Nature*, **1994**, *367*, 630.

b) K. C. Nicolaou, P. G. Nantermet, H. Ueno et al., *J. Am. Chem. Soc.* **1995**, *117*, 624.

c) K. C. Nicolaou, J. J. Liu, Z. Yang et al., *J. Am. Chem. Soc.* **1995**, *117*, 634.

[38] a) J. J. Masters, J. T. Link, L. B. Snyder, W. B. Young, S. J. Danishefski, *Angew. Chem. Int. Ed.* **1995**, *34*, 1723.
b) S. J. Danishefski, J. J. Masters, W. B. Young, J. T. Link et al., *J. Am. Chem. Soc.* **1996**, *118*, 2843.

[39] a) P. A. Wender et al., *J. Am. Chem. Soc.* **1997**, *119*, 2755.
b) P. A. Wender et al., *J. Am. Chem. Soc.* **1997**, *119*, 2757.

[40] a) I. Ojima, I. Habus, M. Zhao, M. Zucco, Y. H. Park, C. M. Sun, T. Brigaud, *Tetrahedron*, **1992**, *48*, 6985-7012.
b) R. A. Holton, US Patent 5,015,744, **1991**.

[41] T. Kirikae, I. Ojima, Z. Ma, F. Kirikae, Y. Hirai, M. Nakano, *Biochem. Bioph. Res. Commun.* **1998**, *245*, 698-704.

[42] D. Sträubig, PhD Thesis, Max-Planck-Institut für Strahlenchemie/University of Essen, **1997**.

[43] M. Eiblmaier, PhD Thesis, Max-Planck-Institut für Strahlenchemie/University of Essen, **1999**.

[44] S. G. Warren, "Designing Organic Synthesis", **1992**, publ. John Wiley&Sons.

[45] a) D. Uzun, PhD Thesis, Max-Planck-Institut für Strahlenchemie/University of Cyprus, **2002**.
b) Y. Makhynya, Diploma Thesis, Max-Planck-Institut für Strahlenchemie/University of Kiew, **2001**.

[46] E.N.Prilezhaeva, *Russ. Chem. Rev.* **2000**, *69*, 367-408.

[47] S. Torii, K. Uneyama, S. Matsunami, *J. Org. Chem.* **1980**, *45*, 16-20.

[48] P. J. Kocienski, B. Lythgoe, I. Waterhouse, *J. Chem. Soc. Perkin Trans 1*, **1980**, 1045-1050.

[49] P. M. Atlani, J. F. Biellmann, S. Dube, J. J. Vicens, *Tetrahedron Lett.* **1974**, *31*, 2665-2668.

[50] I. J. S. Fairlamb, J. M. Dickinson, M. Pegg, *Tetrahedron Lett.* **2001**, *42*, 2205-2208.

[51] X. Yue, Y. Li, *Tetrahedron Lett.* **1996**, *37*, 671-674.

[52] a) E. I. Heiba, R. M. Dessau, *J. Am. Chem. Soc.* **1971**, *93*, 524.
b) E. I. Heiba, R. M. Dessau, *J. Am. Chem. Soc.* **1972**, *94*, 2888.

[53] a) B. B. Snider, J. Y. Kiselgof, *Tetrahedron,* **1998**, *54*, 10641-10648.
b) B. B. Snider, E. Y. Kiselgof, *Tetrahedron,* **1996**, *52*, 6073-6084.

[54] C. Jenson, W. L. Jorgensen, *J. Am. Chem. Soc.* **1997**, *119*, 10846-10854.

[55] W. F. Fleck, B. Schlegel, P. Hoffmann, M. Ritzau, S. Heinze, U. Graefe, *J. Nat. Prod*. **1996**, *59*, 780-781.

[56] D. E. Cane, M. Tandon, *Tetrahedron Lett.* **1994**, *35*, 5355-5358.

[57] M. P. Sibi, S. Manyem, *Tetrahedron*, **2000**, *56*, 8033-8061.

[58] S. D. Evans, R. P. Houghton, *J. Mol. Cat. A: Chem.* **2000**, *164*, 157-164.

[59] D. Müller, G. Umbricht, B. Weber, A. Pfaltz, *Helv. Chim. Acta,* **1991**, *74*, 232-240.

[60] H. Fritschi, U. Leutenegger, K. Siegmann. A. Pfaltz, *Helv. Chim. Acta,* **1988**, *71*, 1541-1552.

[61] H. Fritschi, U. Leutenegger, A. Pfaltz, *Helv. Chim. Acta,* **1988**, *71*, 1553-1565.

[62] J. P. Collman, *Angew. Chem.* **1965**, *4*, 154-161.

[63] A. Guingant, H. Hammami, *Tetrahedron Asymm.* **1991**, *2*, 411-414.

[64] J. Thorhauge, M. Roberson, R. G. Hazell, K. A. Jørgensen, *Chem. Eur. J.* **2002**, *8*, 1888-1898.

[65] Q. Huang, C. A. Roessner, R. Croteau, A. I. Scott, *Bioorg. Med. Chem.* **2001**, *9*, 2237-2242.

[66] D. D. Perrin, W. L. F. Armarego, D. R. Perrin, *Purification of Laboratory Chemicals*, Pergamon press, Oxford, **1980**.

[67] J. W. Bunting, N. P. Fitzgerald, *Can. J. Chem. Eng.* **1984**, *62*, 1301-1307.

[68] A. Armstrong, I. Brackenridge, R. F. W. Jackson, J. M. Kirk, *Tetrahedron Lett.* **1988**, *29*, 2483-2486.

[69] B. Trost, W. C. Vladuchick, *J. Org. Chem.* **1979**, *44*, 148-151.

Abbreviations

The following abbreviations are used in this work:

A	acceptor
BET	back electron transfer
BP	1.1'-biphenyl
BuLi	n-butyllithium
CI	chemical ionisation
COSY	correlation spectroscopy
D	donor
DCTMB	1,4-dicyano-2,3,5,6-tetramethylbenzene
de	diastereomeric excess
DME	1,2-dimethoxyethane
DMF	N,N-dimethylformamide
DMSO	dimethyl sulfoxide
EA	electron affinity
ee	enantiomeric excess
EI	electronic ionisation
ET	electron transfer
HOMO	highest occupied molecular orbital
HRMS	high resolution mass spectroscopy
IP	ionisation potential
IR	infrared spectroscopy
LDA	Lithium diisopropylamide
LUMO	lowest unoccupied molecular orbital
m-CPBA	meta-chloroperbenzoic acid
NMQ	N-methylquinoline
NOESY	nuclear *Overhauser* enhancement spectroscopy
PET	photoelectron transfer
RT	room temperature
TBDMS	*tert*-butyldimethylsilyl
THF	tetrahydrofuran
UV	ultraviolet spectroscopy

Cirriculum vitae

Name	Yevgeny Makhynya
Date of birth	21 February 1978
Place of birth	Kiev, Ukraine
Nationality	Ukrainian
Civil status	married

School Education

September 1985 - Mai 1992	School № 210, Kiev, Ukraine
September 1992 - June 1995	Technical Lyceum of the National Technical University of Ukraine "KPI", Kiev

High School Education

September 1995 - June 2001	Enrolled at National Technical University of Ukraine "KPI", Kiev
June 1999	Bachelor of Science Honours (B.Sc.H), Chemical Technology and Engineering, NTUU "KPI", Kiev
July 2000-February 2001	Preparation of Diploma Thesis (practical part), Max-Planck Institute for Radiation Chemistry, Mülheim an der Ruhr, Germany. *Study of Induced Oxidative Processes of Basic Taxane Skeleton Formation*, under the direction of Prof. M. Demuth
June 2001	Master of Science Honours (M.Sc.H), Chemical Technology of Organic Substances, NTUU "KPI", Kiev
August 2001-December 2004	Ph.D studies, Max-Planck-Institute for Bioinorganic Chemistry (former Max-Planck Institute for Radiation Chemistry), Mülheim an der Ruhr, Germany. *Novel Cu(II)-mediated Methodologies for PET-induced Cyclizations, including Asymmetric Induction, and a Biomimetic Approach to the Basic Taxane Skeleton*, under the direction of Prof. M. Demuth